Ionizing Radiation, DNA Damage Response, and Cancer Therapy Resistance

Serena T Bruens

ISBN: 978-94-6332-295-9

Cover design: Ferdi van der Velden & Paul Munsters
Original design by: Matt Forsythe
Lay-out: Serena Bruens
Printed by: GVO drukkers & vormgevers B.V.

Ionizing Radiation, DNA Damage Response and Cancer Therapy Resistance

Ioniserende straling, DNA schade response en kanker therapie resistentie

Proefschrift

ter verkrijging van de graad van doctor aan de
Erasmus Universiteit Rotterdam
op gezag van de
rector magnificus

prof. dr. H.A.P. Pols

en volgens besluit van het College voor Promoties.

De openbare verdediging zal plaatsvinden op

Woensdag 7 februari 2018 om 15.30
door

Serena Tamara Bruens
geboren te Dordrecht

Erasmus University Rotterdam

Promotiecommissie

Promotor:
Prof. dr. J.H.J. Hoeijmakers

Overige leden:
Prof. dr. R. Kanaar
Prof. dr. ir. G.W. Jenster
Dr. H. Vrieling

Copromotor:

Dr. J. Pothof

Table of Contents

Chapter 1

General Introduction

Serena T Bruens, Joris Pothof, Jan J H Hoeijmakers

1

Cancer

Cancer is one of the most prevalent diseases in the Western world including the Netherlands and a leading cause of mortality and morbidity worldwide (1-3). It is estimated that the incidence of cancer worldwide will increase from 13 million new cases in 2008 to 22 million new cases in 2030, which is due to a growing world population, steadily increased life expectancy and increased exposure to risk factors (e.g. smoking, sunlight, obesity). Cancer is not one disease, but the collective term for a group of diseases that originate from several cell types / tissues, sharing several characteristics such as uncontrolled cell division and metastasis that disrupt normal tissue anatomy / function. Cancer is considered a disease of our genes in which mutations, gross chromosomal rearrangements or epigenetic alterations abrogate tumour-suppressor genes or activate oncogenes, which both drive carcinogenesis. This multistep process is predominantly driven by a combination of genome instability that abrogates or erroneously activates gene function and subsequent clonal selection of the best surviving and growing cells. The complexity of carcinogenesis is even greater and several other processes have to be altered for a tumour (cell) to survive and proliferate (Fig. 1A). These features are regarded the 'hallmarks' of cancer and represent acquired capabilities present in most, if not all, human tumours (4, 5).

Of the aforementioned cancer hallmarks, genome instability is considered the driving force behind carcinogenesis as the spontaneous mutation frequency of normal cells in too low to account for all mutations / chromosomal aberration found in cancer cells and required for mutating relevant combinations of tumour suppressors and oncogenes. Genome instability is often the result of repeated exposure to exogenous DNA-damaging agents (e.g. UV light from the sun, cigarette smoke) or defects in DNA damage repair and/or signalling, collectively designated the DNA damage response (DDR), molecules as one of the first steps in carcinogenesis. Indeed, many hereditary cancer syndromes have germ line mutations in a DDR gene. In addition, most, if not all spontaneous cancers have at least one defect in the DDR.

Uncontrolled cell proliferation is mainly the result of mutations in genes that control cell proliferation and makes a cell grow independent from growth factors. Another important aspect of cancer cells is immortality. During each round of cell division, telomere length is shortened. Critically short or absent telomeres due to repeated cell divisions induce cellular senescence (permanent cell cycle arrest) or apoptosis. Telomere length is thus limiting the number of cell divisions, which have to be overcome by a pre-cancer cell to progress into more malignant states. Therefore, telomere length is maintained by reactivation of the enzyme telomerase, which prolongs telomere length and allows cells to replicate infinitively.

Besides telomere immortalization, cancer cells have acquired resistance to apoptosis to maintain viability. Many mechanisms to evade apoptosis have been discovered that prevent proper induction or execution of apoptosis. One of them is a cancer hallmark on its own, i.e. deregu-

lated metabolism. Cancer cells favour glycolysis over mitochondrial respiration to produce ATP. This effect is known as the Warburg effect and inhibits mitochondrial-dependent apoptosis. The ATP output from glycolysis however, is lower than mitochondrial respiration, therefore most cancer cells have increased expression of membrane-bound glucose transporters to enhance glucose uptake from their environment. Tumour growth is often limited due to lack of nutrients. To propagate cell growth and maintenance of the inner tumour mass, angiogenesis is initiated by the overproduction of vascular growth factors such as VGEF, PDEGF and FGF, leading to migration of endothelial cells into the tumour and formation of capillaries to supply the inner tumour cells with nutrients and oxygen.

In addition to self-sustained proliferation, tumour cells have to avoid clearance by the immune system. Ironically, it is thought that the immune system itself selects for less immunogenic cancer cells by taking out the most highly immunogenic cancer cells thereby allowing less immunogenic cancer cells to survive. Furthermore, pro-inflammatory cytokines secreted by tumour infiltrating immune cells and senescent cells in the tumour stroma enhance tumour maintenance and growth. In addition, a pro-inflammatory environment can induce epithelial-to-mesenchymal transition (EMT) of tumour cells, which is a key process in metastasis.

Cancer therapy

Cancer therapy usually consists of several steps; each designed to reduce the chance of relapse. First-line treatment of non-metastasized solid tumours is surgery to physically remove the tumour from the patient's body. Subsequently, the patient is often treated with radiotherapy, chemo-

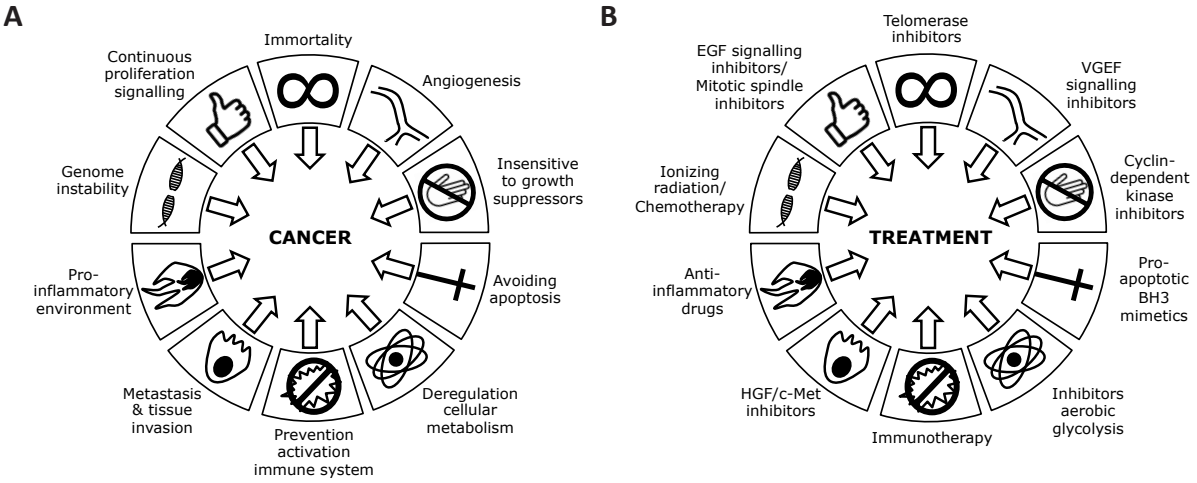

Figure 1: The hallmarks of cancer and treatment targets. A) Cancer cells acquire different hallmarks during carcinogenesis. Often a combination of these hallmarks is found in cancer cells. However, the order in which they are acquired and how many are minimally necessary to induce malignancy are unknown. B) The hallmarks are also used as targets for drug development. Most drugs developed at the moment target one of the hallmarks specifically. Adapted from D. Hanahan and R.A. Weinberg (5).

therapy, targeted therapy and/or immune therapy. First line treatment of primary tumours that cannot be resected or metastasized tumours is often radiotherapy or chemotherapy to offer patients palliation and prolonging of life. Although several interventions are targeting one of the aforementioned cancer hallmarks (Fig 1B), genotoxic/cytotoxic cancer therapies are still the mainstay in medicinal cancer treatment by inducing DNA damage followed by subsequent programmed cell death. Their proven success implies that cancer cells are more sensitive to DNA damage than normal proliferating cells. This increased specific sensitivity of cancer cells is thought to be largely due to intrinsic defects in DNA damage repair and response genes in combination with high cell proliferation in the absence of cell cycle checkpoints, which are so called "proliferation brakes" that arrest the cell cycle in case of DNA damage to allow the cell time to repair the damage.

Currently, three types of genotoxic cancer therapies are being used in the clinic, i.e. radiotherapy, chemotherapy, and targeted therapy. Radiotherapy by ionizing radiation (IR) induces several DNA lesions, but mainly relies on the induction of toxic double strand DNA breaks (DSBs) (6). IR can be applied by i) external beam radiotherapy (EBRT), ii) brachytherapy in which a radioactive source is implanted in or close to the tumour, or iii) radionuclide therapy, a systemic treatment with a radionuclide coupled to a ligand of a highly expressed receptor on the tumour.

A plethora of chemotherapeutic genotoxic/cytotoxic cancer treatments has been developed and is regularly used in the clinic with different modes of action. Examples are platinum-bassed compounds that induce inter- and intrastrand crosslinks, agents that alkylate DNA, compounds that induce DSBs (e.g. bleomycin), etc. Other well-known chemotherapeutic drugs are anthracyclines, which inhibit DNA topoisomerases thereby interfering with DNA and RNA synthesis and preventing relaxation of supercoiled DNA leading to inhibition of DNA replication and transcription, and taxanes that inhibit mitotic spindle formation (7, 8).

Lately, targeted therapies have been developed to primarily target cancer cells with a specific defect in a DNA repair gene. Currently, one targeted therapy is available in the clinic that relies on poly(ADP) ribose polymerase (PARP) inhibition. The effectiveness of PARP inhibition is based on a synthetic lethal interaction with defects in homologous recombination (HR), mainly with BRCA1 and BRCA2. On their own inhibition of PARP or defective BRCA1/BRCA2 are not lethal in cells. Originally it was thought that PARP inhibition leads to spontaneous single strand breaks that result in collapsed replication forks and double strand breaks, which are then repaired via HR. However, when repair requiring BRCA1/BRCA2 is deficient due to mutations, replication induced double-strand breaks are not repaired and the cells go into apoptosis. Recent findings however, indicate that PARP inhibitors exert their function by 'trapping' PARP to the DNA, forming complexes on the DNA that can only be resolved via HR and are therefore cytotoxic (9-11). Interestingly, this mechanism relies on the presence of PARP since the effect PARP inhibition is abrogated when PARP is genetically removed. Treatment with

PARP inhibitors is therefore especially effective in hereditary breast and ovarian cancer in which BRCA1 and BRCA2 are mutated (12-14), although a fraction of several other tumours may also be amenable to this treatment (15).

Since many conventional cancer therapy treatments, including radiotherapy, rely on the induction of DNA damage and most, if not all, tumours have at least one defect in the DDR, it is evident that the status of the DDR is one of the important aspects of determining whether a treatment is successful.

The DNA damage response

DNA is an intrinsic instable molecule and therefore vulnerable to chemical modifications (16, 17). Each day, every cell in the human body may encounter up to 100,000 DNA lesions (18) induced by various endogenous and exogenous sources. For example, endogenous sources include reactive metabolic by-products or spontaneous reactions (mostly hydrolysis). Exogenous sources are e.g. cigarette smoke, UV-light from the sun, or chemicals in food, contaminated water or air (16), but also numerous cancer therapies. Error-prone repair of DNA damage leads to mutations, insertions, deletions and chromosomal aberrations, which all drive carcinogenesis. Per-

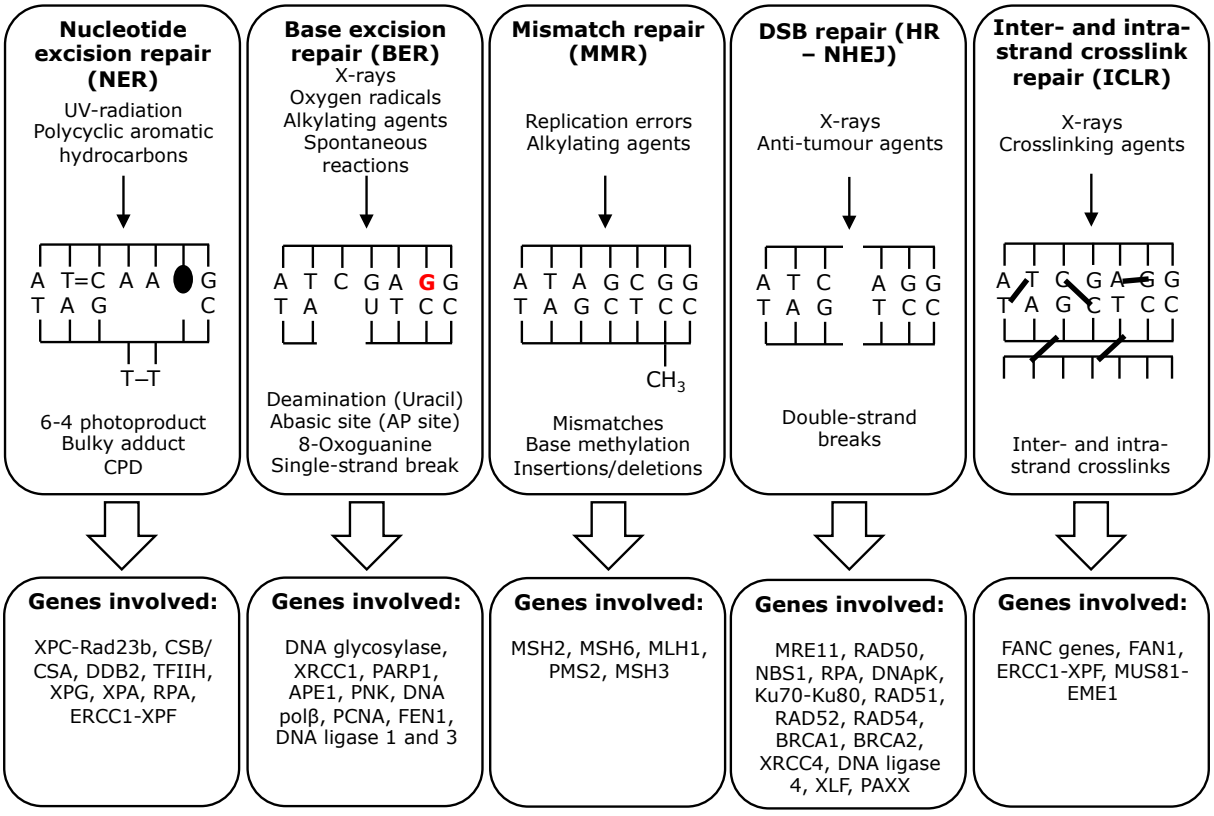

Figure 2: DNA damage, DNA repair pathways and genes involved. Different types of DNA damages are induced via endogenous of exogenous sources. Specific pathways are present to repair these damages, each having specific gene and protein expression. Adapted from J.H.J. Hoeijmakers (21).

sistent DNA damage accumulating throughout life is thought to be a causal driver of the aging process. To counteract the harmful consequences of DNA damage, cells contain various DNA repair systems to correct the damage and DNA damage checkpoints that arrest the cell cycle to allow the cell time to repair the damage, or, in case of damage beyond repair, induce apoptosis or cellular senescence. In addition, several other cellular processes are implicated in the cellular response to DNA damage. The collective cellular response to DNA damage is designated the DNA damage response (DDR).

DNA damage repair

DNA damage comes in many different forms, each being corrected by a different repair pathway (Fig. 2). Radiotherapy induces predominantly single-strand breaks (SSBs) and double-strand breaks (DSBs), which indicate that the SSB and DSB repair systems are most important for the effectiveness of radiotherapy. There are however, additional DNA repair systems. Helix-distorting bulky lesions interfere with base pairing and block transcription and replication in which the consequence is replication fork stalling and collapse, leading to DSBs in S-phase. Another consequence of unrepaired bulky DNA lesions is blocked transcription, which in essence stochastically alters gene expression. These bulky lesions are repaired via nucleotide excision repair (NER). Small chemical modifications of DNA bases, such as oxidation, alkylation damage and deamination, can result in non-canonical base pairing which in turn can lead to incorporation of an incorrect base during S-phase (19), enhancing mutagenesis. These small base damages are repaired by short and long patch base excision repair (BER). The proofreading function of the replication machinery attempts to prevent incorporation of incorrect DNA bases. However when this fails, mismatch repair (MMR) is able to deal with these incorrectly incorporated DNA bases (20). When the DNA replication machinery is blocked by an interstrand crosslink, the covalent binding of the two opposite strands of the DNA helix, the replication fork is stalled and can eventually collapse. Interstrand crosslinks are repaired by interstrand crosslink repair.

As mentioned above radiotherapy mainly induces SSBs and DSBs. Single-strand break repair (SSBR) repairs SSBs via either direct ligation, short patch or long patch BER. SSBs are recognized by PARP and polynu-

Figure 3: DNA damage repair, signalling and factors involved in resistance upon treatment with DNA-damaging agents. This is a simplified schematic representation of the DNA damage response. Different sensor proteins, like MRE11, RAD51 and NBS1, which recruit transducer proteins ATM, ATR and DNApK, detect DNA damage. Dependent on the cell cycle different DNA repair factors are recruited and at the same time other effector proteins, such as CHK1 and CHK2 are phosphorylated. This leads to cellular response that, depending on the severity of the damage, leads to cell cycle arrest, apoptosis, DNA repair and/or senescence. Proteins that are increased in expression during IR resistance are in red. In green are proteins that are decreased in expression during IR resistance. Proteins indicated in white are important players in one or more of these processes, but have not yet been linked to IR resistance.

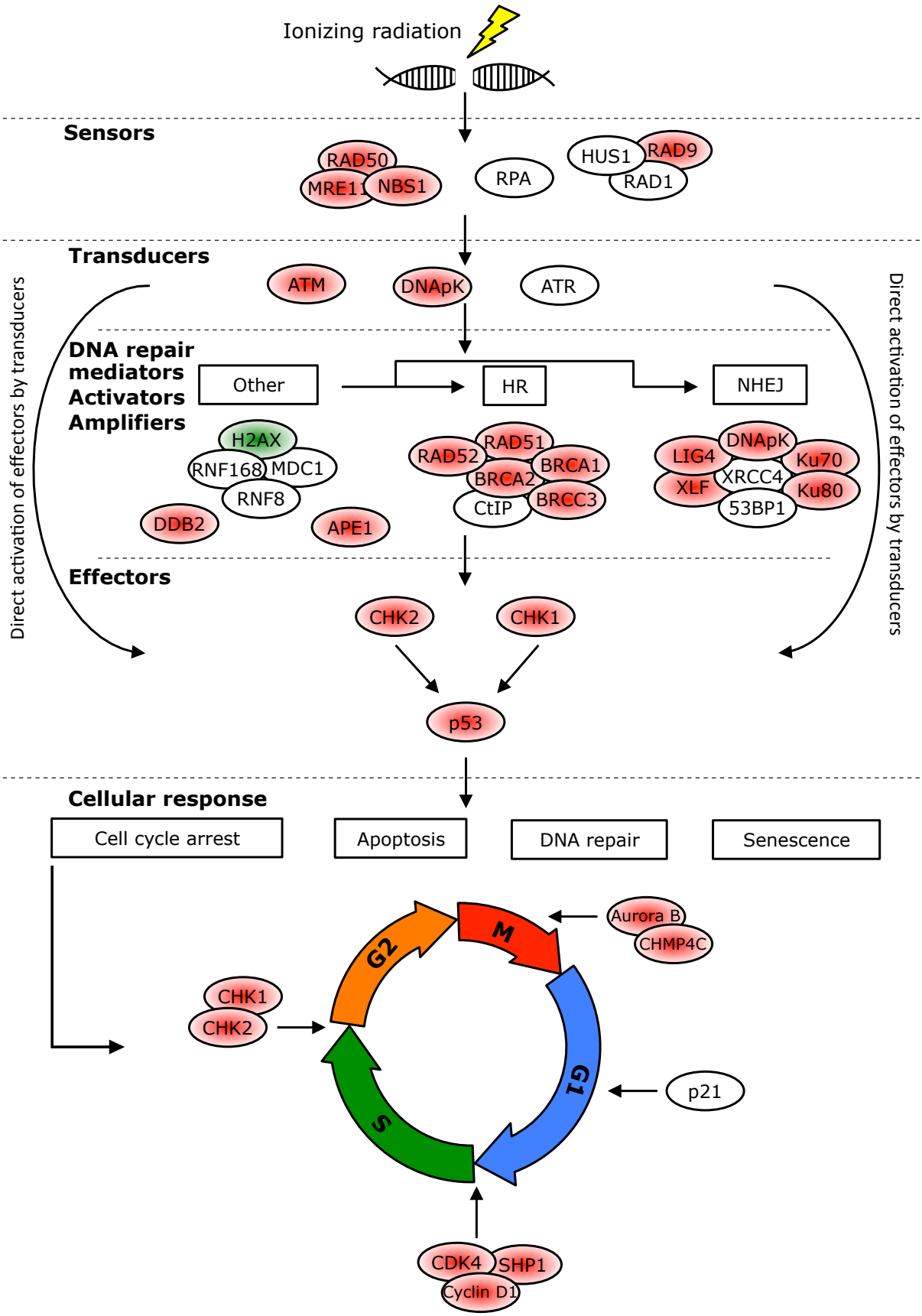
Ionizing radiation
Sensors
RAD50
MRE11
NBS1
RPA
HUS1
RAD9
RAD1
Transducers
ATM
DNApK
ATR
Direct activation of effectors by transducers
Direct activation of effectors by transducers
DNA repair mediators
Activators
Amplifiers
Other
HR
NHEJ
H2AX
RNF168
MDC1
RNF8
DDB2
APE1
RAD51
RAD52
BRCA1
BRCA2
CtIP
BRCC3
DNApK
LIG4
Ku70
XRCC4
XLF
Ku80
53BP1
Effectors
CHK2
CHK1
p53
Cellular response
Cell cycle arrest
Apoptosis
DNA repair
Senescence
G2
M
G1
S
Aurora B
CHMP4C
CHK1
CHK2
p21
CDK4
SHP1
Cyclin D1

cleotide kinase (PNK). DNA polymerase δ/ε together with proliferating cell nuclear antigen (PCNA) adds ±2-8 nucleotides more into the DNA gap, generating a 5'-flap of replaced nucleotides. These nucleotides are then removed by FEN1 (19, 22) and DNA ligase I seals the break. If the SSB is not repaired via BER it will result in a DSB during DNA replication in S-phase.

The two main pathways that repair DSBs are homologous recombination (HR) and non-homologous end joining (NHEJ). HR requires an intact sister chromatid and is therefore only active during the S- and G2-phase of the cell cycle, while NHEJ repairs DSBs during all phases of the cell cycle (23, 24). In HR, a DSB is recognized by the MRN complex (MRE11, RAD50 and NBS1), which recruits CtIP, BRCA1 and other nucleases to generate a 3'-ssDNA overhang at both sides of the DSB, which is bound and covered by replication protein A (RPA). Subsequently, RPA is replaced by RAD51 with the help of BRCA2, thereby forming nucleoprotein filaments. These filaments invade the sister chromatid at the homologous sequence and by using the intact sister chromatid as a template, the DNA is extended. The other end of the DSB is captured and repaired after the junctions are resolved, resulting in a repaired DSB (25). HR is the most accurate DSB repair mechanism.

NHEJ on the other hand is more error-prone. NHEJ is not dependent on cell cycle and does not require a template. The end-joining reaction is initiated by the KU70-KU80 heterodimer that binds to the ends of the DSB and recruits DNA-dependent protein kinase (DNA-PK). If there are no compatible ends, DSB ends are processed by nucleases such as Artemis. Finally, the ligation complex, consisting of DNA ligase IV, XRCC4, XLF and PAXX, ligates the two DNA ends (26, 27). Since NHEJ repairs breaks without homology or template, it is very well possible that small mutations of indels occur.

NHEJ as described above is often referred to canonical NHEJ (c-NHEJ) however; in c-NHEJ disabled systems there is still residual NHEJ present (28). The residual NHEJ is referred to as alternative NHEJ (alt-NHEJ) and functions independent from DNA-PK (29, 30). In alt-NHEJ small stretches of nucleotides serve as a template for micro homology, which is mediated by PARP1. Subsequently, DNA ligase I or DNA ligase III together with XRCC1 repair the break. Although micro homology is used in alt-NHEJ, still mutagenesis and small rearrangements can occur.

DNA damage signalling

DNA repair mechanisms are the first line of defence in the DDR. In addition to DNA repair activation, the cell activates elaborate DNA damage signalling pathways, which are usually referred to as DNA damage/cell cycle checkpoints, since they block transition from G1 to S-phase or G2 to M-phase (31, 32). DNA damage checkpoints halt cell proliferation thereby allowing cell additional time to repair the damage. These DNA damage checkpoints can also induce apoptosis or senescence when damage is beyond repair (Fig. 3).

In order to activate the signalling cascade so-called sensor proteins of which the MRN complex is well known detect DNA damage, especially

DSBs. Upon DNA damage detection transducer proteins, such as ATM, ATR and DNA-PK, are recruited to the site of damage. ATM mainly regulates the response to DSBs (33); whereas ATR primarily regulated the response to SSBs (34). ATM and ATR regulate a broad range of downstream responses, DNA-PK on the other hand directly promotes DSB repair via NHEJ (7, 34). Together, ATM and ATR phosphorylate a plethora of downstream mediator and effector proteins, with each their own specific set of targets (35).

In the DDR ATM kinase activity is activated by MRN and leads to the phosphorylation of mediator protein H2AX (γH2AX). H2AX phosphorylation spreads several kilo bases away from the DSB; subsequently γH2AX recruits other DDR factors and thereby enhances the signalling cascade. Formation of γH2AX foci is important for sustaining the DDR, but γH2AX is not essential for the initial localization of DDR factors such as BCRA1 and 53BP1 (36). Upon phosphorylation of mediator proteins, such as γH2AX, effector proteins are recruited and activated by phosphorylation. However, ATM can also directly phosphorylate effector proteins like CHK2 and p53. Phosphorylation of CHK2 results in an S and G2/M arrest, whereas ATM stabilizes p53 by phosphorylation, leading to increased p21 expression and subsequent G1 arrest (37).

In SSB repair one of the main sensors of DNA damage is RPA that is recruited to ssDNA regions that were generated during DNA replication and DNA repair (34, 38). ATR, which is in complex with ATRIP, recognizes RPA, however ssDNA bound RPA is not sufficient to activate ATR. ATR signalling depends on the 9-1-1 complex (a complex formed by RAD9, RAD1 and HUS1) that recruits TOPBP1. TOPBP1 activates the ATR kinase activity, resulting in the ATR signalling cascade and finally CHK1 phosphorylation. CHK1 phosphorylation eventually results in an S and G2/M arrest (37). Failure of the DDR can have detrimental effects on the cell (16, 17), however for cancer cells DDR failure could be an advantage in order to survive treatment and become resistant.

Cancer therapy resistance

Most tumours display initial sensitivity to aforementioned treatments, but unfortunately also develop resistance that limits therapy effectiveness. Regrettably, therapy resistance is not driven by a single process. Although various cellular resistance mechanisms have been elucidated, these cannot explain all resistance events by far. We can discriminate two main types of resistance to therapy, i.e. intrinsic and acquired resistance. Intrinsic resistance is already present in the tumour before treatment. Intrinsic resistance is usually the result of the cancer cell's specific mutational profile that renders it insensitive to therapy a priori. Acquired resistance is a form of therapy resistance that develops during the course of treatment (39). Here, the tumour is initially sensitive to the treatment, but acquires therapy resistance in the course of treatment often as a result of the therapy itself. A simple explanation could be that genotoxic therapies induce mutations that result in therapy resistance. It has been shown however, that acquired resistance is also induced upon non-genotoxic therapies and often has a tran-

sient nature, suggesting that active processes are on going to maintain cell viability. Several mechanisms of chemotherapy resistance have been described, e.g. alterations of the drug target or increased drug efflux (8, 39).

Since DNA damage induction is the mode of action of genotoxic/cytotoxic therapies including radiotherapy (RT), it is likely that alteration in the DDR could play a role in both intrinsic and acquired resistance. These alterations however, are poorly understood. Here we summarize the role of the DDR in RT-resistance in solid tumours from prostate, lung, head and neck, breast and glioblastoma (GBM) in which RT is often applied as treatment. In addition, we classified studies based on intrinsic or acquired resistance. We published that DNA repair protein expression can be almost absent in human cancer without functionally altering DNA repair capacity (40). Meaning that even small amounts of functional protein are sufficient for efficient and functional DNA repair. Therefore, we added a second classification in which we indicated whether functional DDR data was present: often only a correlation between DDR gene expression/protein level and resistance was published as evidence for the implication of DDR alterations in therapy resistance.

The role of DNA repair in intrinsic RT-resistance

Intrinsic RT-resistance encompasses changes in both HR and NHEJ. Several studies address the role of HR status in RT-resistance. Both BRCA1 and RAD51 are up regulated after IR in the RT-resistant prostate cancer cell line PC3, but down regulated in the IR-sensitive LNCaP prostate cancer cell line, suggesting that HR status plays a role in RT -sensitivity/-resistance (41). Indeed, siRNA-mediated knockdown of RAD51 in CD133+ lung cancer stem cells or overexpression of miR-155, which targets RAD51, in the MCF7 breast cancer cell line, increased IR sensitivity (42, 43). Conversely, BRCA1-defective breast cancer cells are highly radiosensitive. Restoring critical mutated regions of BRCA1 in these cells induced RT-resistance (44, 45). A similar observation was made in BRCA2-deficient Capan-1 pancreatic cancer cells, in which BRCA2 restoration led to RT-resistance (46). DSBs are recognized by the MRN complex, which is involved in both DSB repair via HR and DSB signalling (47). High expression of MRE11 in breast cancer patients is associated with resistance to chemotherapy and RT and decreased disease free and patient survival (48). In line with these results, head and neck squamous cell carcinoma (HNSCC) cells with non-functional RAD50 formed smaller tumours in mice when compared to the control cells after IR treatment (49). In addition, L1CAM expressing gliobastoma multiforme (GBM) stem cells, which are RT-resistant, have increased NBS1 expression and increased phosphorylation of ATM and CHK2 that act downstream in the DNA damage signalling cascade (50).

Several lines of evidence also indicate a role for NHEJ in intrinsic RT-resistance. Restoration of mutant P53 in epidermal carcinoma and lung cancer led to IR sensitivity, which correlated with attenuated DNA repair and lower expression of NHEJ proteins KU70, XRCC4 and DNA-PK (51). In

addition, positive cofactor 4 (PC4), an activator of NHEJ (52), was identified as a regulator of NHEJ in RT-resistance (53). PC4 is up regulated in oesophageal cancer and its knockdown led to IR sensitization in vitro and in vivo by suppression of NHEJ via XLF down regulation (53). In addition, increased expression of KU80 was observed in HPV-negative HNSCC patients, which correlated with loco-regional failure (tumour recurrence at the same site) and mortality after IR (54). Another hint that NHEJ is involved in resistance to IR was derived from studies in colorectal cancer (CRC). Differentiation of colon stem cells is under the control of Wnt/β-catenin signalling, which is often mutated in human colon cancer (55, 56). LIG4, which mediates the final step in NHEJ, is a direct transcriptional target of β-catenin (57). Hyper activation of β-catenin led to increased expression of LIG4 in CRC cells and induced RT-resistance, which was abolished by down regulation of LIG4 or targeting of β-catenin (57).

IR does not only induce DSBs but also 8-oxoguanine and SSBs. SSBs indirectly induce DSBs by collapsing replication forks (58, 59). Both types of lesions are repaired via BER. Cervical cancer and germ cell tumours with high APE1 expression, which functions in BER, correlated with resistant to radiotherapy (60, 61). RAD9 is another factor in BER, but functions in other DNA repair pathways and in damage signalling as well (62). In the prostate cancer cell lines PC3 and Du145 RAD9 knockdown sensitized these cells to RT (63), suggesting a role for BER in RT-resistance. Thus, the cellular status of both DSB repair pathways HR and NHEJ, but possibly BER that repairs IR-induced lesions as well, can determine intrinsic RT-resistance.

The role of DNA damage signalling in intrinsic RT-resistance

DNA repair is not the only line of defence when a cell encounters DNA damage. Cell cycle checkpoints arrest cell proliferation at the G1/S or G2/M transition. Cancer cells often lack a functional G1/S checkpoint, leading to an arrest in the S/G2 phase of the cell cycle. In most cancers the G2/M checkpoint is intact. Cancer cells often rely on the G2/M checkpoint to avoid cell death after DNA damage: DSBs are particularly harmful during mitosis, leading to loss or gain of parts of chromosomes (64, 65). Intrinsic RT-resistance in relation to DNA damage signalling appears to centre on the ATM-CHK1/2-P53 DNA damage signalling axis and downstream alterations in cell cycle control proteins.

Oro-pharyngeal squamous cell carcinoma cells deficient for ATM, due to an 11q copy number loss, require ATR-dependent CHK1 phosphorylation to control the cell cycle and are thus RT-resistant. This is in contrast to AT cells that, without a functional ATM protein, are highly sensitive to IR (66). In the case of an 11q deletion, still some ATM expression is retained, which is sufficient for the cells to survive RT treatment. Therefore, inhibition of CHK1 sensitized these cells to RT (67). DDB2 is a DNA repair protein mainly known for its role in NER (68, 69). DDB has several functions outside NER (70-75) of which one is linked to RT-resistance in non-small cell lung cancer (NSCLC) (76). DDB2 expression promoted RT-resistance by phosphorylati-

on of CHK1, resulting in a G2 cell cycle arrest and increased HR that contributed to RT-resistance in lung cancer cells (77). P53 is a central component of the DDR downstream of CHK1 and CHK2, which is mutated in all cancer types ranging from 5% in cervical cancer to almost 50% in ovarian cancer (78), and activates the G1/S cell cycle checkpoint after damage. P53 deficiency leads to an arrest in S and G2/M phase, which relies on an intact CHK1 and CHK2 protein. Dual inhibition of CHK1 and CHK2 in radiation resistant CD133+ GBM stem cells abolished RT-resistance in vitro and in vivo (79).

These aforementioned results indicate that targeting checkpoint kinases is an effective way to sensitize RT-resistant cancer cells. However, this sensitization depended on the P53 status of the tumour (8, 80). ATM inhibition in P53-deficient cancer cells sensitized them to chemotherapy and radiation, whereas P53-proficient cells became resistant (80-83). Thus, cancer cells that lack functional P53 are vulnerable to G2/M checkpoint inhibition. On the other hand, checkpoint inhibition in cancer cells with normal P53 leads to a reduction of P53-dependent apoptosis (8). Together this points to a complex wiring of the DDR in relation to resistance to DNA-damaging treatments.

Downstream of the ATM-CHK1/2-P53 DNA damage-signalling axis several proteins control the transition of cell cycle to the next phase, which includes cyclins and cyclin-dependent kinases (CDK). Cyclins are positive regulators of CDKs, which in turn promote progression of the cell through the cell cycle and are often overexpressed in cancer cells (84). Knockdown of cyclin D1, which is important for G1/S-phase progression, could sensitize prostate cancer cells to IR, independent of hormone status (85, 86). In line with this finding, knockdown of CDK4, which is a target of cyclin D1, sensitizes breast cancer cells to IR (87), indicating that transition through the G1/S cell cycle checkpoint and subsequent stalling in the S/G2 phase, promotes the survival of RT-resistant cancer cells after DNA damage.

Aurora B is important for progression of mitosis and cytokinesis and plays a role in the abscission checkpoint (checkpoint just before a dividing cell separates into two cells); a direct target of Aurora B is CHMP4C (88). Aurora B and CHMP4C are involved in the repair of chromosome bridges during the last phase of cytokinesis, which prevents chromosome breakage and aneuploidy (89). Often they are up regulated in cancer cells, thereby promoting cancer cell survival (90). Inhibition of Aurora B sensitizes several cancer types to IR (91, 92). In addition, it was recently found that CHMP4C inhibition also sensitizes lung cancer cells to IR in a P53-independent manner (93).

All aforementioned studies depict a picture in which specific DDR defects in cancer cells lead to an arrest or accumulation of cells in the S/G2 checkpoint. This is thought to prevent cell death after DNA damage by utilizing additional DNA repair pathways.

The role of DNA repair in acquired RT-resistance

HR, NHEJ and DNA damage signalling are not only affected in intrinsic resistance also in acquired resistance they were identified to be abro-

gated. Several studies generated RT-resistant cell lines or used recurrent/metastasized tumours to address the role of HR in acquired resistance. The downside, however, is that all studies used different ways of inducing acquired resistance with fractionated IR. Even though the outcome is the same, RT-resistance, mechanistically these studies are difficult to compare. Nevertheless, they provide insights on the role of HR in acquired resistance. BRCA1 and BRCA2 are known to form a complex with RAD51, BARD1, BRCC45 and BRCC3, called the BRCC complex (94). As part of the BRCC complex BRCC3 is a de-ubiquitilating enzyme, which counteracts UBC13-RNF8 ubiquitin enzyme activity (95, 96). In HNSCC high BRCC3 expression is correlated with low overall survival and increased risk of local-regional failure. After in vitro induced acquired resistance, HNSCC cell lines display increased BRCC3 expression, and inhibition of BRCC3 expression sensitized these cells to IR (97). Conversely, RT-resistant lung cancer cells seem to depend on RAD52 expression (98). Rad52 is an essential HR gene in yeast (99), whereas in Rad52-/- mice no DNA repair or recombination phenotype was observed (100). However, RAD52 was found to be functionally redundant with BRCA1, BRCA2 and PALB2 in mediating RAD51-dependent HR (101), indicating its importance in HR. Microarray data of RT-resistant lung cancer cells showed an increased expression of RAD52. Knockdown of RAD52 in RT-resistant lung cancer cells led to decreased colony formation after fractionated IR (98).

Several lines of evidence indicate a role for both HR and NHEJ in acquired RT-resistance of prostate cancer cells. Proteins involved in HR (BRCA1, BRCA2 and RAD51) and NHEJ (KU70/KU80) were up regulated in RT-resistant prostate cancer cells. Whereas phosphorylation of H2AX is down regulated. This effect was reversed by inhibition of the PI3K pathway (102). Suggesting that NHEJ and HR are involved in acquired resistance to IR in prostate cancer. In addition, in acquired RT-resistant lung cancer cells inhibition of NHEJ factor DNA-PK sensitized these cells to additional IR (103). Thus, dependent on the protocol of induction of acquired RT-resistance, DSB repair pathways HR or NHEJ are involved.

The role of DNA damage signalling in acquired RT-resistance

As mentioned previously, the ATM-CHK1/2-P53 DNA damage signalling axis and cell cycle checkpoints are important during intrinsic RT-resistance. However, limited evidence is present on the role of DNA damage signalling in acquired resistance. Nonetheless, present studies indicate roles for DNA damage signalling in acquired RT-resistance (84). Proteomic analysis of acquired RT-resistant breast cancer cell line MCF7 shows that CHK1, CDK1 and CDK2 expression is increased (104). Of those proteins CHK1 is associated with acquired RT-resistance in breast cancer. RT-resistant MCF7 cells exhibit hyperactivity of ATM, which phosphorylates and stabilizes ZEB1 after DNA damage (105). In turn, ZEB1 interacts with USP7, which stabilizes CHK1 and arrests the cells in G2/M phase. As a result, HR was activated and RT-resistance was induced. Moreover, microRNA-205 was found to direct-

ly target ZEB1. Combining RT with microRNA-205 inhibition, RT-resistant breast cancer cell lines were sensitized again. Moreover, direct targeting of CHK1 also has proven to be effective in sensitizing RT-resistant breast cancer cell lines in vitro and breast cancer tumours in mice in vivo (106).

Downstream effectors in the cell cycle are, amongst others, cyclins and CDKs (84). These proteins are phosphorylated by the protein tyrosine phosphatase SHP1, which promotes G1/S phase progression (107, 108). In RT-resistant A549 lung cancer cells and HNSCC cells, SHP1 and its targets cyclin D1 and CDK4 are up regulated, which resulted in S-phase stalling. Down regulation of SHP1 led to G0/1 arrest, down regulation of cyclin D1 and CDK4 and sensitization of A549 to IR (109, 110), highlighting the importance of post-translational modifications in the regulation of RT-resistance. Hence, cells with acquired RT-resistance mainly rely on cell cycle stalling in S or G2/M phase. Targeting checkpoint kinases, such as CHK1, or phosphatases, such as, SHP1 in combination with RT can be an effective strategy to overcome acquired resistance.

Concluding remarks

To maintain a healthy genome, functional DDR pathways are essential. Cancer cells exploit their DDR deficiencies in order to survive treatment and develop therapy resistance. Thus, the DDR has an important role in RT-resistance development. In general, during RT-resistance cancer cells mainly arrest in S- or G2/M-phase due to defective ATM signalling, increased CHK1/2 phosphorylation or increased expression of down stream cell cycle regulators like cyclin D1, CDK4 and Aurora B. This would suggest that by arresting in S- or G2/M-phase RT-resistant cancer cells are able to repair DSBs induced by RT, using the more accurate HR. Indeed, RT-resistant cancer cells have increased expression of HR proteins BRCA1, BRCA2, RAD51, RAD52 and BRCC3. Upstream HR, DSBs are recognized by sensor proteins such as the MRN complex, which consists of MRE11, NBS1 and RAD50. The individual components of the MRN complex were also up regulated in RT-resistant cancer cells. The MRN complex signals not only to downstream HR mediators, it also recruits transducer proteins such as ATM, ATR and DNA-PK. RT-resistant cancer cells with altered MRN complex also have increased phosphorylation of ATM and CHK2, hence the cells arrest in S- and G2/M-phase. Again, highlighting the importance of the S- and G2/M-phase arrest. Next to HR, NHEJ can also repair DSBs, however it is less accurate and can cause small mutations and indels. Evidence is present that NHEJ is involved in RT-resistance. PC4, via XLF, alters NHEJ in RT-resistant cancer cells. Also increased expression of KU70/KU80 and transcriptional regulation of LIG4 by β-catenin were identified as possible mechanism by which NHEJ can cause RT-resistance. However, all NHEJ effects were independent from the cell cycle, suggesting that the ATM-CHK1/2-P53 axis is more important for HR repair in RT-resistant cancer cells. Therefore, effective strategies to sensitize RT-resistant cancer

cells were mostly based on inhibition of checkpoint kinases and checkpoint phosphatases. Moreover, specific inhibition of signal transducer proteins ATM and DNA-PK were also effective. Therefore, designing a personal treatment strategy based on the DDR characteristics of the tumour in combination with IR could be an effective strategy to treat RT-resistant tumours.

Here we focussed primarily on the involvement of the DDR in intrinsic and acquired RT-resistance. Even though most research was performed in intrinsically RT-resistant cancer cells and data on acquired RT-resistance was limited, a general role for the DDR could be found. However, the DDR is just a small part of all processes involved in RT-resistance. Often it is a combination of multiple factors, which together form a resistant phenotype (Fig. 4). Other mechanisms, which are not discussed here, such as de-regulated apoptosis or oncogenic bypass all relate to the cancer hallmarks (5), underlining the complexity of therapy resistance. Therefore, it could be useful to characterize the tumour's characteristics before treatment in order to predict whether the tumour will respond to RT.

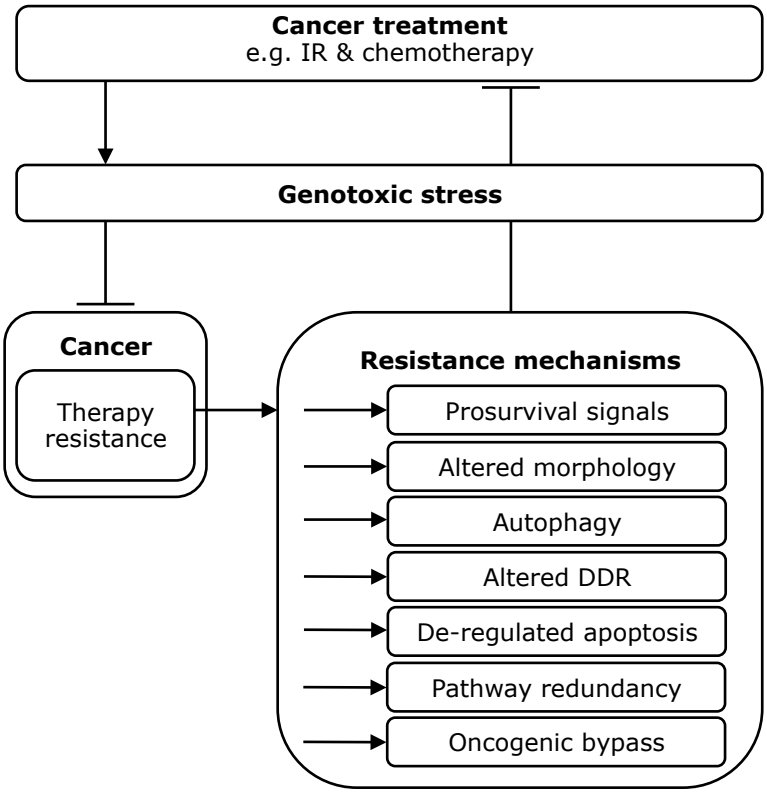

Figure 4: Repetitive treatment with DNA-damaging agents leads to treatment resistance via multiple pathways. Repetitive treatment with IR or chemotherapy leads to DNA damage and/or inhibition of enzymes, which leads to death of cancer cells. However, cancer cells can acquire resistance to these types of treatment and have multiple mechanisms at their disposal to survive treatment. In this review we only focussed on the involvement of the DDR, but many more mechanisms were identified to be involved in therapy resistance.

1

Scope of the thesis

The work described in this thesis aims to elucidate the role of the DNA damage response in acquired resistance to ionizing radiation and its differential regulation upon DNA damage. **Chapter 2** shows that different DNA repair pathways display redundancy in radiotherapy-resistant prostate cancer cells. **Chapter 3** unravels the mRNA response in radiotherapy resistance using next generation sequencing to identify novel pathways. Energy metabolism was identified as one of the main contributors to radiotherapy resistance next to the DNA damage response. **Chapter 4** presents the differential response of an important cell type, embryonic stem cells, to equitoxic dosages of three genotoxic agents. Based on mRNA and small RNA sequencing we were able to identify a novel posttranslational modification, citrullination, that is involved in the proper function of homologous recombination upon induction of double strand breaks (DSBs) in DNA in cancer cells. In **Chapter 5** the role of RNA-binding proteins in DSB repair in cancer cells was investigated. Unexpectedly, we found that proper homologous recombination repair of DSB is dependent on RNA-binding proteins. However, the effect seen in RNA-binding protein knockdown is opposite of the effect seen in **Chapter 4**. This indicates a tight regulation of DSB repair upon genotoxic stress. **Chapter 6** summarizes the main results and discusses the implications of the differential response to DSBs in cancer cells.

References

1. Vineis P, Wild CP. Global cancer patterns: causes and prevention. Lancet. 2014;383(9916):549-57.
2. Bray F, Jemal A, Grey N, Ferlay J, Forman D. Global cancer transitions according to the Human Development Index (2008-2030): a population-based study. The Lancet Oncology. 2012;13(8):790-801.
3. Ferlay J, Shin HR, Bray F, Forman D, Mathers C, Parkin DM. Estimates of worldwide burden of cancer in 2008: GLOBOCAN 2008. International journal of cancer. 2010;127(12):2893-917.
4. Hanahan D, Weinberg RA. The hallmarks of cancer. Cell. 2000;100(1):57-70.
5. Hanahan D, Weinberg RA. Hallmarks of cancer: the next generation. Cell. 2011;144(5):646-74.
6. Ward JF. DNA damage produced by ionizing radiation in mammalian cells: identities, mechanisms of formation, and reparability. Progress in nucleic acid research and molecular biology. 1988;35:95-125.
7. Goldstein M, Kastan MB. The DNA damage response: implications for tumor responses to radiation and chemotherapy. Annual review of medicine. 2015;66:129-43.
8. Bouwman P, Jonkers J. The effects of deregulated DNA damage signalling on cancer chemotherapy response and resistance. Nature reviews Cancer. 2012;12(9):587-98.
9. Pommier Y, O'Connor MJ, de Bono J. Laying a trap to kill cancer cells: PARP inhibitors and their mechanisms of action. Science translational medicine. 2016;8(362):362ps17.
10. Murai J, Huang SY, Renaud A, Zhang Y, Ji J, Takeda S, et al. Stereospecific PARP trapping by BMN 673 and comparison with olaparib and rucaparib. Molecular cancer therapeutics. 2014;13(2):433-43.
11. Murai J, Huang SY, Das BB, Renaud A, Zhang Y, Doroshow JH, et al. Trapping of PARP1 and PARP2 by Clinical PARP Inhibitors. Cancer research. 2012;72(21):5588-99.
12. Bryant HE, Schultz N, Thomas HD, Parker KM, Flower D, Lopez E, et al. Specific killing of BRCA2-deficient tumours with inhibitors of poly(ADP-ribose) polymerase. Nature. 2005;434(7035):913-7.
13. Farmer H, McCabe N, Lord CJ, Tutt AN, Johnson-DA, Richardson TB, et al. Targeting the DNA repair defect in BRCA mutant cells as a therapeutic strategy. Nature. 2005;434(7035):917-21.
14. Audeh MW, Carmichael J, Penson RT, Friedlander M, Powell B, Bell-McGuinn KM, et al. Oral poly(ADP-ribose) polymerase inhibitor olaparib in patients with BRCA1 or BRCA2 mutations and recurrent ovarian cancer: a proof-of-concept trial. Lancet. 2010;376(9737):245-51.
15. Drean A, Lord CJ, Ashworth A. PARP inhibitor combination therapy. Critical reviews in oncology/hematology. 2016;108:73-85.
16. Hoeijmakers JH. DNA damage, aging, and cancer. The New England journal of medicine. 2009;361(15):1475-85.
17. Clark TA, Spittle KE, Turner SW, Korlach J. Direct detection and sequencing of damaged DNA bases. Genome integrity. 2011;2:10.
18. Lindahl T. Instability and decay of the primary structure of DNA. Nature. 1993;362(6422):709-15.
19. Robertson AB, Klungland A, Rognes T, Leiros I. DNA repair in mammalian cells: Base excision repair: the long and short of it. Cellular and molecular life sciences : CMLS. 2009;66(6):981-93.
20. Jiricny J. Postreplicative mismatch repair. Cold Spring Harbor perspectives in biology. 2013;5(4):a012633.
21. Hoeijmakers JH. Genome maintenance mechanisms for preventing cancer. Nature. 2001;411(6835):366-74.
22. Parsons JL, Dianov GL. Co-ordination of base excision repair and genome stability. DNA repair. 2013;12(5):326-33.
23. Wyman C, Kanaar R. DNA double-strand break repair: all's well that ends well. Annual review of genetics. 2006;40:363-83.
24. Heyer WD, Ehmsen KT, Liu J. Regulation of homologous recombination in eukaryotes. Annual review of genetics. 2010;44:113-39.
25. Brandsma I, Gent DC. Pathway choice in DNA double strand break repair: observations of a balancing act. Genome integrity. 2012;3(1):9.
26. Lieber MR. The mechanism of double-strand DNA break repair by the nonhomologous DNA end-joining pathway. Annual review of biochemistry. 2010;79:181-211.
27. Ochi T, Blackford AN, Coates J, Jhujh S, Me-

hmood S, Tamura N, et al. DNA repair. PAXX, a paralog of XRCC4 and XLF, interacts with Ku to promote DNA double-strand break repair. Science. 2015;347(6218):185-8.
28. Feldmann E, Schmiemann V, Goedecke W, Reichenberger S, Pfeiffer P. DNA double-strand break repair in cell-free extracts from Ku80-deficient cells: implications for Ku serving as an alignment factor in non-homologous DNA end joining. Nucleic acids research. 2000;28(13):2585-96.
29. Chiruvella KK, Liang Z, Wilson TE. Repair of double-strand breaks by end joining. Cold Spring Harbor perspectives in biology. 2013;5(5):a012757.
30. Frit P, Barboule N, Yuan Y, Gomez D, Calsou P. Alternative end-joining pathway(s): bricolage at DNA breaks. DNA repair. 2014;17:81-97.
31. Bartek J, Lukas J. Mammalian G1- and S-phase checkpoints in response to DNA damage. Current opinion in cell biology. 2001;13(6):738-47.
32. Pearce AK, Humphrey TC. Integrating stress-response and cell-cycle checkpoint pathways. Trends in cell biology. 2001;11(10):426-33.
33. Bakkenist CJ, Kastan MB. DNA damage activates ATM through intermolecular autophosphorylation and dimer dissociation. Nature. 2003;421(6922):499-506.
34. Ciccia A, Elledge SJ. The DNA damage response: making it safe to play with knives. Molecular cell. 2010;40(2):179-204.
35. Shiloh Y. ATM and related protein kinases: safeguarding genome integrity. Nature reviews Cancer. 2003;3(3):155-68.
36. Celeste A, Petersen S, Romanienko PJ, Fernandez-Capetillo O, Chen HT, Sedelnikova OA, et al. Genomic instability in mice lacking histone H2AX. Science. 2002;296(5569):922-7.
37. Kastan MB, Bartek J. Cell-cycle checkpoints and cancer. Nature. 2004;432(7015):316-23.
38. Cimprich KA, Cortez D. ATR: an essential regulator of genome integrity. Nature reviews Molecular cell biology. 2008;9(8):616-27.
39. Holohan C, Van Schaeybroeck S, Longley DB, Johnston PG. Cancer drug resistance: an evolving paradigm. Nature reviews Cancer. 2013;13(10):714-26.
40. Naipal KA, Raams A, Bruens ST, Brandsma I, Verkaik NS, Jaspers NG, et al. Attenuated XPC expression is not associated with impaired DNA repair in bladder cancer. PloS one. 2015;10(4):e0126029.
41. Young A, Berry R, Holloway AF, Blackburn NB, Dickinson JL, Skala M, et al. RNA-seq profiling of a radiation resistant and radiation sensitive prostate cancer cell line highlights opposing regulation of DNA repair and targets for radiosensitization. BMC cancer. 2014;14:808.
42. Desai A, Webb B, Gerson SL. CD133+ cells contribute to radioresistance via altered regulation of DNA repair genes in human lung cancer cells. Radiotherapy and oncology : journal of the European Society for Therapeutic Radiology and Oncology. 2014;110(3):538-45.
43. Gasparini P, Lovat F, Fassan M, Casadei L, Cascione L, Jacob NK, et al. Protective role of miR-155 in breast cancer through RAD51 targeting impairs homologous recombination after irradiation. Proceedings of the National Academy of Sciences of the United States of America. 2014;111(12):4536-41.
44. Abbott DW, Thompson ME, Robinson-Benion C, Tomlinson G, Jensen RA, Holt JT. BRCA1 expression restores radiation resistance in BRCA1-defective cancer cells through enhancement of transcription-coupled DNA repair. The Journal of biological chemistry. 1999;274(26):18808-12.
45. Mamon HJ, Dahlberg W, Azzam EI, Nagasawa H, Muto MG, Little JB. Differing effects of breast cancer 1, early onset (BRCA1) and ataxia-telangiectasia mutated (ATM) mutations on cellular responses to ionizing radiation. International journal of radiation biology. 2003;79(10):817-29.
46. Xia F, Taghian DG, DeFrank JS, Zeng ZC, Willers H, Iliakis G, et al. Deficiency of human BRCA2 leads to impaired homologous recombination but maintains normal nonhomologous end joining. Proceedings of the National Academy of Sciences of the United States of America. 2001;98(15):8644-9.
47. Williams GJ, Lees-Miller SP, Tainer JA. Mre11-Rad50-Nbs1 conformations and the control of sensing, signaling, and effector responses at DNA double-strand breaks. DNA repair. 2010;9(12):1299-306.
48. Yuan SS, Hou MF, Hsieh YC, Huang CY, Lee YC, Chen YJ, et al. Role of MRE11 in cell proliferation, tumor invasion, and DNA repair in breast cancer. Journal of the National Cancer Institute. 2012;104(19):1485-502.
49. Chang L, Huang J, Wang K, Li J, Yan R, Zhu L, et al. Targeting Rad50 sensitizes human nasopharyngeal carcinoma cells to radiotherapy. BMC cancer.

2016;16:190.
50. Cheng L, Wu Q, Huang Z, Guryanova OA, Huang Q, Shou W, et al. L1CAM regulates DNA damage checkpoint response of glioblastoma stem cells through NBS1. The EMBO journal. 2011;30(5):800-13.
51. Sah NK, Munshi A, Nishikawa T, Mukhopadhyay T, Roth JA, Meyn RE. Adenovirus-mediated wild-type p53 radiosensitizes human tumor cells by suppressing DNA repair capacity. Molecular cancer therapeutics. 2003;2(11):1223-31.
52. Batta K, Yokokawa M, Takeyasu K, Kundu TK. Human transcriptional coactivator PC4 stimulates DNA end joining and activates DSB repair activity. Journal of molecular biology. 2009;385(3):788-99.
53. Qian D, Zhang B, Zeng XL, Le Blanc JM, Guo YH, Xue C, et al. Inhibition of human positive cofactor 4 radiosensitizes human esophageal squmaous cell carcinoma cells by suppressing XLF-mediated nonhomologous end joining. Cell death & disease. 2014;5:e1461.
54. Moeller BJ, Yordy JS, Williams MD, Giri U, Raju U, Molkentine DP, et al. DNA repair biomarker profiling of head and neck cancer: Ku80 expression predicts locoregional failure and death following radiotherapy. Clinical cancer research : an official journal of the American Association for Cancer Research. 2011;17(7):2035-43.
55. Reynolds A, Wharton N, Parris A, Mitchell E, Sobolewski A, Kam C, et al. Canonical Wnt signals combined with suppressed TGFbeta/BMP pathways promote renewal of the native human colonic epithelium. Gut. 2014;63(4):610-21.
56. Polakis P. Wnt signaling in cancer. Cold Spring Harbor perspectives in biology. 2012;4(5).
57. Jun S, Jung YS, Suh HN, Wang W, Kim MJ, Oh YS, et al. LIG4 mediates Wnt signalling-induced radioresistance. Nature communications. 2016;7:10994.
58. Caldecott KW. Protein ADP-ribosylation and the cellular response to DNA strand breaks. DNA repair. 2014;19:108-13.
59. Tubbs A, Nussenzweig A. Endogenous DNA Damage as a Source of Genomic Instability in Cancer. Cell. 2017;168(4):644-56.
60. Herring CJ, West CM, Wilks DP, Davidson SE, Hunter RD, Berry P, et al. Levels of the DNA repair enzyme human apurinic/apyrimidinic endonuclease (APE1, APEX, Ref-1) are associated with the intrinsic radiosensitivity of cervical cancers. British journal of cancer. 1998;78(9):1128-33.
61. Robertson KA, Bullock HA, Xu Y, Tritt R, Zimmerman E, Ulbright TM, et al. Altered expression of Ape1/ref-1 in germ cell tumors and overexpression in NT2 cells confers resistance to bleomycin and radiation. Cancer research. 2001;61(5):2220-5.
62. Broustas CG, Lieberman HB. Contributions of Rad9 to tumorigenesis. Journal of cellular biochemistry. 2012;113(3):742-51.
63. Broustas CG, Lieberman HB. RAD9 enhances radioresistance of human prostate cancer cells through regulation of ITGB1 protein levels. The Prostate. 2014;74(14):1359-70.
64. Chen T, Stephens PA, Middleton FK, Curtin NJ. Targeting the S and G2 checkpoint to treat cancer. Drug discovery today. 2012;17(5-6):194-202.
65. Massague J. G1 cell-cycle control and cancer. Nature. 2004;432(7015):298-306.
66. Choi S, Gamper AM, White JS, Bakkenist CJ. Inhibition of ATM kinase activity does not phenocopy ATM protein disruption: implications for the clinical utility of ATM kinase inhibitors. Cell cycle. 2010;9(20):4052-7.
67. Sankunny M, Parikh RA, Lewis DW, Gooding WE, Saunders WS, Gollin SM. Targeted inhibition of ATR or CHEK1 reverses radioresistance in oral squamous cell carcinoma cells with distal chromosome arm 11q loss. Genes, chromosomes & cancer. 2014;53(2):129-43.
68. Scrima A, Konickova R, Czyzewski BK, Kawasaki Y, Jeffrey PD, Groisman R, et al. Structural basis of UV DNA-damage recognition by the DDB1-DDB2 complex. Cell. 2008;135(7):1213-23.
69. Marteijn JA, Lans H, Vermeulen W, Hoeijmakers JH. Understanding nucleotide excision repair and its roles in cancer and ageing. Nature reviews Molecular cell biology. 2014;15(7):465-81.
70. Zhao R, Han C, Eisenhauer E, Kroger J, Zhao W, Yu J, et al. DNA damage-binding complex recruits HDAC1 to repress Bcl-2 transcription in human ovarian cancer cells. Molecular cancer research : MCR. 2014;12(3):370-80.
71. Stoyanova T, Roy N, Kopanja D, Bagchi S, Raychaudhuri P. DDB2 decides cell fate following DNA damage. Proceedings of the National Academy of Sciences of the United

States of America. 2009;106(26):10690-5.
72. Roy N, Bommi PV, Bhat UG, Bhattacharjee S, Elangovan I, Li J, et al. DDB2 suppresses epithelial-to-mesenchymal transition in colon cancer. Cancer research. 2013;73(12):3771-82.
73. Ennen M, Klotz R, Touche N, Pinel S, Barbieux C, Besancenot V, et al. DDB2: a novel regulator of NF-kappaB and breast tumor invasion. Cancer research. 2013;73(16):5040-52.
74. Roy N, Stoyanova T, Dominguez-Brauer C, Park HJ, Bagchi S, Raychaudhuri P. DDB2, an essential mediator of premature senescence. Molecular and cellular biology. 2010;30(11):2681-92.
75. Yoon T, Chakrabortty A, Franks R, Valli T, Kiyokawa H, Raychaudhuri P. Tumor-prone phenotype of the DDB2-deficient mice. Oncogene. 2005;24(3):469-78.
76. Yang HJ, Kim N, Seong KM, Youn H, Youn B. Investigation of radiation-induced transcriptome profile of radioresistant non-small cell lung cancer A549 cells using RNA-seq. PloS one. 2013;8(3):e59319.
77. Zou N, Xie G, Cui T, Srivastava AK, Qu M, Yang L, et al. DDB2 increases radioresistance of NSCLC cells by enhancing DNA damage responses. Tumour biology : the journal of the International Society for Oncodevelopmental Biology and Medicine. 2016;37(10):14183-91.
78. Olivier M, Hollstein M, Hainaut P. TP53 mutations in human cancers: origins, consequences, and clinical use. Cold Spring Harbor perspectives in biology. 2010;2(1):a001008.
79. Bao S, Wu Q, McLendon RE, Hao Y, Shi Q, Hjelmeland AB, et al. Glioma stem cells promote radioresistance by preferential activation of the DNA damage response. Nature. 2006;444(7120):756-60.
80. Jiang H, Reinhardt HC, Bartkova J, Tommiska J, Blomqvist C, Nevanlinna H, et al. The combined status of ATM and p53 link tumor development with therapeutic response. Genes & development. 2009;23(16):1895-909.
81. Biddlestone-Thorpe L, Sajjad M, Rosenberg E, Beckta JM, Valerie NC, Tokarz M, et al. ATM kinase inhibition preferentially sensitizes p53-mutant glioma to ionizing radiation. Clinical cancer research : an official journal of the American Association for Cancer Research. 2013;19(12):3189-200.
82. Vecchio D, Daga A, Carra E, Marubbi D, Baio G, Neumaier CE, et al. Predictability, efficacy and safety of radiosensitization of glioblastoma-initiating cells by the ATM inhibitor KU-60019. International journal of cancer. 2014;135(2):479-91.
83. Carruthers R, Ahmed SU, Strathdee K, Gomez-Roman N, Amoah-Buahin E, Watts C, et al. Abrogation of radioresistance in glioblastoma stem-like cells by inhibition of ATM kinase. Molecular oncology. 2015;9(1):192-203.
84. Lim S, Kaldis P. Cdks, cyclins and CKIs: roles beyond cell cycle regulation. Development. 2013;140(15):3079-93.
85. Marampon F, Gravina G, Ju X, Vetuschi A, Sferra R, Casimiro M, et al. Cyclin D1 silencing suppresses tumorigenicity, impairs DNA double strand break repair and thus radiosensitizes androgen-independent prostate cancer cells to DNA damage. Oncotarget. 2016;7(5):5383-400.
86. Casimiro MC, Di Sante G, Ju X, Li Z, Chen K, Crosariol M, et al. Cyclin D1 Promotes Androgen-Dependent DNA Damage Repair in Prostate Cancer Cells. Cancer research. 2016;76(2):329-38.
87. Hagen KR, Zeng X, Lee MY, Tucker Kahn S, Harrison Pitner MK, Zaky SS, et al. Silencing CDK4 radiosensitizes breast cancer cells by promoting apoptosis. Cell division. 2013;8(1):10.
88. Carlton JG, Caballe A, Agromayor M, Kloc M, Martin-Serrano J. ESCRT-III governs the Aurora B-mediated abscission checkpoint through CHMP4C. Science. 2012;336(6078):220-5.
89. Carmena M. Abscission checkpoint control: stuck in the middle with Aurora B. Open biology. 2012;2(7):120095.
90. Pharoah PD, Tsai YY, Ramus SJ, Phelan CM, Goode EL, Lawrenson K, et al. GWAS meta-analysis and replication identifies three new susceptibility loci for ovarian cancer. Nature genetics. 2013;45(4):362-70, 70e1-2.
91. Wu X, Liu W, Cao Q, Chen C, Chen Z, Xu Z, et al. Inhibition of Aurora B by CCT137690 sensitizes colorectal cells to radiotherapy. Journal of experimental & clinical cancer research : CR. 2014;33:13.
92. Niermann KJ, Moretti L, Giacalone NJ, Sun Y, Schleicher SM, Kopsombut P, et al. Enhanced radiosensitivity of androgen-resistant prostate cancer: AZD1152-mediated Aurora kinase B inhibition. Radiation research. 2011;175(4):444-51.

93. Li K, Liu J, Tian M, Gao G, Qi X, Pan Y, et al. CHMP4C Disruption Sensitizes the Human Lung Cancer Cells to Irradiation. International journal of molecular sciences. 2015;17(1).
94. Dong Y, Hakimi MA, Chen X, Kumaraswamy E, Cooch NS, Godwin AK, et al. Regulation of BRCC, a holoenzyme complex containing BRCA1 and BRCA2, by a signalosome-like subunit and its role in DNA repair. Molecular cell. 2003;12(5):1087-99.
95. Huen MS, Grant R, Manke I, Minn K, Yu X, Yaffe MB, et al. RNF8 transduces the DNA-damage signal via histone ubiquitylation and checkpoint protein assembly. Cell. 2007;131(5):901-14.
96. Shao G, Lilli DR, Patterson-Fortin J, Coleman KA, Morrissey DE, Greenberg RA. The Rap80-BRCC36 de-ubiquitinating enzyme complex antagonizes RNF8-Ubc13-dependent ubiquitination events at DNA double strand breaks. Proceedings of the National Academy of Sciences of the United States of America. 2009;106(9):3166-71.
97. Tu Z, Xu B, Qu C, Tao Y, Chen C, Hua W, et al. BRCC3 acts as a prognostic marker in nasopharyngeal carcinoma patients treated with radiotherapy and mediates radiation resistance in vitro. Radiation oncology. 2015;10:123.
98. Ghosh S, Krishna M. Role of Rad52 in fractionated irradiation induced signaling in A549 lung adenocarcinoma cells. Mutation research. 2012;729(1-2):61-72.
99. Hanamshet K, Mazina OM, Mazin AV. Reappearance from Obscurity: Mammalian Rad52 in Homologous Recombination. Genes. 2016;7(9).
100. Rijkers T, Van Den Ouweland J, Morolli B, Rolink AG, Baarends WM, Van Sloun PP, et al. Targeted inactivation of mouse RAD52 reduces homologous recombination but not resistance to ionizing radiation. Molecular and cellular biology. 1998;18(11):6423-9.
101. Lok BH, Carley AC, Tchang B, Powell SN. RAD52 inactivation is synthetically lethal with deficiencies in BRCA1 and PALB2 in addition to BRCA2 through RAD51-mediated homologous recombination. Oncogene. 2013;32(30):3552-8.
102. Chang L, Graham PH, Hao J, Ni J, Bucci J, Cozzi PJ, et al. PI3K/Akt/mTOR pathway inhibitors enhance radiosensitivity in radioresistant prostate cancer cells through inducing apoptosis, reducing autophagy, suppressing NHEJ and HR repair pathways. Cell death & disease. 2014;5:e1437.
103. Li Y, Li H, Peng W, He XY, Huang M, Qiu D, et al. DNA-dependent protein kinase catalytic subunit inhibitor reverses acquired radioresistance in lung adenocarcinoma by suppressing DNA repair. Molecular medicine reports. 2015;12(1):1328-34.
104. Guo L, Xiao Y, Fan M, Li JJ, Wang Y. Profiling global kinome signatures of the radioresistant MCF-7/C6 breast cancer cells using MRM-based targeted proteomics. Journal of proteome research. 2015;14(1):193-201.
105. Zhang P, Wei Y, Wang L, Debeb BG, Yuan Y, Zhang J, et al. ATM-mediated stabilization of ZEB1 promotes DNA damage response and radioresistance through CHK1. Nature cell biology. 2014;16(9):864-75.
106. Zhang Y, Lai J, Du Z, Gao J, Yang S, Gorityala S, et al. Targeting radioresistant breast cancer cells by single agent CHK1 inhibitor via enhancing replication stress. Oncotarget. 2016;7(23):34688-702.
107. Lopez-Ruiz P, Rodriguez-Ubreva J, Cariaga AE, Cortes MA, Colas B. SHP-1 in cell-cycle regulation. Anti-cancer agents in medicinal chemistry. 2011;11(1):89-98.
108. Rodriguez-Ubreva FJ, Cariaga-Martinez AE, Cortes MA, Romero-De Pablos M, Ropero S, Lopez-Ruiz P, et al. Knockdown of protein tyrosine phosphatase SHP-1 inhibits G1/S progression in prostate cancer cells through the regulation of components of the cell-cycle machinery. Oncogene. 2010;29(3):345-55.
109. Cao R, Ding Q, Li P, Xue J, Zou Z, Huang J, et al. SHP1-mediated cell cycle redistribution inhibits radiosensitivity of non-small cell lung cancer. Radiation oncology. 2013;8:178.
110. Peng G, Cao RB, Li YH, Zou ZW, Huang J, Ding Q. Alterations of cell cycle control proteins SHP1/2, p16, CDK4 and cyclin D1 in radioresistant nasopharyngeal carcinoma cells. Molecular medicine reports. 2014;10(4):1709-16.

Chapter 2

Persistent DNA double strand breaks and transient rewiring of the DNA damage response induce acquired radio-resistance

Serena Bruens[1], Nicole Verkaik[1], Marjolein Baar[1], Aranka Ambags[1], Marjolijn Ladan[1], Dik van Gent[1], Wytkse van Weerden[2], Guido Jenster[2], Jan Hoeijmakers[1,3,4], Joris Pothof[1*]

[1] Department of Molecular Genetics, Erasmus Medical Center, Rotterdam, The Netherlands
[2] Department of Urology, Erasmus Medical Center, Rotterdam, The Netherlands
[3] CECAD Research Center, University of Cologne, Cologne, Germany
[4] Princess Maxima Center for Pediatric Oncology, Utrecht, The Netherlands

* Corresponding author: j.pothof@erasmusmc.nl

Submitted

Abstract

Radiation therapy by ionizing radiation is an integral part of cancer therapy. Initially sensitive tumours can acquire resistance to radiotherapy, seriously frustrating curing patients. ~12% of prostate cancer patients experience clinical failure, in which the recurrent or metastasized tumour has acquired resistance to radiotherapy. Ionizing radiation induces DNA damage of which double strand DNA breaks are most toxic for a cell. Currently, our knowledge about the role of DSB repair and signalling in acquired radiotherapy resistance is still limited. We generated transient radio-resistant prostate cancer cells using a radiotherapy regimen identical to clinical practice, which could be reversed by withholding radiotherapy for >2 weeks. These radio-resistant cancer cells were retained in the G2-phase of the cell cycle in combination with ATM activation. In addition we observed persistent double strand breaks in G1-phase cells and reduced canonical non-homologous end joining. The NHEJ repair deficiency was compensated by enhanced homologous recombination in S/G2-phase. Only combined ATM and DNA-PK or ATM and PARP inhibition could sensitize radio-resistant cancer cells. In summary, we provide a new paradigm in radio-resistance, indicating that DSB repair is in part attenuated instead of increased to establish resistance.

Introduction

Radiotherapy (RT) is one of the most frequently used cancer therapies for solid tumours, which relies on inducing cytotoxic DNA damage. Prostate cancer is the second most common form of cancer in men worldwide and is treated with RT, chemotherapy or hormone deprivation therapy, often in combination (1). First-line therapy of non-metastasized tumours is often surgical removal. Some prostate tumours however, cannot be resected. In these cases, RT can be a curative treatment. First-line RT options in localized prostate cancer are external beam radiotherapy (EBRT) or internal radiotherapy (RT) (2). Although initially sensitive, about 12% of patients have clinical failure (CF) within the first five years after treatment, which further increases to 26% after ten years (3). In the majority of these patients the recurrent or metastasized tumours are resistant to therapy, resulting in a decreased patient survival (4, 5).

Several mechanisms of radiotherapy resistance in prostate cancer have been identified (5-8). For example, activation of PI3K/AKT/mTOR and Erk pathways in radio-resistant prostate cancer cells is associated with cancer stem cell (CSC) phenotypes as well as epithelial-to-mesenchymal transition (5, 9). Inhibition of the PI3K/AKT/mTOR pathway could sensitize radio-resistant prostate cancer cells.

RT induces different types of DNA lesions of which DSBs are most toxic to the cell (10). DSBs are repaired via either non-homologous end joining (NHEJ) in all phases the cell cycle or homologous recombination (HR) that only takes place in S- and G2-phase of the cell cycle. NHEJ does not re-

quire a DNA template to repair a DSB, whereas HR needs a sister chromatid for repair, hence its cell cycle specificity (11, 12). In NHEJ KU70/KU80 bind to the ends of a DSB and recruit DNA-PK, which leads via several steps to ligation of the DSB. An alternative form of NHEJ (Alt-EJ) requires micro-homology in the opposite sides of the DSB, which anneal and overhanging flaps are removed (13). Alt-EJ is intrinsically mutagenic as micro-homology annealing leads to deletions. The MRN complex can also recognized DSBs, which results in the recruitment of HR factors but also ATM that activates DNA damage checkpoints. Defects in DNA damage repair and signalling cause genome instability and are causally implicated in carcinogenesis (12). It is thought that these defects in combination with continuous cell proliferation may also sensitize tumours to genotoxic cancer treatments, including RT.

Here, we show that a RT regimen as applied in the clinic can induce radio-resistance in prostate cancer cells. We identified transient alterations of the DNA damage response, which are implicated in radio-resistance.

Materials & Methods

Cell culture

Du145 and PC3 prostate cancer cells were cultured in RPMI-1640 (RPMI-1640 Medium, R2405-500ML, Sigma-Aldrich) supplemented with penicillin-streptomycin (100× diluted, Penicillin-Streptomycin, P0781-100ML, Sigma-Aldrich) and 10% fetal bovine serum (Fetal Bovine Serum (FBS) South America, S1810-500, Biowest) at 5% CO2 and 37°C. A549 and MCF7 were cultured in DMEM supplemented with penicillin-streptomycin (100× diluted, Penicillin-Streptomycin, P0781-100ML, Sigma-Aldrich) and 10% fetal bovine serum (Fetal Bovine Serum (FBS) South America, S1810-500, Biowest) at 5% CO2 and 37°C.

Generation of radio-resistant Du145, PC3, MCF7 and A549

Du145, PC3, A549 and MCF7 were seeded in 6-well plates and maintained as described. The day after seeding all cell lines were radiated (Gammacell 40 Cesium 137 irradiation unit, Atomic Energy) with 2 Gy/day (from Monday-Friday; no IR during Saturday and Sunday) up to a cumulative dose of 78 Gy. After cells have received the indicated IR dosages (see figures), they were not radiated for two days. On the third day after IR experiments were done. For an "IR holiday", cells were analyzed after 10, 17, 24, 31 and 38 days after the last dose of IR.

Clonogenic cell survival assay

Cells were trypsinised (Trypsin-EDTA solution, T3924-500ML, Sigma-Aldrich) and counted (Z2 Coulterparticle count and size analyzer, Beckman Coulter). 600 cells per well in triplicates per condition were seeded in 6-well plates. Next day the cells were treated with different compounds at least 15 minutes prior to IR (0-2-4-6-8 Gy): DMSO; ATMi (KU55933, Selleckchem; 10 mM stock; 10 μM final); PI3Ki (LY294002, Cell Signaling 50 mM stock; 50 μM final); DNApKi (NU7441/KU57788, Selleckchem; 5

mM stock; 10 μM final); PARPi (Olaparib, AstraZeneca, 10 mM stock; 4 μM final); CHK2i (C3742-5mg, Sigma-Aldrich, 1.5 mM stock; 120 nM final); Nutlin (Nutlin3, N6287, Sigma-Aldrich, 10 mM stock; 10 μM final). Cells were incubated for 8-9 days. Then, cells were washed once with PBS and fixed and stained with 0.1% Coomassie Brilliant Blue (50% (v/v) Methanol, 43% (v/v) H2O, 7% (v/v) Acetic Acid, 0.1% (m/v) Coomassie Brilliant Blue). Colonies were counted using Gelcount (Oxford Optronix).

Immunofluorescence

Cells were seeded on coverslips, irradiated with 2 Gy the next day and fixed 1, 2, 4, 8, and 24h after IR. Briefly, the coverslips were washed once with PBS, fixed with 2% PFA, washed with PBS + 0.1% triton X-100 3× short and 2× 10 minutes, once washed with PBS+ (100 ml PBS + 0.5 g BSA + 0.15 g Glycine), incubated 1-2h at RT with primary antibodies. After incubation coverslips were washed with PBS + 0.1% triton X-100 3× short and 2× 10 minutes, once washed with PBS+, incubated 1-2h at RT with secondary antibodies. After incubation coverslips were washed with PBS + 0.1% triton X-100 3× short and 2× 10', once washed with PBS+. For RAD51 staining (commercial antibody, see primary antibodies) the coverslips were washed once with PBS, fixed with 4% PFA. Subsequently, cells were permeabilised for 20' with PBS + 0.2% triton X-100 and washed with PBS. After permeabilization cells were treated with 10× diluted DNAse I (04536282001, Roche Life Sciences) for 1h at 37°C in a humidified chamber and washed with PBS. Blocking was performed using IFF buffer (PBS + 1% BSA + 2% FCS) for at least 30'. After blocking cells were incubated with primary antibodies for 1-2h at RT. After incubation coverslips were washed 3× for 5' with PBS and incubated with secondary antibodies 1-2h at RT. After incubation coverslips were washed 3× for 5' with PBS. Coverslips were mounted in DAPI Vectashield mounting medium (H1200, Vector Laboratories). Images were made using a LSM700 microscope (Carl Zeiss Microimaging Inc.).

Immunoblot analysis

Cells were lysed in 2× sample buffer and boiled at 99°C for 5 minutes. Samples were run on a SDS-PAGE gel and transferred to a PVDF membrane (Immobilon FL PVDF Transfer membrane 0.45um, IPFL00010, Millipore). Membranes were blocked in 5% milk in PBS for 1-2h at RT. After blocking, membranes were incubated with primary antibodies 1-2h at RT. Then the membranes were washed 5 times for 5 minutes with PBS + 0.05% Tween-20 and incubated with secondary antibodies at RT for 1-2h. Again the membranes were washed 5× for 5 minutes. Membranes were visualized using Odyssey CLx Infrared Imaging System (LI-COR Biosciences).

BrdU and PI labelling for cell cycle analysis

Cells were labelled with 5 μM BrdU (B5002, Sigma-Aldrich) for 15 minutes at 37°C. Subsequently, cells were harvested and fixed in 70% ethanol at least overnight at 4°C. Fixed cells were washed with ice-cold PBS and re-sus-

pended in pepsin solution (5 mg pepsin in 10 ml 0.1N HCl) and incubated 20 minutes at RT. After pepsin-treatment blocking solution (PBS + 0.5% Tween-20 + 0.1% BSA) was added and cells were washed. Next, cell were re-suspended in 2N HCl for 12 minutes at 37°C. To neutralise, borate buffer (100 mM, pH8.5) was added and the cells were pelleted. BrdU antibody was added and the cells were incubated for 2h on ice in the dark. Stained cells were washed in blocking solution and re-suspended in 500 µl PBS supplemented with 12.5 µl RNase A and 1 µl PI (P3566, Invitrogen). Cell cycle was analysed the next day using BD LSRFortessa (BD Biosciences). Flow Cytometry data was analysed using FlowJo vX.0.7 (Tree Star Inc.).

Primary antibodies
53BP1 (1000×, 05-726, Millipore); 53BP1 (1000×, sc-22760, Santa Cruz Biotechnology); Akt (Pan) (500×, #4691, Cell Signaling); p-Akt (T308) (500×, #2956, Cell Signaling); p-Akt (S473) (500×, #4060, Cell Signaling); p-ATM (500×, #4526, Cell Signaling); BRCA1 (50×, sc-6954, Santa Cruz Biotechnology); BrdU Kit (50×, 556028, BD Sciences); CHK2 (500×, #3440, Cell Signaling); p-CHK2 (500×, #2197, Cell Signaling); Geminin (400×, 10802-1-AP, Proteintech); γH2AX (Ser139) (1000×, 05-636, Millipore); MDC1 (1000×, ab50003, Abcam); p53 (1000×, sc-126, Santa Cruz Biotechnology); RAD51 (200×, GTX70230, GeneTex); p-SQ/TQ (1000×, #2851, Cell Signaling); Tubulin (2000×, sc-12462-R, Santa Cruz Biotechnology); Tubulin (5000×, T5168, Sigma-Aldrich)

Secondary antibodies
GoatαMouse Alexa 488 (1000×, A11034, Life Technologies); GoatαRabbit Alexa 555 (1000×, A21429, Life Technologies); DonkeyαMouse IRDye 800CW (5000×, 926-32212, LI-COR Biosciences); DonkeyαRabbit IRDye 680RD (5000×, 926-32223, LI-COR Biosciences)

Apoptosis assay
Cells were treated with Cisplatin (20 µM; 1 mg/ml, Accord Healthcare), Docetaxel (1 µM), UV-C (16 J/m2; 254 nm germicidal lamp, Philips) and Caspase 3 activator (100 µM; PAC-1, ab142074, Abcam). After treatment the cells were incubated for 48h. Apoptotic cells were analysed according to the protocol published by Smid et al. (14). In brief, medium and cells were collected and re-suspended in 998 µl FACS buffer (0.5% BSA + 0.05% NaN3 in PBS) pre-heated to 37°C. 1 µl diluted Hoechst 33342 (10 mg/ml, H3570, Life Technologies) was added and the cells were vortexed and incubated for exactly 7 minutes at 37°C. Subsequently, the cells were immediately placed on ice and 1 µl 7-AAD (1 mg/ml, A1310, Invitrogen) was added. Cells were analysed within 1h after adding 7-AAD using BD LSRFortessa (BD Biosciences). Flow Cytometry data was analysed using FlowJo vX.0.7 (Tree Star Inc.).

RNA isolation, cDNA synthesis and qPCR
Total RNA was isolated using Trizol reagent (TriPure Isolation Reagent,

11667165001, Roche Life Science). In brief cells were lysed in Trizol reagent and chloroform was added. Lysates were spun for 15' at 4°C. The aqueous phase was transferred to a new eppendorf tube and isopropanol was added. The aqueous phase was incubated at RT for 10', then spun down for 10' at 4°C. RNA pellets were washed once with 75% ethanol. After washing RNA pellets were dried and dissolved in 30 µl of RNAse-free H2O. RNA concentration and quality was assed using Nanodrop (NanoDrop™ 2000/2000c Spectrophotometers, ThermoFischer Scientific). Subsequently, cDNA was made using iScript cDNA Synthesis Kit (170-8891, Biorad) according to the manufacturer's protocol. qPCR was performed using Platinum® Taq DNA Polymerase (10966018, Invitrogen) according to the manufacturer's protocol complemented with SYBR Green I (SYBR® Green I nucleic acid gel stain, S9430, Sigma-Aldrich) for detection. The reaction mix was run according to the following cycling program: 3' - 95°C; 45× 15'' - 95°C/30'' - 60°C/30'' - 72°C; 1' - 95°C; 1' - 65°C; 65× 30'' - 65°C. Data was analyzed using ΔCt method (15).

Primers

	Forward primer (5'-3')	Reversed primer (5'-3')
Hsa-*NQO1*	GGAGAGTTTGCTTACACTTACGC	AGTGGTGATGGAAGCACTGCCTTC
Hsa-*HO-1*	AAGACTGCGTTCCTGCTCAAC	AAAGCCCTACAGCAACTGTCG
Hsa-*GADPH*	AAGGTGAAGGTCGGAGTCAA	ACCATGTAGTTGAGGTCAATG
Hsa-*UbC*	CTGGAAGATGGTCGTACCCTG	GGTCTTGCCAGTGAGTGTCT

End-joining assay

The end-joining assay was performed as described in (16), with some minor changes. In short, cells were grown in a 3-cm dish to 50-80% confluency. Cells were transiently transfected with 2 µg of a blunt-ended linear DNA substrate (EcoRV/Eco47III digested pDvG94 plasmid (16)) using X-treme GENE HP DNA Transfection Reagent (Sigma Aldrich), following manufacturers protocol. Two days after transfection, extra-chromosomal DNA was isolated and re-suspended in a final volume of 20 µl water (17). From this solution, 1 µl was PCR amplified with the DAR5 and FM30 primers (16), using PuReTaq ready-To-Go PCR beads (GE Healthcare). The PCR product was digested with BstXI. Restriction fragments were separated on a 6% polyacrylamide gel in TBE buffer, stained with ethidiumbromide. The relative level of micro homology-directed end joining was determined by quantification of the BstXI digested PCR product using the ImageJ software.

Statistical analysis

Data was processed using GraphPad Prism v7.0a (GraphPad Software Inc.). Statistical test used were Student's T-test and Mann-Whitney U test. P-values equal or lower than 0.05 were accepted as significant.

Results

Prostate cancer cells acquire a transient resistance phenotype early during IR treatment

In order to study the underlying mechanisms of radio-resistance, we mimicked IR treatment regimen applied in the clinic to prostate cancer cells in vitro by daily exposure to IR to examine whether they develop radio-resistance (Fig. 1A). Briefly, cells were seeded and the next day received 2 Gy IR, which was continued the subsequent days except for weekends. After receiving the indicated final dose, cells were incubated over the weekend without IR and then used for experiments. Prostate cancer cells received the indicated cumulative dose at a dose rate of 2 Gy/day (Fig. 1A) and resistance was investigated using a colony survival assay. We chose a colony survival assay because it measures both sensitivity as well as the ability of a cell to continue proliferation. Resistance occurred between a cumulative dose of 8 Gy and 28 Gy (Fig. 1B + C). Therefore, we determined at what cumulative dose resistance approximately occurred. From 8 Gy onwards we used cumulative dosages of 5 Gy in which the last dose consists of 1 Gy up to a cumulative dose of 28 Gy. Increased resistance was already observed at a cumulative dose of 23 Gy. A cumulative dose of 28 Gy rendered the cells fully resistant, which remained up to a cumulative dose of 78 Gy (Fig. 1B + C). The generation of radio-resistant cells (RR cells, which received a cumulative dose of 28 Gy in future experiments) was not confined to only one cancer cell line. PC3 (prostate cancer), A549 (lung cancer) and MCF7 (breast cancer) cell lines also acquired a similar IR resistance phenotype. BPH1 cells, a non-cancerous prostate epithelial cell line, did not acquire a radio-resistance phenotype (Supplementary Fig. 1A – D), consistent with the idea that IR resistance is a general phenomenon confined to cancer cells.

The colony survival assay demonstrated an additional feature of the RR-cells, i.e. a reduced capacity to form colonies (Fig. 1D + E), indicating that either specific mutations were introduced that drive resistance or that many surviving cells enter a state of quiescence. The latter has been found in chemotherapy-resistant cancer cells, in which the resistance phenotype was transient (18). We generated RR cells, withheld IR for 10, 17, 24 or 31 days (IR holiday) and assessed radio-resistance. Interestingly, the observed RT resistance was transient and could be reversed by an IR holiday of at least 17 days (Fig. 1D). We will refer to these as time re-sensitized cells. Subsequently, we determined whether re-sensitization was permanent or transient as well. Time re-sensitized cells by a 17-day IR holiday were again irradiated with the aforementioned regimen of daily 2 Gy doses up to a cumulative dose of 48 Gy (Fig. 1E). These time re-sensitized cells developed RT resistance again, indicating that also time re-sensitization is not permanent (Fig. 1F). Thus, IR resistance is an early, but transient phenomenon during RT treatment.

DNA damage-associated cell fates are altered in RR cells

DNA damage can lead to several cell fates: transient cell cycle arrest, per-

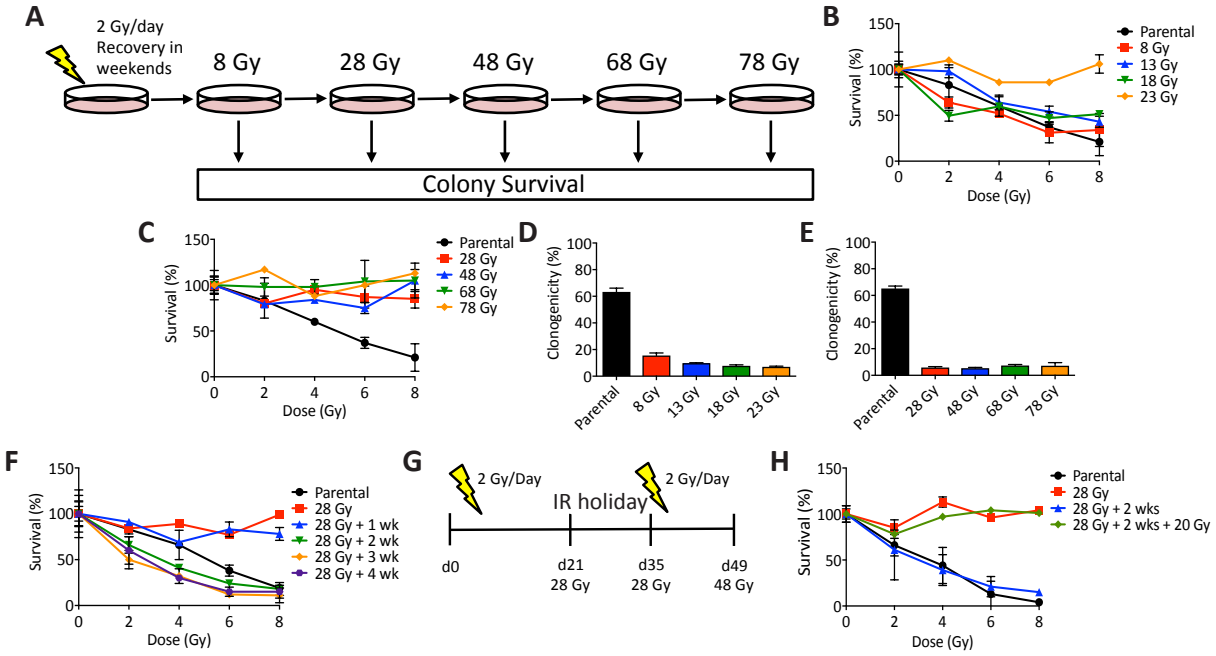

Figure 1: Du145 become IR resistant after fractionated IR treatment. A) Treatment protocol. Beginning 1 day after seeding Du145 cells were radiated with 2 Gy/day in 5 sequential dosages followed by 2 days rest. IR resistance was assessed using colony survival assay. B + C) Du145 cells were tested for IR resistance after different accumulated dosages of IR by colony survival. For 13 and 23 Gy the final dose of IR was 1 Gy instead of 2 Gy. D + E) Percentages of colonies formed by radiated cells relative to parental (unirradiated) cells. F) After receiving IR treatment IR-resistant Du145 were incubated for different periods of time after receiving the last IR dose. IR resistance was addressed using colony survival. G) Treatment schedule. Du145 were radiated up to 28 Gy, then they received IR holiday of 17 days. After the IR holiday IR treatment was continued with 2 Gy/day for five consecutive days with 2 days rest in between up to an additional dose of 20 Gy (total dose is 48 Gy). H) IR resistance was assessed at baseline, after 28 Gy, after IR holiday and after additional IR treatment. Every experiment was repeated at least three times. Mean ± SEM are depicted.

manent cell cycle arrest (senescence), polyploidization and cell death. To further characterize RR cells, we first measured cellular senescence using senescence marker HMGB1, in which loss of HMGB1 expression represents cellular senescence (19). Almost all parental Du145 cells expressed HMGB1. In RR cell cultures however, only normal-sized nuclei expressed HMGB1 and micronuclei are present (white arrow tips), which indicate severe DNA damage and chromosomal instability (Fig. 2A). Next, we analysed whether RR cells with normal-sized nuclei or polyploid RR cells form visible colonies. We seeded RR cells at low density to allow single cells to grow into colonies and stained these with DAPI to determine nuclear size and expression of geminin, a marker for S- and G2-phase cells to determine proliferation status. Only RR cells with normal-sized nuclei could form colonies (Fig. 2B), indicating that RR cells retain normal-sized nuclei and do not exhibit signs of cellular senescence.

Resistance to chemotherapy has been associated with a prolonged stay in G1/G0 phase of the cell cycle. It is thought that chemotherapy

is less toxic to a cancer cell in the quiescent state. When chemotherapy and its associated effect on a cancer cell are alleviated, quiescent cancer cells enter the cell cycle again to continue proliferation (18). We performed a cell cycle analysis based on BrdU incorporation and PI staining to determine the cell cycle profile of RR cells by flow cytometry analysis. We observed a shift towards retention in the G2/M-phase, which was normalized again in time re-sensitized cells (Fig. 2C). The G2/M block in RR cells led us to investigate the response of RR cells to docetaxel, a conventional chemotherapeutic drug often used in prostate cancer treatment that blocks microtubule formation. The apoptotic response in RR cells treated with docetaxel for 48h was attenuated (Fig. 2D). The observed resistance to apoptosis could be due to a strong G2/M block that prevents early entry in M-phase, increased activity of drug clearance systems or a general resistance to apoptosis. To test these possibilities, we treated parental and RR cells with cisplatin, a chemotherapeutic drug that interferes with DNA replication, UV-C irradiation that directly induces DNA damage and subsequent apoptosis and is not affected by drug clearance systems and a Caspase 3 activator that induces apoptosis independent of damage (Fig. 2E – G). We observed a clear reduction in cell death induction in RR

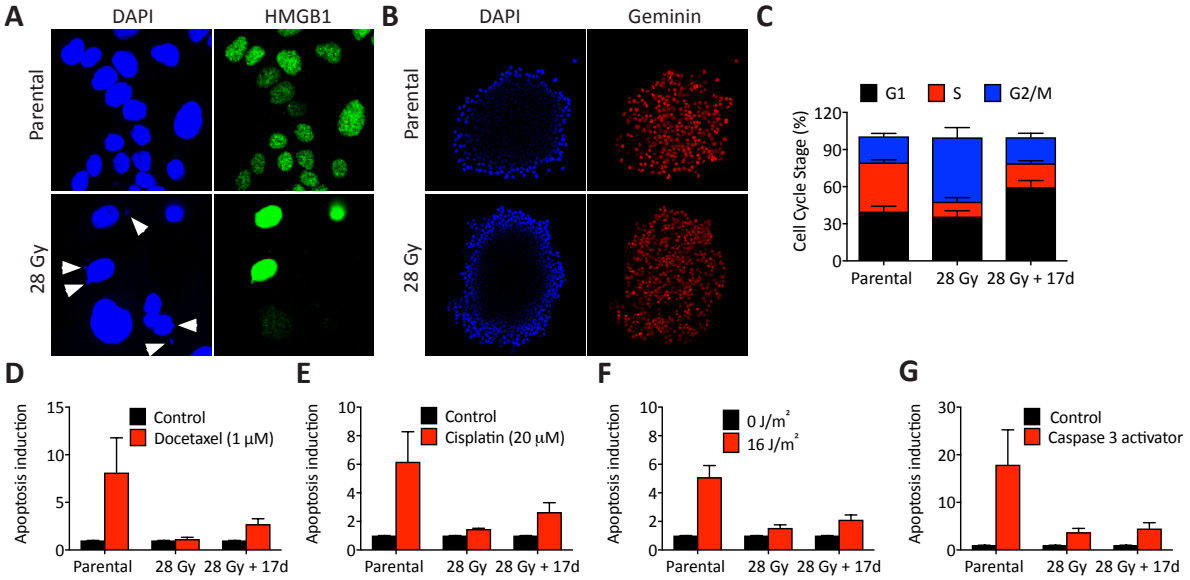

Figure 2: Altered DNA damage-associated cell fates in Du145 RR cells. A) Immunofluorescent staining of parental and RR cells for DAPI and HMGB1. White arrow tips indicate micronuclei. Images were taken at 63× magnification. B) Immunofluorescent staining of colonies formed by parental and RR cells for DAPI and geminin. Note that the DAPI stain only visualized the peripheral nuclei of the colony. Images were taken at 20× magnification. C) Cell cycle profile was determined by flow cytometry analysis using BrdU incorporation and PI staining. RR cells have a block in G2/M-phase, which is reversed after IR holiday. D – G) Cells were incubated for 48 with docetaxel (D) or cisplatin (E), radiated with UVC (F) or incubated with caspase-3 activator (G) at the indicated dose. Using flow cytometry, apoptotic cells were measured by Hoechst 33342 and 7-AAD staining. Every experiment was repeated at least three times. Mean ± SEM are depicted.

cells in all conditions, but not in parental cancer cells. However, apoptosis was still attenuated in time re-sensitized cells, indicating that attenuation of apoptosis is not the mechanism by which RT resistance is induced.

Targeting the ATM signalling pathway did not sensitize RR cells to IR

To understand the mechanistic basis of resistance in RR cells, we first tested known resistance mechanisms. We could not implicate the NRF2 anti-oxidant/cytoprotection pathway in RT resistance, which was measured by qRT-PCR of target genes *NQO1* and *HO-1* (Supplementary fig. 2A). Cancer stem cell (CSC) formation/stabilization has been implicated in the development of RT resistance. We did not observe an increase in cell surface markers associated with prostate cancer CSC except for CD49b and CD133, as was measured by flow cytometry (Suppelmentary fig. 2B – F) (5). Furthermore, it was shown that the PI3 Kinase signalling pathway is involved in RT resistance (9). We could not implicate the PI3 Kinase signalling pathway in the RT resistance model that we developed (Supplementary Fig. 2G). An increased fraction of cells in G2/M-phase is usually observed after a single dose of IR to allow the cell time to repair IR-induced DSBs before entering mitosis. One of the central factors of the G2/M checkpoint is the phosphatidyl inositol 3-kinase like serine/threonine kinase ATM, which amplifies the damage signal via phosphorylation of SQ/TQ motifs in target proteins (20, 21). We analysed phosphorylation of ATM (S1981) and general ATM target phosphorylation on SQ/TQ motifs and found increased phosphorylation of ATM (S1981) and SQ/TQ motifs in RR cells (Fig. 3A + B). Furthermore, P53, which is phosphorylated directly and indirectly by ATM leading to its stabilization, is modestly increased. CHK2, another target of ATM, is highly phosphorylated during IR resistance (Fig. 3C), but also CHK2 levels itself are increased. Thus, ATM activation is increased in RR cells.

Since ATM and its downstream targets are activated in RR cells, we

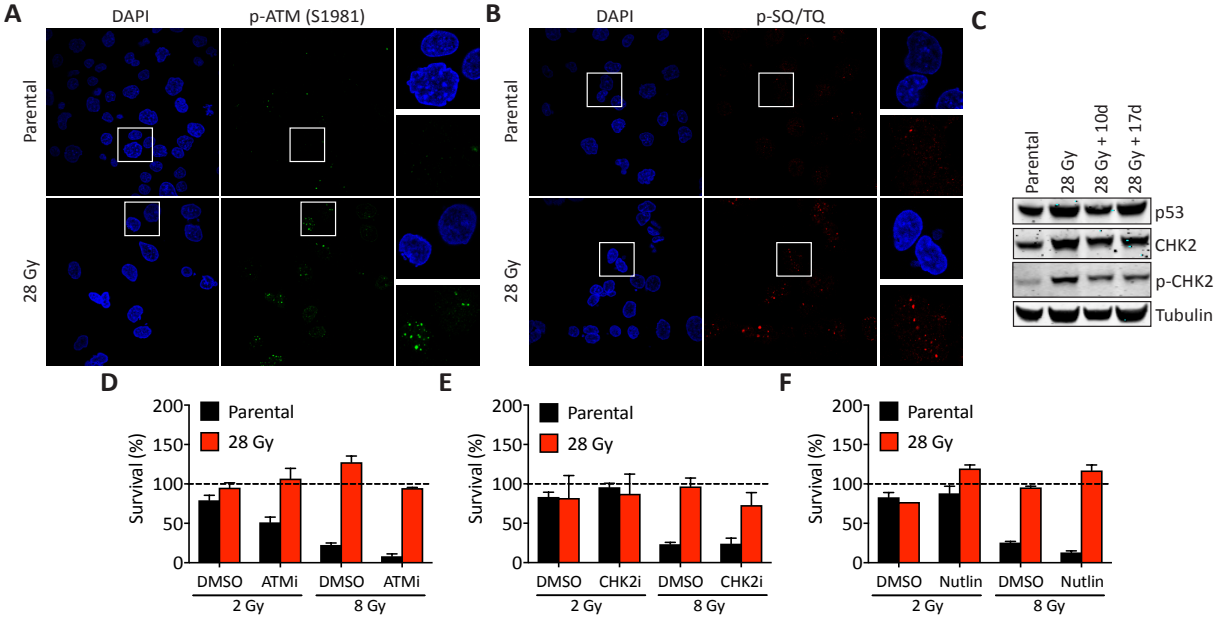

Figure 3: Activation of ATM and DSB repair during IR resistance. A) Immunofluorescent images of p-ATM (S1981; in green) in parental and RR cells. Images were taken at 63× magnification. DAPI was used to stain the nuclei. B) Immunofluorescent images of p-SQ/TQ (in red) in parental and RR cells. Images were taken at 63× magnification. DAPI was used to stain the nuclei. C) Immunoblot of whole cell extract of parental, IR resistant, IR holiday 10 days and IR holiday 17 days cells for p53, CHK2 and p-CHK2. Tubulin was used as loading control. D – F) Parental and RR cells were seeded for colony survival and pre-treated with ATM inhibitor KU55933 (D), CHK2 inhibitor (E) and P53 activator Nutlin (F) to assess IR resistance after inhibition of the DDR signalling pathway. Colonies formed in non-radiated wells were set 100% (dashed line). Every experiment was performed at least three times and mean ± SEM are depicted.

tested whether inhibition could sensitize RR cells. An IR colony survival with RR cells pre-treated with ATM inhibitor, CHK2 inhibitor or Nutlin (p53 activator) demonstrated that RR cells could not be sensitized to IR after treatment with either one of these inhibitors (Fig. 3D – F), indicating that ATM inhibition is not sufficient to abolish the observed resistance phenotype.

DSB repair is altered in RR cells

ATM is rapidly activated by DSBs (22). RR cells still exhibit ATM activation three days after receiving the last dose of 2 Gy, indicating the presence of more persistent DSBs. Note that RR cells that recovered for three days are able to proliferate at day three as seen in colony survival assays. We hypothesized that ATM activation in RR cells is due to more persistent DSBs. We measured the presence of DSBs using the marker γH2AX in combination with cell cycle marker geminin, which indicates whether cells are in G1 (geminin$^-$) or in S/G2 (geminin$^+$) phase of the cell cycle. This distinction is important, since we observed a larger fraction of RR cells in the G2-phase of the cell cycle. At baseline, RR cells that reside in the G1-phase exhibited a 8-fold increase in γH2AX foci when compared to parental cells. A 10-day recovery of RR cells, which were still resistant at this stage, also exhibited an increased number of γH2AX foci. Time re-sensitized cells that were allowed to recover for 17 days had similar levels of DSBs as compared to parental cells (Fig. 4A). We did not observe a difference in γH2AX foci between RR and parental cells, which resided in the S/G2-phase of the cell cycle (Fig. 4B). This indicates that DSBs in general or a subset of DSBs are poorly repaired during the G1-phase in RR cells.

A reduced DSB repair capacity or differences in repair kinetics can be visualized by how fast cells are able to resolve DSBs as seen by a reduction of γH2AX foci in time, which are induced by an additional dose of IR. We applied 2 Gy IR and observed γH2AX foci increase in both parental and RR cells 1h after IR (Fig. 4C + D and Supplementary Fig. 3A + B). The kinetics of resolving DSBs appeared to be slower in RR cells compared to parental cells between 4 and 24 hours after IR irrespective of geminin status, but more prominently in G1-phase cells (Fig. 4C + D). Moreover, RR cells in G1-phase still did not reach parental background γH2AX foci levels 24h after IR. In addition to γH2AX foci, we also measured 53BP1 foci, which is recruited by phosphorylated H2AX and directs DSB repair pathway choice towards NHEJ

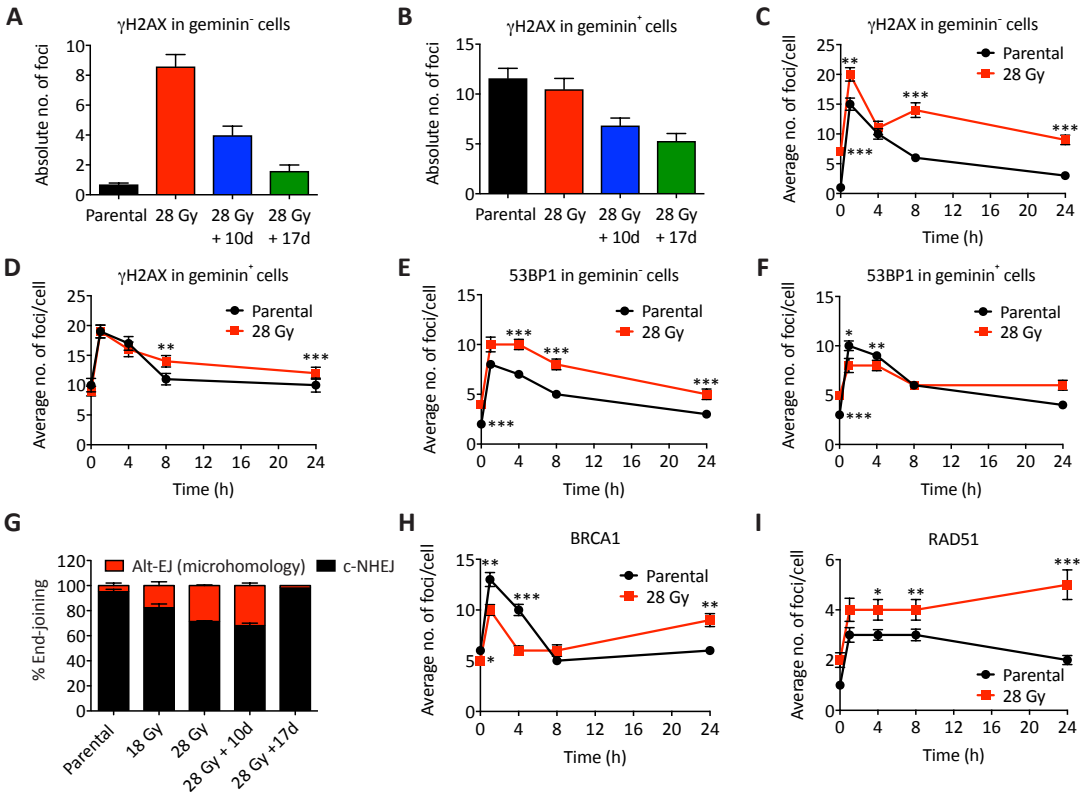

Figure 4: Clearance of DDR foci is slower in RR cells. A + B) Quantification of γH2AX foci in at least 25 nuclei/experiment of parental (black) and RR cells (red), time re-sensitized cells 10 days (blue) and time re-sensitized cells 17 days (green). Geminin was used to discriminate between G1 (A) and S/G2 phase cells (B). C + D) RR cells were radiated with 2 Gy and after indicated time points γH2AX foci in at least 25 nuclei/experiment of parental (black) and RR cells (red) were counted in G1 (C) or S/G2 phase cells (D). E + F) Quantification of 53BP1 foci in at least 25 nuclei/experiment of parental (black) and RR cells (red). Geminin was used to discriminate between G1 (E) and S/G2 phase cells (F). G) End joining assay was use to determine c-NHEJ (black) and microhomology (Red) efficiency in parental, partially resistant cells (18 Gy) RR cells (28 Gy) and time re-sensitized cells (28 Gy + 10d and 28 Gy + 17d). H) Absolute number of BRCA1 foci per geminin positive nucleus. At least 25 nuclei/experiment were counted for parental (black) and RR cells (red). I) Absolute number of RAD51 foci per geminin positive nucleus. At least 25 nuclei/experiment were counted for parental (black) and RR cells (red). Every experiment was performed at least three times and mean ± SEM are depicted. Unpaired two-sided Mann-Whitney test was performed to determine statistical significance, *P<0.05, **P<0.01, ***P<0.001.

(23). We already observed an increase in 53BP1 foci at basal level, indicating the presence of persistent DSBs in RR cells. Moreover, clearance of 53BP1 foci appeared to be slower in RR cells as well again more prominent in G1 (geminin-) cells (Fig. 4E + F). Thus, DSB repair capacity is altered in RR cells and a subset of difficult to repair DSBs are present during the G1-phase of RR cells.

Since NHEJ and Alt-EJ are the only DSB repair pathway active in the G1-phase, we determined NHEJ capacity using a plasmid-based assay (16). This NHEJ assay measures the repair ratio between canonical NHEJ (c-NHEJ) and Alt-EJ, in which the latter uses micro-homology to

repair DSBs. In partially resistant (18 Gy) and RR cells end-joining activity is shifted from c-NHEJ to Alt-EJ (Fig. 4G). Such a shift is usually seen when c-NHEJ is less functional (24). The observed Alt-EJ phenotype is reversed again in time re-sensitized RR cells. Therefore, RR cells preferentially use Alt-EJ or in combination with the observed increase in DSBs during the G1-phase in RR cells, c-NHEJ activity is reduced.

In case of reduced c-NHEJ capacity, it is expected that HR is more active to explain the IR resistance phenotype and the clearance of DSBs in S/G2. We performed foci analysis of HR proteins BRCA1 and RAD51 in geminin+ cells to select S/G2-phase cells. At baseline we did not observe any obvious differences in BRCA1 and RAD51 foci between parental and RR cells (Fig. 4I + J). After an additional dose of IR, BRCA1 and RAD51 foci are induced in both parental and RR cells (Fig. 4I + J). Interestingly, DSB repair by HR in the first hours appeared normal as seen by a reduction in foci. Remarkably, 24 hours after IR both BRCA1 and RAD51 foci are increased again up to, or even higher than, just irradiated RR cells. We interpret this observation, as a compensation mechanism by HR to repair DSBs that otherwise would have been resolved by NHEJ. Together, our data indicate that DSB repair pathways are differentially wired in RR cells in which c-NHEJ is reduced and/or Alt-EJ is increased after which HR compensates for total DSB repair capacity.

Interference with DNA repair together with ATM signalling sensitizes RR cells to IR

Since RR cells exhibited an altered end joining phenotype, we first targeted c-NHEJ using a DNA-PK inhibitor (25). Parental and RR cells were treated with DNA-PK inhibitor followed by IR sensitivity measurements. While parental cells were sensitive to DNA-PK inhibition, RR cells remained resistant (Fig. 5A). Next, we targeted Alt-EJ. Several proteins have been implicated in this pathway of which one is PARP (25, 26). Both parental and RR cells were pre-treated with the PARP inhibitor Olaparib and sensitivity was assessed. Again, parental cells were sensitized to IR, but RR cells maintained their resistance phenotype (Fig. 5B), indicating that inhibiting c-NHEJ or Alt-EJ is not sufficient to reverse RT resistance.

The unsuccessful attempts to sensitize RR cells by inhibition of ATM signalling, DNA-PK or PARP could be due to redundancy. Therefore, we performed combination treatments with aforementioned inhibitors. While the combination DNA-PK and PARP did not sensitize RR cells, either the ATM – PARP and the ATM – DNA-PK inhibitor combination led to increased RT sensitivity in RR cells (Fig. 5C – E), which suggests that IR resistance is dependent on at least two DSB repair and signalling sub-pathways in which PARP and DNA-PK belong to one epistasis group and ATM to another.

Discussion

Here we showed that RR cells are established relatively early during RT using a protocol that closely mimics patient RT treatment in the

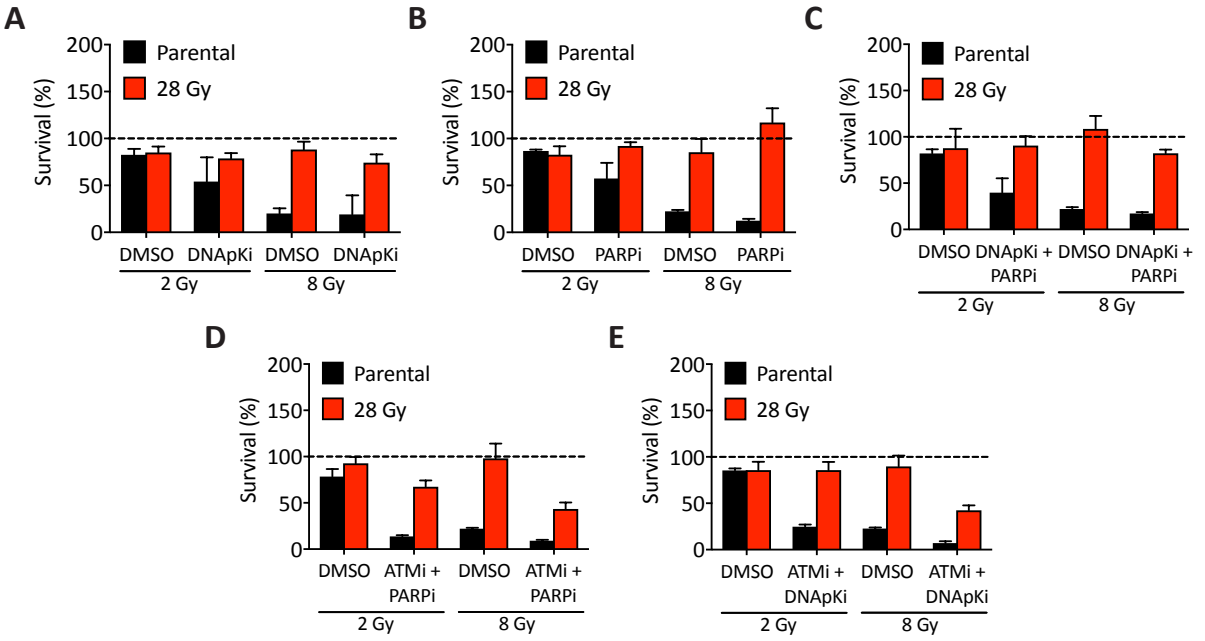

Figure 5: RR cells are sensitized to IR by dual inhibition of ATM with PARPi or DNApKi. A + B) Parental and RR cells were seeded for colony survival and pre-treated with DNApKi inhibitor NU7441 (A) and PARP inhibitor Olaparib (B) to assess IR resistance after inhibition of the DDR signalling pathway. Colonies formed in non-radiated wells were set 100% (dashed line). C – E) Parental and RR cells were seeded for colony survival and pre-treated with a combination of DNApKi inhibitor NU7441 and PARP inhibitor Olaparib (C), ATM inhibitor KU55933 and PARP inhibitor Olaparib (D) and ATM inhibitor KU55933 and DNApK inhibitor NU7441 (E) to assess IR resistance after inhibition of multiple components of the DDR signalling pathway. Colonies formed in non-radiated wells were set 100% (dashed line). Every experiment was performed at least three times and mean ± SEM are depicted.

clinic. IR resistance was maintained up to the end of RT treatment. Importantly, it could be reversed by an 'IR holiday', which demonstrates not only its dynamic, transient nature, but also suggests that an adjusted RT schedule could reduce therapy resistance and tumour relapse. Furthermore, we show that ATM is activated, RR cells remain longer in G2/M-phase and DSB repair by NHEJ is altered. Finally, we demonstrate that RT resistance is dependent on two epistasis groups of which ATM belongs to one, while PARP and DNA-PK to another. On the other hand, inhibition of ATR or the combination of ATR inhibition with either PARP inhibition or DNA-PK inhibition did not induce sensitivity (data not shown).

Our interpretation of the data provides evidence for a model in which repetitive exposure to IR reduces c-NHEJ capacity thereby relying on Alt-EJ. Alternatively, Alt-EJ activity is increased, which subsequently competes with c-NHEJ. The consequence of this alteration in DSB repair is an increased number of DSBs in the G1-phase of the cell cycle. During cell cycle progression, these DSBs activate a strong G2/M block, which allows a resistant cell time to repair unresolved DSBs. Paradoxically, our data points to a reduction in DSB repair rather than an improvement to establish a RT-resistant phenotype. Based on our intervention experiments we can implicate ATM function as essential

to maintain IR resistance and another branch consists of PARP and DNA-PK.

Since all three DDR molecules ATM, DNA-PK and PARP have multiple functions in DSB repair and signalling, their exact molecular mechanistic implication in radio-resistance is not yet clear. However, we can speculate that the inhibition of either ATM or DNA-PK affects the response to DSBs. Since they belong to the same family of PI3K-like protein kinases (PIKKs) together with ATR, it could be likely that their activity is increased to partially compensate for the missing member (27). That, in turn, can explain why single inhibition of ATM and DNA-PK does not sensitize RR cells to IR.

DSBs are recognized by PARP, which is involved in facilitating recruitment of MRE11 and NBS1 (which are part of the MRN complex that senses DSBs) (28-31). The MRN complex, especially NBS1, is required for ATM activation and subsequent downstream signalling and repair by HR (27, 32). Inhibition of PARP will therefore not abolish DNA repair, but delays the activation of downstream DDR proteins that need ATM phosphorylation for their activation (33). Simultaneously, ATM is dispensable for HR functioning, although HR will not be as efficient as normal (34). Therefore we postulate that PARP and ATM are redundant and that explains why single PARP or ATM inhibition in RR cells does not sensitize them to IR, whereas double inhibition of ATM and PARP does. Interestingly, *Atm/Parp1*$^{-/-}$ mice are embryonically lethal, suggesting that ATM and PARP are also important for normal cell development (PMID: 11238919).

A striking observation was the reduced repair of DSB in G1-phase of the cell cycle in RR cells. It is known that about 80% of IR-induced DSBs in G1-phase are repaired via c-NHEJ independent from ATM (35, 36). The remaining 20% of DSBs is localized close to, or reside in, highly condensed regions in heterochromatin (HC). Often these breaks are referred to as persistent or 'complex' breaks and need ATM signalling for repair (35). Under normal circumstances HC is condensed by factors such as KAP-1, HP1, HDAC1 and HDAC2 (37), thereby keeping the damaged DNA inaccessible for DNA repair proteins in the case of a DSB. ATM-dependent phosphorylation of KAP-1, which is mediated by 53BP1 (38-40), relaxes the compact chromatin structure and facilitate DNA repair. Following chromatin relaxation DNA repair factors like ARTEMIS and DNA-PK are required for DSB repair (36). Based on these observations we hypothesize that the observed persistent DSBs are located near or in HC regions in RR cells. Inhibition of both ATM and DNA-PK will disrupt downstream DSB signalling to other DNA repair factors, impairs c-NHEJ in G1-phase and in combination with less efficient HR due to ATM inhibition lead to lethal persistent DSBs. This hypothesis could explain the observed redundancy between ATM and PARP and ATM and DNA-PK. However, more in depth characterization of DSB repair and signalling in RR cells is required.

In summary, we showed that a transient IR resistance phenotype is acquired early during RT treatment, which can be reversed by an IR holiday. We have outlined a mechanistic basis for the observed radio-resistance induced by repetitive RT using a regimen identical to the clinic. This new paradigm in radio-resistance states that DSB repair is in part

attenuated instead of increased to establish resistance. Further dissection of the transient rewiring of DSB repair and signalling pathways in RT-resistant cancers can lead to the development of novel combination therapies to sensitize tumours and improve cancer therapy outcome.

Acknowledgements

The authors would like to thank members of the Molecular Genetics department en the Experimental Urology department of the Erasmus Medical Center Rotterdam for their contributions to the manuscript. This research was supported by Dutch Cancer Society (KWF) grant nr. 2011-5030.

Disclosure

The authors declare no conflict of interest.

References

1. Torre LA, Bray F, Siegel RL, Ferlay J, Lortet-Tieulent J, Jemal A. Global cancer statistics, 2012. CA: a cancer journal for clinicians. 2015;65(2):87-108.
2. Heidenreich A, Bastian PJ, Bellmunt J, Bolla M, Joniau S, van der Kwast T, et al. EAU guidelines on prostate cancer. part 1: screening, diagnosis, and local treatment with curative intent-update 2013. European urology. 2014;65(1):124-37.
3. Fitch DL, McGrath S, Martinez AA, Vicini FA, Kestin LL. Unification of a common biochemical failure definition for prostate cancer treated with brachytherapy or external beam radiotherapy with or without androgen deprivation. International journal of radiation oncology, biology, physics. 2006;66(5):1430-9.
4. Fitzgerald TJ, Wang T, Goel HL, Huang J, Stein G, Lian J, et al. Prostate carcinoma and radiation therapy: therapeutic treatment resistance and strategies for targeted therapeutic intervention. Expert review of anticancer therapy. 2008;8(6):967-74.
5. Kyjacova L, Hubackova S, Krejcikova K, Strauss R, Hanzlikova H, Dzijak R, et al. Radiotherapy-induced plasticity of prostate cancer mobilizes stem-like non-adherent, Erk signaling-dependent cells. Cell death and differentiation. 2015;22(6):898-911.
6. Chang L, Graham PH, Hao J, Ni J, Bucci J, Cozzi PJ, et al. PI3K/Akt/mTOR pathway inhibitors enhance radiosensitivity in radioresistant prostate cancer cells through inducing apoptosis, reducing autophagy, suppressing NHEJ and HR repair pathways. Cell death & disease. 2014;5:e1437.
7. Josson S, Xu Y, Fang F, Dhar SK, St Clair DK, St Clair WH. RelB regulates manganese superoxide dismutase gene and resistance to ionizing radiation of prostate cancer cells. Oncogene. 2006;25(10):1554-9.
8. Kong Z, Xie D, Boike T, Raghavan P, Burma S, Chen DJ, et al. Downregulation of human DAB2IP gene expression in prostate cancer cells results in resistance to ionizing radiation. Cancer research. 2010;70(7):2829-39.
9. Ni J, Cozzi P, Hao J, Beretov J, Chang L, Duan W, et al. Epithelial cell adhesion molecule (EpCAM) is associated with prostate cancer metastasis and chemo/radioresistance via the PI3K/Akt/mTOR signaling pathway. The international journal of biochemistry & cell biology. 2013;45(12):2736-48.
10. Ward JF. DNA damage produced by ionizing radiation in mammalian cells: identities, mechanisms of formation, and reparability. Progress in nucleic acid research and molecular biology. 1988;35:95-125.
11. Hoeijmakers JH. Genome maintenance mechanisms for preventing cancer. Nature. 2001;411(6835):366-74.
12. ackson SP, Bartek J. The DNA-damage response in human biology and disease. Nature. 2009;461(7267):1071-8.
13. Seol JH, Shim EY, Lee SE. Microhomology-mediated end joining: Good, bad

and ugly. Mutation research. 2017.
14. Schmid I, Uittenbogaart C, Jamieson BD. Live-cell assay for detection of apoptosis by dual-laser flow cytometry using Hoechst 33342 and 7-amino-actinomycin D. Nature protocols. 2007;2(1):187-90.
15. Livak KJ, Schmittgen TD. Analysis of relative gene expression data using real-time quantitative PCR and the 2(-Delta Delta C(T)) Method. Methods. 2001;25(4):402-8.
16. Verkaik NS, Esveldt-van Lange RE, van Heemst D, Bruggenwirth HT, Hoeijmakers JH, Zdzienicka MZ, et al. Different types of V(D)J recombination and end-joining defects in DNA double-strand break repair mutant mammalian cells. European journal of immunology. 2002;32(3):701-9.
17. van Gent DC, Ramsden DA, Gellert M. The RAG1 and RAG2 proteins establish the 12/23 rule in V(D)J recombination. Cell. 1996;85(1):107-13.
18. Sharma SV, Lee DY, Li B, Quinlan MP, Takahashi F, Maheswaran S, et al. A chromatin-mediated reversible drug-tolerant state in cancer cell subpopulations. Cell. 2010;141(1):69-80.
19. Davalos AR, Kawahara M, Malhotra GK, Schaum N, Huang J, Ved U, et al. p53-dependent release of Alarmin HMGB1 is a central mediator of senescent phenotypes. The Journal of cell biology. 2013;201(4):613-29.
20. Kim ST, Lim DS, Canman CE, Kastan MB. Substrate specificities and identification of putative substrates of ATM kinase family members. The Journal of biological chemistry. 1999;274(53):37538-43.
21. O'Neill T, Dwyer AJ, Ziv Y, Chan DW, Lees-Miller SP, Abraham RH, et al. Utilization of oriented peptide libraries to identify substrate motifs selected by ATM. The Journal of biological chemistry. 2000;275(30):22719-27.
22. Marechal A, Zou L. DNA damage sensing by the ATM and ATR kinases. Cold Spring Harbor perspectives in biology. 2013;5(9).
23. Brandsma I, Gent DC. Pathway choice in DNA double strand break repair: observations of a balancing act. Genome integrity. 2012;3(1):9.
24. Iliakis G, Murmann T, Soni A. Alternative end-joining repair pathways are the ultimate backup for abrogated classical non-homologous end-joining and homologous recombination repair: Implications for the formation of chromosome translocations. Mutation research Genetic toxicology and environmental mutagenesis. 2015;793:166-75.
25. Mladenov E, Iliakis G. Induction and repair of DNA double strand breaks: the increasing spectrum of non-homologous end joining pathways. Mutation research. 2011;711(1-2):61-72.
26. Wang M, Wu W, Wu W, Rosidi B, Zhang L, Wang H, et al. PARP-1 and Ku compete for repair of DNA double strand breaks by distinct NHEJ pathways. Nucleic acids research. 2006;34(21):6170-82.
27. Shiloh Y, Ziv Y. The ATM protein kinase: regulating the cellular response to genotoxic stress, and more. Nature reviews Molecular cell biology. 2013;14(4):197-210.
28. Sukhanova MV, Abrakhi S, Joshi V, Pastre D, Kutuzov MM, Anarbaev RO, et al. Single molecule detection of PARP1 and PARP2 interaction with DNA strand breaks and their poly(ADP-ribosyl)ation using high-resolution AFM imaging. Nucleic acids research. 2016;44(6):e60.
29. Langelier MF, Pascal JM. PARP-1 mechanism for coupling DNA damage detection to poly(ADP-ribose) synthesis. Current opinion in structural biology. 2013;23(1):134-43.
30. Ali AAE, Timinszky G, Arribas-Bosacoma R, Kozlowski M, Hassa PO, Hassler M, et al. The zinc-finger domains of PARP1 cooperate to recognize DNA strand breaks. Nature structural & molecular biology. 2012;19(7):685-92.
31. Haince JF, McDonald D, Rodrigue A, Dery U, Masson JY, Hendzel MJ, et al. PARP1-dependent kinetics of recruitment of MRE11 and NBS1 proteins to multiple DNA damage sites. The Journal of biological chemistry. 2008;283(2):1197-208.
32. Lee JH, Paull TT. Direct activation of the ATM protein kinase by the Mre11/Rad50/Nbs1 complex. Science. 2004;304(5667):93-6.
33. Haince JF, Kozlov S, Dawson VL, Dawson TM, Hendzel MJ, Lavin MF, et al. Ataxia telangiectasia mutated (ATM) signaling network is modulated by a novel poly(ADP-ribose)-dependent pathway in the early response to DNA-damaging agents. The Journal of biological chemistry. 2007;282(22):16441-53.
34. Blackford AN, Jackson SP. ATM, ATR, and DNA-PK: The Trinity at the Heart of the DNA Damage Response. Molecular cell. 2017;66(6):801-17.
35. Goodarzi AA, Noon AT, Deckbar D, Ziv Y, Shiloh Y,

Lobrich M, et al. ATM signaling facilitates repair of DNA double-strand breaks associated with heterochromatin. Molecular cell. 2008;31(2):167-77.
36. Riballo E, Kuhne M, Rief N, Doherty A, Smith GC, Recio MJ, et al. A pathway of double-strand break rejoining dependent upon ATM, Artemis, and proteins locating to gamma-H2AX foci. Molecular cell. 2004;16(5):715-24.
37. Goodarzi AA, Jeggo P, Lobrich M. The influence of heterochromatin on DNA double strand break repair: Getting the strong, silent type to relax. DNA repair. 2010;9(12):1273-82.
38. Noon AT, Shibata A, Rief N, Lobrich M, Stewart GS, Jeggo PA, et al. 53BP1-dependent robust localized KAP-1 phosphorylation is essential for heterochromatic DNA double-strand break repair. Nature cell biology. 2010;12(2):177-84.
39. Lee JH, Goodarzi AA, Jeggo PA, Paull TT. 53BP1 promotes ATM activity through direct interactions with the MRN complex. The EMBO journal. 2010;29(3):574-85.
40. Ziv Y, Bielopolski D, Galanty Y, Lukas C, Taya Y, Schultz DC, et al. Chromatin relaxation in response to DNA double-strand breaks is modulated by a novel ATM- and KAP-1 dependent pathway. Nature cell biology. 2006;8(8):870-6.

Supplemental information

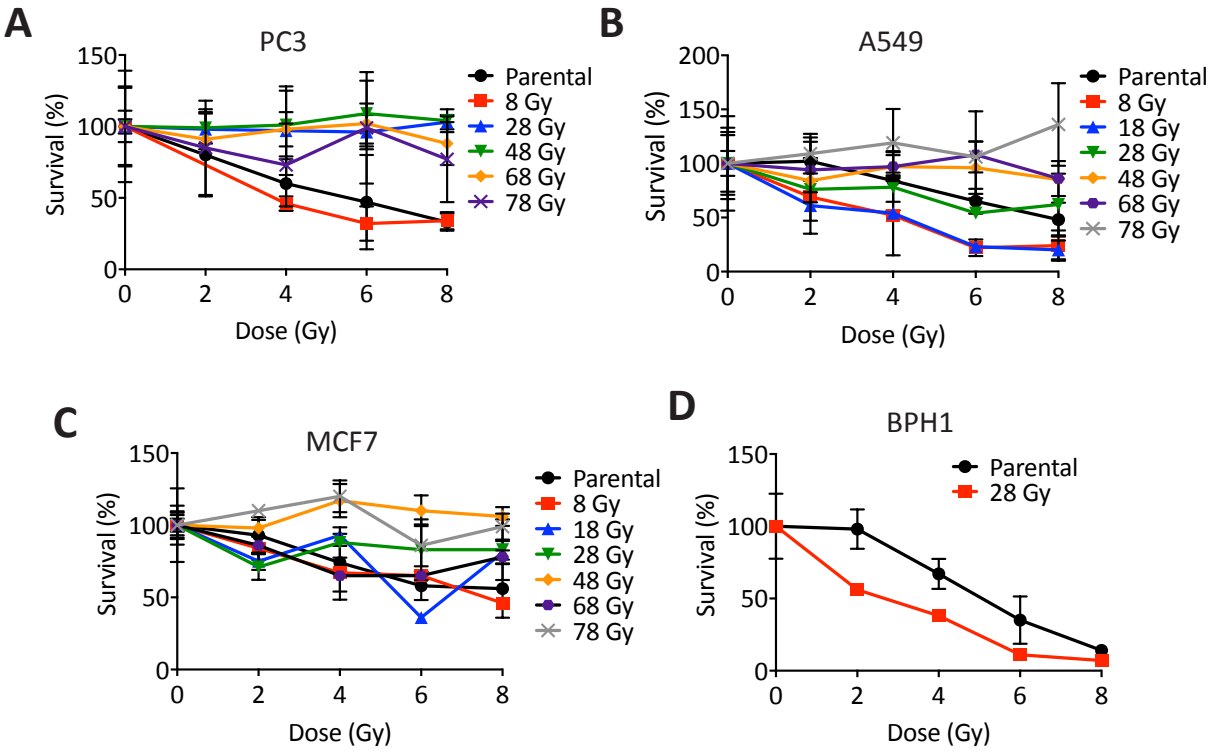

Supplementary Figure 1: IR-resistant phenotype is not restricted to Du145 only. A + B + C) PC3, A549 and MCF7 cells received the same IR treatment as Du145. IR resistance was assessed using colony survival. D) BPH-1 cells were treated like Du145, PC3, A549 and MCF7 up to 28 Gy. IR resistance was addressed using colony survival. Every experiment was repeated at least three times. Mean ± SEM are depicted.

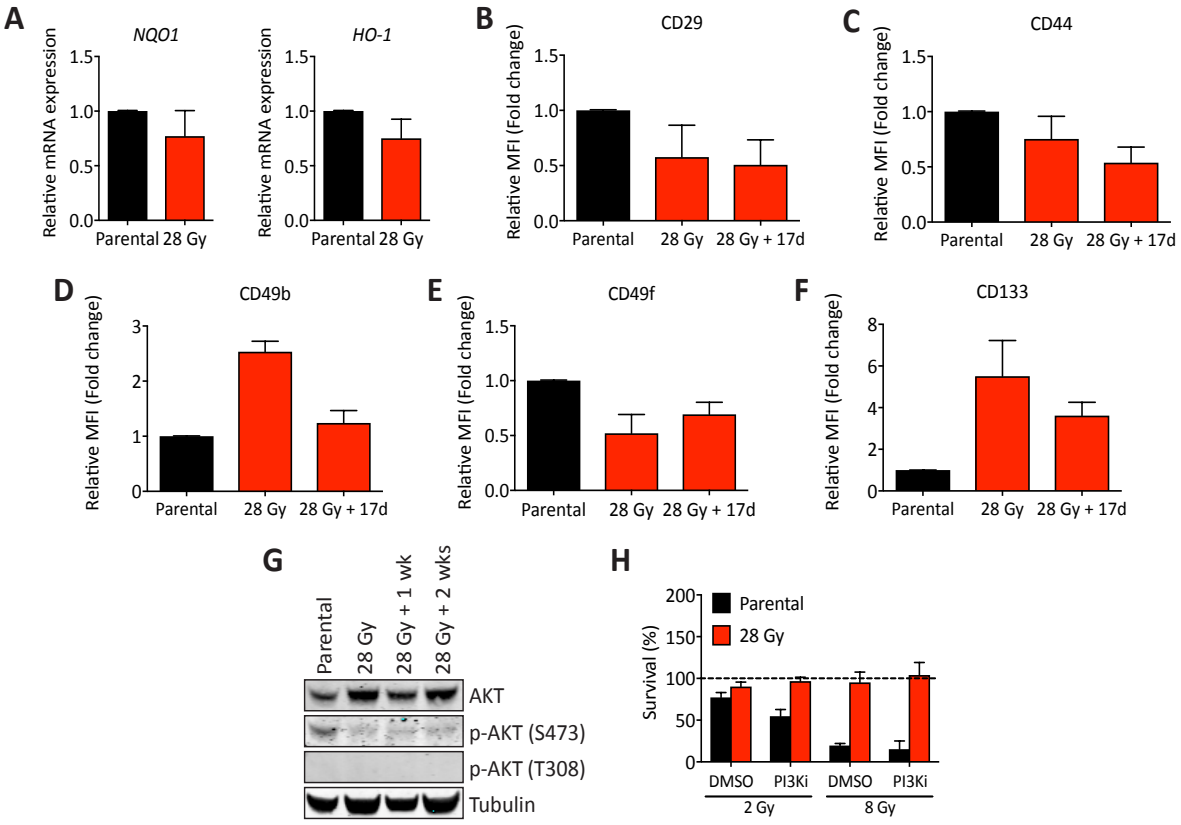

Supplementary Figure 2: Known resistance mechanisms are not altered in RR cells. A) mRNA levels of *NQO1* and *HO-1* were determined by qPCR. B – F) Parental and RR cells were stained for prostate CSC markers CD29 (B), CD44 (C), CD49b (D), CD49f (E) and CD133 (F) and expression was addressed using flow cytometry. G) Immunoblot for AKT, p-AKT (S473), p-AKT (T308) and Tubulin. WCE were isolated from parental, RR cells, time re-sensitized cells 10 days and time re-sensitized cells 17 days. H) RR cells were pre-treated with 50 μM of PI3K inhibitor LY294002 and colony survival was performed to address IR sensitivity upon PI3K inhibitor treatment. Colonies formed in non-radiated wells were set 100% (dashed line). Every experiment was repeated at least three times. Mean ± SEM are depicted.

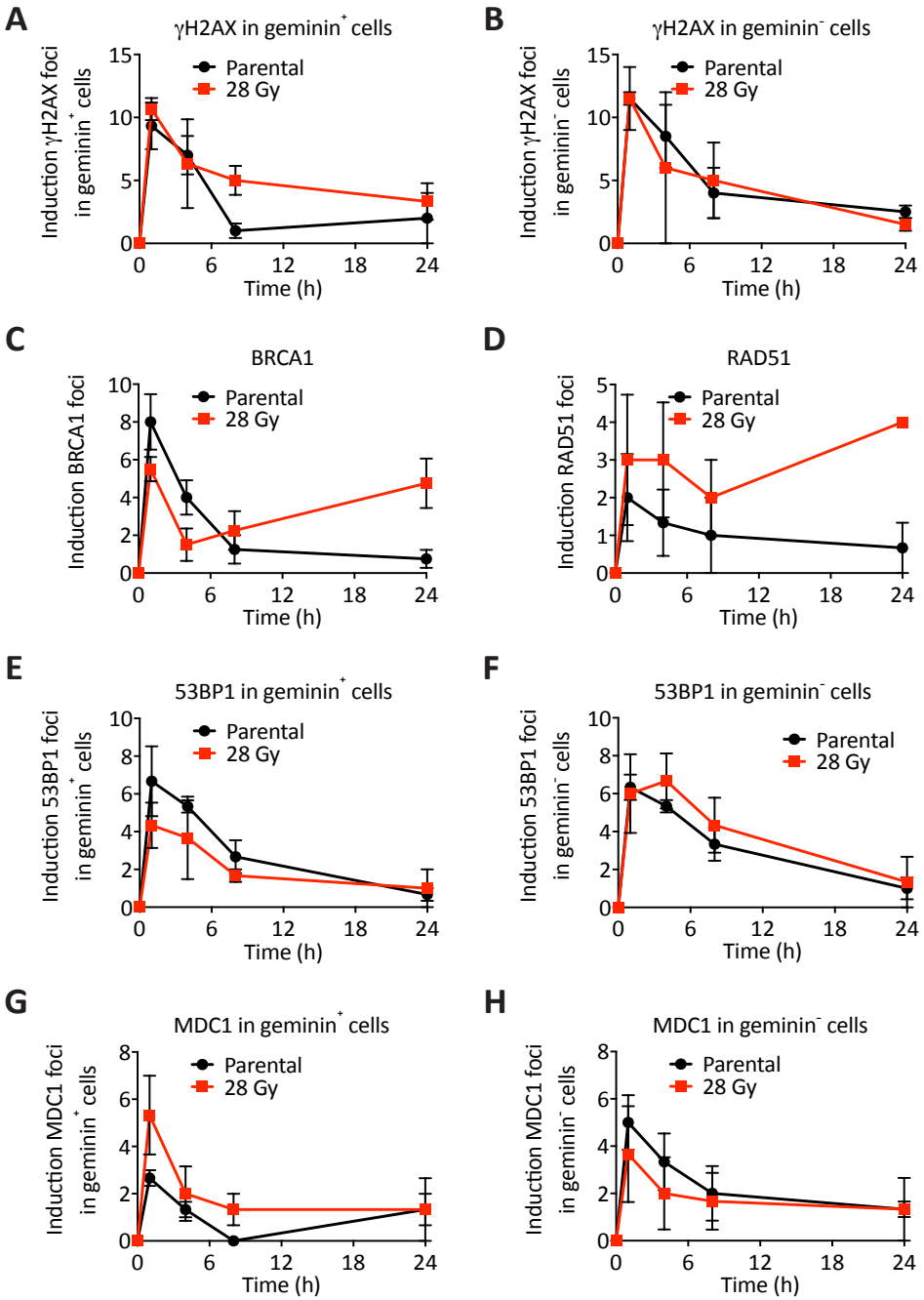

Supplementary Figure 3: DNA damage foci are induced in parental and RR cells. A + B) Absolute number of number of γH2AX foci per geminin negative (A) and positive (B) nucleus per time point were counted and averaged per experiment. At least 25 nuclei per experiment were quantified per time point in parental and RR cells. C + D) Absolute number of number of BRCA1 (C) and RAD51 (D) foci per geminin positive nucleus per time point were counted and averaged per experiment. At least 25 nuclei per experiment were quantified per time point in parental and RR cells. (E – H) Absolute number of number of 53BP1 and MDC1 foci per geminin negative (G + H) and positive (E + F) nucleus per time point were counted and averaged per experiment. At least 25 nuclei per experiment were quantified per time point in parental and RR cells. Every experiment was performed at least three times and mean ± SEM are depicted.

Chapter 3

Increased metabolic activity contributes to acquired radio-resistance

Serena Bruens[1], Jiang Chang[1], Chiara Milanese[1], Akos Gyenis[1,2], Kasper Derks[1], Marjolijn Ladan[1], Pier Mastroberardino[1], Wytkse van Weerden[3], Guido Jenster[3], Jan Hoeijmakers[1,3,4], Joris Pothof[1]*

[1] Department of Molecular Genetics, Erasmus Medical Center, Rotterdam, The Netherlands
[2] CECAD Research Center, University of Cologne, Cologne, Germany
[3] Department of Urology, Erasmus Medical Center, Rotterdam, The Netherlands
[4] Princess Maxima Center for Pediatric Oncology, Utrecht, The Netherlands

* Corresponding author: j.pothof@erasmusmc.nl

To be submitted

Abstract

Non-metastasized prostate cancer is usually resected by surgery followed by radiotherapy. In a substantial number of patients, resection is not possible and curative treatment solely relies on radiotherapy. Unfortunately, about 12% of prostate cancer patients experience relapse or metastasis. These recurrent or metastasized tumours can acquire resistance to the initial radiotherapy treatment, which is a significant problem for patient recovery and survival. To address this problem, we generated transient radio-resistant cancer cells using a radiotherapy regimen identical to the clinic. These transient therapy-resistant cancer cells can be re-sensitized by withholding radiotherapy for 17 days. To identify novel processes in acquired radio-resistant prostate cancer, we defined four distinct experimental groups, I) parental cells, II) radio-resistant cells, III) radio-resistant cells followed by 10 days without IR and IV) radio-resistant cells followed by 17 days with out IR, which exhibit radio-sensitivity again. These experimental groups were used for mRNA sequencing. We performed expression signature recognition analysis to identify processes potentially involved in radio-resistance and identified mitochondrial respiration. Experimental validation demonstrated normal glycolysis levels, but a dramatic increase in mitochondrial respiration in radio-resistant cells. Furthermore, ATP and NAD+ levels were increased, which also points to increased mitochondrial respiration. Finally, we found that shifting the bio-energetic profile of parental (radio-sensitive) prostate cancer cells from glycolysis to mitochondrial respiration by 2-deoxyglucose led to increased radio-resistance. Thus, the data show that increased metabolic respiration contributes to acquired radio-resistance in prostate cancer, providing a new target for radiotherapy sensitization.

Introduction

Non-metastasized solid tumours are treated via a multi-step approach to reduce the chance of relapse and metastasis. In general, the tumour is resected, which is often followed by radiotherapy and/or chemotherapy. Examples of radiotherapy (RT) are external beam radiotherapy (EBRT), internal RT, brachytherapy and radionuclide therapy (1, 2). EBRT, internal RT and brachytherapy could be selected for first line treatment in prostate cancer, which is the second most common cancer in men worldwide (3). Unfortunately, about 12% of patients have clinical failure (CF) within the first five years after treatment. CF even increases up to 26% after ten years (4). The recurrent or metastasized tumours in the majority of these patients are resistant to RT, resulting in decreased patient survival (5, 6). RT induces different types of DNA damage of which double-strand DNA breaks (DSBs) are the most deleterious to the cell (7). When not properly repaired, DSBs lead to apoptosis or cellular senescence (8). Although most cancer cells are initially sensitive to RT, cancer cells can develop RT resistance, which may lead to relapse and metastasis. This process is known as acquired resistance.

Currently, protocols used to generate RT-resistant cells vary widely between studies. Therefore, we generated RT-resistant cells using a clinically relevant treatment protocol in which we treated prostate cancer cells with 2 Gy per day for 5 days followed by 2 days of rest up to a cumulative dose of 78 Gy (9). RT resistance is already fully present after a cumulative dose of 28 Gy (10). When these RT-resistant cells were subjected to an 'IR holiday', in which the cells did not receive treatment for a certain time period after the final IR dose, the resistant phenotype was reversed (10).

Several mechanisms have been described by which acquired RT resistance is induced. One example is the induction of cancer stem cells (CSC) or tumour-initiating cells (TIC), which are characterized by their ability to self-renew and to restore tumour growth (11-13). In addition, several signalling pathways have been identified to contribute to RT resistance such as the epidermal growth factor receptor (EGFR) pathway (14, 15). Another example of a signalling pathway is the PI3K/AKT pathway, which could be activated directly by IR or by the EGFR pathway during RT (16). The activation of the PI3K/AKT/mTOR pathway in radio-resistant cancer cells is associated with CSC phenotypes as well as epithelial-to-mesenchymal transition (6, 17-19). The inhibition of the PI3K/AKT/mTOR pathway also led to the sensitisation of radio-resistant prostate cancer cells to radiation. Many of these studies however, use different protocols to generate RT-resistant cells. Our approach to generate RT-resistant prostate cancer cells based on a clinically relevant protocol indicated that CSC and the PI3K pathway are not involved in RT resistance in prostate cancer (10). Since RT induces DSBs, we speculated that the transient alterations in DSB repair and/or signalling were involved in the acquired RT resistance phenotype. Indeed, we showed that the DNA damage response (DDR) is affected in acquired RT resistance (10).

In addition to alterations in DSB repair and signalling, supplementary processes could be involved in acquired RT resistance or act in conjunction with the observed alterations in DSB repair and signalling. To identify these new processes in acquired radio-resistance we designed RT-resistant and -sensitive experimental groups based on IR treatment and IR holiday followed by mRNA sequencing. Overrepresented pathway analysis identified energy metabolism, which we verified via bio-energetic measurements. Moreover, adjusting the bio-energetic profile of parental cancer cells induced RT resistance, indicating the validity of this approach.

Materials & Methods

Cell culture

Du145 prostate cancer cells (20) were cultured in RPMI-1640 (RPMI-1640 Medium, R2405-500ML, Sigma-Aldrich) supplemented with penicillin-streptomycin (100× diluted, Penicillin-Streptomycin, P0781-100ML, Sigma-Aldrich) and 10 % foetal bovine serum (Foetal Bovine Serum (FBS) South America, S1810-500, Biowest) at 5% CO2 and 37°C.

Generation of radio-resistant Du145

Du145 were seeded in 6-well plates and maintained as described. The day after seeding all cell lines were radiated (Gammacell 40 Cesium 137 irradiation unit, Atomic Energy) with 2 Gy/day (from Monday-Friday; Saturday-Sunday no IR) up to 28 Gy of cumulative dose, comparable to clinical radiation regimen (9). After cells obtained the indicated dosage of IR (see Figure 1A), they were not radiated for two days. On the third day after the last dose experiments were done. For "IR holiday" the cells were analysed after 10 days and 17 days after the last dose of IR.

Clonogenic cell survival assay

Cells were trypsinised (Trypsin-EDTA solution, T3924-500ML, Sigma-Aldrich) and counted (Z2 Coulterparticle count and size analyzer, Beckman Coulter). 600 cells per well in triplicates per condition were seeded in 6-well plates. The next day, cells were irradiated with IR (0-2-4-6-8 Gy). Cells were then incubated for 8-9 days and washed once with PBS followed by 0.1% Coomassie Brilliant Blue staining (50% (v/v) Methanol, 43% (v/v) H2O, 7% (v/v) Acetic Acid, 0.1% (m/v) Coomassie Brilliant Blue). Colonies were counted using Gelcount (Oxford Optronix). Clonogenic survivals with 2-Deoxy-Glucose (2-DG) were performed as described above, with the addition of 5 mM 2-DG (D6134-1G, Sigma Aldrich, 1 M stock; 5 mM final) at least 15 minutes prior to IR dosages.

mRNA sequencing

Total RNA was isolated using the miRNeasy Mini Kit (217004, Qiagen) according to the manufacturer's protocol. RNA quality was assed using capillary gel electrophoresis (RIN >7.6) (Bioanalyzer 2100, Agilent Technologies). The resulting 50-bp single-ended sequencing files were aligned to the human reference genome (hg19) using Tophat (21) with the –g 1 option. The resulting aligned reads were then analysed by Cufflinks (22). FPKM (fragments per kilo base of exon per million fragments mapped) was applied to quantify the expression of each transcript. To identify differentially expression genes, the average transcripts level was calculated for each set (three 3 time points damage-induced experiments). Lowly expressed transcripts were removed from analysis (cut-off: at least 10 reads in each sample). Differentially expressed genes were identified with cuffdiff, with the cut-off of Log2 fold-change > 1.5 and FDR < 0.05. The statistics plots (i.e. Principal component analysis, Pearson's correlation, heatmap) were created by Rstudio (v0.99.486) (RStudio Team (2015). RStudio: Integrated Development for R. RStudio, Inc., Boston, MA URL http://www.rstudio.com/). Short Time-series Expression Miner (STEM) was used to perform clustering analysis (23). The data was summarized and visualized by Graphpad Prism. (One-way ANOVA with Dunnett's posttest was performed using GraphPad Prism version 7.00 for Windows, GraphPad Software, San Diego California USA, www.graphpad.com). The functional analysis was performed in Ingenuity Pathway Analysis (IPA) (version 36601845, QIAGEN Redwood City, www.qiagen.com/ingenuity)

for canonical pathway, molecular function and upstream regulator analysis.

Bio-energetic profiling

The Seahorse XF24 Extracellular Flux Analyzer (Seahorse Biosciences) was used to generate bio-energetic profiles of irradiated Du145 cells by simultaneous measure of oxygen consumption rates (OCR) and glycolysis (ECAR; extracellular acidification rate) in real time (Ambrosi 2014). Cells were seeded on a cell-tak coated Seahorse XF-24 plate (3.5 µg/cm2; BD biosciences) at a density of 50,000 cells and incubated 30 minutes at 37° C in presence of CO2 in un-buffered DMEM (XF Assay Medium; Agilent Technologies, Santa Clara, Ca, USA) supplemented with 5 mM glucose and 1 mM pyruvate. Medium was adjusted to pH 7.4 prior to use. The plate was additionally incubated 30 minutes at 37° C in absence of CO2 and then moved to the Seahorse machine for the analysis. After four baseline measurements of OCR and ECAR levels, cells were challenged with sequential injections of mitochondrial toxins: 0.5 µM oligomycin (ATP synthase inhibitor), 0.3 µM FCCP (mitochondrial respiration uncoupler), 0.5 µM rotenone (complex I inhibitor), and 0.5 µM antimycin (complex III inhibitor); 3 measurements per injection were performed.

Acetyl CoA, Citrate, NADP(H) and NAD(H) assay

Acetyl CoA (Acetyl-Coenzyme A Assay Kit, MAK039-1KT, Sigma-Aldrich), Citrate (Citrate Assay Kit, MAK057-1KT, Sigma-Aldrich), NADP(H) (NADP/NADPH Quantitation Kit, MAK038-1KT, Sigma-Aldrich) and NAD(H) (NAD/NADH Quantitation Kit, MAK-037-1KT, Sigma-Aldrich) concentrations were determined using their respective kits according to the manufacturer's protocol.

Statistical analysis

Data was processed using GraphPad Prism v7.0a (GraphPad Software Inc.). Statistical test used were unpaired and paired Student's T-test and Mann-Whitney U test. P-values equal or lower than 0.05 were accepted as significant.

Results

Repetitive IR treatment leads to IR resistance, which is reversed by IR holiday

To identify pathways involved in IR resistance by mRNA sequencing we designed 4 experimental groups of which one group is the IR-sensitive Du145 parental prostate cancer cell line. We obtained radio-resistant (RR) cells according to the protocol shown in Fig. 1A (10). Prostate cancer cells received 2 Gy/day on weekdays and no radiation during weekends. Once a total dose of 28 Gy was reached, one group was incubated over the weekend (3 days); one group was incubated for 10 days and one group for 17 days without RT. First, IR sensitivity/resistance of these experimental groups was tested. Compared to parental cells, RR cells (3 days) and RR cells that were cultured for 10 days without RT exhibited resistance, while 17 day-incubated RR cells without RT treatment (IR holiday) were re-sensitized (Fig. 1B). Thus, our

experimental design for mRNA sequencing includes two IR-sensitive groups (parental cell line and RR cells with 17 day IR holiday) and two IR-resistant groups (RR cells with 3 and 10 day incubation). This experimental set up allows us to correlate IR resistance/sensitivity to gene expression patterns.

Subsequently, total RNA was isolated for mRNA sequencing (Fig. 1C). Raw data with an average of approximately 25.6 million reads per sample were aligned to the human reference genome of which more than 90% could be uniquely mapped (Fig. 1D). A Pearson correlation analysis shows a high similarity between all conditions (Supplementary Fig. 1), indicating that IR treatment and IR holiday do not induce large numbers of differential expressed genes (DEGs) nor the presence of substantial technical variation. Next, we identified DEGs by comparing the treated experimental groups to the sensitive parental cell line. Transcripts with at least 2.8 fold difference (log2 fold change (FC) of >1.5 and <-1.5; false discovery rate (FDR)<0.05) were classified as DEGs. We observed large numbers of DEGs and overlapping genes in radiated samples over time (Fig. 1E). Genes overlapping across all three conditions correlated with a persistent DNA damage response, while genes that overlap between 28 Gy and 28 Gy + 10 days correlated with an IR resistance response.

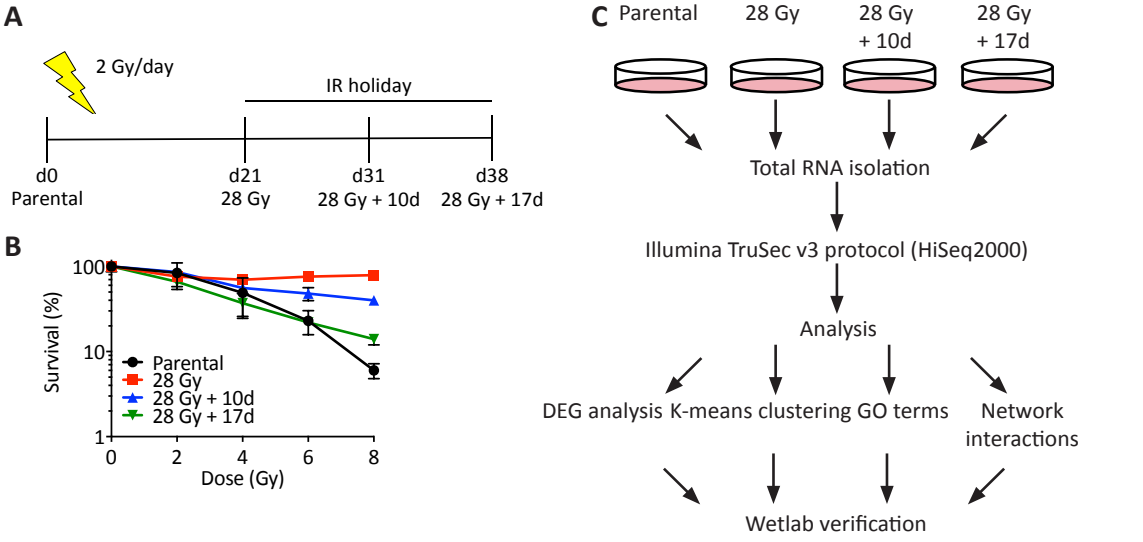

D

Sample	Total reads	Mapped reads	Mapping rate
Parental #1	28689673	26709229	93.10%
Parental #2	31584077	29708845	94.06%
Parental #3	24467539	22857976	93.42%
28 Gy #1	21686343	20158618	92.96%
28 Gy #2	26590935	24870148	93.53%
28 Gy #3	24287935	22471422	92.52%
28 Gy + 10d #1	31226765	29128873	93.28%
28 Gy + 10d #2	25101521	23196103	92.41%
28 Gy + 10d #3	28560201	26713718	93.53%
28 Gy + 17d #1	31880350	29279703	91.84%
28 Gy + 17d #2	28558054	26460559	92.66%
28 Gy + 17d #3	28470707	26385342	92.68%

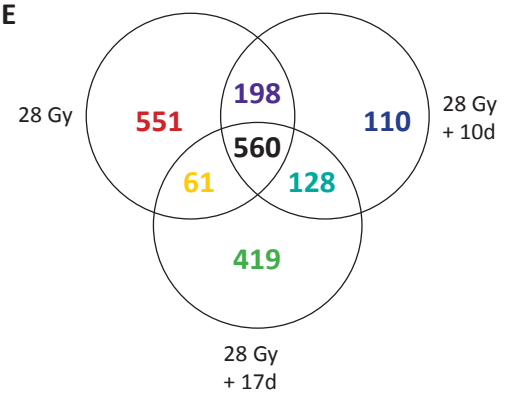

Figure 1: Generation of RR cells and subsequent NGS sequencing. A) Radiation protocol for the generation of RR cells and time re-sensitized cells. B) Colony survival assay of RR cells and time re-sensitized cells. RR cells are resistant to additional IR and time re-sensitized cells have a similar survival curve as parental cells. C) Workflow sequencing different RT-resistant populations. Of each population 3 independent RNA samples were collected, total RNA isolated and run via Illumina TruSec v3 protocol. The data generated was analysed using different analysis programs. The outcomes of these analyses have been verified by experimental approaches. D) Mapping rate of all samples run. All samples have a mapping rate of at least 90%. E) Venn diagram of DEGs between different populations, which were normalized to parental cells. The diagram shows subsets of uniquely regulated genes and overlapping genes between the different populations. All experiments were performed at least three times.

Gene clusters analysis reveals involvement of energy metabolism in RT resistance

Since we have one experimental group without IR treatment and three experimental groups that were exposed to 28 Gy, we are able to isolate DEGs that correlate with a persisting response after IR treatment. Similarly, we have two IR- sensitive and two IR-resistant groups, which allows us to detect DEGs that correlate with IR sensitivity/resistance. Because our data represents a time series, we used Short Time-series Expression Miner (STEM) to perform gene expression profile clustering. STEM analysis allows identification of significant temporal expression profiles in genes associated with these profiles and the comparison of the behaviour of these genes across multiple conditions (23). To prevent underrepresentation of significant gene expression patterns, total DEGs were used to analyse significant gene expression patterns instead of the overlapping genes from the Venn diagram (Fig. 1E). Gene expression patterns of interest were designated as persistent or resistant patterns. Indeed, we identified significant persistent up- and down-regulated DEG patterns (Fig. 2A). Using Ingenuity pathway analysis (IPA), we analysed up- and down-regulated persistent patterns separately, which showed enrichment of cell cycle related pathways and ATM signalling in the up-regulated DEGs and pathways related to senescence and apoptosis such as HMGB1 signalling and Myc-mediated apoptosis in the down-regulated DEGs (Fig. 2C + Supplementary Fig. 2B). In addition, we applied a gene ontology term (GO term) analysis that implicated several processes in the persistent response to IR treatment (Supplementary Fig. 3A + B). Thus, repeated IR treatment leads to long-term changes in several cellular processes and pathways regardless of sensitivity status.

Subsequently, we analysed DEGs that correlate with IR resistance (Fig. 2A). IPA analysis of canonical pathways correlating with IR resistance using upregulated genes identified metabolic processes such as NADH repair, arginine degradation and glutamine biosynthesis (Fig. 2D + Supplementary Fig. 2C). IPA analysis of canonical pathways correlating with IR resistance using downregulated genes also identified alterations in metabolism such as acetate conversion to acetyl-coA and nicotine degradation (Fig. 2E + Supplementary Fig. 2D). Although only few significant GO terms were identified, metabolism was also present in the gene expres-

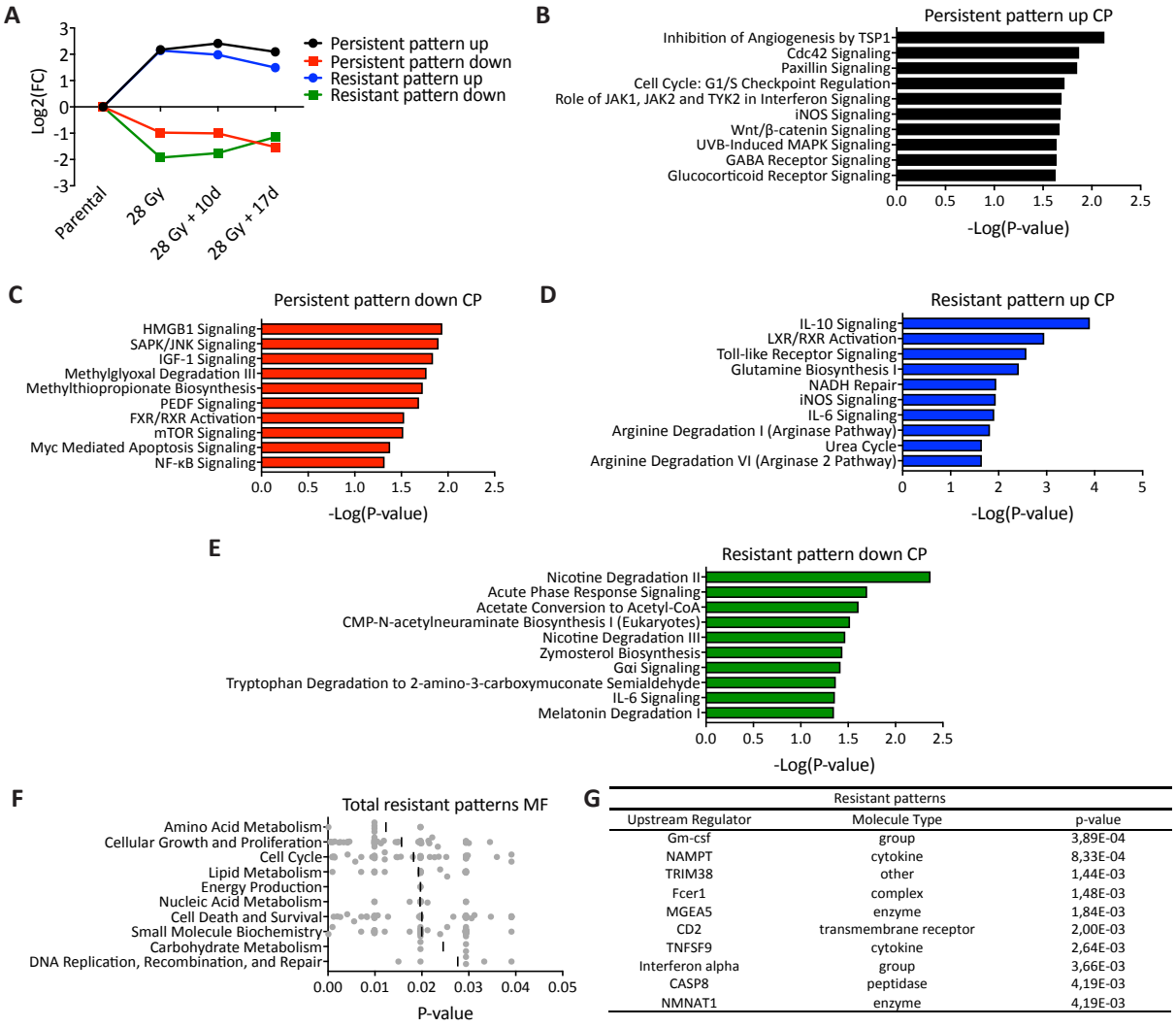

Resistant patterns		
Upstream Regulator	Molecule Type	p-value
Gm-csf	group	3,89E-04
NAMPT	cytokine	8,33E-04
TRIM38	other	1,44E-03
Fcer1	complex	1,48E-03
MGEA5	enzyme	1,84E-03
CD2	transmembrane receptor	2,00E-03
TNFSF9	cytokine	2,64E-03
Interferon alpha	group	3,66E-03
CASP8	peptidase	4,19E-03
NMNAT1	enzyme	4,19E-03

Figure 2: Analysis of persistent gene expression patterns and resistant gene expression patterns. A) Significant expression patterns of DEG, which show persistent (black and red) or resistant (blue and green) expression patterens. Patterns were generated by STEM analysis. Mean ± SEM are depicted. B – E) Canonical pathway (CP) analysis of persistent pattern with up-regulated genes (B), persistent pattern with down-regulated genes (C), resistant pattern with up-regulated genes (D) and resistant pattern with down-regulated genes (E). For all CP analysis the top 10 and the –Log(p-value) are depicted. F) Analysis of molecular functions (MF) of resistant patterns combined, the top 10 per pattern is given sorted based on average p-value. Each dot per function represents a significant pathway within the molecular function. G) Upstream regulator analysis of resistant patterns combined. The top 10 of upstream regulators is depicted.

sion patterns correlating with resistance (Supplementary Fig. 3C + D).

Since a recurrent theme in our analyses was energy metabolism, we performed a molecular function analysis using IPA in which we combined both up- and down-regulated DEGs derived from STEM analysis that correlate with resistance. Indeed, we observed that processes such as DNA repair, cell cycle, apoptosis, energy metabolism and carbohydrate metabolism were altered (Fig. 2F). Next, we also performed an up-

stream regulator analysis, which predicts which factors could control the altered expression of the observed DEGs. This analysis identified NAMPT and NMNAT1 as upstream regulators (Fig. 2G), which are both involved in the *de novo* synthesis of NAD^+ by the salvage pathway (24). This finding is also in accordance with the canonical pathway analysis in which NADH repair was enriched (Fig. 2D). Together our analyses indicate that IR resistance is correlated with genes involved in energy metabolism.

Bio-energetic alterations in IR-resistant cancer cells

Our mRNA sequencing analyses supports the observation that high metabolic activity, as measured by labelled glucose uptake by the tumour, is associated with cancer therapy resistance (25-27). We measured the bioenergetics profile of parental, RR cells and re-sensitized RR cells by IR holiday.

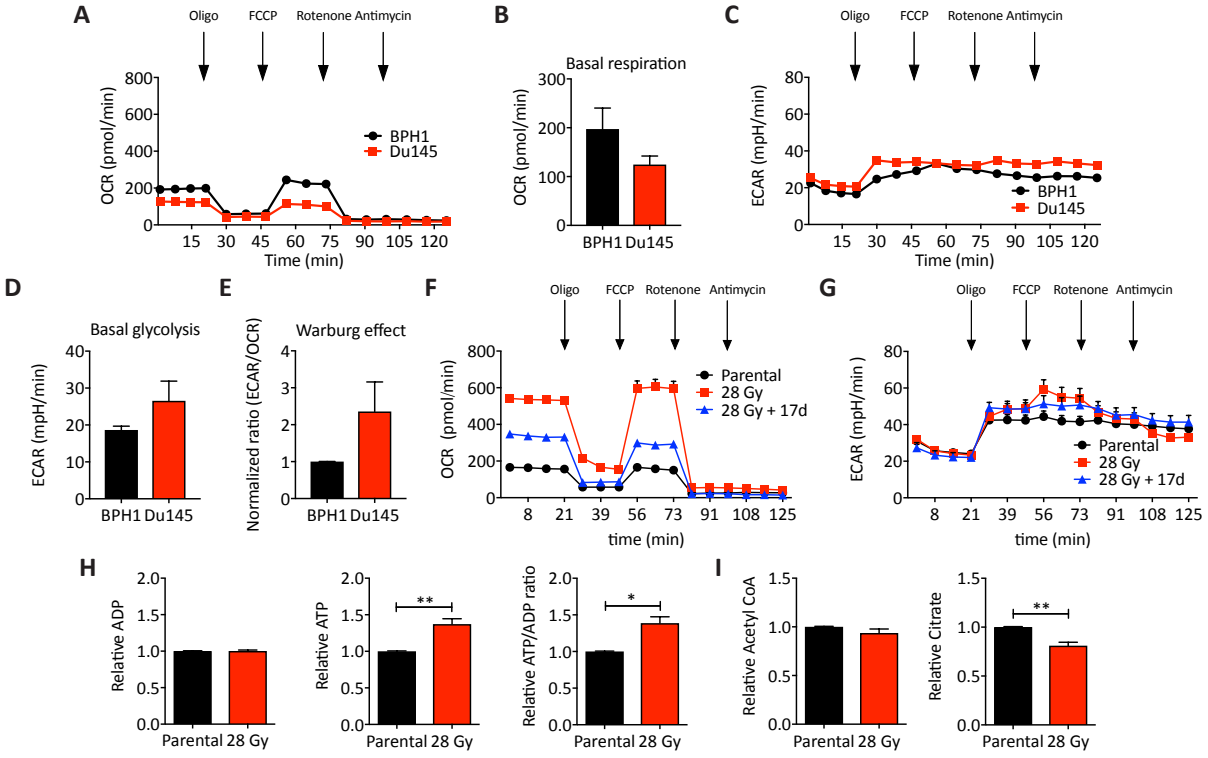

Figure 3: Increased metabolic activity in RR cells. A) Oxygen consumption rate (OCR) was measured in normal prostate epithelial cells BPH1 (black) and Du145 (red) cells. B) Quantification of the basal respiration rate based on the first four time points of the OCR measurement (A). C) Glycolysis was measured in BPH1 (black) and Du145 (red) cells by measuring the extracellular acidification rate (ECAR). D) Quantification of basal glycolysis based on the first four time points of the ECAR measurement (B). E) Normalized ratio of ECAR over OCR as a measure for the Warburg effect, where the ratio of BPH1 cells was set to 1. F) OCR measurement for parental (black), RR cells (red) and RR cells with a 2-week IR holiday (blue). G) ECAR measurement for parental (black), RR cells (red) and RR cells with a 2-week IR holiday (blue). H) Relative ADP, ATP and ATP/ADP ratio in parental (black) and RR cells (red). I) Relative Acetyl CoA and citrate levels in parental (black) and RR cells (red). All experiments were repeated at least three times and mean ± SEM are depicted. Unpaired two-sided T-test was performed to determine statistical significance. * P>0.05; ** P>0.01

First, we compared the bio-energetics profiles of normal prostate epithelial cells (BPH1 cells), which do not acquire resistance upon repetitive IR treatment (10), with prostate cancer cells. We observed that the basal respiration of normal prostate epithelial cells as measured by the oxygen consumption rate (OCR) is higher than prostate cancer cells (Fig. 3A, 3B). On the other hand, glycolysis, which was measured by the extracellular acidification rate (ECAR), is increased in prostate cancer cells when compared to normal prostate epithelial cells (Fig. 3C, 3D). This shift from oxidative phosphorylation to glycolysis is also known as the Warburg effect, in which cancer cells prefer glycolysis instead of oxidative phosphorylation for ATP production (28). Indeed, the ECAR/OCR ratio indicates increased glycolysis levels in prostate cancer cells, indicating the presence of the Warburg effect (Fig. 3E). Subsequently, we performed bioenergetics profiling of parental, RR cells and RR cells with a 17-day IR holiday. We observed that the OCR of RR cells is tremendously increased when compared to parental cells (Fig. 3F) and returns towards parental cell levels after a 17-day IR holiday. On the other hand, glycolysis does not differ between the three groups (Fig. 3G). This indicates that RT-resistant prostate cancer cells have increased mitochondrial respiration.

Increased ATP levels are expected to increase, because of the observed increase in mitochondrial respiration. While ADP levels between parental cells and RR cells are similar, ATP levels are increased (Fig. 3H). As a consequence, the ATP/ADP ratio is also increased (Fig. 3H). The increase in ATP levels and the OCR in RR cells is not due to increased activity of upstream parts of the energy metabolism chain: glycolysis was not altered (Fig. 3G), but also the citric acid cycle was not altered as measured by acetyl CoA and citrate levels (Fig. 3I). Thus, increased oxidative phosphorylation and ATP production during RT resistance is not due to increased activity of upstream components of energy metabolic pathways.

Next, we measured the coenzymes $NADP^+$/NADPH and NAD^+/NADH that are involved in the mitochondrial electron transport chain (ETC). The pentose phosphate pathway (PPP) mainly produces $NADP^+$/NADPH that are involved in cellular redox capacity and nucleotide synthesis (29, 30). NAD^+/NADH shuttle electrons produced during oxidative reactions in the citric acid cycle to the ETC. During IR resistance, $NADP^+$ and NADPH are both increased compared to parental cells, but the ratio between $NADP^+$ and NADPH remains similar (Fig. 4A), indicating increased activity of the PPP. However, more experiments need to be done to confirm the involvement of the PPP in IR resistance. In addition, we observed that the NAD^+ concentration is increased in RR cells, but NADH is not altered. The ratio NAD^+/NADH is by extension also increased during IR resistance (Fig. 4B). This observation is in agreement with the mRNA sequencing data in which we observed NADH repair as a significant enriched process (Fig. 2D).

Our observations indicate that a shift in the bio-energetic profile from glycolysis to mitochondrial respiration could be causally involved in RT resistance. To test this hypothesis, we determined in a clonogenic survival assay whether parental prostate cancer cells could

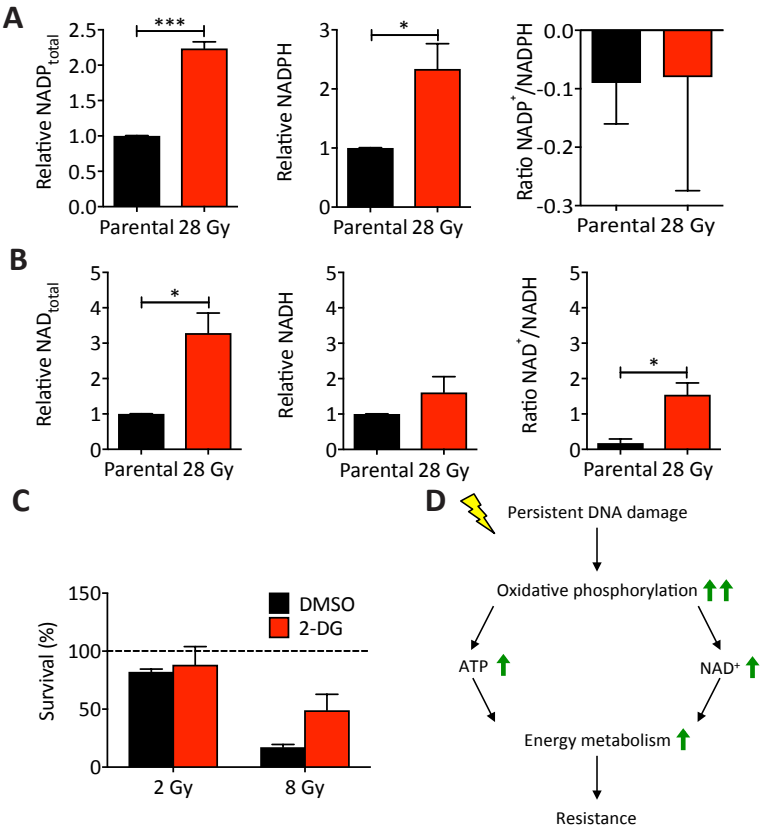

Figure 4: Increased levels NAD⁺ in RR cells. A) Total NADP (NADP⁺ and NADPH) and NADPH were measured in the same batch of cells. Ratio NADP⁺/NADPH was calculated by subtracting NADPH from total NADP, which was then divided by NADPH. B) Total NAD (NAD⁺ and NADH) and NADH were measured in the same batch of cells. NAD⁺/NADH ratio was calculated by subtracting NADH form total NAD, which was then divided by NADH. C) Colony survival of parental cells treated with DMSO (black) or 5 mM 2-DG (red) prior to additional IR. Percentages are relative to the numbers of colonies formed at 0 Gy (dotted line). D) Simplified schematic model of induction of acquired resistance. Repetitive DNA damage leads to increased oxidative phosphorylation and subsequent increase in ATP and NAD⁺ levels. In turn this leads to increased energy metabolism, which contributes to the development of acquired RT resistance. Every experiment was performed at least three times and mean ± SEM are depicted. Unpaired two-sided T-test was performed to determine statistical significance. *P>0.05, **P>0.01.

acquire RT resistance when we shift their bio-energetic profile from glycolysis to mitochondrial respiration using 2-deoxyglucose (2-DG), which blocks ATP production by glycolysis and forces cells to use oxidative phosphorylation (31). Interestingly, parental cells are more resistant to IR after 2-DG treatment (Fig. 4C), indicating that increased mitochondrial respiration contributes to RT resistance in prostate cancer cells.

Discussion

We have previously shown that repeated IR treatment leads to radio-resistance, which can be reversed by an 'IR holiday' (10). Here, we designed well-defined experimental groups to identify genes and cellular processes by

mRNA sequencing that could be causally involved in RT resistance. We showed that DNA repair was associated with RT resistance, which verified our previous findings in which specific transient alterations in the DNA damage response were functionally implicated in acquired RT resistance (10). In addition, we found that the expression of genes involved in energy metabolism was altered in RT resistance. We verified our RNA sequencing data by bio-energetic profiling, in which we observed increased mitochondrial respiration in RR cells, which was reversed after an IR holiday. Glycolysis however, was not altered. The changes in energy metabolism are likely important for RT resistance, since an experimentally-induced shift from glycolysis to mitochondrial respiration increased RT resistance in parental prostate cancer cells.

Based on these data, we propose a model in which repetitive IR treatment leads to RT resistance via increased oxidative phosphorylation and subsequent increased ATP and NAD^+ levels (Fig. 4D). Several lines of evidence further support this model. For instance, glioblastoma cancer cells and oesophageal adenocarcinoma cells are both treated with RT in the clinic and often acquire resistance to RT. When metabolic parameters were analysed, both showed increased oxidative phosphorylation and ATP production (32, 33). The emerging model is likely more complicated, because hepatocellular carcinoma cells, cervical cancer cells and medulloblastoma stem-like cells showed increased glycolysis in acquired RT resistance, which can be sensitized by 2-DG treatment (34, 35). We speculate that the complex wiring of all energy metabolic components and pathways may be different for distinct tumour types, each with their specific genomic alterations.

In addition, we also observed increased levels of NAD^+ but not NADH. NAD^+ is produced *de novo* or via the salvage pathway (24). In the salvage pathway NAMPT is the rate-limiting enzyme in the production of NAD^+ and it is up-regulated in several cancers (24, 36-39). We identified NAMPT as an upstream regulator in our data set, suggesting that the increased amounts of NAD^+ are due to an increased production via the salvage pathway. Moreover, genes involved in the de novo synthesis of NAD^+ or the Preiss-Handler pathway (40) were not differentially expressed in our dataset, which indicates that the increased NAD^+ level could be attributed to increased NAD^+ production by the salvage pathway. NAD^+ is not only a coenzyme in mitochondrial respiration, but it is also a substrate for the sirtuin class of histone deacetylases (SIRT) (40). Seven SIRT proteins have been identified each with a different cellular location. SIRT1, SIRT 6 and SIRT7 are located in the nucleus, whereas SIRT2 is the only SIRT situated in the cytosol and SIRT3, SIRT4 and SIRT5 reside in the mitochondria (41). *SIRT5* was the only sirtuin that was differentially expressed in our data set (data not shown). Interestingly, it was shown that SIRT5 is highly expressed in non-small cell lung cancer (NSCLC) patients and its high expression correlated with poor survival and drug resistance (42). Not only SIRTs but also PARP uses NAD^+ as a substrate to exert its function(43), we speculate that high NAD^+ levels prevents PARP to deplete the NAD^+ pool that leads to cell death (44), but also maintains DNA repair capacity in RR cells.

At this moment we do not know exactly how the elevated and altered energy metabolism contributes to RT resistance, since inhibition of the different essential components of oxidative phosphorylation has proven to be difficult, either all cells died or inhibition was incomplete (data not shown). Furthermore, we have previously shown that the DNA damage response also contributes to acquired RT resistance (10). Therefore, it is plausible that these two pathways work together in accomplishing resistance to RT.

In summary, we have shown that by using well-defined groups of radio-resistant and -sensitive prostate cancer cells, novel pathways involved in RT resistance can be identified by mRNA sequencing, which includes energy metabolism. Further experiments showed increased mitochondrial respiration in RR cells and increased metabolic parameters such as ATP and NAD^+, indicating that energy metabolism is indeed more active in RR cells. Targeting energy metabolism led to a change in radiosensitivity, indicating that energy metabolism could be a promising target, despite its essential role in cells. Future research should focus on exactly pinpointing the role of energy metabolism in acquired RT resistance to design novel interventions to sensitize prostate cancer.

Acknowledgements

The authors would like to thank members of the Molecular Genetics department and the Experimental Urology department of the Erasmus Medical Center Rotterdam for their contributions to the manuscript. The authors would also like to thank the members of the Center for Biomics of the Erasmus Medical Center for their help with sequencing. This research was supported by the Dutch Cancer Society (KWF) grant nr. 2011-5030.

Disclosure

The authors declare no conflict of interest.

References

1. Connell PP, Hellman S. Advances in radiotherapy and implications for the next century: a historical perspective. Cancer research. 2009;69(2):383-92.
2. Baskar R, Itahana K. Radiation therapy and cancer control in developing countries: Can we save more lives? International journal of medical sciences. 2017;14(1):13-7.
3. Heidenreich A, Bastian PJ, Bellmunt J, Bolla M, Joniau S, van der Kwast T, et al. EAU guidelines on prostate cancer. part 1: screening, diagnosis, and local treatment with curative intent-update 2013. European urology. 2014;65(1):124-37.
4. Fitch DL, McGrath S, Martinez AA, Vicini FA, Kestin LL. Unification of a common biochemical failure definition for prostate cancer treated with brachytherapy or external beam radiotherapy with or without androgen deprivation. International journal of radiation oncology, biology, physics. 2006;66(5):1430-9.
5. Fitzgerald TJ, Wang T, Goel HL, Huang J, Stein G, Lian J, et al. Prostate carcinoma and radiation therapy: therapeutic treatment resistance and strategies for targeted therapeutic intervention. Expert review of anticancer therapy. 2008;8(6):967-74.
6. Kyjacova L, Hubackova S, Krejcikova K, Strauss R, Hanzlikova H, Dzijak R, et al. Radiotherapy-induced plasticity of prostate cancer mobilizes stem-like non-adherent, Erk signaling-dependent cells. Cell

death and differentiation. 2015;22(6):898-911.
7. Ward JF. DNA damage produced by ionizing radiation in mammalian cells: identities, mechanisms of formation, and reparability. Progress in nucleic acid research and molecular biology. 1988;35:95-125.
8. Hoeijmakers JH. DNA damage, aging, and cancer. The New England journal of medicine. 2009;361(15):1475-85.
9. Incrocci L, Wortel RC, Alemayehu WG, Aluwini S, Schimmel E, Krol S, et al. Hypofractionated versus conventionally fractionated radiotherapy for patients with localised prostate cancer (HYPRO): final efficacy results from a randomised, multicentre, open-label, phase 3 trial. The Lancet Oncology. 2016;17(8):1061-9.
10. Serena Bruens NV, Marjolein Baar, Aranka Ambags, Marjolijn Ladan, Dik van Gent, Wytkse van Weerden, Guido Jenster, Jan Hoeijmakers, Joris Pothof*. Altered DNA damage response is causative for acquired radiation resistance in cancer. 2017.
11. Chang L, Graham PH, Hao J, Ni J, Bucci J, Cozzi PJ, et al. Acquisition of epithelial-mesenchymal transition and cancer stem cell phenotypes is associated with activation of the PI3K/Akt/mTOR pathway in prostate cancer radioresistance. Cell death & disease. 2013;4:e875.
12. Yun HS, Baek JH, Yim JH, Um HD, Park JK, Song JY, et al. Radiotherapy diagnostic biomarkers in radioresistant human H460 lung cancer stem-like cells. Cancer biology & therapy. 2016;17(2):208-18.
13. Mihatsch J, Toulany M, Bareiss PM, Grimm S, Lengerke C, Kehlbach R, et al. Selection of radioresistant tumor cells and presence of ALDH1 activity in vitro. Radiotherapy and oncology : journal of the European Society for Therapeutic Radiology and Oncology. 2011;99(3):300-6.
14. Liu H, Yang W, Gao H, Jiang T, Gu B, Dong Q, et al. Nimotuzumab abrogates acquired radioresistance of KYSE-150R esophageal cancer cells by inhibiting EGFR signaling and cellular DNA repair. OncoTargets and therapy. 2015;8:509-18.
15. Saki M, Toulany M, Rodemann HP. Acquired resistance to cetuximab is associated with the overexpression of Ras family members and the loss of radiosensitization in head and neck cancer cells. Radiotherapy and oncology : journal of the European Society for Therapeutic Radiology and Oncology. 2013;108(3):473-8.
16. Toulany M, Baumann M, Rodemann HP. Stimulated PI3K-AKT signaling mediated through ligand or radiation-induced EGFR depends indirectly, but not directly, on constitutive K-Ras activity. Molecular cancer research : MCR. 2007;5(8):863-72.
17. Skvortsova I, Skvortsov S, Stasyk T, Raju U, Popper BA, Schiestl B, et al. Intracellular signaling pathways regulating radioresistance of human prostate carcinoma cells. Proteomics. 2008;8(21):4521-33.
18. Gomez-Casal R, Epperly MW, Wang H, Proia DA, Greenberger JS, Levina V. Radioresistant human lung adenocarcinoma cells that survived multiple fractions of ionizing radiation are sensitive to HSP90 inhibition. Oncotarget. 2015;6(42):44306-22.
19. Perri F, Pacelli R, Della Vittoria Scarpati G, Cella L, Giuliano M, Caponigro F, et al. Radioresistance in head and neck squamous cell carcinoma: Biological bases and therapeutic implications. Head & neck. 2015;37(5):763-70.
20. Stone KR, Mickey DD, Wunderli H, Mickey GH, Paulson DF. Isolation of a human prostate carcinoma cell line (DU 145). International journal of cancer. 1978;21(3):274-81.
21. Trapnell C, Pachter L, Salzberg SL. TopHat: discovering splice junctions with RNA-Seq. Bioinformatics. 2009;25(9):1105-11.
22. 22. Trapnell C, Williams BA, Pertea G, Mortazavi A, Kwan G, van Baren MJ, et al. Transcript assembly and quantification by RNA-Seq reveals unannotated transcripts and isoform switching during cell differentiation. Nature biotechnology. 2010;28(5):511-5.
23. Ernst J, Bar-Joseph Z. STEM: a tool for the analysis of short time series gene expression data. BMC bioinformatics. 2006;7:191.
24. Canto C, Menzies KJ, Auwerx J. NAD(+) Metabolism and the Control of Energy Homeostasis: A Balancing Act between Mitochondria and the Nucleus. Cell metabolism. 2015;22(1):31-53.
25. Wang W, Larson SM, Tuttle RM, Kalaigian H, Kolbert K, Sonenberg M, et al. Resistance of [18f]-fluorodeoxyglucose-avid metastatic thyroid cancer lesions to treatment with high-dose radioactive iodine. Thyroid : official journal of the American Thyroid Association. 2001;11(12):1169-75.
26. Nakaigawa N, Kondo K, Ueno D, Namura K, Makiyama K, Kobayashi K, et al. The accelerati-

on of glucose accumulation in renal cell carcinoma assessed by FDG PET/CT demonstrated acquisition of resistance to tyrosine kinase inhibitor therapy. BMC cancer. 2017;17(1):39.
27. Hendlisz A, Deleporte A, Delaunoit T, Marechal R, Peeters M, Holbrechts S, et al. The Prognostic Significance of Metabolic Response Heterogeneity in Metastatic Colorectal Cancer. PloS one. 2015;10(9):e0138341.
28. Liberti MV, Locasale JW. The Warburg Effect: How Does it Benefit Cancer Cells? Trends in biochemical sciences. 2016;41(3):211-8.
29. Hamanaka RB, Chandel NS. Cell biology. Warburg effect and redox balance. Science. 2011;334(6060):1219-20.
30. Pavlova NN, Thompson CB. The Emerging Hallmarks of Cancer Metabolism. Cell metabolism. 2016;23(1):27-47.
31. Woodward GE, Hudson MT. The effect of 2-desoxy-D-glucose on glycolysis and respiration of tumor and normal tissues. Cancer research. 1954;14(8):599-605.
32. Vlashi E, Lagadec C, Vergnes L, Matsutani T, Masui K, Poulou M, et al. Metabolic state of glioma stem cells and nontumorigenic cells. Proceedings of the National Academy of Sciences of the United States of America. 2011;108(38):16062-7.
33. Mims J, Bansal N, Bharadwaj MS, Chen X, Molina AJ, Tsang AW, et al. Energy metabolism in a matched model of radiation resistance for head and neck squamous cell cancer. Radiation research. 2015;183(3):291-304.
34. Shimura T, Noma N, Sano Y, Ochiai Y, Oikawa T, Fukumoto M, et al. AKT-mediated enhanced aerobic glycolysis causes acquired radioresistance by human tumor cells. Radiotherapy and oncology : journal of the European Society for Therapeutic Radiology and Oncology. 2014;112(2):302-7.
35. Sun L, Moritake T, Ito K, Matsumoto Y, Yasui H, Nakagawa H, et al. Metabolic analysis of radioresistant medulloblastoma stem-like clones and potential therapeutic targets. PloS one. 2017;12(4):e0176162.
36. Bi TQ, Che XM, Liao XH, Zhang DJ, Long HL, Li HJ, et al. Overexpression of Nampt in gastric cancer and chemopotentiating effects of the Nampt inhibitor FK866 in combination with fluorouracil. Oncology reports. 2011;26(5):1251-7.
37. Wang B, Hasan MK, Alvarado E, Yuan H, Wu H, Chen WY. NAMPT overexpression in prostate cancer and its contribution to tumor cell survival and stress response. Oncogene. 2011;30(8):907-21.
38. Hasmann M, Schemainda I. FK866, a highly specific noncompetitive inhibitor of nicotinamide phosphoribosyltransferase, represents a novel mechanism for induction of tumor cell apoptosis. Cancer research. 2003;63(21):7436-42.
39. Van Beijnum JR, Moerkerk PT, Gerbers AJ, De Bruine AP, Arends JW, Hoogenboom HR, et al. Target validation for genomics using peptide-specific phage antibodies: a study of five gene products overexpressed in colorectal cancer. International journal of cancer. 2002;101(2):118-27.
40. Xiao W, Wang RS, Handy DE, Loscalzo J. NAD(H) and NADP(H) Redox Couples and Cellular Energy Metabolism. Antioxidants & redox signaling. 2017.
41. Michishita E, Park JY, Burneskis JM, Barrett JC, Horikawa I. Evolutionarily conserved and nonconserved cellular localizations and functions of human SIRT proteins. Molecular biology of the cell. 2005;16(10):4623-35.
42. Lu W, Zuo Y, Feng Y, Zhang M. SIRT5 facilitates cancer cell growth and drug resistance in non-small cell lung cancer. Tumour biology : the journal of the International Society for Oncodevelopmental Biology and Medicine. 2014;35(11):10699-705.
43. Schreiber V, Dantzer F, Ame JC, de Murcia G. Poly(ADP-ribose): novel functions for an old molecule. Nature reviews Molecular cell biology. 2006;7(7):517-28.
44. Alano CC, Garnier P, Ying W, Higashi Y, Kauppinen TM, Swanson RA. NAD+ depletion is necessary and sufficient for poly(ADP-ribose) polymerase-1-mediated neuronal death. The Journal of neuroscience : the official journal of the Society for Neuroscience. 2010;30(8):2967-78.

Supplemental information

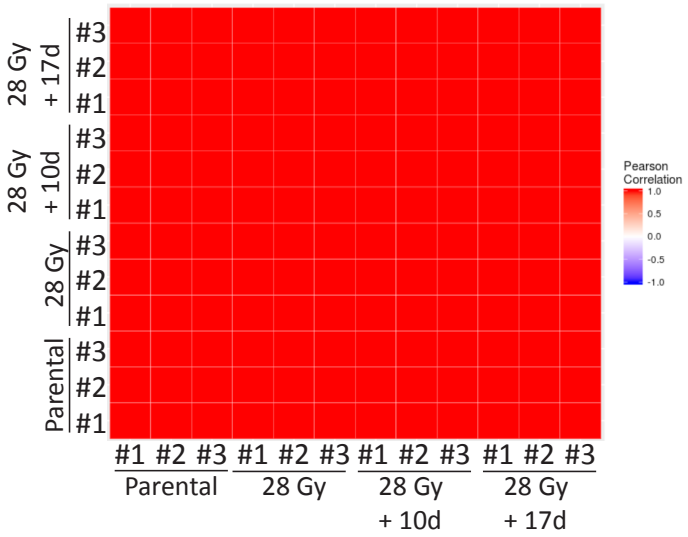

Supplementary Figure 1: Pearson correlation plot of all sequenced samples. Pearson correlation analysis of all samples shows a significant correlation between samples and between the different groups.

A

Persistent pattern up	
Ingenuity Canonical Pathways	-log(p-value)
Inhibition of Angiogenesis by TSP1	2,13E00
Cdc42 Signaling	1,85E00
Paxillin Signaling	1,73E00
Cell Cycle: G1/S Checkpoint Regulation	1,72E00
Role of JAK1, JAK2 and TYK2 in Interferon Signaling	1,69E00
iNOS Signaling	1,68E00
Wnt/β-catenin Signaling	1,67E00
UVB-Induced MAPK Signaling	1,64E00
GABA Receptor Signaling	1,64E00
Glucocorticoid Receptor Signaling	1,63E00
p38 MAPK Signaling	1,6E00
Renin-Angiotensin Signaling	1,56E00
ErbB Signaling	1,49E00
Toll-like Receptor Signaling	1,48E00
Assembly of RNA Polymerase III Complex	1,47E00
Regulation of eIF4 and p70S6K Signaling	1,44E00
EIF2 Signaling	1,43E00
IL-6 Signaling	1,43E00
IL-15 Signaling	1,41E00
Cyclins and Cell Cycle Regulation	1,39E00
Chronic Myeloid Leukemia Signaling	1,38E00
ATM Signaling	1,35E00
UDP-D-xylose and UDP-D-glucuronate Biosynthesis	1,31E00
Taurine Biosynthesis	1,31E00
Protein Ubiquitination Pathway	1,31E00
Chronic Myeloid Leukemia Signaling	1,38E00
ATM Signaling	1,35E00
UDP-D-xylose and UDP-D-glucuronate Biosynthesis	1,31E00
Taurine Biosynthesis	1,31E00
Protein Ubiquitination Pathway	1,31E00

B

Persistent pattern down	
Ingenuity Canonical Pathways	-log(p-value)
HMGB1 Signaling	1,94E00
SAPK/JNK Signaling	1,9E00
IGF-1 Signaling	1,84E00
Methylglyoxal Degradation III	1,77E00
Methylthiopropionate Biosynthesis	1,73E00
PEDF Signaling	1,69E00
FXR/RXR Activation	1,53E00
mTOR Signaling	1,52E00
Myc Mediated Apoptosis Signaling	1,38E00
NF-κB Signaling	1,32E00

C

Resistant pattern up	
Ingenuity Canonical Pathways	-log(p-value)
IL-10 Signaling	3,9E00
LXR/RXR Activation	2,95E00
Toll-like Receptor Signaling	2,58E00
Glutamine Biosynthesis I	2,42E00
NADH Repair	1,95E00
iNOS Signaling	1,94E00
IL-6 Signaling	1,91E00
Airway Inflammation in Asthma	1,82E00
Arginine Degradation I (Arginase Pathway)	1,82E00
Urea Cycle	1,65E00
Arginine Degradation VI (Arginase 2 Pathway)	1,65E00
TREM1 Signaling	1,54E00
Citrulline Biosynthesis	1,53E00
IL-15 Signaling	1,48E00

D

Resistant pattern down	
Ingenuity Canonical Pathways	-log(p-value)
Nicotine Degradation II	2,37E00
Acute Phase Response Signaling	1,7E00
Acetate Conversion to Acetyl-CoA	1,61E00
CMP-N-acetylneuraminate Biosynthesis I (Eukaryotes)	1,52E00
Nicotine Degradation III	1,47E00
Zymosterol Biosynthesis	1,44E00
Gαi Signaling	1,42E00
LPS/IL-1 Mediated Inhibition of RXR Function	1,4E00
Tryptophan Degradation to 2-amino-3-carboxymuconate Semialdehyde	1,37E00
IL-6 Signaling	1,36E00
Melatonin Degradation I	1,35E00

Supplementary Figure 2: Canonical pathway analysis of the different significant STEM patterns. Complete tables with all significant canonical pathways identified in persistent pattern up (A), persistent pattern down (B), resistant pattern up (C) and resistant pattern down (D) using Ingenuity Pathway Analysis. The tables depict the pathways and –Log(p-value).

A

Persistent pattern up	
GO-terms	P-value
GO: 0009749 response to glucose	0.004
GO: 0030195 negative regulation of blood coagulation	0.005
GO: 0048247 lymphocyte chemotaxis	0.009
GO: 2000145 regulation of cell motility	0.009
GO: 0006954 inflammatory response	0.011
GO: 0007182 common-partner SMAD protein phosphorylation	0.012
GO: 0006893 Golgi to plasma membrane transport	0.013
GO: 0070374 positive regulation of ERK1 and ERK2 cascade	0.016
GO: 0019221 cytokine-mediated signaling pathway	0.017
GO: 0006417 regulation of translation	0.019
GO: 0050729 positive regulation of inflammatory response	0.022
GO: 0070723 response to cholesterol	0.022
GO: 0007369 gastrulation	0.024
GO: 0042127 regulation of cell proliferation	0.024
GO: 0007173 epidermal growth factor receptor signalling pathway	0.026
GO: 0060021 palate development	0.026
GO: 0006959 humoral immune response	0.028
GO: 0071346 cellular response to interferon-gamma	0.028
GO: 0055088 lipid homeostasis	0.029
GO: 0050679 positive regulation of epithelial cell proliferation	0.034
GO: 0051149 positive regulation of muscle cell differentiation	0.034
GO: 0035265 organ growth	0.034
GO: 0097191 extrinsic apoptotic signalling pathway	0.036
GO: 0034067 protein localization to Golgi apparatus	0.041
GO: 0042592 homeostatic process	0.041
GO: 0060338 regulation of type I interferon-mediated signalling pathway	0.042
GO: 0023014 signal transduction by protein phosphorylation	0.042
GO: 0001822 kidney development	0.044
GO: 0051384 response to glucocorticoid	0.045
GO: 0030838 positive regulation of actin filament polymerization	0.045
GO: 0030593 neutrophil chemotaxis	0.048
GO: 0008334 histone mRNA metabolic process	0.048

B

Persistent pattern down	
GO-terms	P-value
GO: 0045187 regulation of circadian sleep/wake cycle sleep	0.007
GO: 0042503 tyrosine phosphorylation of Stat3 protein	0.007
GO: 0007608 sensory perception of smell	0.010
GO: 0051216 cartilage development	0.010
GO: 0007160 cell-matrix adhesion	0.016
GO: 0000387 spliceosomal snRNP assembly	0.024
GO: 0007030 Golgi organization	0.026
GO: 0048706 embryonic skeletal system development	0.029
GO: 0051492 regulation of stress fiber assembly	0.033
GO: 0006486 protein glycosylation	0.042

C

Resistant pattern up	
GO-terms	P-value
GO: 1901896 positive regulation of calcium-transporting ATPase activity	0.021
GO: 0031642 negative regulation of myelination	0.037
GO: 0032057 negative regulation of translational initiation in response to stress	0.037
GO: 0051646 mitochondrion localization	0.037
GO: 0002467 germinal center formation	0.042
GO: 0001825 blastocyst formation	0.042
GO: 0034599 cellular response to oxidative stress	0.045

D

Resistant pattern down	
GO-terms	P-value
GO: 0071456 cellular response to hypoxia	0.022
GO: 0042572 retinol metabolic process	0.069

Supplementary Figure 3: GO-term analysis of the different significant STEM patterns. GO-term analysis of persistent pattern up (A), persistent pattern down (B), resistant pattern up (C) and resistant pattern down (D) using DAVID array tools. Only significant GO-terms are depicted (A – C) or all GO-terms are depicted (D).

Chapter 4

A time-resolved transcriptional map induced by DNA damage reveales citrullination as a novel process in the DNA damage response

Serena Bruens[1]*, Jiang Chang[1]*, Kasper Derks[1]*, Akos Gyenis[1,2], Nicole Verkaik[1], Dik van Gent[1], Jan Hoeijmakers[1,2,3], Joris Pothof[1]¶

[1] Department of Molecular Genetics, Erasmus Medical Center, Rotterdam, The Netherlands
[2] CECAD Research Center, University of Cologne, Cologne, Germany
[3] Princess Maxima Center for Pediatric Oncology, Utrecht, The Netherlands

* Contributed equally to this work
¶ Corresponding author: j.pothof@erasmusmc.nl

Submitted

Abstract

Since damaged DNA cannot be replaced by a newly synthesized DNA molecule, genetic integrity solely dependent on DNA repair. Loss or dysfunction of genetic information is particularly harmful, because it has been causally linked to carcinogenesis, the aging process and age-related diseases. Genome stability is maintained by DNA repair systems, but also elaborate DNA damage signaling pathways that transiently halt cell proliferation to allow repair and in case of extensive damage, induce cell death, cellular senescence or terminal differentiation. This DNA damage response network is comprised of numerous factors and cellular processes, but the intricate wiring of the DNA damage response and regulatory steps are still unclear. Here, we mapped the transcriptional response of both genes as well as microRNAs in time to three types of genotoxic agents, i.e. UV-C, ionizing radiation and cisplatin, which induce their own spectrum of DNA lesions. We delineated a general DNA damage-induced transcriptional signature and identified several upstream regulators, in which microRNAs predominantly control gene expression only in the first hours after DNA damage after which more permanent transcriptional changes take over. Moreover, we identified several novel processes in the DNA damage response, one of which is protein citrullination, the intra-peptidal conversion of amino acid arginine into citrulline. We show that citrullination facilitates replication fork stability and is required for homologous recombination repair of double strand DNA breaks. In conclusion, we provide a time-resolved mechanistic framework of the transcriptional response to DNA damage in mouse embryonic stem cells that integrates gene and microRNA expression as well as post-translational modifications. Our extensive resource permits identification of novel processes in the DNA damage response, with relevance to cancer and aging.

Introduction

DNA is continuously damaged by genotoxic agents from both exogenous sources (e.g. ultraviolet (UV) light, cigarette smoke) and endogenous sources (e.g. replication, transcription, metabolism) (1). Each genotoxic agent induces its own spectrum of DNA lesions, which in turn is repaired by a specific DNA repair pathway to maintain genome integrity. Single strand breaks (SSB) and subtle lesions are mainly repaired via base excision repair, base-pair-disrupting lesions via nucleotide excision repair, interstrand crosslinks via interstrand crosslink repair and double strand breaks (DSB) by either non-homologous end joining (NHEJ), homologous recombination (HR) or single strand annealing (SSA) (2). In addition to DNA repair activation, DNA damage can induce DNA damage checkpoint signalling pathways, which determine cell fate. First, a temporary cell cycle arrest is induced to allow the cell time to repair the damage. DNA damage that is too extensive and beyond repair triggers cell death, cellular senescence or terminal differenti-

ation (2-4). The cellular outcome of DNA damage signalling is dependent on the number and type of lesions, their intrinsic characteristics (e.g. genomic location), cell type and cellular context (e.g. cell proliferation status) (5). Collectively, the response to DNA damage that includes DNA damage repair and signalling is designated the DNA damage response (DDR). DNA damage accumulation has several clinical implications. Exposure to environmental genotoxic agents induces mutations that drive carcinogenesis. In addition, genetic defects in the DDR are causal drivers of carcinogenesis as well. Moreover, many cancer therapies such as radiation and chemotherapy act via induction of DNA damage (6). During surgical procedures, ischemia reperfusion injury inflicts DNA damage that impairs organ function (7). Furthermore, defects in specific DNA repair pathways can lead to severe premature aging syndromes. Finally, it is becoming clear that gradual accumulation of DNA damage causing genome dysfunction and cell death can cause common age-related diseases and pathologies (1, 8, 9). For finding effective interventions for both cancer and ageing associated diseases, it is important to understand the complex wiring of the DDR network.

The complex DDR network needs to be tightly regulated and fine-tuned. Decreased activity will lead to mutations and chromosomal aberrations that drive cancer. Hyper-activation induces premature apoptosis and senescence that accelerate aging. Many regulatory steps in the DDR have been discovered. Directly after DNA damage is inflicted, protein–protein interactions and a wealth of post-translational modifications (PTMs) such as phosphorylation, acetylation, methylation, glycosylation, sumoylation, unbiquitylation, neddylation and polyADP-ribosylation are required for activation of DNA repair, the DNA damage checkpoint and cell cycle arrest (10, 11). To maintain a prolonged cell cycle arrest, but also to direct a damaged cell into a specific cell fate such as apoptosis, senescence or terminal differentiation, gene expression programs are induced. Several transcription factors have been identified to play a role in the DDR. For example, transcription factor P53 induces expression of genes that maintain cell cycle arrest and induce apoptosis (12, 13). Besides the relatively fast protein-protein interactions and PTMs on one hand and the relatively slow gene expression changes via transcription factors on the other hand, we identified another level of DDR regulation by microRNAs that act between the fast protein/PTM level and relatively slow transcription factor-controlled gene expression changes (14). MicroRNAs are small (± 22 nucleotides) endogenously encoded non-coding RNAs, which repress gene expression by binding to complementary target sites that mainly reside in the 3'UTR of mRNAs, leading to mRNA degradation and/or translation inhibition (15). Since one microRNA can target several mRNAs at once, a comprehensive set of gene expression patterns can be rapidly altered by only a few microRNAs. The mechanistic basis of microRNA action in the DDR relies on their fast maturation. A pool of primary microRNA transcripts is present in the nucleus. The DDR signalling kinase ATM directly phosphorylates and activates microRNA-binding protein KHSRP, which detects and binds

specific primary microRNAs from this nuclear pool and preferentially directs them into the microRNA biogenesis/maturation pathway (16). Since post-transcriptional regulation of microRNAs bypasses transcription, it is much faster than gene expression changes by altering promoter activity.

Numerous studies have been published in which global gene expression changes after genotoxic stress have been documented using micro-array or next generation sequencing technology. However, comparing these studies is difficult, since conditions, cell types, tissues, doses, timing, but also the number of replicates, are all different. Moreover, most DNA-damaging agents are not completely specific for DNA and will damage additional cellular macromolecules, which hampers mapping specific transcriptional responses induced by DNA damage. Here, we generated an extensive sequencing dataset in which gene and microRNA expression changes are analysed after three types of genotoxic stresses (UV-C, IR and cisplatin) at equitoxic doses in mouse embryonic stem (mES) cells at three time points (4, 8, 12 hours) to construct a map of the early transcriptional response to DNA damage. Each genotoxic agent induces a specific spectrum of DNA lesions: UV-C causes mainly helix-distorting lesions, ionizing radiation (IR) induces a range of oxidative DNA lesions, SSBs and DSBs, and cisplatin generates inter- and intra-strand crosslinks (4, 6, 17). Each DNA-damaging agent has its own side effects, e.g. UV-C causes very abundant transcription blocking lesions, with slow repair kinetics and replication bypass, causing lower relative toxicity (18). In addition, UV-C can damage cell membranes and RNA (19). IR causes very abundant SSBs, most of which are quickly repaired, and few DSBs, which are strong signalling-type of lesions in replicating cells (17). Furthermore, IR can oxidize proteins as well (20). Cisplatin induces the less abundant interstrand and intrastrand DNA crosslinks with a strong S-phase block and cell death (21). Besides DNA, cisplatin also damages RNA and can not only react with, but can also crosslink proteins (22). Covering this spectrum of DNA lesions allowed us to map a general gene and microRNA expression response to genotoxic stress, which likely is not influenced by the side effects of each treatment. In addition, we can map genotoxic stress-specific processes. Finally, we show that our rich and well-curated dataset allows for the identification of novel processes in the DDR.

Materials & Methods

Total RNA isolation

mES cells (HM1; 129/ola) were cultured as described (23). One vial of mES cells was thawed and grown for two passages on feeder-coated plates followed by one passage on gelatin-coated plates before taken into experiment. The mES cells in experiment were treated with 5μM cisplatin (Platosin), exposed to 4J/m2 UVC or, 4 Gy IR or mock-treated. Treatments with cisplatin, UVC and IR were carefully calibrated to be equitoxic, resulting in a 50% survival based on clonogenic assays (or 'colony-forming ability') (24, 25). After 4, 8 and 12h exposure total RNA was iso-

lated using Qiazol Lysis Reagent (Qiagen) and total RNA was purified with the miRNeasy kit (Qiagen), according to manufacturer's protocols. The integrity of the RNA was determined on the Agilent 2100 Bioanalyzer (Agilent) according to manufacturer's instructions. All scores were >9.0. This procedure was repeated three times to obtain independent biological replicates. Subsequent sequencing protocols were performed on the total RNA from the same biological samples.

RNA Sequencing Library Preparation and Deep Sequencing

Total RNA enrichment for sequencing poly(A)$^+$ RNAs was performed with the TruSeq mRNA sample preparation kit (Illumina) according to the manufacturer's protocols. In short, 1 µg of total RNA for each sample was used for poly(A)$^+$ RNA selection using magnetic beads coated with poly-dT, followed by thermal fragmentation. The fragmented poly(A)$^+$ RNA enriched samples were subjected to cDNA synthesis using Illumina TruSeq preparation kit according to the manufacturer's protocol. Then, cDNA was synthesized by reverse transcriptase (Super-Script II) using poly-dT and random hexamer primers. These cDNA fragments were subsequently blunt-ended by end-repair reaction, followed by dA-tailing. Finally, specific double-stranded bar-coded adapters were ligated and library amplification for 15 cycles was performed. cDNA libraries for small RNA sequencing were generated by Illumina TruSeq smallRNA kit v1.5 (smallRNASeq), according to the manufacturer's instructions. In short, specific bar-coded adapters were ligated to 1 µg of total RNA followed by reverse transcriptase and amplification for 11 cycles. Small RNAs were enriched by fractionation on a 15% Tris-borate-EDTA gel, excising the RNAs of 15-30 nucleotide of length. Pooled cDNA libraries all consisted of equal concentrations of bar-coded samples. The pooled libraries were sequenced, all 36bp single read on the HiSeq2000 (Illumina).

Analysis of sequencing data

The resulting 50-bp single-ended sequencing files were aligned to the Mus musculus genome (mm9) using Tophat (26) with the –g 1 option. The resulting aligned reads were then analysed by Cufflinks (27). FPKM (fragments per kilobase of exon per million fragments mapped) was applied to quantify the expression of each transcript. To identify the differentially expression genes (DEG), the average transcript level was calculated for each set (three damage-induced experiments consisting of three time points). The transcripts at low level were removed by requiring an average of at least 10 reads in each sample. Differentially expressed genes were identified using EdgeR (28), Deseq2 (29) and limma-voom (30, 31), with the cut-off of fold-change > 2 and FDR < 0.05. The statistics plots (i.e. principal component analysis, Pearson's correlation, heatmap) were created by Rstudio (v0.99.486) (RStudio Team (2015). RStudio: Integrated Development for R. RStudio, Inc., Boston, MA URL http://www.rstudio.com/). Short Time-series Expression Miner (STEM) using STEM clustering method was used to perform clustering analysis (32). The data were sum-

marized and visualized by Graphpad Prism. (One-way ANOVA with Dunnett's posttest was performed using GraphPad Prism version 5.00 for Windows, GraphPad Software, San Diego California USA, www.graphpad.com). Functional analysis was performed in Ingenuity Pathway Analysis (IPA) (QIAGEN Redwood City, www.qiagen.com/ingenuity) for canonical pathway analysis and upstream regulator analysis. The GO enrichment analysis was performed with PANTHER (33). Networks of GO term interactions were created using Cytoscape (34) under the BINGO package (35).

Cell culture

U2OS cells were cultured in DMEM supplemented with penicillin-streptomycin (100× diluted, Penicillin-Streptomycin, P0781-100ML, Sigma-Aldrich) and 10 % fetal bovine serum (Fetal Bovine Serum (FBS) South America, S1810-500, Biowest) at 5% CO2 and 37°C. To induce PADI4 KD cells were incubated with Cl-amidine (200 mM stock; 200 µM final, 506282-10MG, Millipore) for 48h.

Clonogenic cell survival assay

After treatment with Cl-amidine cells were trypsinised (Trypsin-EDTA solution, T3924-500ML, Sigma-Aldrich) and counted (Z2 Coulter-particle count and size analyzer, Beckman Coulter). 300 cells per well in triplicates per condition were seeded in 6-well plates. Cells were incubated 8-9 days, after incubation the cells were washed once with PBS, then stained with 0.1% Coomassie Brilliant Blue (50% (v/v) Methanol, 43% (v/v) H2O, 7% (v/v) Acetic Acid, 0.1% (m/v) Coomassie Brilliant Blue). Colonies were counted using Gelcount (Oxford Optronix).

Proliferation assay

Cell proliferation was assessed using xCelligence RTCA DP (Roche Life Sciences). Briefly, cells were treated with Cl-amidine for 48h and trypsinised and counted. All wells of a special 2-row 96-well plate (E plate VIEW 16, 06 324 738 001, Acea bioscience) were filled with 50 µl pre-warmed medium (DMEM + 10% FCS + pen/strep). The remainder spaces were filled with pre-heated PBS. The plate was put in the xCelligence machine to measure background. 1000 cells/150 µl cell suspension was added to the wells. The cells were adhered for 30' at RT. The plate was put in the machine and measured for 96h with a measurement every 30'.

Immunofluorescence

U2OS were seeded on coverslips and incubated with Cl-amidine for 48h. The cells were radiated with 1 Gy and fixed 1, 2, 4, 8, and 24h after IR. Briefly, the coverslips were washed once with PBS, fixed with 2% PFA, washed with PBS + 0.1% triton X-100 3× short and 2× 10 minutes, once washed with PBS+ (100 ml PBS + 0.5 g BSA + 0.15 g Glycine), incubated 1-2h at RT with primary antibodies. After incubation coverslips were washed with PBS + 0.1% triton X-100 3× short and 2× 10 minutes, once washed with PBS+, incubated 1-2h at RT with secondary antibodies. After incubation coverslips were washed

with PBS + 0.1% triton X-100 3× short and 2× 10', once washed with PBS+. For RAD51 staining the coverslips were washed once with PBS, fixed with 4% PFA. Subsequently, cells were permeabilised for 20' with PBS + 0.2% triton X-100 and washed with PBS. After permeabilization cells were treated with 10× diluted DNAse I (04536282001, Roche Life Sciences) for 1h at 37°C in a humidified chamber and washed with PBS. Blocking was performed using IFF buffer (PBS + 1% BSA + 2% FCS) for at least 30'. After blocking cells were incubated with primary antibodies for 1-2h at RT. After incubation coverslips were washed 3× for 5' with PBS and incubated with secondary antibodies 1-2h at RT. After incubation coverslips were washed 3× for 5' with PBS. Coverslips were mounted in DAPI Vectashield mounting medium (H1200, Vector Laboratories). Images were made using a LSM700 microscope (Carl Zeiss Microimaging Inc.).

Immuno-blot analysis

Cells were lysed in 2× sample buffer and boiled at 99°C for 5 minutes. Samples were run on a SDS-PAGE gel and transferred to a PVDF membrane (Immobilon FL PVDF Transfer membrane 0.45um, IPFL00010, Millipore). Membranes were blocked in 5% milk in PBS for 1-2h at RT. After blocking, membranes were incubated with primary antibodies 1-2h at RT. Then the membranes were washed 5 times for 5 minutes with PBS + 0.05% Tween-20 and incubated with secondary antibodies at RT for 1-2h. Again the membranes were washed 5× for 5 minutes. Membranes were visualized using Odyssey CLx Infrared Imaging System (LI-COR Biosciences). For (phospho-)RPA32 analysis cells were treated with Cl-amidine for 48h. Medium was replaced for medium containing Cl-amidine and 4 mM HU. Cell lysates were made directly, 1h or 5h after HU treatment.

BrdU and PI labelling for cell cycle analysis

Cells were labelled with 5 μM BrdU (B5002, Sigma-Aldrich) for 15 minutes at 37°C. Subsequently, cells were harvested and fixed in 70% ethanol at least overnight at 4°C. Fixed cells were washed with ice-cold PBS and re-suspended in pepsin solution (5 mg pepsin in 10 ml 0.1N HCl) and incubated 20 minutes at RT. After pepsin-treatment blocking solution (PBS + 0.5% Tween-20 + 0.1% BSA) was added and cells were washed. Next, cell were re-suspended in 2N HCl for 12 minutes at 37°C. To neutralise, borate buffer (100 mM, pH8.5) was added and the cells were pelleted. BrdU antibody was added and the cells were incubated for 2h on ice in the dark. Stained cells were washed in blocking solution and re-suspended in 500 μl PBS supplemented with 12.5 μl RNase A and 1 μl PI (P3566, Invitrogen). Cell cycle was analysed the next day using BD LSRFortessa (BD Biosciences). Flow Cytometry data was analysed using FlowJo vX.0.7 (Tree Star Inc.).

Primary antibodies

ATM (500×, #2873, Cell Signaling); p-ATM (500×, #4526, Cell Signaling); BRCA1 (50×, sc-6954, Santa Cruz Biotechnology); BrdU Kit

(50×, 556028, BD Sciences); Geminin (400×, 10802-1-AP, Proteintech); γH2AX (Ser139) (1000×, 05-636, Millipore); p53 (1000×, sc-126, Santa Cruz Biotechnology); RAD51 (200×, GTX70230, GeneTex); RPA32 (2000×, A300-244A, Bethyl Laboratories); phopho-RPA32 (S4/S8) (2000×, A300-245A, Bethyl Laboratories); phospho-RPA32 (S33) (2000×, A300-246A, Bethyl Laboratories); Tubulin (2000×, sc-12462-R, Santa Cruz Biotechnology); Tubulin (5000×, T5168, Sigma-Aldrich)

Secondary antibodies

Goatαmouse Alexa 488 (1000×, A11034, Life Technologies); GoatαRabbit Alexa 555 (1000×, A21429, Life Technologies); Donkeyαmouse IRDye 800CW (5000×, 926-32212, LI-COR Biosciences); Donkeyαrabbit IRDye 680RD (5000×, 926-32223, LI-COR Biosciences)

Apoptosis assay

Apoptotic cells were analysed according to the protocol published by Smid et al. (36). In brief, medium and cells were collected and re-suspended in 998 µl FACS buffer (0.5% BSA + 0.05% NaN3 in PBS) pre-heated to 37°C. 1 µl Hoechst 33342 (10 mg/ml, H3570, Life Technologies) was added and the cells were vortexed and incubated for exactly 7 minutes at 37°C. Subsequently, the cells were immediately placed on ice and 1 µl 7-AAD (1 mg/ml, A1310, Invitrogen) was added. Cells were analysed within 1h after adding 7-AAD using BD LSRFortessa (BD Biosciences). Flow Cytometry data was analysed using FlowJo vX.0.7 (Tree Star Inc.).

RNA isolation, cDNA synthesis and qPCR

Total RNA was isolated using Trizol reagent (TriPure Isolation Reagent, 11667165001, Roche Life Science). In brief cells were lysed in Trizol reagent and chloroform was added. Lysates were spun 12000 g for 15’ at 4°C. The aqueous phase was transferred to a new eppendorf tube and isopropanol was added. The aqueous phase was incubated at RT for 10’, then spun 12000 g for 10’ at 4°C. RNA pellets were washed once with 75% ethanol. After washing RNA pellets were dried and dissolved in 30 µl of RNAse-free H2O. RNA concentration and quality was assessed using Nanodrop (NanoDrop™ 2000/2000c Spectrophotometers, ThermoFischer Scientific). Subsequently, cDNA was made using iScript cDNA Synthesis Kit (170-8891, Biorad) according to the manufacturer’s protocol. qPCR was performed using Platinum® Taq DNA Polymerase (10966018, Invitrogen) according to the manufacturer’s protocol complemented with SYBR Green I (SYBR® Green I nucleic acid gel stain, S9430, Sigma-Aldrich) for detection. The reaction mix was run according to the following cycling program: 3’ - 95°C; 45× 15’’ - 95°C/30’’ - 60°C/30’’ - 72°C; 1’ - 95°C; 1’ - 65°C; 65× 30’’ - 65°C. Data was analyzed using ΔCt method (37).

Primers

	Forward primer (5'-3')	Reversed primer (5'-3')
Mmu-*Padi1*	TAGTGGCGGACACAGTCAGTA	ACAGCAGTTAGGTAGAGCAC
Mmu-*Padi2*	AAGGGGCTATCCTGCTGGT	GACCTTTTCGTCACTACAGTCC
Mmu-*Padi3*	CTACAGAGGATTGTGCGTGTG	AGGAACCGCCCCATAAATGTC
Mmu-*Padi4*	TCTGCTCCTAAGGGCTACACA	GTCCAGAGGCCATTTGGAGG
Hsa-*PADI4*	TTCTCTAAGGCGGAAGCTTTT	AGCAGGGAACACACCTTCTC
Mmu-*Tubg2*	CAGACCAACCACTGCTACAT	AGGGAATGAAGTTGGCCAGT
Mmu-*B2m*	CCCTGGTCTTTCTGGTGCTT	ATTTCAATGTGAGGCGGGTG
Hsa-*GADPH*	AAGGTGAAGGTCGGAGTCAA	ACCATGTAGTTGAGGTCAATG
Hsa-*UbC*	CTGGAAGATGGTCGTACCCTG	GGTCTTGCCAGTGAGTGTCT

End-joining assay

The end-joining assay was performed as described in (38), with some minor changes. In short, cells were grown in a 3-cm dish to 50-80% confluency. Cells were transiently transfected with 2 µg of a blunt-ended linear DNA substrate (EcoRV/Eco47III digested pDvG94 plasmid (38)) using X-treme GENE HP DNA Transfection Reagent (Sigma Aldrich), following manufacturers protocol. Two days after transfection, extrachromosomal DNA was isolated and resuspended in a final volume of 20 µl water (39). From this solution, 1 µl was PCR amplified with the DAR5 and FM30 primers (38), using PuReTaq ready-To-Go PCR beads (GE Healthcare). The PCR product was digested with BstXI. Restriction fragments were separated on a 6% polyacrylamide gel in TBE buffer, stained with ethidium bromide. The relative level of microhomology-directed end-joining was determined by quantification of the BstXI-digested PCR product using the ImageJ software.

Statistical analysis

Data was processed using GraphPad Prism v7.0a (GraphPad Software Inc.). Statistical tests used were Student's T-test and Mann-Whitney U test. P-values equal or lower than 0.05 were accepted as significant.

Results

A general gene expression response after DNA damage

To generate a time-resolved map of differentially expressed genes (DEGs) induced by genotoxic stress we used mES cells because of they are non-transformed, wild-type cells with high proliferation rates in which the effects of DNA damage are immediately present. Therefore, mES cells were exposed to cisplatin, UV-C and IR each with its own spectrum of specific DNA lesions. These genotoxic agents together cover a wide range of DNA lesions, which enable identification of both general as well as lesion-specific genotoxic stress responses. To obtain total RNA for mRNA sequencing we thawed

one vial of mES cells that were grown for two passages on feeder-coated plates followed by one passage on gelatin-coated plates and exposed those cell cultures to cisplatin, UV-C, IR or mock-treatment. Genotoxic stress was applied in equitoxic doses, correlating with 50% survival in a colony formation assay. Total RNA was isolated 4, 8 and 12 hours after treatment. This complete procedure was repeated three times to obtain independent, complete biological replicates for statistical analysis (Fig. 1A). After the raw sequence data was obtained we designed an informatics workflow to identify DEGs (Fig. 1B). Briefly, raw datasets with on average 28 million reads per sample were aligned to the mouse reference genome. More than 70% of all reads could be uniquely mapped. The number of mapped reads to each open reading frame (ORF) was counted and used as input for statistical analysis.

First, we analysed total transcript numbers per sample and observed similar percentages of transcripts in each sample with the expected distribution in classes (on average 69.1% in exonic regions) (Fig. 1C). A Pearson correlation between all conditions showed >94% overlap between different conditions (Supplemental Figure 1), indicating very low technical or biological variation, which could negatively influence data analysis and indicates, as expected, that only a relatively small subset of genes (<10% of total genes) is significantly altered by DNA damage. Next, we performed variation analysis using a principal component analysis (PCA), which shows that samples belonging to the same condition cluster largely together indicating distinct effects on transcription and gene expression (Fig. 1D). PC1 (34.8%) seems to mostly discriminate based on treatment, whereas PC2 (19.2%) appears to predominantly correlate with time. Of note: the PCA indicated that only few DEGs are present 4h after UV-C exposure as seen by its clustering together with the control samples. However, at later time points the UV profiles start to deviate progressively more from the 4h time point. This contrasts with IR, in which the 4h time point deviates quite strongly from mock, but progression in time is relatively modest. The 8h and 12h time points demonstrate that the DEGs induced by UV-C are most similar to mES cells exposed to IR. Furthermore, the PCA indicates that cisplatin treatment results in much more and different DEGs compared to UV and IR.

To further investigate gene expression kinetics after DNA damage, we determined DEGs in all conditions. We only identified 3 DEGs in the 4h UV-C time point consistent with the PCA plot analyses. We calculated correlations between all conditions and clustered them using a dendrogram, using DEG-fold changes over mock-treatment (Fig. 1E). A high correlation in DEGs between all conditions was observed, except for 4h after UV-C. For example, at least 50% of all DEGs identified after IR and cisplatin treatment overlapped in each time point, indicating that the same genes are regulated in the general response to DNA damage. Importantly, most genes that are differentially expressed at 4h after IR and cisplatin were also regulated in the same direction 4h after UV-C, but to a much lesser extent. This indicates that gene expression changes after UV-C is delayed, which is confirmed by comparing correlation values of IR 4h and cisplatin 4h with UV 4h and the correlation

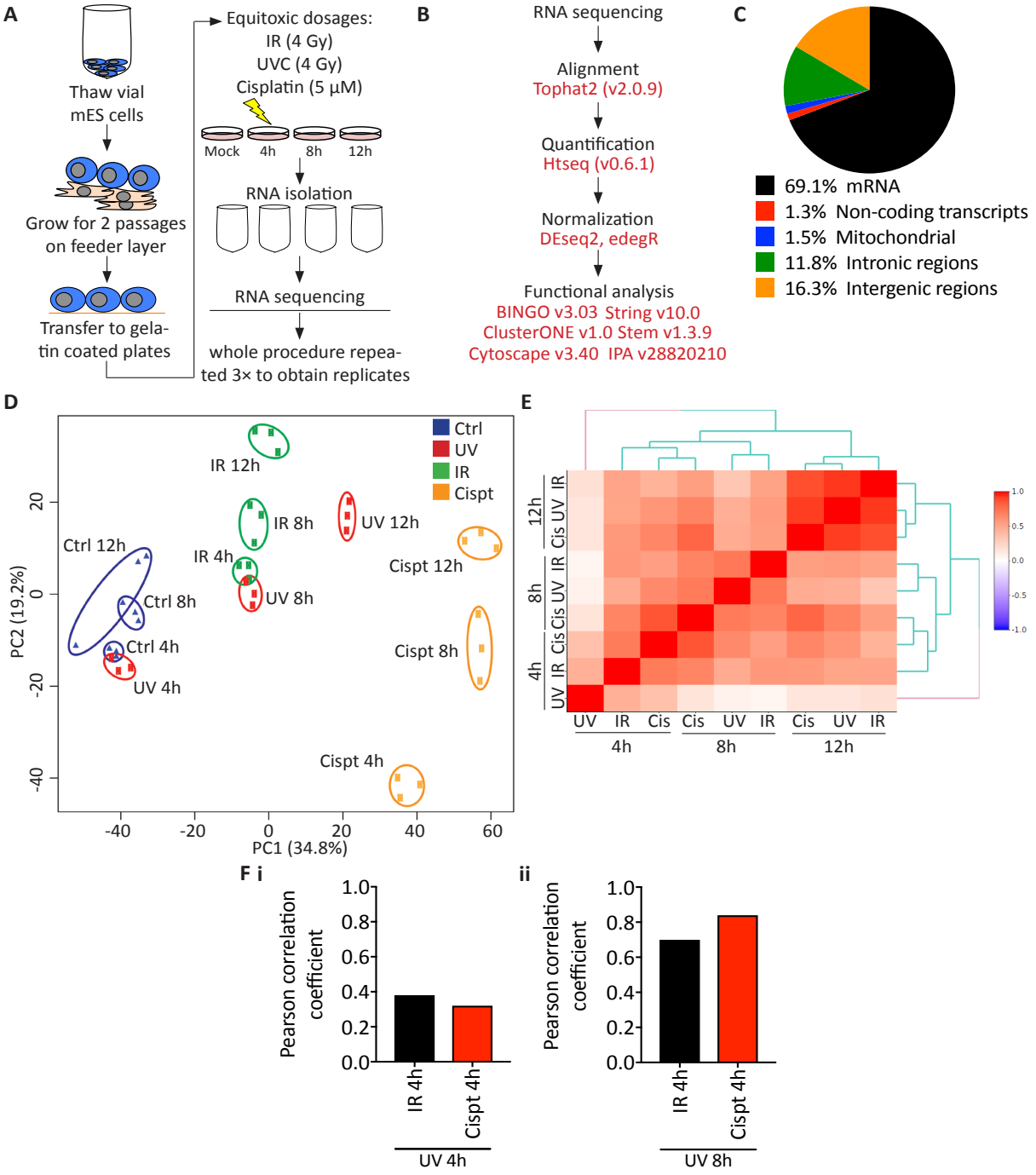

Figure 1: General gene expression profiles after different genotoxic stresses in mES cells. A) Schematic representation of the workflow from cells to RNA. B) Schematic representation of the bioinformatics analysis pipeline. C) Distribution of different RNA classes analysed by mRNA sequencing. D) Principal component analysis of all samples. E) Dendrogram of Pearson correlation coefficient using fold changes of all DEGs in each condition. Fi + ii) Correlation values of IR 4h and cisplatin 4h compared to UV 4h (i) and correlation values of UV 8h compared to IR 4h and cisplatin 4h (ii).

value of UV 8h with IR 4h and cisplatin 4h (Fig. 1Fi + ii). Finally, we observed the strongest overlap in the 12 hour time point across all three genotoxic

stresses, which indicates that although differences between treatments are present in earlier time points, the general gene expression pattern in response to DNA damage evolves and culminates into a common response.

Upstream regulator analysis identifies transcription factors and microRNAs

In order to classify transcriptional programs of the mES cell transcriptome after DNA damage, we performed gene expression pattern clustering using Short Time-series Expression Miner (STEM). STEM identifies significant temporal expression profiles in genes and compares the behaviour of these genes across multiple conditions (32). First, we selected all DEGs from one genotoxic agent and performed a genotoxic stress-based clustering. ~50% of DEGs clustered in one significant pattern, which is a gradual up regulation in all treatments (Fig. 2A). We performed an upstream regulator analysis using ingenuity pathway analysis (IPA) on this cluster and identified predominantly overrepresented transcription factors, growth factors and to a minor extend microRNAs (Fig. 2B). As expected, transcription factors such as TP73 and TP53 were present (Fig. 2C and Supplementary Table 1). In addition, we identified a second significant expression pattern (Fig. 2D), in which DEGs are up regulated only at the 8h and 12h time point. Upstream regulator analysis on the DEGs in these patterns showed a predicted increase of microRNAs (Fig. 2E + F and Supplementary Table 2), suggesting that a subset of genes is regulated by microRNAs after DNA damage.

Canonical pathway analysis of the upstream regulators identified in Fig. 2B and Fig. 2E showed expected pathways related to embryonic cell development such as Wnt/β-catenin signalling and the DDR such as ATM signalling in both analysis (Fig. 2G + H and Supplementary Table 3 and 4). Remarkably, the overlap in upstream regulators between the two expression patterns is ~30%, which indicates that either a transcription factor can establish two different expression patterns or a large proportion of genes are regulated by a secondary process as well.

microRNAs and mRNAs have different expression kinetics upon DNA damage

To confirm the upstream regulator analysis, we performed microRNA sequencing on the very same samples as used for gene expression analysis. We designed an informatics workflow to identify differential expressed microRNAs (DEmiRs) (Fig. 3A). In short, the raw sequencing data with an average of 12 million reads per sample was aligned to the mouse small RNA reference genome (including rRNA, tRNA, miRBase database (microRNA) and piwi-interaction RNA database). On average 73.3% of all reads per sample could be uniquely mapped to the small RNA reference database and statistical analysis identified several DEmiRs (Fig. 3B). In contrast to the PCA plot generated from mRNA expression data (Fig. 1D), the microRNA PCA plot shows a classification per time point rather than genotoxic stress (Fig. 3C). Importantly, the 4h after UV-C condition is similar to the 4h IR and cisplatin conditions, indicating that sam-

A

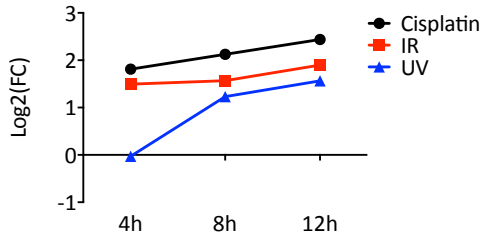

B

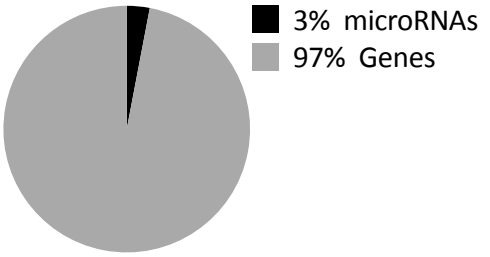

C

Upstream Regulator	Molecule Type	p-value of overlap
TP73	transcription regulator	5,14E-06
MYOG	transcription regulator	2,32E-05
TGFB1	growth factor	1,49E-04
TP53	transcription regulator	3,76E-04
MYF6	transcription regulator	5,47E-04
Sry	transcription regulator	8,32E-04
SREBF1	transcription regulator	1,04E-03
HTT	transcription regulator	1,43E-03
SP1	transcription regulator	1,57E-03
CREBBP	transcription regulator	2,39E-03
TAF7L	transcription regulator	2,75E-03
CUX1	transcription regulator	4,10E-03
SRF	transcription regulator	4,48E-03
SMAD7	transcription regulator	4,75E-03
KMT2D	transcription regulator	4,75E-03
EPC1	transcription regulator	4,80E-03
KLF2	transcription regulator	4,94E-03
BRCA1	transcription regulator	5,20E-03
HR	transcription regulator	6,95E-03
mir-365	microrna	7,85E-03

D

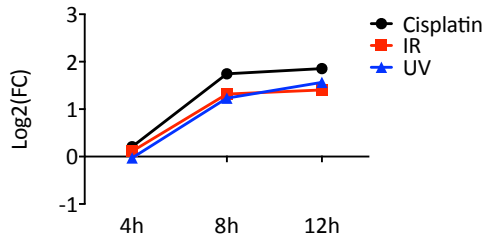

E

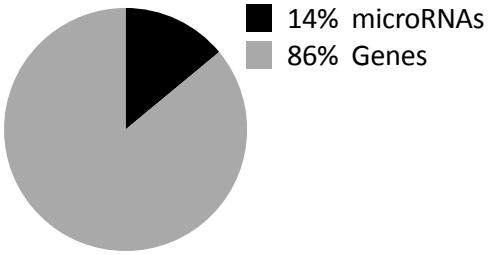

F

Upstream Regulator	Molecule Type	p-value of overlap
SIM1	transcription regulator	8,36E-04
NGF	growth factor	1,78E-03
ARNT2	transcription regulator	3,16E-03
miR-130a	microrna	4,45E-03
PAX7	transcription regulator	4,50E-03
TAL1	transcription regulator	4,64E-03
HDAC4	transcription regulator	5,06E-03
CREB1	transcription regulator	6,71E-03
NOTCH1	transcription regulator	8,55E-03
ISL1	transcription regulator	8,75E-03
NFKBIL1	transcription regulator	9,27E-03
POU5F2	transcription regulator	9,27E-03
OTP	transcription regulator	9,27E-03
miR-675-5p	mature microrna	9,27E-03
miR-688-3p	mature microrna	9,27E-03
mir-668	microrna	9,27E-03
mir-1258	mature microrna	9,27E-03
miR-1343-5p	microrna	9,27E-03
mir-939	microrna	9,27E-03
ZFP36L1	transcription regulator	9,27E-03

G

Ingenuity Canonical Pathways	-log(p-value)
TGF-β Signaling	1,1E01
p38 MAPK Signaling	7,01E00
Aryl Hydrocarbon Receptor Signaling	6,5E00
Sumoylation Pathway	6,2E00
ATM Signaling	6,09E00
Wnt/β-catenin Signaling	5,84E00
p53 Signaling	5,81E00
ERK5 Signaling	5,63E00
Neurotrophin/TRK Signaling	5,26E00
Human Embryonic Stem Cell Pluripotency	5,12E00

H

Ingenuity Canonical Pathways	-log(p-value)
Neurotrophin/TRK Signaling	5,36E00
Human Embryonic Stem Cell Pluripotency	5,24E00
ERK5 Signaling	4,29E00
Circadian Rhythm Signaling	3,8E00
FLT3 Signaling in Hematopoietic Progenitor Cells	3,79E00
FGF Signaling	3,69E00
PPAR Signaling	3,66E00
ATM Signaling	3,6E00
RAR Activation	3,5E00
Embryonic Stem Cell Differentiation into Cardiac Lineages	3,35E00

Figure 2: STEM analysis identifies different expression patterns and leads to identification of upstream regulators and transcription factors. A) STEM analysis of significant up-regulated DEGs in cisplatin, IR and UV treated mES cells. B) Top-20 of predicted upstream regulators of all genes identified in (A). C) Percentage of predicted microRNAs and genes in the upstream regulator analysis identified in (B). D) STEM analysis of 'delayed' up-regulated genes in cisplatin, IR and UV treated mES cells. E) Top-20 of predicted upstream regulators of all genes identified in (D). F) Per-

centage of predicted microRNAs and genes in the upstream regulator analysis identified in (E). G + H) Canonical pathway analysis of the significant upstream regulators identified in (B = G) and (E = H).

ple preparation for mRNA sequencing was performed correctly, since the identical RNA samples were used to analyse microRNA expression. At the same time this indicates that UV, IR and cisplatin treated mES cells have similar and rapid responses at the microRNA level. Similarly, the Pearson correlation plot in which we used the fold change of all DEmiRs per condition shows that time after treatment is the main determinant for microRNA expression (Fig. 3D). This implies that either each four hours another set of microRNAs is regulated in all three genotoxic stresses or the presence of one dominant microRNA signature across all three genotoxic agents. To further dissect these microRNA expression changes we performed a STEM analysis to identify microRNA expression signatures. We identified a large subset of microRNAs (81% of total DEmiRs) exhibiting a single expression signature: up-regulated 4h after DNA damage that returns to basal levels or is down-regulated 8h and 12h after DNA damage (Fig. 3E). Thus, our data indicate that microRNAs act predominantly in the first hours after DNA damage, which verifies and strengthens our previous finding (14).

To examine the observation that microRNAs are mainly active in the first hours after DNA damage on a global scale, we performed an exon-intron split analysis (EISA) that measures changes in mature mRNA (exonic sequences) and pre-mRNA (intronic sequences) across different experimental conditions to quantify transcriptional and post-transcriptional regulation of gene expression (40). While the majority of sequence reads are mapped in exonic regions due to mRNA selection in the procedure, mRNA sequencing also detects some intronic reads (Fig 1C), which serve as a proxy for nascent transcription. Therefore, expression changes between treatment and control were identified separately for exonic (Δexon (treatment – control)) and intronic (Δintron (treatment – control)) reads and the relationship between Δexon and Δintron was investigated. If a gene is regulated at the transcriptional level, we expected an increase or decrease in both the Δexon and Δintron in the same direction, while post-transcriptional regulation results in a decrease or increase in Δexon, but not in Δintron, as transcription of this gene is not affected. Thus, the ratio of Δexon to Δintron can reflect whether genes are under transcriptional or post-transcriptional control, e.g. by microRNAs. Dividing Δexon by Δintron leads to a value in which 1 represents either similar expression levels between control and treatment or gene regulation by transcription. Values <1 indicate increased post-transcriptional silencing, e.g. by microRNAs, and a value >1 indicates decreased post-transcriptional silencing. Indeed, EISA analysis showed that the majority of DEGs 4h after DNA damage had a low ratio of Δexon to Δintron, indicating that post-transcriptional gene regulation is mainly occurring 4h after DNA damage (Fig. 3G). We conclude that microRNA-controlled gene expression acts mainly in the first hours after DNA damage.

Classification of transcriptional responses after DNA damage

We further explored which processes and pathways were altered by DNA damage in mES cells. DEGs that were identified using STEM analysis (Fig. 2A + D) were subjected to canonical pathway analysis using IPA. In both analyses pathways related to embryonic development such as the role of NANOG (Fig. 4A) and Oct4 (Fig. 4B) in mammalian embryonic stem cell pluripotency were identified. In the canonical pathway analysis related to Fig. 2A we also found DDR related pathways such as p53 signalling (Fig. 4A). Interestingly, in the canonical pathway analysis related to Fig. 2D we found pathways re-

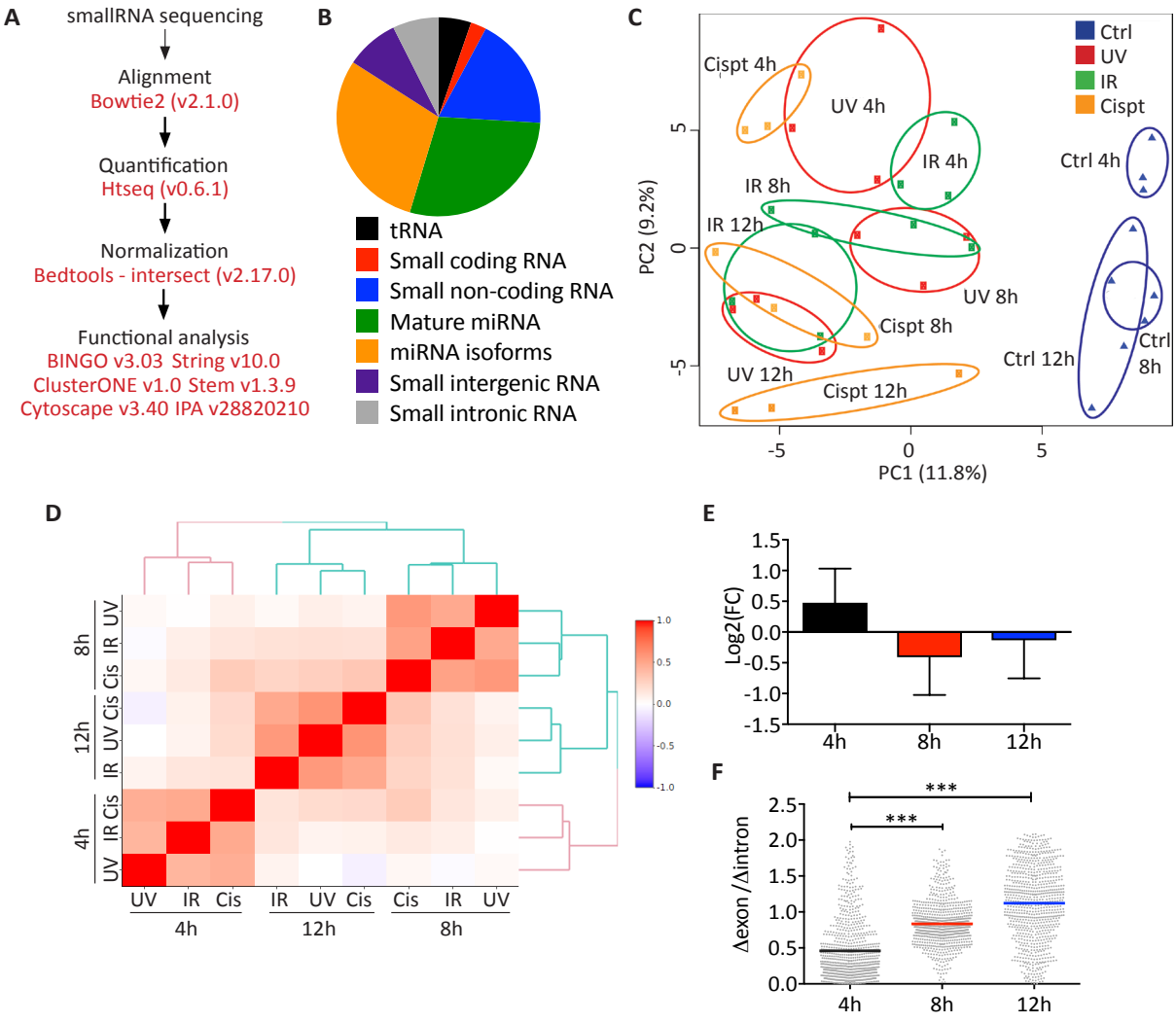

Figure 3: Expression patterns of microRNAs and mRNAs differ after different genotoxic stresses. A) Schematic representation of the bioinformatics pipeline to analyse small RNAs. B) Distribution of different small RNA classes analysed by microRNA sequencing. C) Principal component analysis of differentially expressed microRNAs in all samples. D) Dendrogram of Pearson correlation coefficient using fold changes of all DEmiRs in each condition. E) Dominant pattern in STEM analysis using all differentially expressed microRNAs. F) Exon-intron split analysis.

lated to metabolism such as NAD biosynthesis and Uracil degradation (Fig. 4B). Remarkably, in both analyses protein citrullination was highly significant.

In addition we constructed enriched canonical pathway network by IPA for both Fig. 4A and Fig. 4B. All significant overrepresented canonical pathways were connected if they share at least one gene. As expected, we identified several well-known DDR pathways, such as the p53 pathway (Fig. 4C). Several pathways that are essential for stem cell self-renewal, pluripotency and cellular differentiation (Wnt signalling, Oct4 signalling and NANOG signalling) were linked to damage signalling in this network (Fig. 4C + D), indicating that DNA damage signalling can crosstalk to stem cell self-renewal and pluripotency pathways. Interestingly, one pathway appeared unconnected with the main DNA damage transcriptional network, which is protein citrullination. Protein citrullination was also identified as one of the significant overrepresented canonical pathways in the STEM analysis (Fig. 4A + B). Protein citrullination is the intra-peptide conversion of arginine into the amino acid citrulline (41, 42) and is controlled by the peptidyl arginine deiminase (PADI) enzyme family, which consists of 5 genes. In the analysis of Fig. 4C *PADI1*, *PADI2*, *PADI3* and *PADI4* were found, whereas in Fig. 4D *PADI6* was found in protein citrullination. In summary, GO term and canonical pathway network analysis demonstrates that cell death and terminal differentiation are the main cell fates induced by DNA damage in mES cells. Moreover, several, previously unidentified, GO terms and canonical pathways could be linked to DNA damage signalling, indicating the implication of novel processes in the DDR.

Citrullination inhibition induces replication stress

Protein citrullination is the intra-peptide conversion of arginine into the amino acid citrulline (41, 42) and is controlled by the peptidyl arginine deiminase (PADI) enzyme family, which consists of 5 genes. Arginine to citrulline conversion alters amino acid mass and acidity (arginine is strongly basic, while citrulline is neutral). As a consequence the overall charge and charge distribution of the peptide or protein changes when arginine is converted into citrulline. First, we confirmed differential expression of PADI genes by qRT-PCR in mES cells (Supplementary Fig. 2A + B). Next, we analysed whether PADI gene expression induction is specific for mES cells. We focused on PADI4, the only member that has a known nuclear localization signal (42). We exposed U2OS cell cultures to cisplatin, IR or UV-C and performed qRT-PCR and immunoblot to determine mRNA and protein levels. We observed that PADI4 mRNA and protein levels are increased after DNA damage (Supplementary Fig. 2C – F), indicating that at least PADI4 expression is increased after DNA damage in another cell type as well.

Since 4 out of 5 PADI genes are up-regulated in our dataset, we used Cl-amidine, which is a chemical inhibitor of total citrullination (43). First, we tested if Cl-amidine inhibits citrullination and indeed observed a reduction in citrullinated H3 expression (Supplementary Fig. 2G + H). Next we tested the effect of citrullination inhibition on cellular outcomes such as

A

Ingenuity Canonical Pathways	-log(p-value)
Protein Citrullination	5,47E00
Human Embryonic Stem Cell Pluripotency	3,56E00
Regulation of the Epithelial-Mesenchymal Transition Pathway	2,9E00
Superpathway of Inositol Phosphate Compounds	2,84E00
GP6 Signaling Pathway	2,74E00
PCP pathway	2,73E00
Phospholipases	2,69E00
Role of NANOG in Mammalian Embryonic Stem Cell Pluripotency	2,53E00
Eicosanoid Signaling	2,49E00
eNOS Signaling	2,35E00
Antioxidant Action of Vitamin C	1,88E00
3-phosphoinositide Biosynthesis	1,85E00
p53 Signaling	1,81E00
D-myo-inositol-5-phosphate Metabolism	1,7E00
Endothelin-1 Signaling	1,64E00
Notch Signaling	1,63E00
Dopamine Receptor Signaling	1,62E00
Wnt/β-catenin Signaling	1,54E00
Sorbitol Degradation I	1,54E00
Gustation Pathway	1,5E00
D-myo-inositol (1,4,5)-Trisphosphate Biosynthesis	1,37E00
VEGF Family Ligand-Receptor Interactions	1,37E00
Pregnenolone Biosynthesis	1,34E00
nNOS Signaling in Neurons	1,33E00

B

Ingenuity Canonical Pathways	-log(p-value)
Tryptophan Degradation to 2-amino-3-carboxymuconate Semialdehyde	2,65E00
NAD biosynthesis II (from tryptophan)	2,09E00
Role of Oct4 in Mammalian Embryonic Stem Cell Pluripotency	2,06E00
G-Protein Coupled Receptor Signaling	1,85E00
Cholecystokinin/Gastrin-mediated Signaling	1,85E00
cAMP-mediated signaling	1,73E00
Tryptophan Degradation III (Eukaryotic)	1,69E00
Tetrahydrobiopterin Biosynthesis I	1,56E00
Tetrahydrobiopterin Biosynthesis II	1,56E00
L-serine Degradation	1,56E00
TNFR2 Signaling	1,51E00
TREM1 Signaling	1,5E00
GP6 Signaling Pathway	1,45E00
Uracil Degradation II (Reductive)	1,44E00
Thymine Degradation	1,44E00
Protein Citrullination	1,35E00

C

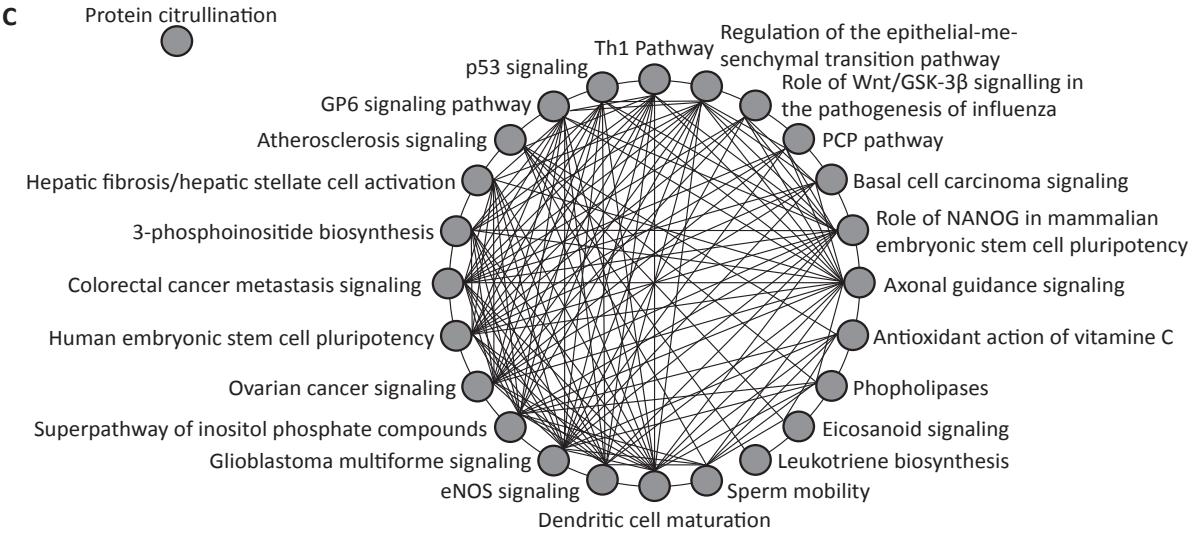

D

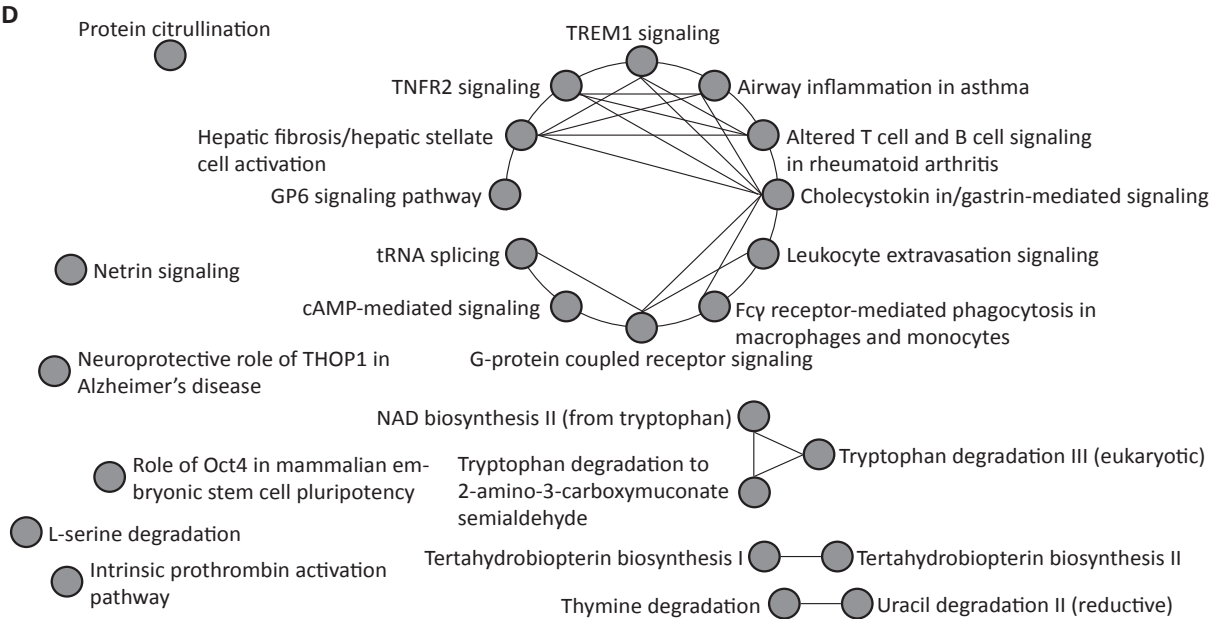

Figure 4: Protein citrullination is a novel process in the DDR. A) Canonical pathway analysis of genes identified in Fig. 2A. All significant canonical pathways are depicted. B) Canonical pathway analysis of genes identified in Fig. 2D. All significant canonical pathways are depicted. C) Network analysis of significant canonical pathways ($p<0.05$) by IPA of overlapping DEGs identified in Fig. 2A. D) Network analysis of significant canonical pathways ($p<0.05$) by IPA of overlapping DEGs identified in Fig. 2D.

proliferation, apoptosis and cell cycle and noted reduced proliferation (Fig. 5A). In accordance with reduced proliferation, we observed a significant decrease in clonogenicity by citrullination inhibition (Fig. 5B). Similar results were obtained by a siRNA against PADI4 (data not shown). Reduced colony forming capacity could be explained by increased apoptosis. However, we failed to observe increased apoptosis (Fig. 5C), indicating that a cell cycle arrest rather than apoptosis is involved. Insteas, we observed a higher proportion of cells in S-phase after citrullination inhibition. Thus, our data indicate that citrullination facilitates progression through S-phase.

Cell cycle stalling in S-phase could indicate that inhibition of citrullination induces replication stress. RPA32 phosphorylation of serine 33 (Ser^{33}) and serine 4/8 (Ser^{4}/Ser^{8}) is induced by replication stress, which is a mark for stalled or collapsed replication forks, respectively (44, 45). To determine whether inhibition of citrullination affected replication stress, we treated cells with 4 mM hydroxyurea (HU) for 1h (enrichment for stalled replication forks) and 5h (enrichment for collapsed replication forks) in the presence or absence of inhibition of citrullination. HU exposure for 1h already led to an increase in stalled replication forks as represented by phospho-Ser33 (Fig. 5E). 5h after HU exposure both stalled and collapsed replication forks (represented by phospho-$Ser^{4/8}$) are significantly increased after citrullination inhibition. Together, these data indicate that protein citrullination is necessary in maintaining replication forks.

Citrullination inhibition reduces DSB repair during S-phase

Citrullination facilitates progression through S-phase. All three genotoxic agents used in this study block DNA synthesis, leading to stalled and collapsed replication forks. Collapsed replication forks will result in DSBs and require DSB repair to correct the damage and replication fork restart to continue DNA synthesis. We determined DSB levels after inhibition of citrullination by γH2AX foci formation. To discriminate between G1-phase and S/G2-phase cells we co-stained with geminin in which geminin-negative cells represent G1-phase cells, whereas geminin-positive cells represent S/G2-phase cells (46). We observed 11-fold more γH2AX foci after citrullination inhibition in S/G2-phase cells (Fig. 6A; Supplementary Fig. 3A). The increase in DSBs during S-phase could be due to persistent DSBs in the G1-phase that are transferred to S-phase or to poor repair of DSBs in S-phase. We only observed a modest 1.7 fold increase in γH2AX foci in G1-phase cells by citrullination inhibition, indicating that DNA repair in S-phase is not defective (Fig. 6B; Supplementary Fig. 3A). Next, we assessed DSB repair in both G1-phase and S/G2-phase cells by applying an additional dose of IR and monitoring γH2AX foci clearance in time, which is an indication of DSB repair

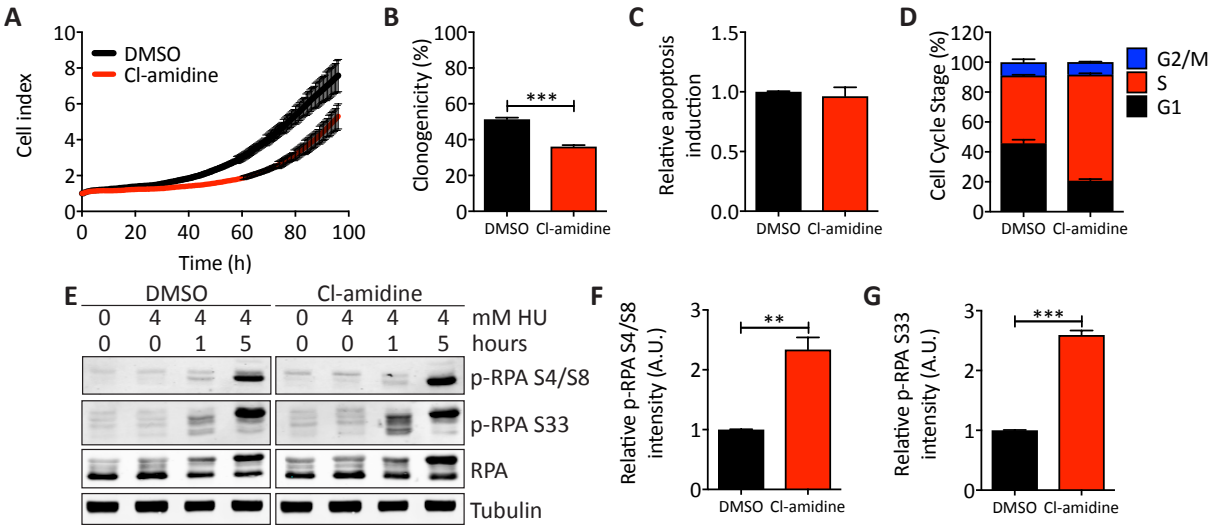

Figure 5: Inhibition of protein citrullination leads to replication stress. A) U2OS cells were incubated with DMSO or Cl-amidine for 48h and proliferation rate was measured for 96h. B) Colony forming assay with or without Cl-amidine, colonies were fixed 8-9 days later. C) Apoptosis assay based on Hoechst 33342 and 7-AAD labelling 48h after citrullination inhibition. D) Cell cycle analysis based on BrdU and PI labelling 48h after Cl-amidine treatment in U2OS cells. E – F) Analysis and quantification of replication fork stalling or collapsed replication forks. Cl-amidine treated cells (48h incubation with Cl-amidine prior HU treatment) were incubated with 4 mM HU for 1h or 5h. WCE-based immunoblot for total RPA and phosphorylated RPA (S4/8 and S33). All experiments were performed at least three times. Mean ± SEM are indicated. ** P<0.01; *** P<0.001

capacity. DSB repair in G1-phase cells was only modestly slower by citrullination inhibition (Fig. 6C). Interestingly, in S/G2-phase cells γH2AX foci were increased by IR and remained present up to 24h after inhibition of citrullination (Fig 6D), indicating that DSB repair in S/G2-phase cells was impaired. We conclude that citrullination is required for DSB repair during S/G2 phase.

The observation that citrullination is probably important for DSB repair in S/G2-phase, likely implicates DDR activation in which DNA damage checkpoint kinase ATM plays a central role. Therefore, we stained for activated phosphorylated ATM (S1981) and ATM target proteins that are phosphorylated on SQ/TQ motifs. We observed increased numbers of phospho-ATM and phospho-SQ/TQ foci were present at basal levels (Fig. 6E + F; Supplementary Fig. 3B). Interestingly, the general kinetics of p-ATM and p-SQ/TQ foci induction and clearance after IR was similar between control and citrullination inhibited cells, indicating that ATM signalling itself is not affected.

DSBs are repaired by NHEJ in all phases of the cell cycle, while HR repairs DSBs only in S/G2-phase. We first analysed whether citrullination inhibition leads to NHEJ defects by monitoring 53BP1 foci formation after IR. 53BP1 in DSB foci directs DSB repair choice towards NHEJ (47). Both G1- and S/G2-phase cells showed only a modest increase in basal 53BP1 foci at un-irradiated levels by inhibition of citrullination. After IR however, we observed increased 53BP1 foci formation directly after IR independent of cell cycle phase after citrullination inhibition and

normal repair kinetics (Fig. 6G + H; Supplementary Fig. 3C), indicating that NHEJ is not affected and might even compensate for a putative repair defect of other DSB repair pathways. Indeed, a plasmid-based end-joining assay demonstrated normal and functional NHEJ (Fig. 6I) (38).

The increase in DSBs primarily in S/G2-phase cells suggests that HR, which can only repair DSBs in S/G2 when a sister chromatid is present, is reduced by inhibition of citrullination. We monitored foci formation of HR proteins BRCA1 and RAD51 at base line as well as after IR. Both BRCA1 and RAD51 foci were already increased in unirradiated cells after citrullination inhibition, which is in agreement with the elevated γH2AX foci levels (Fig. 6J + 6K; Supplementary Fig. 3D). After IR, citrullination inhibition resulted only in a modestly increased number of BRCA1 foci and a slight decrease of BRCA1 foci in time, suggesting a mild HR defect (Fig. 6J). Although RAD51 foci exhibited different kinetics compared to BRCA1 foci after IR, an altered HR response was also apparent. RAD51 foci were induced by IR, but were not cleared (Fig. 6K), indicating that HR is stalled at the RAD51 level. Together the data indicate that citrullination is important for proper HR repair of DSBs in S/G2-phase. Insufficient HR is probably leading to collapsed replication forks.

Discussion

Here, we generated a time-resolved transcriptional map of the cellular response to DNA damage in mES cells. These extensive RNA sequencing datasets will not only be a major resource to identify novel pathways in the DDR, but can also be used to analyse DDR-related diseases such as cancer or medical treatments that utilize or generate DNA damage such as cancer therapy or ischemia reperfusion injury. Several studies have been published in which gene and/or microRNA expression profiling have been performed after DNA damage. However, each study uses different time points, cell types, genotoxic stresses, dosages and technologies to generate expression profiles (23, 48-54). Hence, comparisons between studies to derive specific DNA damage-induced transcriptional signatures are hampered. Our experimental design allows us to compare different types of genotoxic stresses, each with their own spectrum of DNA lesions, in the first 12 hours of the transcriptional response to DNA damage. Such a design could furthermore discriminate RNA expression responses induced by DNA damage from possible side effects, since genotoxic agents are usually not only damaging DNA. Cisplatin can also damage proteins and RNAs, IR generates oxidative stress that damages all cellular macromolecules and UV-C also damages RNA and lipid membranes. These side effects are likely to elicit additional cellular responses, including transcriptional alterations. Indeed, differences between genotoxic agents are apparent. The general transcriptional DDR map deduced from those three genotoxic agents however, contains several pathways known to respond to DNA damage of which the P53 pathway is the best-studied example.

This study provides a mechanistic framework of the transcriptional

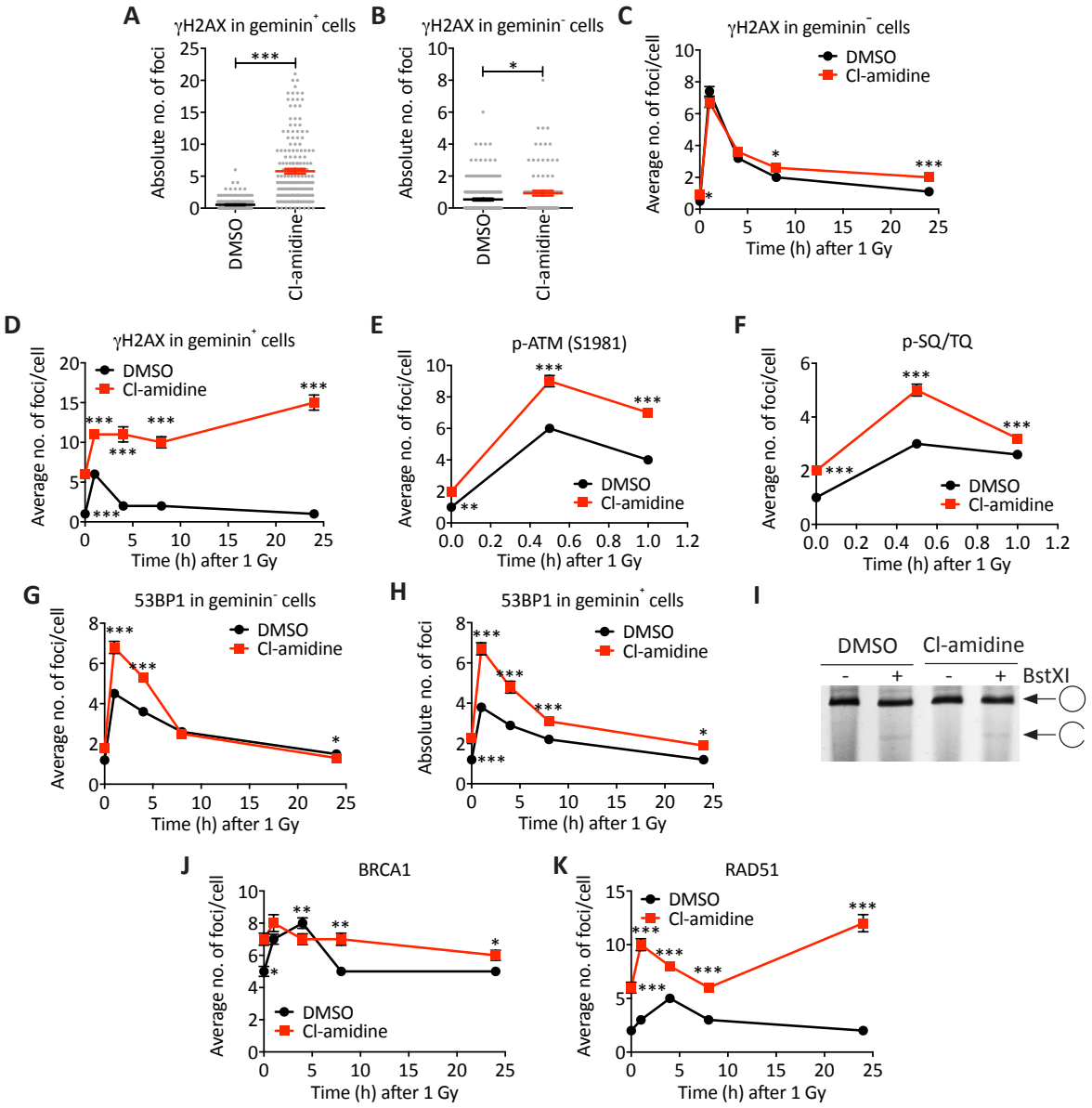

Figure 6: More spontaneous DSBs and reduced DNA repair in S-phase after protein citrullination inhibition. A + B) γH2AX foci formation G1-phase cells (A) and S-/G2-phase U2OS cells (B) 48h after Cl-amidine treatment using immunofluorescent staining. At least 50 cells per experiment were quantified using Image J imaging software. C + D) Kinetics of γH2AX foci formation after additional IR over time in G1- (C) and S-/G2-phase (D) cells 48h after Cl-amidine treatment using immunofluorescent staining. At least 50 cells per experiment were quantified using Image J software. E + F) p-ATM (S1981) (E) and p-SQ/TQ (F) foci kinetics 48 after Cl-amidine treatment and additional IR using immunofluorescent staining. At least 50 cells per experiment were quantified using Image J imaging software. G + H) Kinetics of 53BP1 foci formation after additional IR over time in G1- (G) and S-/G2-phase (H) cells 48h after Cl-amidine treatment using immunefluorescent staining. At least 50 cells per experiment were quantified using Image J software. I) Plasmid-based end joining assay 48h after Cl-amidine treatment. J + K) Kinetics of BRCA1 (J) and RAD51 (K) foci formation after additional IR over time in S-/G2-phase cells 48h after Cl-amidine treatment using immunefluorescent staining. At least 50 cells per experiment were quantified using Image J software. All experiments were performed at least three times. Mean ± SEM are indicated. * P<0.05; ** P<0.01; *** P<0.001

DDR in mES cells (Fig. 7). The most dominant gene expression signature that represents most DEGs is a linear up-regulation across time. Furthermore, two additional gene expression signatures were found: a gradual up regulation starting from 8h onwards with a lag at 4h and a gradual down regulation of genes. The high overlap between DEGs 12h after treatment compared to earlier time points indicates that all three types of genotoxic stress, each with their own characteristics and expression kinetics, culminate into a single end point. Although gene expression changes were highly similar across time and different genotoxic stresses, some noticeable differences were observed in which the virtual absence of DEGs 4 hours after UV-C treatment was most obvious. The experimental set up renders technical errors as unlikely. Moreover, many DEGs that were identified 4h after IR and cisplatin treatment were already regulated in the same direction 4h after UV-C exposure (Fig. 1E), but to a much lesser extent. Finally, the identification of DEmiRs from the identical 4h UV-C treated samples that are overlapping with IR and cisplatin also argue against technical errors. Thus, we conclude that the transcriptional response to a dose of 4 J/m2 UV-C in mES cells is delayed.

The observed delayed UV-response in mES cells could be explained by

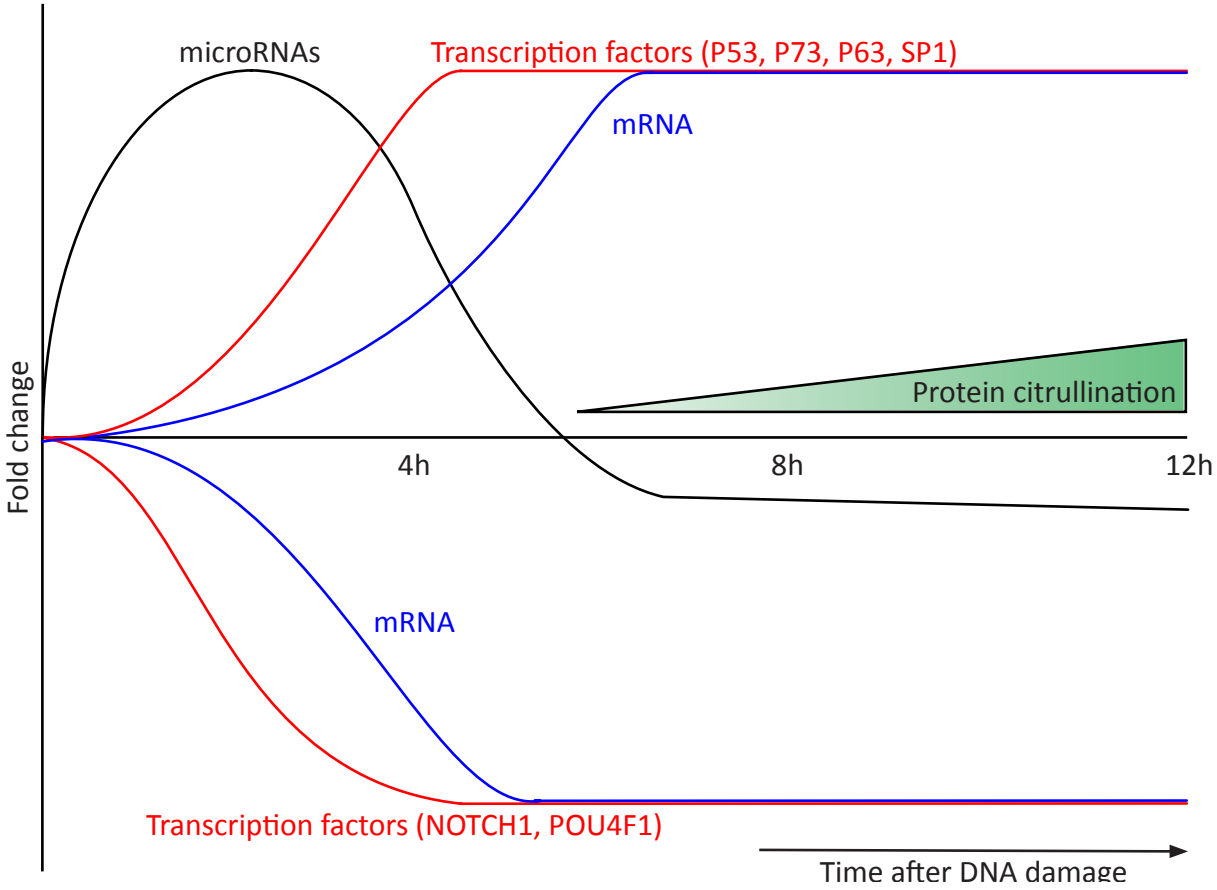

Figure 7: Schematic representation of microRNA and mRNA expression patterns over time after DNA damage. Gene and microRNA expression patterns after DNA damage are visualized, including upstream regulators, canonical pathways and citrullination. Protein citrullination as seen by PADI gene expression is also indicated.

DDR characteristics that are induced by UV-lesions. UV-lesions can induce DDR signalling by blocking DNA replication, leading to replication fork collapse and DDR signalling or by blocking transcription, which also poses a signal for DDR activation (2, 18, 55). Specialized trans-lesion DNA polymerases bypass damaged DNA during S-phase, which initially prevents replication fork arrest and DDR activation (56). In addition, nucleotide excision repair (NER) is the main DNA repair machinery to repair UV-lesions. NER consists of two sub-branches: transcription-coupled NER (TC-NER) that repairs UV-lesions in transcribed DNA strands and global genome NER (GG-NER), which repairs UV-lesions across the genome (18). Since mES cells rely more on GG-NER and to a lesser extent on TC-NER in combination with trans-lesion synthesis (24), it is conceivable that the transcriptional response elicited by TC-NER is delayed. Studies that have identified DEGs early after UV treatment all use much higher doses UV, which could accelerate the transcriptional response.

In addition to the specific transcriptional signatures themselves, we identified several significantly overrepresented upstream regulators that were predicted to control the expression of the identified DEGs. As expected, the P53 pathway was identified, but also transcription factors that control stem cell self-renewal, pluripotency and terminal differentiation. Moreover, our analyses predicted that microRNAs could control numerous DEGs as well. Small RNA sequencing of the identical samples used for mRNA sequencing and subsequent analyses showed that a single dominant microRNA signature was induced after DNA damage in general, in which DEmiR expression is increased 4 hours after genotoxic stress treatment and returned to basal levels at 8 and 12 hours. This is further strengthened by microRNA-gene interaction analysis, demonstrating that many DEGs are under microRNA control in the first hours after damage. This is in agreement with our earlier proposed model in which microRNAs act between the fast protein post-translational modification responses and relatively slow transcription activation/repression (14). The observed fast and transient induction of microRNAs themselves is likely due to post-transcriptional regulation. Specialized microRNA-binding proteins can bind specific primary microRNA transcripts from the nuclear pool and present them to the microRNA biogenesis/maturation pathway. Both the DNA damage checkpoint proteins ATM and p53 are shown to control post-transcriptional microRNA expression via this mechanism (16, 57). These microRNA kinetics could have several implications for the DDR. For example, microRNA expression induction likely contributes to the timing of gene expression and thereby the timing of or fine-tuning specific steps in the DDR. Moreover, these microRNAs are likely acting in concert with transcription factors, since several predicted upstream transcription factors are also target genes of these microRNAs. Thus, this study favours a model in which DDR-related transcription factors activate a general gene expression response, while microRNAs control the fine-tuning and timing of these events in the first hours after DNA damage exposure.

Finally, we also mapped significantly overrepresented pathways. Indeed, we observed several expected pathways such as P53 signalling. Mo-

reover, overrepresented pathways also demonstrated the various cell fates associated with DNA damage in mES cells. The applied equitoxic doses of genotoxic stresses will lead to ~50% mES cell survival in a colony survival assay and ~50% of mES cells that cannot form colonies due to cell death or terminal differentiation. The latter two cell fates of DNA damage in mES cells are well reflected in the transcriptional signature of DNA damage. The transcriptional changes induced by genotoxic stress in mES cells implicates several new cellular processes in the DDR such as protein citrullination, the intra-peptidal conversion of arginine into citrulline by PADI enzymes. It has been shown that PADI4 expression is induced by P53, which lead to subsequent histone modifications, which opened chromatin structure (58-60). We provide evidence that citrullination is required for replication fork stability. Chemical inhibition of citrullination enhances cell cycle stalling in S-phase and replication fork stalling and collapse, particularly for IR and cisplatin. DNA lesions induced by the used genotoxic stresses will block the DNA polymerase machinery, which stalls replication and lead to replication fork collapse and associated DSBs. It is conceivable that citrullination is not needed for replication fork restart, but repair of these collapsed replication forks. Indeed, we observed that DNA damage-induced DSBs are poorly repaired in S and G2-phase cells after inhibition of protein citrullination. We show that both γH2AX and RAD51 foci are not resolved as well, indicating that DSBs are poorly repaired likely due to a homologous recombination deficiency. The exact molecular mechanism by which citrullination is required in the HR pathway is not known. Whether DSB repair by HR is attenuated or RAD51 and γH2AX foci are not properly cleared from the site of damage remain an open question. It is also conceivable that RAD51 is not translocated from the repaired double-stranded DNA (dsDNA). Translocation of RAD51 from dsDNA is performed by RAD54 and loss of RAD54 leads to an accumulation of RAD51 independent of DNA damage sites (61). Thus, we propose that up regulation of PADI enzymes after DNA damage will facilitate replication fork repair by enhancing HR. In conclusion, we generated an extensive resource that describes the transcriptional responses, pathways and upstream regulators after genotoxic stress exposure in mES cells. We provide a mechanistic framework of gene and microRNA expression in the DDR, including the identification of new processes. This will not only serve as a resource for future DDR studies, but can also be used to analyse cancer and cancer therapy responses.

Acknowledgements

The authors would like to thank the Molecular Genetics department of the Erasmus Medical Center Rotterdam and the members of the Center for Biomics of the Erasmus Medical Center for their help with sequencing.for their contributions to the manuscript. This research was supported by the Dutch Cancer Society (KWF) grant nr. 2011-5030.

Disclosure

The authors declare no conflict of interest.

References

1. Hoeijmakers JH. DNA damage, aging, and cancer. The New England journal of medicine. 2009;361(15):1475-85.
2. Hoeijmakers JH. Genome maintenance mechanisms for preventing cancer. Nature. 2001;411(6835):366-74.
3. Campisi J. Aging, tumor suppression and cancer: high wire-act! Mechanisms of ageing and development. 2005;126(1):51-8.
4. Wingert S, Rieger MA. Terminal differentiation induction as DNA damage response in hematopoietic stem cells by GADD45A. Experimental hematology. 2016;44(7):561-6.
5. Blanpain C, Mohrin M, Sotiropoulou PA, Passegue E. DNA-damage response in tissue-specific and cancer stem cells. Cell stem cell. 2011;8(1):16-29.
6. Woods D, Turchi JJ. Chemotherapy induced DNA damage response: convergence of drugs and pathways. Cancer biology & therapy. 2013;14(5):379-89.
7. Pressly JD, Park F. DNA repair in ischemic acute kidney injury. American journal of physiology Renal physiology. 2017;312(4):F551-F5.
8. Vermeij WP, Hoeijmakers JH, Pothof J. Genome Integrity in Aging: Human Syndromes, Mouse Models, and Therapeutic Options. Annual review of pharmacology and toxicology. 2016;56:427-45.
9. O'Driscoll M. Diseases associated with defective responses to DNA damage. Cold Spring Harbor perspectives in biology. 2012;4(12).
10. Marechal A, Zou L. DNA damage sensing by the ATM and ATR kinases. Cold Spring Harbor perspectives in biology. 2013;5(9).
11. Oberle C, Blattner C. Regulation of the DNA Damage Response to DSBs by Post-Translational Modifications. Current genomics. 2010;11(3):184-98.
12. Williams AB, Schumacher B. p53 in the DNA-Damage-Repair Process. Cold Spring Harbor perspectives in medicine. 2016;6(5).
13. Purvis JE, Karhohs KW, Mock C, Batchelor E, Loewer A, Lahav G. p53 dynamics control cell fate. Science. 2012;336(6087):1440-4.
14. Pothof J, Verkaik NS, van IW, Wiemer EA, Ta VT, van der Horst GT, et al. MicroRNA-mediated gene silencing modulates the UV-induced DNA-damage response. The EMBO journal. 2009;28(14):2090-9.
15. Bartel DP. MicroRNAs: target recognition and regulatory functions. Cell. 2009;136(2):215-33.
16. Zhang X, Wan G, Berger FG, He X, Lu X. The ATM kinase induces microRNA biogenesis in the DNA damage response. Molecular cell. 2011;41(4):371-83.
17. Ward JF. DNA damage produced by ionizing radiation in mammalian cells: identities, mechanisms of formation, and reparability. Progress in nucleic acid research and molecular biology. 1988;35:95-125.
18. Marteijn JA, Lans H, Vermeulen W, Hoeijmakers JH. Understanding nucleotide excision repair and its roles in cancer and ageing. Nature reviews Molecular cell biology. 2014;15(7):465-81.
19. Schwarz T. UV light affects cell membrane and cytoplasmic targets. Journal of photochemistry and photobiology B, Biology. 1998;44(2):91-6.
20. Reisz JA, Bansal N, Qian J, Zhao W, Furdui CM. Effects of ionizing radiation on biological molecules--mechanisms of damage and emerging methods of detection. Antioxidants & redox signaling. 2014;21(2):260-92.
21. Roberts JJ, Friedlos F. Quantitative estimation of cisplatin-induced DNA interstrand cross-links and their repair in mammalian cells: relationship to toxicity. Pharmacology & therapeutics. 1987;34(2):215-46.
22. Li H, Zhao Y, Phillips HI, Qi Y, Lin TY, Sadler PJ, et al. Mass spectrometry evidence for cisplatin as a protein cross-linking reagent. Analytical chemistry. 2011;83(13):5369-76.
23. Kruse JJ, Svensson JP, Huigsloot M, Giphart-Gassler M, Schoonen WG, Polman JE, et al. A portrait of cisplatin-induced transcriptional changes in mouse embryonic stem cells reveals a dominant p53-like response. Mutation research. 2007;617(1-2):58-70.
24. de Waard H, Sonneveld E, de Wit J, Esveldt-van Lange R, Hoeijmakers JH, Vrieling H, et al. Cell-type-specific consequences of nucleotide excision repair deficiencies: Embryonic stem cells versus fibroblasts. DNA repair. 2008;7(10):1659-69.
25. Carreras Puigvert J, von Stechow L, Siddappa R, Pines A, Bahjat M, Haazen LC, et al. Systems biology approach identifies the kinase Csnk1a1 as a regulator of the DNA damage response in embryonic stem cells. Science signaling. 2013;6(259):ra5.
26. Trapnell C, Pachter L, Salzberg SL. TopHat: discovering splice junctions with RNA-Seq. Bioinformatics. 2009;25(9):1105-11.

27. Trapnell C, Williams BA, Pertea G, Mortazavi A, Kwan G, van Baren MJ, et al. Transcript assembly and quantification by RNA-Seq reveals unannotated transcripts and isoform switching during cell differentiation. Nature biotechnology. 2010;28(5):511-5.
28. Robinson MD, McCarthy DJ, Smyth GK. edgeR: a Bioconductor package for differential expression analysis of digital gene expression data. Bioinformatics. 2010;26(1):139-40.
29. Love MI, Huber W, Anders S. Moderated estimation of fold change and dispersion for RNA-seq data with DESeq2. Genome biology. 2014;15(12):550.
30. Ritchie ME, Phipson B, Wu D, Hu Y, Law CW, Shi W, et al. limma powers differential expression analyses for RNA-sequencing and microarray studies. Nucleic acids research. 2015;43(7):e47.
31. Law CW, Chen Y, Shi W, Smyth GK. voom: Precision weights unlock linear model analysis tools for RNA-seq read counts. Genome biology. 2014;15(2):R29.
32. Ernst J, Bar-Joseph Z. STEM: a tool for the analysis of short time series gene expression data. BMC bioinformatics. 2006;7:191.
33. Mi H, Huang X, Muruganujan A, Tang H, Mills C, Kang D, et al. PANTHER version 11: expanded annotation data from Gene Ontology and Reactome pathways, and data analysis tool enhancements. Nucleic acids research. 2017;45(D1):D183-D9.
34. Shannon P, Markiel A, Ozier O, Baliga NS, Wang JT, Ramage D, et al. Cytoscape: a software environment for integrated models of biomolecular interaction networks. Genome research. 2003;13(11):2498-504.
35. Maere S, Heymans K, Kuiper M. BiNGO: a Cytoscape plugin to assess overrepresentation of gene ontology categories in biological networks. Bioinformatics. 2005;21(16):3448-9.
36. Schmid I, Uittenbogaart C, Jamieson BD. Live-cell assay for detection of apoptosis by dual-laser flow cytometry using Hoechst 33342 and 7-amino-actinomycin D. Nature protocols. 2007;2(1):187-90.
37. Livak KJ, Schmittgen TD. Analysis of relative gene expression data using real-time quantitative PCR and the 2(-Delta Delta C(T)) Method. Methods. 2001;25(4):402-8.
38. Verkaik NS, Esveldt-van Lange RE, van Heemst D, Bruggenwirth HT, Hoeijmakers JH, Zdzienicka MZ, et al. Different types of V(D)J recombination and end-joining defects in DNA double-strand break repair mutant mammalian cells. Eur J Immunol. 2002;32(3):701-9.
39. van Gent DC, Ramsden DA, Gellert M. The RAG1 and RAG2 proteins establish the 12/23 rule in V(D)J recombination. Cell. 1996;85(1):107-13.
40. Gaidatzis D, Burger L, Florescu M, Stadler MB. Analysis of intronic and exonic reads in RNA-seq data characterizes transcriptional and post-transcriptional regulation. Nature biotechnology. 2015;33(7):722-9.
41. Gyorgy B, Toth E, Tarcsa E, Falus A, Buzas EI. Citrullination: a posttranslational modification in health and disease. The international journal of biochemistry & cell biology. 2006;38(10):1662-77.
42. Vossenaar ER, Zendman AJ, van Venrooij WJ, Pruijn GJ. PAD, a growing family of citrullinating enzymes: genes, features and involvement in disease. BioEssays : news and reviews in molecular, cellular and developmental biology. 2003;25(11):1106-18.
43. uo Y, Arita K, Bhatia M, Knuckley B, Lee YH, Stallcup MR, et al. Inhibitors and inactivators of protein arginine deiminase 4: functional and structural characterization. Biochemistry. 2006;45(39):11727-36.
44. Anantha RW, Vassin VM, Borowiec JA. Sequential and synergistic modification of human RPA stimulates chromosomal DNA repair. The Journal of biological chemistry. 2007;282(49):35910-23.
45. Kim TM, Son MY, Dodds S, Hu L, Hasty P. Deletion of BRCA2 exon 27 causes defects in response to both stalled and collapsed replication forks. Mutation research. 2014;766-767:66-72.
46. McGarry TJ, Kirschner MW. Geminin, an inhibitor of DNA replication, is degraded during mitosis. Cell. 1998;93(6):1043-53.
47. Brandsma I, Gent DC. Pathway choice in DNA double strand break repair: observations of a balancing act. Genome integrity. 2012;3(1):9.
48. Melis JP, Derks KW, Pronk TE, Wackers P, Schaap MM, Zwart E, et al. In vivo murine hepatic microRNA and mRNA expression signatures predicting the (non-)genotoxic carcinogenic potential of chemicals. Archives of toxicology. 2014;88(4):1023-34.
49. Li G, Qiu Y, Su Z, Ren S, Liu C, Tian Y, et al. Genome-wide analyses of radioresistance-associated miRNA expression profile in nasopharyngeal carcinoma using next generation deep sequencing. PloS one. 2013;8(12):e84486.
50. Hart M, Nolte E, Wach S, Szczyrba J, Taubert H, Rau TT, et al. Comparative microRNA profiling of prostate carcinomas with increasing tumor stage by deep sequencing. Molecular cancer research : MCR. 2014;12(2):250-63.
51. Liu Q, Ullery J, Zhu J, Liebler DC, Marnett LJ,

Zhang B. RNA-seq data analysis at the gene and CDS levels provides a comprehensive view of transcriptome responses induced by 4-hydroxynonenal. Molecular bioSystems. 2013;9(12):3036-46.
52. Kanematsu S, Tanimoto K, Suzuki Y, Sugano S. Screening for possible miRNA-mRNA associations in a colon cancer cell line. Gene. 2014;533(2):520-31.
53. Kenzelmann Broz D, Spano Mello S, Bieging KT, Jiang D, Dusek RL, Brady CA, et al. Global genomic profiling reveals an extensive p53-regulated autophagy program contributing to key p53 responses. Genes & development. 2013;27(9):1016-31.
54. Li A, Wei G, Wang Y, Zhou Y, Zhang XE, Bi L, et al. Identification of intermediate-size non-coding RNAs involved in the UV-induced DNA damage response in C. elegans. PloS one. 2012;7(11):e48066.
55. Tresini M, Warmerdam DO, Kolovos P, Snijder L, Vrouwe MG, Demmers JA, et al. The core spliceosome as target and effector of non-canonical ATM signalling. Nature. 2015;523(7558):53-8.
56. Sale JE, Lehmann AR, Woodgate R. Y-family DNA polymerases and their role in tolerance of cellular DNA damage. Nature reviews Molecular cell biology. 2012;13(3):141-52.
57. Suzuki HI, Yamagata K, Sugimoto K, Iwamoto T, Kato S, Miyazono K. Modulation of microRNA processing by p53. Nature. 2009;460(7254):529-33.
58. Tanikawa C, Ueda K, Nakagawa H, Yoshida N, Nakamura Y, Matsuda K. Regulation of protein Citrullination through p53/PADI4 network in DNA damage response. Cancer research. 2009;69(22):8761-9.
59. Li P, Wang D, Yao H, Doret P, Hao G, Shen Q, et al. Coordination of PAD4 and HDAC2 in the regulation of p53-target gene expression. Oncogene. 2010;29(21):3153-62.
60. Tanikawa C, Espinosa M, Suzuki A, Masuda K, Yamamoto K, Tsuchiya E, et al. Regulation of histone modification and chromatin structure by the p53-PADI4 pathway. Nature communications. 2012;3:676.
61. Mason JM, Dusad K, Wright WD, Grubb J, Budke B, Heyer WD, et al. RAD54 family translocases counter genotoxic effects of RAD51 in human tumor cells. Nucleic acids research. 2015;43(6):3180-96.

Supplemental information

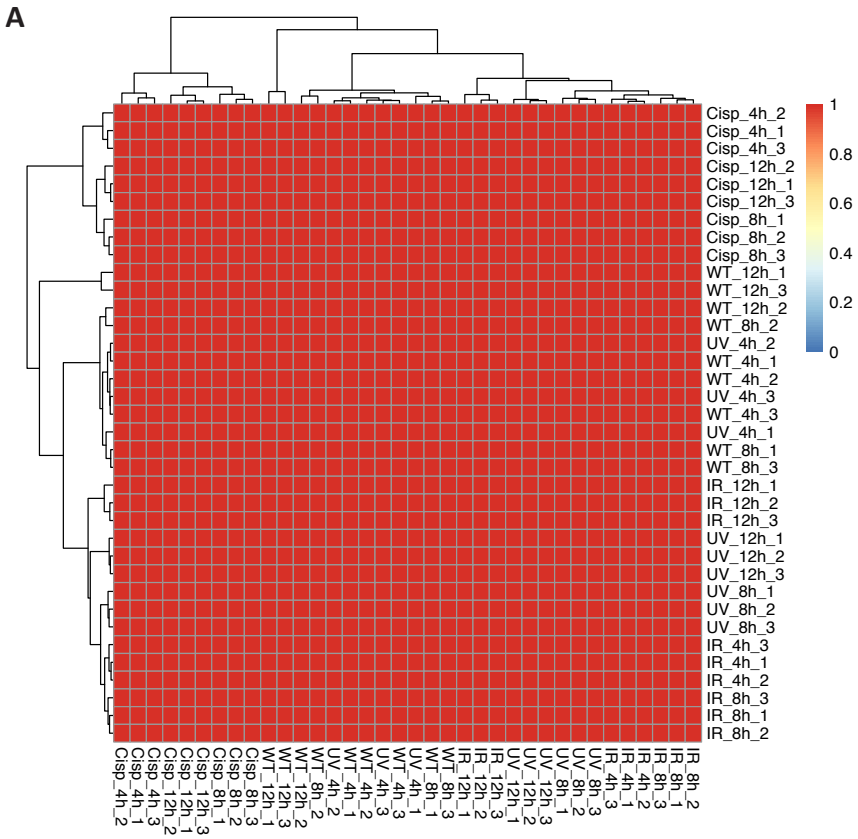

Supplementary figure 1: Pearson correlation of all samples. Pearson correlation coefficient plot of all samples together based on all genes.

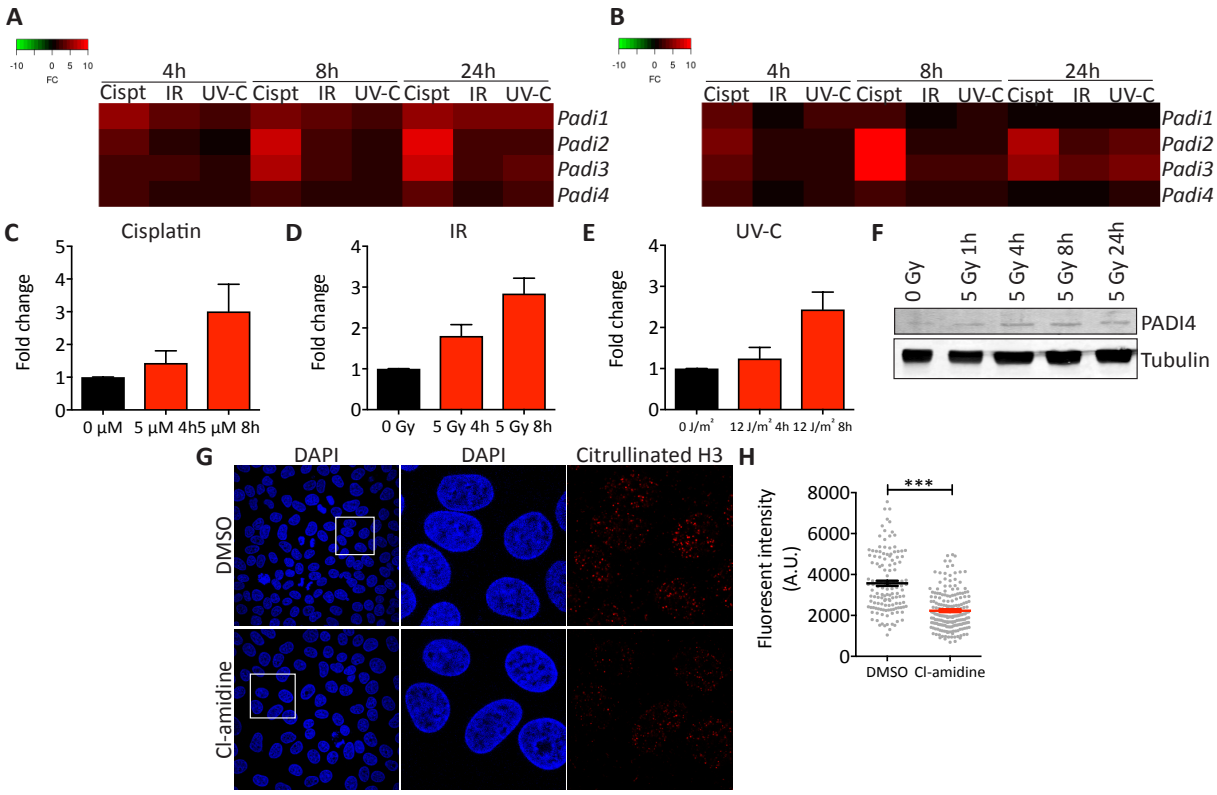

Supplementary figure 2: Verification of PADI expression on mRNA and protein level. A) Heatmap constructed from gene expression levels determined after mRNA sequencing. B) qPCR verification of PADI mRNA expression levels in the same mES cell samples that were used for mRNA sequencing. C – E) PADI4 mRNA expression in U2OS cells over time after cisplatin, IR and UVC. F) PADI4 protein expression in U2OS cells over time after IR. G) Immunofluorescent staining of citrullinated histone H3 after mock and Cl-amidine treatment. H) Quantification of citrullinated histone H3 expression in U2OS cells after mock and Cl-amidine treatment. All experiments were performed at least three times. Mean ± SEM are indicated. *** P<0.001

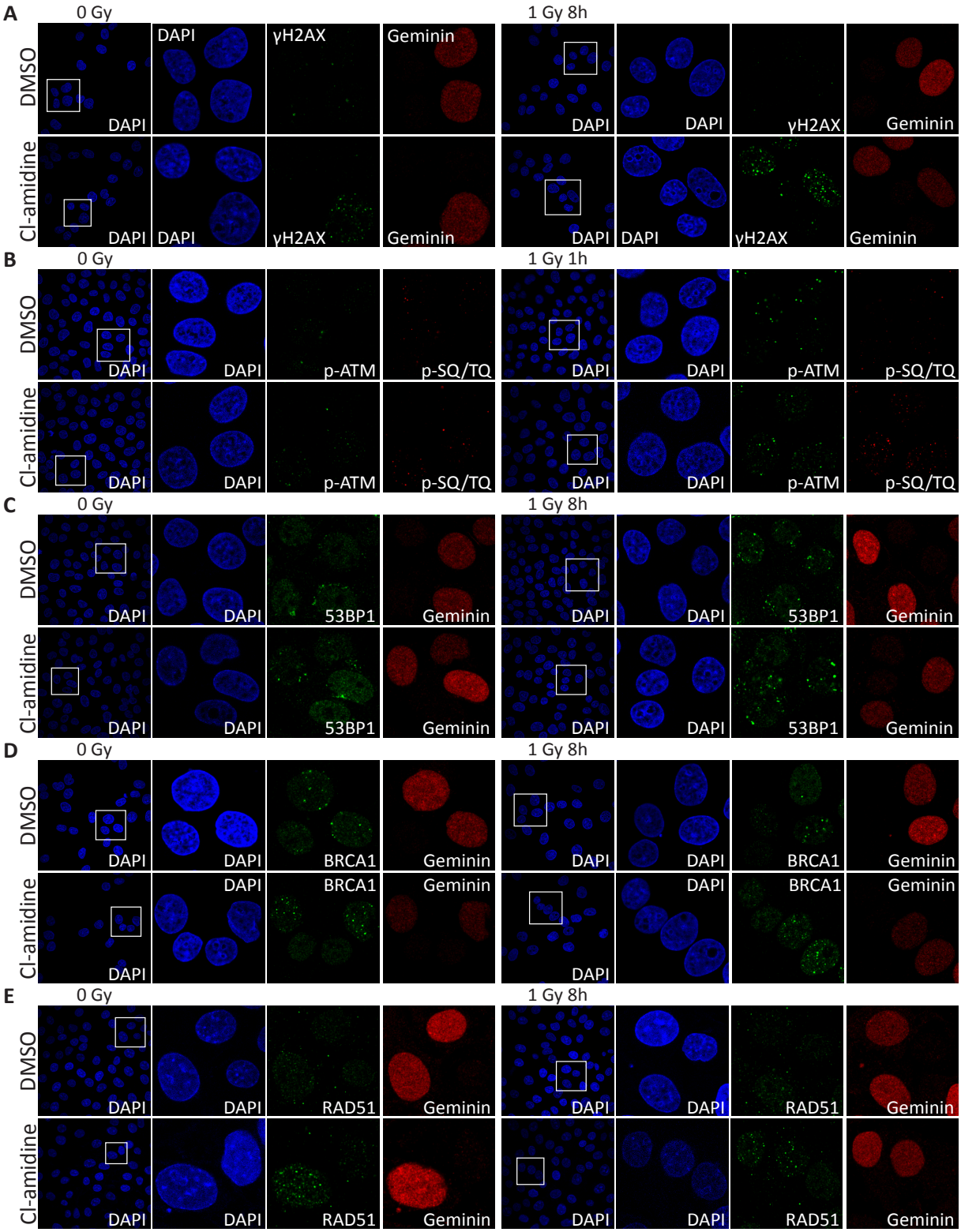

Supplementary figure 3: Foci formation of different DDR markers after DNA damage. Immunofluorescent staining of basal levels and after 1 Gy IR of γH2AX (A), p-ATM and p-SQ/TQ (B), 53BP1 (C), BRCA1 (D) and RAD51 (E) foci after 48h Cl-amidine treatment. Images were generated using Image J software. A representative image out of three independent experiments is shown.

Supplementary Table 1

Upstream Regulator	Molecule Type	p-value of overlap
TP73	transcription regulator	5,14E-06
MYOG	transcription regulator	2,32E-05
TGFB1	growth factor	1,49E-04
TP53	transcription regulator	3,76E-04
MYF6	transcription regulator	5,47E-04
Sry	transcription regulator	8,32E-04
SREBF1	transcription regulator	1,04E-03
HTT	transcription regulator	1,43E-03
SP1	transcription regulator	1,57E-03
CREBBP	transcription regulator	2,39E-03
TAF7L	transcription regulator	2,75E-03
CUX1	transcription regulator	4,10E-03
SRF	transcription regulator	4,48E-03
SMAD7	transcription regulator	4,75E-03
KMT2D	transcription regulator	4,75E-03
EPC1	transcription regulator	4,80E-03
KLF2	transcription regulator	4,94E-03
BRCA1	transcription regulator	5,20E-03
HR	transcription regulator	6,95E-03
mir-365	microrna	7,85E-03
INHA	growth factor	1,05E-02
SOX15	transcription regulator	1,16E-02
JUN	transcription regulator	1,16E-02
PRDM1	transcription regulator	1,23E-02
FOSL2	transcription regulator	1,32E-02
NOTCH1	transcription regulator	1,34E-02
BCL6	transcription regulator	1,63E-02
CDX1	transcription regulator	1,68E-02
SIM2	transcription regulator	1,89E-02
EED	transcription regulator	1,95E-02
NGF	growth factor	1,95E-02
BDNF	growth factor	2,02E-02
SIM1	transcription regulator	2,06E-02
PLAG1	transcription regulator	2,10E-02
PAX2	transcription regulator	2,16E-02
MYOD1	transcription regulator	2,17E-02
RUNX2	transcription regulator	2,21E-02
GATA2	transcription regulator	2,25E-02
SP3	transcription regulator	2,27E-02
NKX2-3	transcription regulator	2,50E-02
USF1	transcription regulator	2,52E-02
HMGB1	transcription regulator	2,52E-02
EP300	transcription regulator	2,62E-02
FGF3	growth factor	2,62E-02
MNX1	transcription regulator	2,62E-02
NLRC5	transcription regulator	2,76E-02

Supplementary Table 1 - continuation

TCFL5	transcription regulator	2,89E-02
MEF2B	transcription regulator	2,89E-02
EAF1	transcription regulator	2,89E-02
EID1	transcription regulator	2,89E-02
TP63	transcription regulator	2,96E-02
NFYA	transcription regulator	3,12E-02
NODAL	growth factor	3,44E-02
CRX	transcription regulator	3,44E-02
MKL2	transcription regulator	3,46E-02
TGFB3	growth factor	3,55E-02
NKX2-1	transcription regulator	3,66E-02
EGF	growth factor	3,67E-02
ARNT2	transcription regulator	3,74E-02
KLF11	transcription regulator	3,76E-02
MYF5	transcription regulator	3,85E-02
POU4F1	transcription regulator	4,03E-02
IRF8	transcription regulator	4,23E-02
mir-193	microrna	4,60E-02
ZFHX3	transcription regulator	4,60E-02
FOXC2	transcription regulator	4,93E-02

Supplementary Table 2

Upstream Regulator	Molecule Type	p-value of overlap
SIM1	transcription regulator	8,36E-04
NGF	growth factor	1,78E-03
ARNT2	transcription regulator	3,16E-03
miR-130a-3p	mature microrna	4,45E-03
PAX7	transcription regulator	4,50E-03
TAL1	transcription regulator	4,64E-03
HDAC4	transcription regulator	5,06E-03
CREB1	transcription regulator	6,71E-03
NOTCH1	transcription regulator	8,55E-03
ISL1	transcription regulator	8,75E-03
NFKBIL1	transcription regulator	9,27E-03
POU5F2	transcription regulator	9,27E-03
OTP	transcription regulator	9,27E-03
miR-675-5p	mature microrna	9,27E-03
miR-668-3p	mature microrna	9,27E-03
mir-668	microrna	9,27E-03
miR-1258	mature microrna	9,27E-03
mir-1258	microrna	9,27E-03
miR-1343-5p	mature microrna	9,27E-03
mir-939	microrna	9,27E-03
ZFP36L1	transcription regulator	9,27E-03
LHX9	transcription regulator	9,27E-03
DMRT1	transcription regulator	1,27E-02
TLX3	transcription regulator	1,32E-02
MNT	transcription regulator	1,32E-02
SRF	transcription regulator	1,36E-02
GFI1	transcription regulator	1,36E-02
TWIST1	transcription regulator	1,45E-02
ETV1	transcription regulator	1,45E-02
GATA3	transcription regulator	1,46E-02
FIGLA	transcription regulator	1,59E-02
SRA1	transcription regulator	1,60E-02
ADNP	transcription regulator	1,84E-02
ASH2L	transcription regulator	1,84E-02
STAG2	transcription regulator	1,84E-02
CREB5	transcription regulator	1,84E-02
UHRF1	transcription regulator	1,84E-02
WDR77	transcription regulator	1,90E-02
POU4F1	transcription regulator	1,93E-02
FGF2	growth factor	2,03E-02
TLX1	transcription regulator	2,23E-02
NODAL	growth factor	2,23E-02
NTF3	growth factor	2,23E-02
FOXL2	transcription regulator	2,25E-02
CBX5	transcription regulator	2,36E-02
VAV1	transcription regulator	2,40E-02

Supplementary Table 2 - continuation

RELB	transcription regulator	2,43E-02
ATOH1	transcription regulator	2,58E-02
miR-199a-5p	mature microrna	2,73E-02
LHX5	transcription regulator	2,75E-02
LHX8	transcription regulator	2,75E-02
miR-125b-1-3p	mature microrna	2,75E-02
mir-132	microrna	2,76E-02
POU5F1	transcription regulator	2,91E-02
NEUROG3	transcription regulator	2,93E-02
CITED2	transcription regulator	3,33E-02
ASCC1	transcription regulator	3,66E-02
IRF2BP2	transcription regulator	3,66E-02
SIX4	transcription regulator	3,66E-02
CTNNB1	transcription regulator	3,71E-02
MSX2	transcription regulator	4,16E-02
FOSB	transcription regulator	4,16E-02
FOXN4	transcription regulator	4,55E-02
SSBP2	transcription regulator	4,55E-02
TRIM27	transcription regulator	4,55E-02
ZIC1	transcription regulator	4,55E-02
SOX18	transcription regulator	4,55E-02
MYOCD	transcription regulator	4,58E-02
STAT5A	transcription regulator	4,80E-02
EP300	transcription regulator	4,81E-02

Supplementary Table 3

Ingenuity Canonical Pathways	-log(p-value)
TGF-β Signaling	1,1E01
p38 MAPK Signaling	7,01E00
Aryl Hydrocarbon Receptor Signaling	6,5E00
Sumoylation Pathway	6,2E00
ATM Signaling	6,09E00
Wnt/β-catenin Signaling	5,84E00
p53 Signaling	5,81E00
ERK5 Signaling	5,63E00
Neurotrophin/TRK Signaling	5,26E00
Human Embryonic Stem Cell Pluripotency	5,12E00
Corticotropin Releasing Hormone Signaling	4,49E00
RAR Activation	4,43E00
Regulation of the Epithelial-Mesenchymal Transition Pathway	4,41E00
BMP signaling pathway	4
VDR/RXR Activation	3,87E00
Prolactin Signaling	3,78E00
Inhibition of Angiogenesis by TSP1	3,74E00
PEDF Signaling	3,7E00
PPARα/RXRα Activation	3,57E00
HIF1α Signaling	3,24E00
Cell Cycle: G2/M DNA Damage Checkpoint Regulation	3,23E00
NGF Signaling	3,18E00
Glucocorticoid Receptor Signaling	3,17E00
Estrogen Receptor Signaling	3,09E00
HMGB1 Signaling	3,07E00
Adipogenesis pathway	3,02E00
Granzyme A Signaling	2,95E00
GNRH Signaling	2,93E00
Cell Cycle: G1/S Checkpoint Regulation	2,91E00
EGF Signaling	2,81E00
GADD45 Signaling	2,74E00
DNA damage-induced 14-3-3σ Signaling	2,74E00
Sirtuin Signaling Pathway	2,69E00
Cyclins and Cell Cycle Regulation	2,66E00
Calcium Signaling	2,6E00
NF-κB Signaling	2,57E00
FGF Signaling	2,45E00
PPAR Signaling	2,43E00
Circadian Rhythm Signaling	2,26E00
Androgen Signaling	2,25E00
Telomerase Signaling	2,25E00
UVC-Induced MAPK Signaling	2,04E00
iNOS Signaling	2,02E00
P2Y Purigenic Receptor Signaling Pathway	2
Role of Oct4 in Mammalian Embryonic Stem Cell Pluripotency	2
Activation of IRF by Cytosolic Pattern Recognition Receptors	1,88E00

Supplementary Table 3 - continuation

Transcriptional Regulatory Network in Embryonic Stem Cells	1,88E00
Role of CHK Proteins in Cell Cycle Checkpoint Control	1,83E00
Tight Junction Signaling	1,77E00
Wnt/Ca+ pathway	1,72E00
Ephrin Receptor Signaling	1,7E00
UVB-Induced MAPK Signaling	1,7E00
IL-10 Signaling	1,68E00
Lymphotoxin β Receptor Signaling	1,68E00
ErbB2-ErbB3 Signaling	1,66E00
NRF2-mediated Oxidative Stress Response	1,63E00
ILK Signaling	1,6E00
Gap Junction Signaling	1,59E00
ERK/MAPK Signaling	1,57E00
Role of BRCA1 in DNA Damage Response	1,53E00
Macropinocytosis Signaling	1,53E00
LPS-stimulated MAPK Signaling	1,48E00
FLT3 Signaling in Hematopoietic Progenitor Cells	1,47E00
HER-2 Signaling in Breast Cancer	1,47E00
PDGF Signaling	1,44E00
IL-7 Signaling Pathway	1,44E00
Protein Kinase A Signaling	1,42E00
Phospholipase C Signaling	1,41E00
TR/RXR Activation	1,4E00
ErbB Signaling	1,39E00
CDK5 Signaling	1,38E00
SAPK/JNK Signaling	1,35E00
DNA Double-Strand Break Repair by Homologous Recombination	1,34E00
IGF-1 Signaling	1,33E00
UVA-Induced MAPK Signaling	1,32E00
Mouse Embryonic Stem Cell Pluripotency	1,31E00

Supplementary Table 4

Ingenuity Canonical Pathways	-log(p-value)
Neurotrophin/TRK Signaling	5,36E00
Human Embryonic Stem Cell Pluripotency	5,24E00
ERK5 Signaling	4,29E00
Circadian Rhythm Signaling	3,8E00
FLT3 Signaling in Hematopoietic Progenitor Cells	3,79E00
FGF Signaling	3,69E00
PPAR Signaling	3,66E00
ATM Signaling	3,6E00
RAR Activation	3,5E00
Embryonic Stem Cell Differentiation into Cardiac Lineages	3,35E00
p38 MAPK Signaling	3,33E00
NGF Signaling	3,26E00
Transcriptional Regulatory Network in Embryonic Stem Cells	3,21E00
Wnt/Ca+ pathway	2,97E00
Wnt/β-catenin Signaling	2,69E00
Calcium Signaling	2,68E00
ILK Signaling	2,52E00
Regulation of the Epithelial-Mesenchymal Transition Pathway	2,52E00
ERK/MAPK Signaling	2,48E00
Gαs Signaling	2,32E00
Corticotropin Releasing Hormone Signaling	2,29E00
Phospholipase C Signaling	2,25E00
P2Y Purigenic Receptor Signaling Pathway	2,06E00
Role of Oct4 in Mammalian Embryonic Stem Cell Pluripotency	2,04E00
GNRH Signaling	2,01E00
Ephrin Receptor Signaling	1,76E00
NF-κB Signaling	1,75E00
Glucocorticoid Receptor Signaling	1,73E00
Lymphotoxin β Receptor Signaling	1,73E00
CREB Signaling in Neurons	1,68E00
Ephrin B Signaling	1,65E00
Growth Hormone Signaling	1,56E00
Prolactin Signaling	1,55E00
LPS-stimulated MAPK Signaling	1,52E00
TGF-β Signaling	1,52E00
AMPK Signaling	1,52E00
PEDF Signaling	1,51E00
cAMP-mediated signaling	1,49E00
Protein Kinase A Signaling	1,49E00
CDK5 Signaling	1,42E00
Mouse Embryonic Stem Cell Pluripotency	1,35E00
p53 Signaling	1,34E00
Granzyme A Signaling	1,33E00

Chapter 5

KHSRP is involved in DNA repair by regulating homologous recombination

Serena Bruens[1], Nicole Verkaik[1], Dik van Gent[1], Jan Hoeijmakers[1,2,3], Joris Pothof[1]*

[1] Department of Molecular Genetics, Erasmus Medical Center, Rotterdam, The Netherlands
[2] CECAD Research Center, University of Cologne, Cologne, Germany
[3] Princess Maxima Center for Pediatric Oncology, Utrecht, The Netherlands

*Corresponding author: j.pothof@erasmusmc.nl

In preparation

Abstract

RNA binding proteins are causally implicated in many cellular processes and control RNA expression, stability and function. It is becoming clear that RNA and RNA binding proteins are an essential element of the DNA damage response. One of those proteins is KHSRP, which is phosphorylated by ATM that leads to the specific processing of microRNAs. The specific functions and implications of KHSRP in the DNA damage response are not well known. Here, we show that siRNA-mediated silencing of KHSRP does not affect DNA damage signalling outcomes such as cell cycle arrest and apoptosis, but reduces DSB repair by homologous recombination. KHSRP knockdown has no effect on general DNA repair kinetics, but specifically diminishes HR function by affecting the accumulation kinetics of RPA, BRCA1 and RAD51 in the early time points after DNA damage. Based on these results we hypothesize that KHSRP interacts with BRCA1, thereby promoting HR via displacement of RPA and loading of RAD51 on the break.

Introduction

RNA binding proteins (RBPs) are a large family of proteins that bind RNA, each with different degrees of sequence-specificity and affinity, and target RNA species (1, 2). RBPs are classified according to their RNA-binding domain and perform their function in either the nucleus or the cytoplasm. In the nucleus, RBPs control transcription, pre-mRNA splicing and polyadenylation (2-7). In the cytoplasm, RBPs regulate processes such as transport, translation, RNA modification, RNA localization and RNA turnover (2, 8-12). It is becoming apparent that RBPs play pivotal roles in many cellular processes.

Proteome-wide and RNAi screens have implicated RBPs in the response to DNA damage (13-15). To counteract the harmful consequences of DNA damage, cells have various DNA repair systems and elaborate DNA damage checkpoint pathways that halt cell proliferation and if DNA damage is too extensive, activate apoptotic or senescent programs (16-19). The combined response to DNA damage is designated the DNA damage response (DDR). Several RBPs are directly phosphorylated by DNA damage checkpoint kinases ATR/ATM or CHK1/CHK2 (14, 15, 20). Interestingly, known DDR proteins such as KU70, KU80, DNA-PK, 53BP1 and BRCA1 were identified as novel RBPs themselves (21).

A plethora of RBP functions in the DDR have been described. For example, RNAse H1/2 is required to prevent harmful R-loop formation (22). RBPs control the expression of DDR genes p53, p21 and RhoB via promotion of mRNA translation by HuR after DNA damage (23-25). Another RBP, EWS, mediates alternative splicing of DDR genes CHK2 and MDM2 after DNA damage by dissociating from the transcribed RNA (26). In addition, RBPs are also directly involved in DNA repair (1). PSF is an RBP that binds to DNA, RAD51D and TOPBP1 thereby affecting DSB repair via non-homologous end joining (NHEJ) and homologous recom-

bination (HR) (27, 28). Furthermore, hnRNPUL directly interacts with the double strand DNA break (DSB) recognition complex MRN, thereby promoting end resection and subsequent DSB repair via HR (29).

One of the RBPs identified in DNA damage-induced phosphoproteomic screens is the KH-type splicing regulatory protein (KHSRP or KSRP, also known as FBP2 or FUBP2). It is characterized by four KH-domains and has multiple functions in RNA biogenesis, including mRNA decay and promotion of pre-microRNA maturation (13). Several studies link KHSRP to the DDR (13, 30-32). It was shown that BRCA1 negatively regulates KHSRP, although it was not linked to its DNA repair function (31). In addition, ATM directly phosphorylates KHSRP after DNA damage, which resulted in KHSRP-dependent microRNA processing of specific microRNAs (30). Another described function of KHSRP in the DDR is cell cycle progression control downstream of the p38/MK2 kinase complex (32).

Currently, KHSRP has been implicated in the DDR, but its exact role is not clear. We analyzed KHSRP function in the DDR and provide evidence that KHSRP is involved in proper functioning of HR after DNA damage.

Materials & Methods

Cell culture and transfection

U2OS cells were cultured in DMEM supplemented with penicillin-streptomycin (100× diluted, Penicillin-Streptomycin, P0781-100ML, Sigma-Aldrich) and 10 % fetal bovine serum (Fetal Bovine Serum (FBS) South America, S1810-500, Biowest) at 5% CO2 and 37°C. Single siRNA transfections were performed using Lipofectamine RNAiMax (56532, Invitrogen) according to manufacturer's instructions. Experiments were carried out 48h after transfection. Non-targeting siRNA #5 (D-001210-05-50, Dharmacon) and SMARTpool: ON-TARGETplus KHSRP siRNA (L-009490-00-0020, Dharmacon) were used to carry out transfections.

Clonogenic cell survival assay

After siRNA treatment cells were trypsinised (Trypsin-EDTA solution, T3924-500ML, Sigma-Aldrich) and counted (Z2 Coulterparticle count and size analyzer, Beckman Coulter). 500 cells per well in triplicates per condition were seeded in 6-well plates. The next day, cells were irradiated by ionizing radiation (IR) (Gammacell 40 Cesium 137 irradiation unit, Atomic Energy). Cells were incubated 8-9 days and afterwards washed once with PBS, then stained with 0.1% Coomassie Brilliant Blue (50% (v/v) Methanol, 43% (v/v) H2O, 7% (v/v) Acetic Acid, 0.1% (m/v) Coomassie Brilliant Blue). Colonies were counted using Gelcount (Oxford Optronix).

Primary antibodies

53BP1 (1000×, sc-22760, Santa Cruz Biotechnology); BRCA1 (50×, sc-6954, Santa Cruz Biotechnology); BrdU Kit (50×, 556028, BD Sciences); CHK2 (500×, #3440, Cell Signaling); p-CHK2 (500×, #2197, Cell Signaling); Ge-

minin (400×, 10802-1-AP, Proteintech); γH2AX (Ser139) (1000×, 05-636, Millipore); KHSRP (1000×, ab140648, Abcam); RAD51 (5000×, Home made); p53 (1000×, sc-126, Santa Cruz Biotechnology); RAD51 (200×, GTX70230, GeneTex); RPA34 (500×, NA18, Calbiochem); Tubulin (2000×, sc-12462-R, Santa Cruz Biotechnology); Tubulin (5000×, T5168, Sigma-Aldrich).

Secondary antibodies
Goat-α-mouse Alexa 488 (1000×, A11034, Life Technologies); Goat-α-Rabbit Alexa 555 (1000×, A21429, Life Technologies); Donkey-α-mouse IRDye 800CW (5000×, 926-32212, LI-COR Biosciences); Donkey-α-rabbit IRDye 680RD (5000×, 926-32223, LI-COR Biosciences).

Immunofluorescence
After siRNA treatment U2OS cells were seeded on coverslips. The cells were irradiated with 5 Gy and fixed 1, 2, 4, 8, and 24h after IR. Briefly, the coverslips were washed once with PBS, fixed with 2% PFA, washed with PBS + 0.1% triton X-100 3× short and 2× 10 minutes, once washed with PBS+ (100 ml PBS + 0.5 g BSA + 0.15 g Glycine), incubated 1-2h at RT with primary antibodies. After incubation coverslips were washed with PBS + 0.1% triton X-100 3× short and 2× 10 minutes, once washed with PBS+, incubated 1-2h at RT with secondary antibodies. After incubation coverslips were washed with PBS + 0.1% triton X-100 3× short and 2× 10', once washed with PBS+. For RAD51 staining (commercial antibody) the coverslips were washed once with PBS, fixed with 4% PFA. Subsequently, cells were permeabilised for 20' with PBS + 0.2% triton X-100 and washed with PBS. After permeabilization cells were treated with 10× diluted DNAse I (04536282001, Roche Life Sciences) for 1h at 37°C in a humidified chamber and washed with PBS. Blocking was performed using IFF buffer (PBS + 1% BSA + 2% FCS) for at least 30'. After blocking cells were incubated with primary antibodies for 1-2h at RT. After incubation coverslips were washed 3× for 5' with PBS and incubated with secondary antibodies 1-2h at RT. After incubation coverslips were washed 3× for 5' with PBS. Coverslips were mounted in DAPI Vectashield mounting medium (H1200, Vector Laboratories). Images were made using a LSM700 microscope (Carl Zeiss Microimaging Inc.). Analysis of the images was performed using the ImageJ software.

Alpha track assay
The Alpha track assay was performed as previously described (33). In brief, cells were transfected with siRNA and seeded on mylar dishes 24h after transfection. 48h after transfection, dishes were radiated three times for 30'' with ^{241}americium source. Cells were washed once with ice-cold PBS. Extraction was performed with cold CSK buffer (10 mM HEPES-KOH, pH7.9; 100 mM NaCl; 300 mM sucrose; 3 mM MgCl2; 1 mM EGTA; 0.5% (v/v) triton-X100) and cold CSS buffer (10 mM Tris-HCl, pH7.4; 10 mM NaCl; 3 mM MgCl2; 1% (v/v) tween-20; 0.5% (w/v) sodium deoxycholate) for 5' each. After extraction cells were fixed in 4% PFA in PBS for 20' at RT and stain-

ed according to the protocol for immunofluorescence as described above.

Immunoblot assay
Cells were lysed in 2× sample buffer and boiled at 99°C for 5 minutes. Samples were run on a SDS-PAGE gel and transferred to a PVDF membrane (Immobilon FL PVDF Transfer membrane 0.45um, IPFL00010, Millipore). Membranes were blocked in 5% milk in PBS for 1-2h at RT. After blocking, membranes were incubated with primary antibodies 1-2h at RT. Then the membranes were washed 5 times for 5 minutes with PBS + 0.05% Tween-20 and incubated with secondary antibodies at RT for 1-2h. Again the membranes were washed 5× for 5 minutes. Membranes were visualized using Odyssey CLx Infrared Imaging System (LI-COR Biosciences).

BrdU and PI labelling for cell cycle analysis
Cells were labelled with 5 μM BrdU (B5002, Sigma-Aldrich) for 15 minutes at 37°C. Subsequently, cells were harvested and fixed in 70% ethanol at least overnight at 4°C. Fixed cells were washed with ice-cold PBS and re-suspended in pepsin solution (5 mg pepsin in 10 ml 0.1N HCl) and incubated 20 minutes at RT. After pepsin-treatment blocking solution (PBS + 0.5% Tween-20 + 0.1% BSA) was added and cells were washed. Next, cell were re-suspended in 2N HCl for 12 minutes at 37°C. To neutralise, borate buffer (100 mM, pH8.5) was added and the cells were pelleted. BrdU antibody was added and the cells were incubated for 2h on ice in the dark. Stained cells were washed in blocking solution and re-suspended in 500 μl PBS supplemented with 12.5 μl RNase A and 1 μl PI (P3566, Invitrogen). Cell cycle was analysed the next day using BD LSRFortessa (BD Biosciences). Flow Cytometry data was analysed using FlowJo vX.0.7 (Tree Star Inc.).

Apoptosis assay
Apoptotic cells were analysed according to the protocol published by Smid et al. (34). In brief, medium and cells were collected and re-suspended in 998 μl FACS buffer (0.5% BSA + 0.05% NaN3 in PBS) pre-heated to 37°C. 1 μl diluted Hoechst 33342 (10 mg/ml, H3570, Life Technologies) was added and the cells were vortexed and incubated for exactly 7 minutes at 37°C. Subsequently, the cells were immediately placed on ice and 1 μl 7-AAD (1 mg/ml, A1310, Invitrogen) was added. Cells were analysed within 1h after adding 7-AAD using BD LSRFortessa (BD Biosciences). Flow Cytometry data was analysed using FlowJo vX.0.7 (Tree Star Inc.).

Homologous recombination reporter assay
The homologous recombination reporter assay was performed as described previously (35). In brief, 48h after transfection of U2OS cells with an I-Sce restriction site were transfected using X-tremeGENE HP DNA Transfection Reagent (06366244001, Roche Life Sciences) with I-Sce-GFP plasmid. 48h after transfection GFP positive cells were analysed using BD LSRFortessa (BD Biosciences). Flow Cytometry data was analysed using FlowJo vX.0.7 (Tree Star Inc.).

End joining assay
The end-joining assay was performed as described in (36), with some minor changes. In short, cells were grown in a 3-cm dish to 50-80% confluency. Cells were transiently transfected with 2 µg of a blunt-ended linear DNA substrate (EcoRV/Eco47III digested pDvG94 plasmid (36)), using X-treme GENE HP DNA Transfection Reagent (Sigma Aldrich), following manufacturers protocol. Two days after transfection, extrachromosomal DNA was isolated and resuspended in a final volume of 20 µl water (37). From this solution, 1 µl was PCR amplified with the DAR5 and FM30 primers (36), using PuReTaq ready-To-Go PCR beads (GE Healthcare). The PCR product was digested with BstXI. Restriction fragments were separated on a 6% polyacrylamide gel in TBE buffer, stained with ethidium bromide. The relative level of microhomology-directed end-joining was determined by quantification of the BstXI digested PCR product using the ImageJ software.

Statistical analysis
Data was processed using GraphPad Prism v5.0a (GraphPad Software Inc.). Statistical test used were Student's T-test and Mann-Whitney U test. P-values equal or lower than 0.05 were accepted as significant.

Results

KHSRP is not essential for maintaining cell cycle and apoptosis

In literature the role of KHSRP in the DDR is described to some extend (REF 13, 30-32), but more information on how KHSRP exactly functions in the DDR is unknown. Therefore, in order to determine the role of KHSRP in the DDR, we first analysed KHSRP expression on protein and mRNA level using immunofluorescence, qRT-PCR and western blot. KHSRP is mainly expressed in the nucleus of U2OS cells in a speckled pattern with different intensities per nucleus (Fig. 1A). IR resulted in increased KHSRP mRNA levels 24h after damage (Fig. 1B) and a gradual increase in protein levels (Fig. 1C), indicating that DNA damage induces KHSRP mRNA and protein levels.

Next, we analysed standard cellular outcomes of DDR. First, we optimized KHSRP knockdown (Fig. 1D) and assessed cell cycle distribution. KHSRP silencing did not affect cell cycle distribution compared to control cells (Fig. 1E), indicating that KHSRP does not control cell cycle status. We also monitored whether KHSRP silencing altered the apoptotic response. We saw a very modest, but non-significant, increase in apoptosis (Fig. 1F). Finally, we assessed whether KHSRP affects cell survival after DNA damage. A colony survival assay after IR indicated that KHSRP silencing by siRNAs did not alter sensitivity (Fig. 1G). In addition, colony survival after cisplatin or UV-C treatment was also not affected (data not shown). Thus, KHSRP silencing does not alter cell fates induced by DNA damage.

The DNA damage response is activated in the absence of KHSRP

An important signalling molecule in the DDR is the phosphatidyl ino-

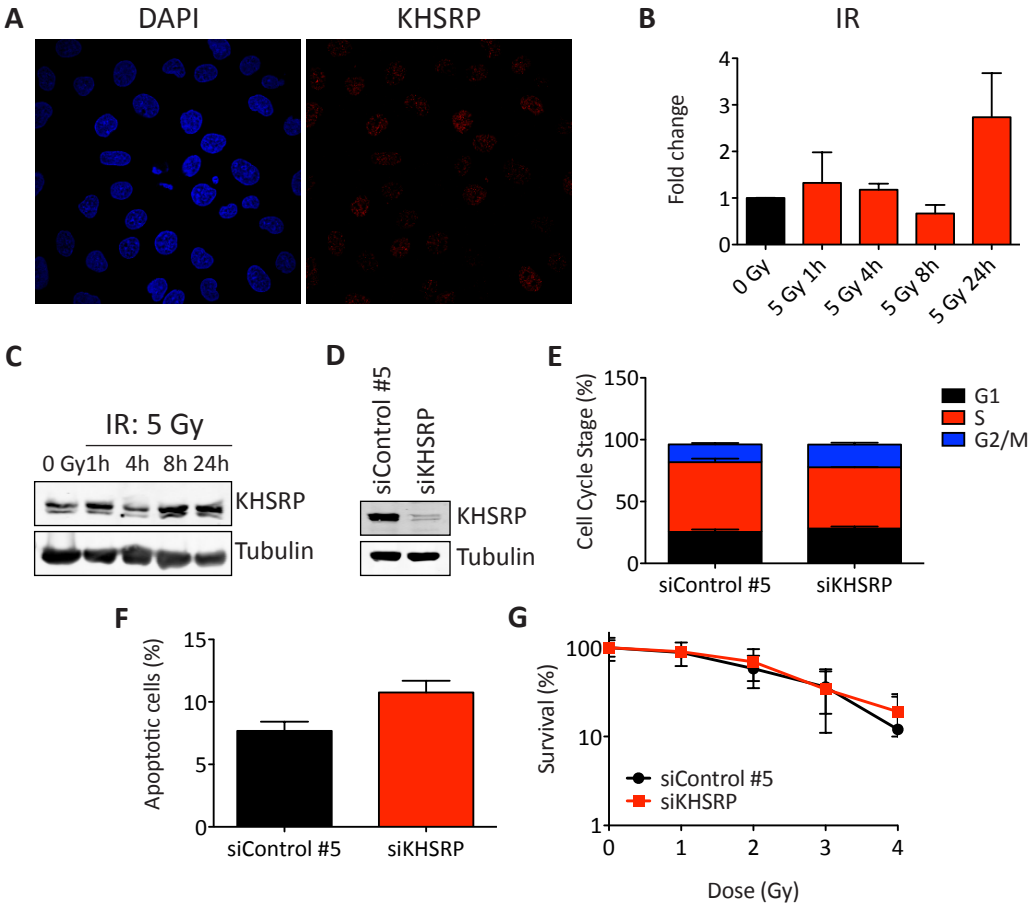

Figure 1: KHSRP knockdown does not affect cellular processes. A) Expression pattern of KHSRP in U2OS cells was determined using immunofluorescence. B) mRNA expression of KHSRP at different time points after 5 Gy of IR. qPCR was used to determine mRNA levels, n = 3 and mean with SEM are given. C) Western blot was used to determine protein expression of KHSRP at different time points after 5 Gy IR. A representative of 3 independent experiments is shown. D) Western blot for KHSRP after siKHSRP treatment. E) Cell cycle analysis after siKHSRP treatment. Cells were pulse labelled with BrdU and then stained for BrdU and with PI. Expression analysis was performed using flow cytometry, n = 3 and mean with SEM are depicted. F) Apoptotic cells were stained with Hoechst 33342 and 7-AAD after siKHSRP treatment. n = 3, mean and SEM are depicted. G) Colony survival was performed seeding 500 cells in triplicates per condition. Than cells were treated with IR in different dosages and colonies were fixed 8-9 days later. The graphs are representatives of 3 independent experiments.

sitol 3-kinase like serine/threonine kinase ATM, which phosphorylates target proteins on SQ/TQ motifs (38, 39). KHSRP was identified as a direct phosphorylation target of ATM (30), which resulted in the enhanced maturation of specific microRNAs. We analyzed ATM activity by monitoring phosphorylation of ATM (S1981) and its target protein phosphorylation on SQ/TQ motifs before and after IR. Before IR, KHSRP depletion resulted in an induction of phosphorylated ATM foci (Fig. 2B). After IR, we observed a 3-fold increase of phosphorylated ATM foci in the absence of KHSRP (Fig. 2A + B), indicating that ATM is more active in the absence of

KHSRP. However, we observed a much smaller increase of SQ/TQ phosphorylation (Fig. 2A + C) or phosphorylation of ATM target protein CHK2 (Fig. 2D). This indicates that KHSRP restricts ATM phosphorylation after IR, but does not alter ATM-dependent phosphorylation of target proteins.

Since ATM is activated by DSBs and an induction of phosphorylated ATM foci were observed already before irradiation, we analyzed γH2AX foci, which marks DSBs. Indeed, a modest, but significant 1.6 fold in-

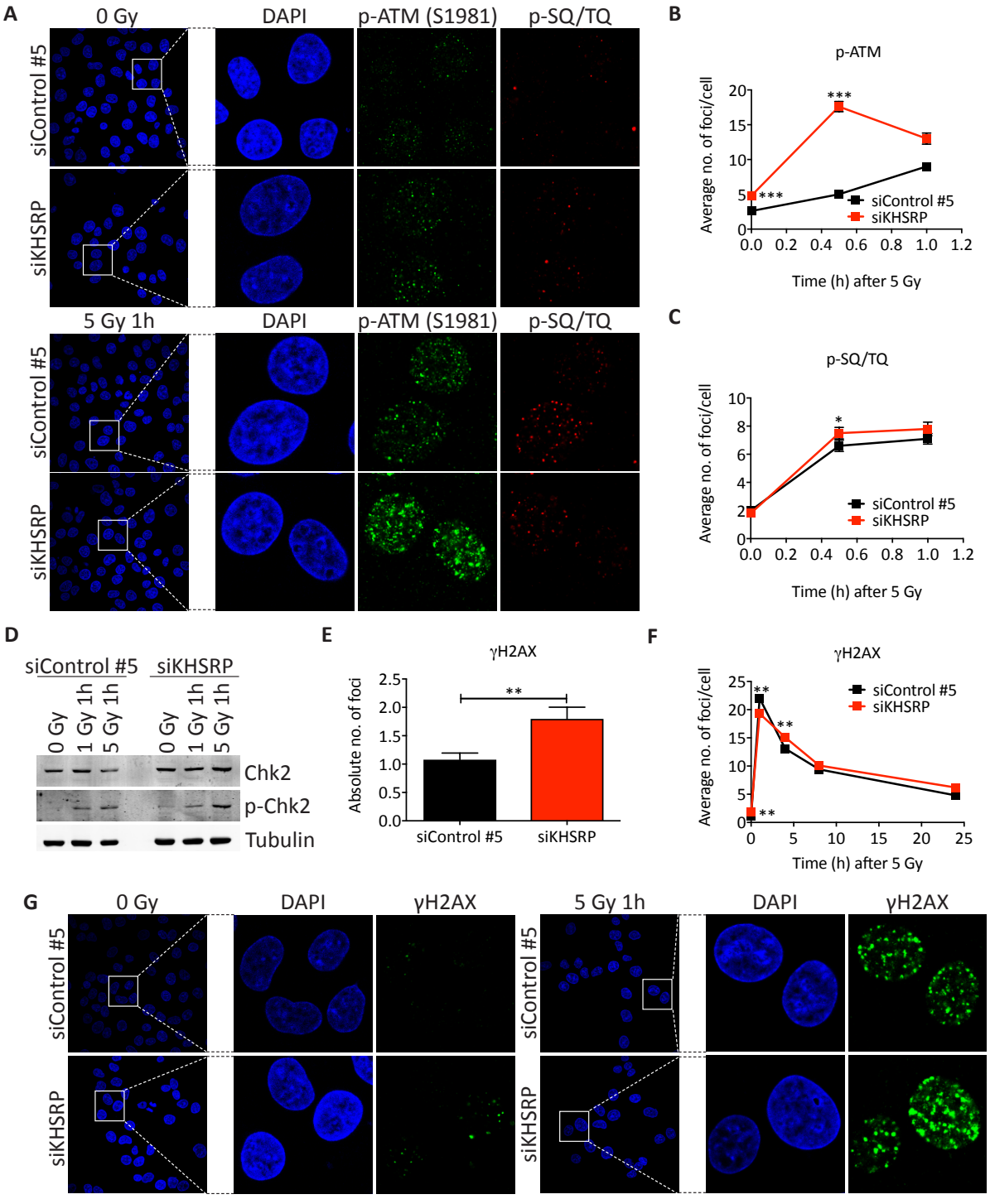

Figure 2: Activation of the DDR after KHSRP knockdown. A) Representative immunofluorescence images of siControl or siKHSRP treated U2OS cells stained with DAPI and for p-ATM (S1981) and p-SQ/TQ at t=0 and 1h after 5 Gy. Magnification 63× for left panel, the right panels are enlarged using ImageJ analysis software. B + C) Foci kinetics of p-ATM (S1981) and p-SQ/TQ over time after 5 Gy. The graph shows foci kinetics over time after 5 Gy. At least 50 cells were quantified per time point per experiment. The experiment was repeated three times. D) Western blot analysis of p53 and CHK2 at 1h after 1 and 5 Gy IR. A representative of 3 experiments is given. E) Absolute numbers of γH2AX foci per cell in non-radiated conditions were determined using ImageJ analysis software. F) Average number of γH2AX foci per cell was determined using ImageJ software. The graph shows foci kinetics over time after 5 Gy. At least 50 cells were quantified per time point per experiment. The experiment was repeated three times. G) Representative immunofluorescence images at 0 G and 1h after 5 Gy of siControl or siKHSRP treated U2OS cells stained with DAPI and for γH2AX. Magnification 63× for left panel, the right panels are enlarged using ImageJ analysis software. Mean and SEM are depicted, Mann-Whitney U test was performed to determine statistical significance. * $p<0.05$; ** $p<0.01$; *** $p<0.001$.

duction of γH2AX foci was observed after KHSRP depletion (Fig. 2E + G). Next, we analysed DSB repair kinetics by following clearance of γH2AX foci after IR. We observed a slightly reduced induction of γH2AX foci 1h after IR and a slightly reduced clearance of γH2AX foci (Fig. 2F + G). Since γH2AX foci clearance kinetics are similar between control and KHSRP depleted cells, the overall DSB repair capacity is only modestly altered.

KHSRP does not affect NHEJ, but is required for HR

DSBs are repaired by non-homologous end joining (NHEJ) or homologous recombination (HR) (17). Since we observed a slight increase in γH2AX and phospho-ATM foci, we assessed both HR and NHEJ function via plasmid-based assays. Interestingly, HR capacity after KHSRP depletion was markedly reduced (Fig. 3A), whereas NHEJ capacity was not altered (Fig. 3B). Next, we monitored 53BP1 foci formation, which direct DSB repair pathway choice towards NHEJ (40). Although at baseline more 53BP1 foci are present in the absence of KHSRP (Fig. 3C + D), 53BP1 foci kinetics after IR was not different between control and KHSRP depleted cells, suggesting normal functional NHEJ.

KHSRP depletion results in HR phenotype.

Next, we further dissected the apparent HR phenotype as observed in Fig. 3A. First, we monitored foci formation of essential HR proteins BRCA1 and RAD51. Since HR only takes place in the S- and G2-phase of the cell cycle when a sister chromatid is present, we co-stained for Geminin. Geminin is a cell cycle marker and is only expressed in the S/G2-phase (41). Interestingly, both the BRCA1 and RAD51 focus formation induction after IR was blunted in the absence of KHSRP (Fig. 4A – D), but is at control levels 24h after IR. These observations suggest a defect in HR.

The reduced induction of BRCA1 by KHSRP silencing suggests that BRCA1 loading on resected DNA ends is impaired. The replication protein A complex (RPA) covers single strand overhangs of the DSB, which is displaced by the BRCA1-PALB2-BRCA2 complex that leads to assembly of RAD51 nucleoprotein filaments (42-44). A defect in BRCA1 recruitment will lead to increased

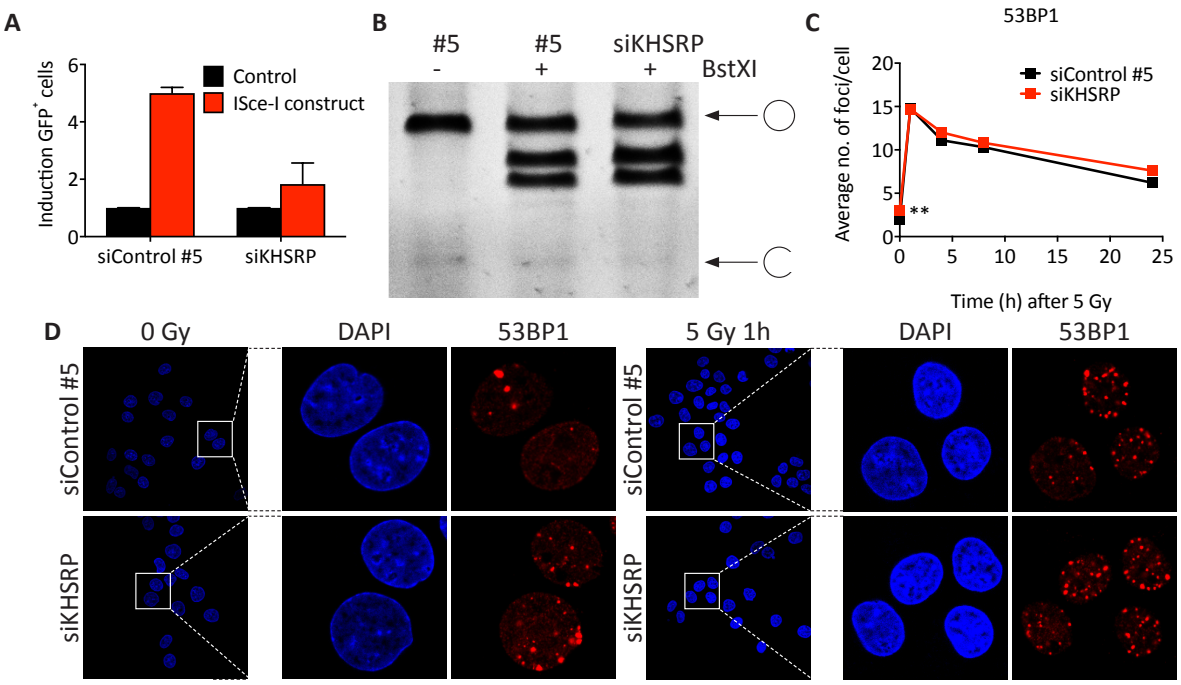

Figure 3: KHSRP is not involved in NHEJ, but is needed for HR. A) HR reporter assay was performed as described in materials and methods. GFP signal induction is depicted relative to its own mock-transfected control. NHEJ assay was performed as described in the materials and methods. B) A representative image of 3 experiments is shown. The arrows indicate the size of the circular plasmid (top arrow with circle) and the digested plasmid (bottom arrow with incomplete circle). C) Average number of 53BP1 foci per cell at different time points after 5 Gy IR were counted using ImageJ analysis software. At least 50 cells were quantified per time point per experiment. The experiment was repeated three times. D) Representative immunofluorescence images of non-irradiated and 1h after 5 Gy U2OS cells treated with siControl or siKHSRP and stained with DAPI and for 53BP1. For left panel magnification is 63×, the right panels are enlarged using ImageJ analysis software. N = 3, mean and SEM are depicted, Mann-Whitney U test was performed to determine statistical significance, ** $p<0.01$.

numbers of RPA-coated DSBs, which can be monitored by the α-track assay (33). 53BP1 staining was used to locate DSB tracks (Supplementary Fig. 1A). In the absence of KHSRP, an increase in RPA$^+$ 53BP1$^+$ α-tracks were observed at DSB tracks (Fig. 4F), suggesting that KHSRP is involved in removal of RPA from the single strand overhangs of DSBs or efficient loading of BRCA1.

HR phenotype in the absence of KHSRP is not due to inhibition of microRNA biogenesis

KHSRP has several described functions, but microRNA maturation after DNA damage is the most prominently studied role in the DDR (30, 31, 45). We assessed whether the observed HR phenotype by KHSRP depletion was induced by its microRNA biogenesis function. We transfected U2OS cells with a siRNA that targets DGCR8, one of the master regulators of microRNA biogenesis. DGCR8 inhibition inhibits microRNA biogenesis (46). First, the effect of DGCR8 knockdown was measured by qRT-PCR of three mature microRNAs (miR-30e, Let-7c and miR-26a), which resulted in a re-

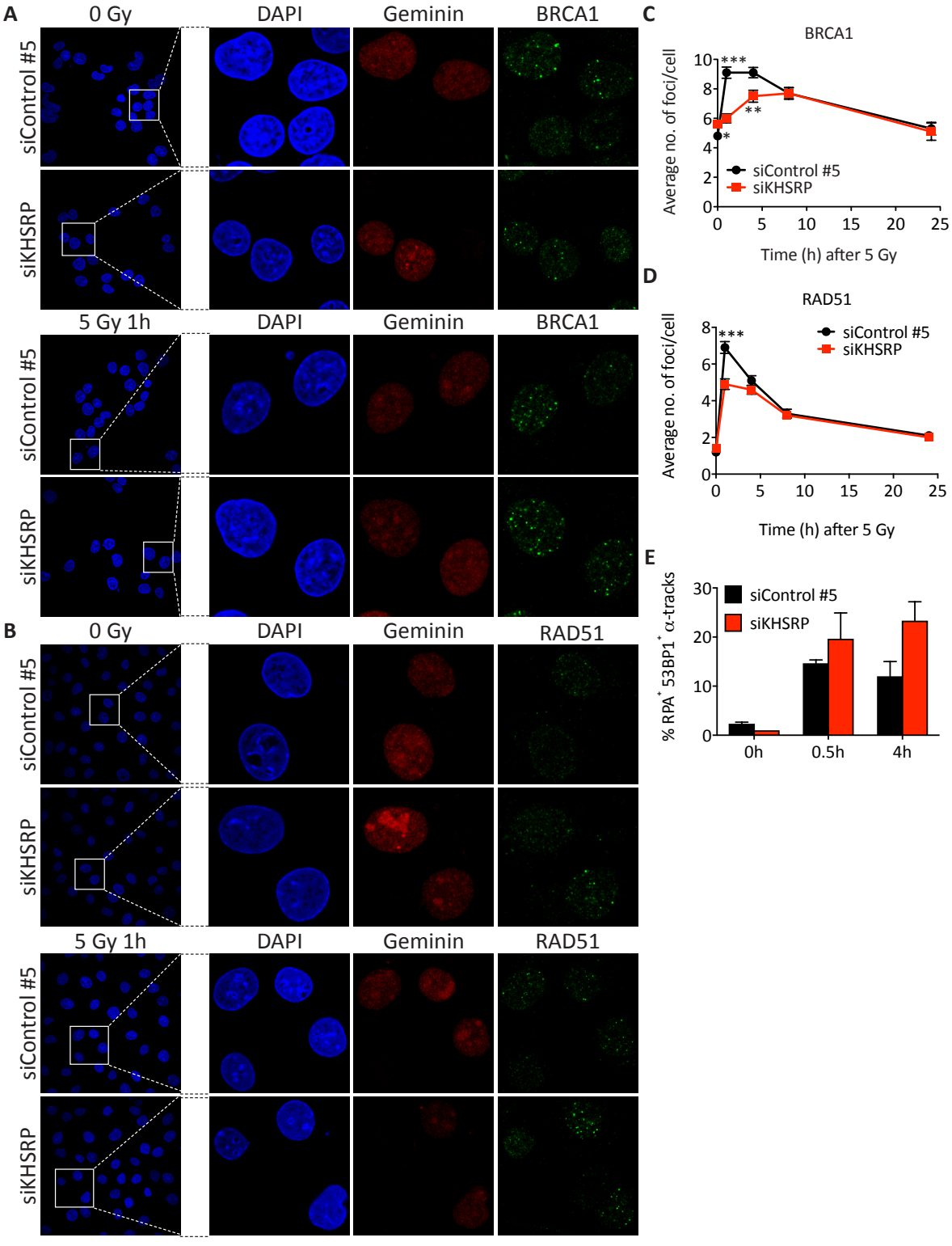

Figure 4: KHSRP knockdown affect HR-related proteins. A) Representative immunofluorescence images of non-irradiated and 1h after 5 Gy siControl or siKHSRP treated U2OS cells stained with DAPI and for BRCA1 (green) and geminin (red). Magnification 63× for left panel, the right panels are enlarged using ImageJ analysis software. B) Representative immunofluorescence images of non-irradiated and 1h after 5 Gy siControl or siKHSRP treated U2OS cells stained with DAPI and for

RAD51 (green) and geminin (red). Magnification 63× for left panel, the right panels are enlarged using ImageJ analysis software. C) Average number of BRCA1 foci per geminin positive cell were determined using ImageJ analysis software. Foci numbers were determined at different time points after 5 Gy IR. At least 50 cells were quantified per time point per experiment. The experiment was repeated three times. D) Average number of RAD51 foci per geminin positive cell were determined using ImageJ analysis software. Foci numbers were determined at different time points after 5 Gy IR. At least 50 cells were quantified per time point per experiment. The experiment was repeated three times. E) Quantification of 53BP1 and RPA positive tracks. N = 3, mean and SEM are depicted, Mann-Whitney U test was performed to determine statistical significance, * $p<0.05$; ** $p<0.01$.a

duction in mature microRNAs (Supp. Fig. 1B). Then, we analysed BRCA1 and RAD51 foci formation 1h after 5 Gy IR, a time point in which we observed the largest differences, and observed normal foci induction (Supplementary Fig. 1C + D). In addition, HR function was also not affected in the absence of DGCR8 (Supplementary Fig. 1E), suggesting that the defect in HR by KHSRP depletion is independent of its microRNA biogenesis function.

Discussion

Here, we showed that KHSRP depletion resulted in increased activation of ATM and reduced HR as seen by blunted RAD51 and BRCA1 focus formation after IR. Interestingly, RPA coating of resected ends of DSBs was increased, which suggests that KHSRP is involved in proper displacement of RPA from the single strand overhangs or facilitates BRCA1 loading onto these single strand overhangs that also does not displace RPA. We propose a model in which KHSRP acts in during RPA displacement and BRCA1 loading (Fig. 5).

A commonly used assay to measure HR is the DR-GFP assay, which was used in this manuscript (35, 40). However, this assay is prone to artefacts and therefore other assays to measure HR should be performed, for instance the sister chromatin exchange assay (SCE assay) (40). Nevertheless, we can still speculate on how KHSRP is involved in HR. After DSB recognition by PARP, the MRN complex is recruited to and binds to DSBs and facilitated DSB repair by HR (47). Then, the MRN complex recruits CtIP, which together with exonucleases EXO1, BLM and DNA2 results in end resection (48, 49). RPA coats the single strand overhangs to stabilize single strand DNA (50, 51). In the next step, RPA is displaced from the break by the BRCA1-BRCA2-PALB2 complex (42-44), which subsequently promotes RAD51 filament formation. Therefore, it is conceivable that a defect in BRCA1 loading or a defect in RPA displacement from single strand overhangs by KHSRP depletion leads to reduced RAD51 foci formation as well. Although we did not study the role CtIP, BRCA2 and PALB2 after KHSRP depletion, it is conceivable that their recruitment to DSBs is also reduced.

It is currently not clear how KHSRP interacts with the HR machinery. We performed a search in the Biogrid and Genemania databases, which list all known protein-protein interactions from literature and proteome-wide screens (52, 53). Both databases did not predict a direct interaction between BRCA1 and KHSRP, RAD51 and KHSRP, or KHSRP any

other HR factor. In some cases, an intermediary interaction was found, which is a common protein to which KHSRP and a HR protein both can bind (data not shown). It is conceivable that a direct interaction between BRCA1 and KHSRP is not yet identified or does not exist. Both BRCA1 and KHSRP can bind RNA species. BRCA1 was found to bind several types of RNA (21, 54, 55). After DNA damage, DDSR1, a long non-coding RNA (lncRNA), interacts with BRCA1 and the RBP hnRNPUL1, which prevents unwanted DNA binding by BRCA1 and as a consequence fine-tunes HR (54). Furthermore, hnRNPUL1/2 associates with the MRN complex thereby stimulating end resection, signalling and DNA repair via HR (29). These data imply that KHSRP and BRCA1 could interact via a RNA component, similarly as observed for the polycomb repressor complex 2 (56).

In conclusion, we have established a role for KHSRP in restricting ATM activation and HR, in which KHSRP facilitates RPA displacement or BRCA1 loading onto single strand overhangs. Future experiments should further dissect the role of KHSRP in the DDR.

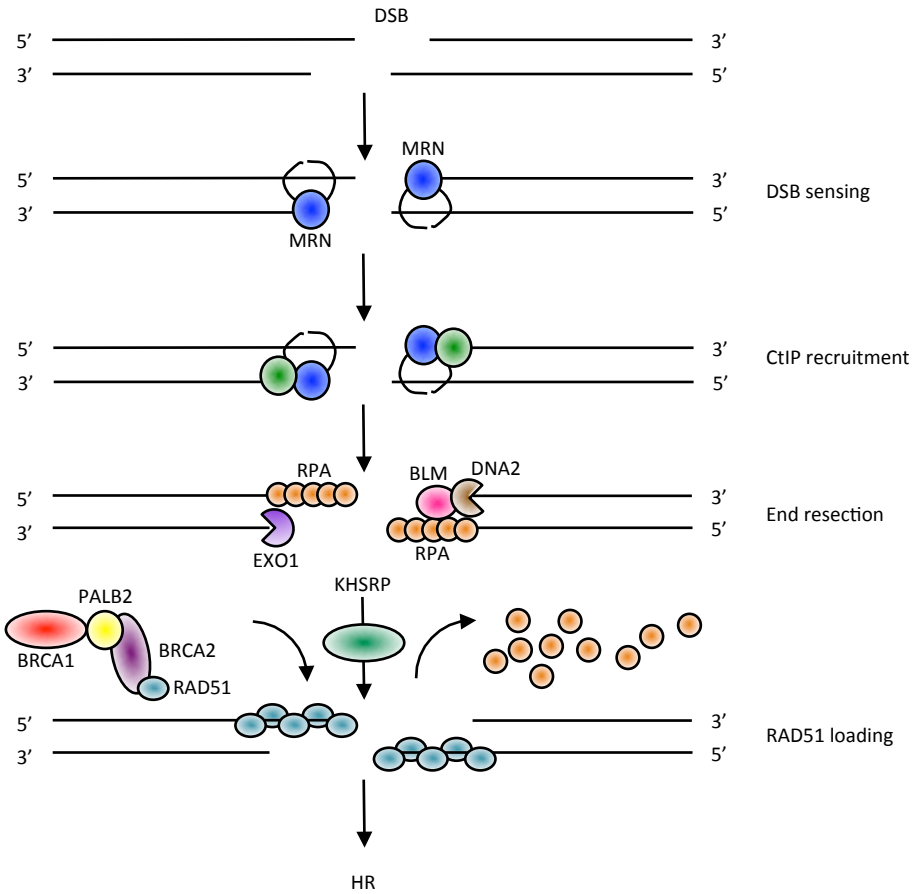

Figure 5: Model. KHSRP promotes RPA displacement and/or BRCA1 loading followed by RAD51 filament formation. DSBs are detected by the MRN complex and recruits CtIP. CtIP EXO1, DNA2 and BLM for end resection and RPA to coat single strand overhangs. The BRCA1 –PALB2 – BRCA2 complex displaces RPA, promoting strand evasion and subsequent repair, via forming RAD51 filaments.

Acknowledgements

The authors would like to thank the Molecular Genetics department of the Erasmus Medical Center Rotterdam for their contributions to the manuscript. This research was supported by Dutch Cancer Society (KWF) grant nr. 2011-5030.

Disclosure

The authors declare no conflict of interest.

References

1. Dutertre M, Lambert S, Carreira A, Amor-Gueret M, Vagner S. DNA damage: RNA-binding proteins protect from near and far. Trends in biochemical sciences. 2014;39(3):141-9.
2. Glisovic T, Bachorik JL, Yong J, Dreyfuss G. RNA-binding proteins and post-transcriptional gene regulation. FEBS letters. 2008;582(14):1977-86.
3. Hayakawa-Yano Y, Suyama S, Nogami M, Yugami M, Koya I, Furukawa T, et al. An RNA-binding protein, Qki5, regulates embryonic neural stem cells through pre-mRNA processing in cell adhesion signaling. Genes & development. 2017.
4. Cornella N, Tebaldi T, Gasperini L, Singh J, Padgett RA, Rossi A, et al. The hnRNP RALY regulates transcription and cell proliferation by modulating the expression of specific factors, including the proliferation-marker E2F1. The Journal of biological chemistry. 2017.
5. Kajitani N, Glahder J, Wu C, Yu H, Nilsson K, Schwartz S. hnRNP L controls HPV16 RNA polyadenylation and splicing in an Akt kinase-dependent manner. Nucleic acids research. 2017;45(16):9654-78.
6. Bondy-Chorney E, Baldwin RM, Didillon A, Chabot B, Jasmin BJ, Cote J. RNA binding protein RALY promotes Protein Arginine Methyltransferase 1 alternatively spliced isoform v2 relative expression and metastatic potential in breast cancer cells. The international journal of biochemistry & cell biology. 2017;91(Pt B):124-35.
7. Moumen A, Masterson P, O'Connor MJ, Jackson SP. hnRNP K: an HDM2 target and transcriptional coactivator of p53 in response to DNA damage. Cell. 2005;123(6):1065-78.
8. Brown AS, Mohanty BK, Howe PH. Computational Identification of Post Translational Modification Regulated RNA Binding Protein Motifs. PloS one. 2015;10(9):e0137696.
9. Pullmann R, Jr., Kim HH, Abdelmohsen K, Lal A, Martindale JL, Yang X, et al. Analysis of turnover and translation regulatory RNA-binding protein expression through binding to cognate mRNAs. Molecular and cellular biology. 2007;27(18):6265-78.
10. Huttelmaier S, Zenklusen D, Lederer M, Dictenberg J, Lorenz M, Meng X, et al. Spatial regulation of beta-actin translation by Src-dependent phosphorylation of ZBP1. Nature. 2005;438(7067):512-5.
11. Gherzi R, Lee KY, Briata P, Wegmuller D, Moroni C, Karin M, et al. A KH domain RNA binding protein, KSRP, promotes ARE-directed mRNA turnover by recruiting the degradation machinery. Molecular cell. 2004;14(5):571-83.
12. Stutz F, Bachi A, Doerks T, Braun IC, Seraphin B, Wilm M, et al. REF, an evolutionary conserved family of hnRNP-like proteins, interacts with TAP/Mex67p and participates in mRNA nuclear export. Rna. 2000;6(4):638-50.
13. Matsuoka S, Ballif BA, Smogorzewska A, McDonald ER, 3rd, Hurov KE, Luo J, et al. ATM and ATR substrate analysis reveals extensive protein networks responsive to DNA damage. Science. 2007;316(5828):1160-6.
14. Bennetzen MV, Larsen DH, Bunkenborg J, Bartek J, Lukas J, Andersen JS. Site-specific phosphorylation dynamics of the nuclear proteome during the DNA damage response. Molecular & cellular proteomics : MCP. 2010;9(6):1314-23.
15. Blasius M, Forment JV, Thakkar N, Wagner SA, Choudhary C, Jackson SP. A phospho-proteomic screen identifies substrates of the checkpoint kinase Chk1. Genome biology. 2011;12(8):R78.
16. Hoeijmakers JH. DNA damage, aging, and cancer. The New England jour-

nal of medicine. 2009;361(15):1475-85.
17. Hoeijmakers JH. Genome maintenance mechanisms for preventing cancer. Nature. 2001;411(6835):366-74.
18. Campisi J. Aging, tumor suppression and cancer: high wire-act! Mechanisms of ageing and development. 2005;126(1):51-8.
19. Wingert S, Rieger MA. Terminal differentiation induction as DNA damage response in hematopoietic stem cells by GADD45A. Experimental hematology. 2016;44(7):561-6.
20. Bensimon A, Schmidt A, Ziv Y, Elkon R, Wang SY, Chen DJ, et al. ATM-dependent and -independent dynamics of the nuclear phosphoproteome after DNA damage. Science signaling. 2010;3(151):rs3.
21. Dutertre M, Vagner S. DNA-Damage Response RNA-Binding Proteins (DDRBPs): Perspectives from a New Class of Proteins and Their RNA Targets. Journal of molecular biology. 2016.
22. Tresini M, Warmerdam DO, Kolovos P, Snijder L, Vrouwe MG, Demmers JA, et al. The core spliceosome as target and effector of non-canonical ATM signalling. Nature. 2015;523(7558):53-8.
23. Mazan-Mamczarz K, Galban S, Lopez de Silanes I, Martindale JL, Atasoy U, Keene JD, et al. RNA-binding protein HuR enhances p53 translation in response to ultraviolet light irradiation. Proceedings of the National Academy of Sciences of the United States of America. 2003;100(14):8354-9.
24. Glorian V, Maillot G, Poles S, Iacovoni JS, Favre G, Vagner S. HuR-dependent loading of miRNA RISC to the mRNA encoding the Ras-related small GTPase RhoB controls its translation during UV-induced apoptosis. Cell death and differentiation. 2011;18(11):1692-701.
25. Wang W, Furneaux H, Cheng H, Caldwell MC, Hutter D, Liu Y, et al. HuR regulates p21 mRNA stabilization by UV light. Molecular and cellular biology. 2000;20(3):760-9.
26. Paronetto MP, Minana B, Valcarcel J. The Ewing sarcoma protein regulates DNA damage-induced alternative splicing. Molecular cell. 2011;43(3):353-68.
27. Rajesh C, Baker DK, Pierce AJ, Pittman DL. The splicing-factor related protein SFPQ/PSF interacts with RAD51D and is necessary for homology-directed repair and sister chromatid cohesion. Nucleic acids research. 2011;39(1):132-45.
28. Kuhnert A, Schmidt U, Monajembashi S, Franke C, Schlott B, Grosse F, et al. Proteomic identification of PSF and p54(nrb) as TopBP1-interacting proteins. Journal of cellular biochemistry. 2012;113(5):1744-53.
29. Polo SE, Blackford AN, Chapman JR, Baskcomb L, Gravel S, Rusch A, et al. Regulation of DNA-end resection by hnRNPU-like proteins promotes DNA double-strand break signaling and repair. Molecular cell. 2012;45(4):505-16.
30. Zhang X, Wan G, Berger FG, He X, Lu X. The ATM kinase induces microRNA biogenesis in the DNA damage response. Molecular cell. 2011;41(4):371-83.
31. Santarosa M, Del Col L, Viel A, Bivi N, D'Ambrosio C, Scaloni A, et al. BRCA1 modulates the expression of hnRNPA2B1 and KHSRP. Cell cycle. 2010;9(23):4666-73.
32. Boucas J, Fritz C, Schmitt A, Riabinska A, Thelen L, Peifer M, et al. Label-Free Protein-RNA Interactome Analysis Identifies Khsrp Signaling Downstream of the p38/Mk2 Kinase Complex as a Critical Modulator of Cell Cycle Progression. PloS one. 2015;10(5):e0125745.
33. Stap J, Krawczyk PM, Van Oven CH, Barendsen GW, Essers J, Kanaar R, et al. Induction of linear tracks of DNA double-strand breaks by alpha-particle irradiation of cells. Nature methods. 2008;5(3):261-6.
34. Schmid I, Uittenbogaart C, Jamieson BD. Live-cell assay for detection of apoptosis by dual-laser flow cytometry using Hoechst 33342 and 7-amino-actinomycin D. Nature protocols. 2007;2(1):187-90.
35. Pierce AJ, Johnson RD, Thompson LH, Jasin M. XRCC3 promotes homology-directed repair of DNA damage in mammalian cells. Genes & development. 1999;13(20):2633-8.
36. Verkaik NS, Esveldt-van Lange RE, van Heemst D, Bruggenwirth HT, Hoeijmakers JH, Zdzienicka MZ, et al. Different types of V(D)J recombination and end-joining defects in DNA double-strand break repair mutant mammalian cells. European journal of immunology. 2002;32(3):701-9.
37. van Gent DC, Ramsden DA, Gellert M. The RAG1 and RAG2 proteins establish the 12/23 rule in V(D)J recombination. Cell. 1996;85(1):107-13.
38. O'Neill T, Dwyer AJ, Ziv Y, Chan DW, Lees-Miller SP, Abraham RH, et al. Utilization of oriented peptide libraries to identify substra-

te motifs selected by ATM. The Journal of biological chemistry. 2000;275(30):22719-27.
39. Kim ST, Lim DS, Canman CE, Kastan MB. Substrate specificities and identification of putative substrates of ATM kinase family members. The Journal of biological chemistry. 1999;274(53):37538-43.
40. Brandsma I, Gent DC. Pathway choice in DNA double strand break repair: observations of a balancing act. Genome integrity. 2012;3(1):9.
41. McGarry TJ, Kirschner MW. Geminin, an inhibitor of DNA replication, is degraded during mitosis. Cell. 1998;93(6):1043-53.
42. Sy SM, Huen MS, Chen J. PALB2 is an integral component of the BRCA complex required for homologous recombination repair. Proceedings of the National Academy of Sciences of the United States of America. 2009;106(17):7155-60.
43. Zhang F, Fan Q, Ren K, Andreassen PR. PALB2 functionally connects the breast cancer susceptibility proteins BRCA1 and BRCA2. Molecular cancer research : MCR. 2009;7(7):1110-8.
44. Zhang F, Ma J, Wu J, Ye L, Cai H, Xia B, et al. PALB2 links BRCA1 and BRCA2 in the DNA-damage response. Current biology : CB. 2009;19(6):524-9.
45. Trabucchi M, Briata P, Garcia-Mayoral M, Haase AD, Filipowicz W, Ramos A, et al. The RNA-binding protein KSRP promotes the biogenesis of a subset of microRNAs. Nature. 2009;459(7249):1010-4.
46. Gregory RI, Yan KP, Amuthan G, Chendrimada T, Doratotaj B, Cooch N, et al. The Microprocessor complex mediates the genesis of microRNAs. Nature. 2004;432(7014):235-40.
47. Haince JF, McDonald D, Rodrigue A, Dery U, Masson JY, Hendzel MJ, et al. PARP1-dependent kinetics of recruitment of MRE11 and NBS1 proteins to multiple DNA damage sites. The Journal of biological chemistry. 2008;283(2):1197-208.
48. Nimonkar AV, Genschel J, Kinoshita E, Polaczek P, Campbell JL, Wyman C, et al. BLM-DNA2-RPA-MRN and EXO1-BLM-RPA-MRN constitute two DNA end resection machineries for human DNA break repair. Genes & development. 2011;25(4):350-62.
49. Sartori AA, Lukas C, Coates J, Mistrik M, Fu S, Bartek J, et al. Human CtIP promotes DNA end resection. Nature. 2007;450(7169):509-14.
50. Chen H, Lisby M, Symington LS. RPA coordinates DNA end resection and prevents formation of DNA hairpins. Molecular cell. 2013;50(4):589-600.
51. Wold MS. Replication protein A: a heterotrimeric, single-stranded DNA-binding protein required for eukaryotic DNA metabolism. Annual review of biochemistry. 1997;66:61-92.
52. Chatr-Aryamontri A, Oughtred R, Boucher L, Rust J, Chang C, Kolas NK, et al. The BioGRID interaction database: 2017 update. Nucleic acids research. 2017;45(D1):D369-D79.
53. Montojo J, Zuberi K, Rodriguez H, Bader GD, Morris Q. GeneMANIA: Fast gene network construction and function prediction for Cytoscape. F1000Research. 2014;3:153.
54. Sharma V, Khurana S, Kubben N, Abdelmohsen K, Oberdoerffer P, Gorospe M, et al. A BRCA1-interacting lncRNA regulates homologous recombination. EMBO reports. 2015;16(11):1520-34.
55. Savage KI, Gorski JJ, Barros EM, Irwin GW, Manti L, Powell AJ, et al. Identification of a BRCA1-mRNA splicing complex required for efficient DNA repair and maintenance of genomic stability. Molecular cell. 2014;54(3):445-59.
56. Cifuentes-Rojas C, Hernandez AJ, Sarma K, Lee JT. Regulatory interactions between RNA and polycomb repressive complex 2. Molecular cell. 2014;55(2):171-85.

Supplemental information

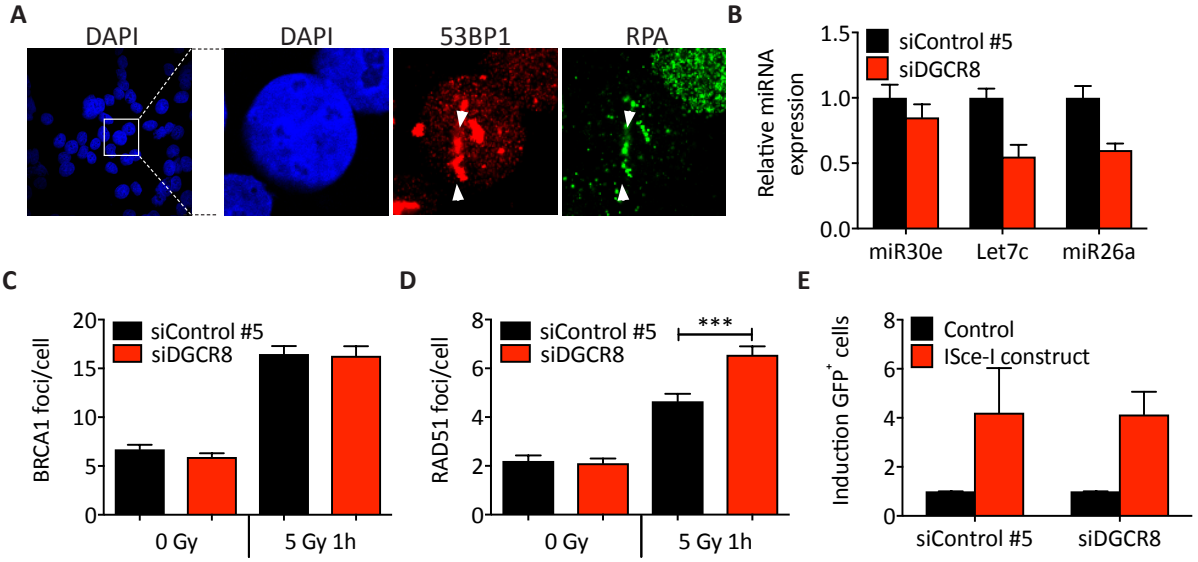

Supplementary Figure 1: The effect on HR by KHSRP silencing is not regulated by microRNAs. A) A representative image of U2OS cells treated with ^{241}americium source. Magnification of lest panel is 63×, right panels are enlarged using ImageJ analysis software. 53BP1 was used to locate DSB tracks (in between white arrow heads in red), next the track was scored for RPA staining (in between white arrow heads in green). The effect of DGCR8 knockdown was determined by qPCR of miR-30e, Let-7C and miR-26a. Mean and standard deviation are depicted. B + C) Immunofluorescence of BRCA1 (B) and RAD51 (C) was used to determine absolute number of foci per geminin positive cell. At least 50 cells were quantified per time point per experiment. N = 3, mean and SEM are depicted, Mann-Whitney U test was performed to determine statistical significance, *** $p<0.001$. D) HR reporter assay after DGCR8 knockdown. N = 3, mean and SEM are depicted.

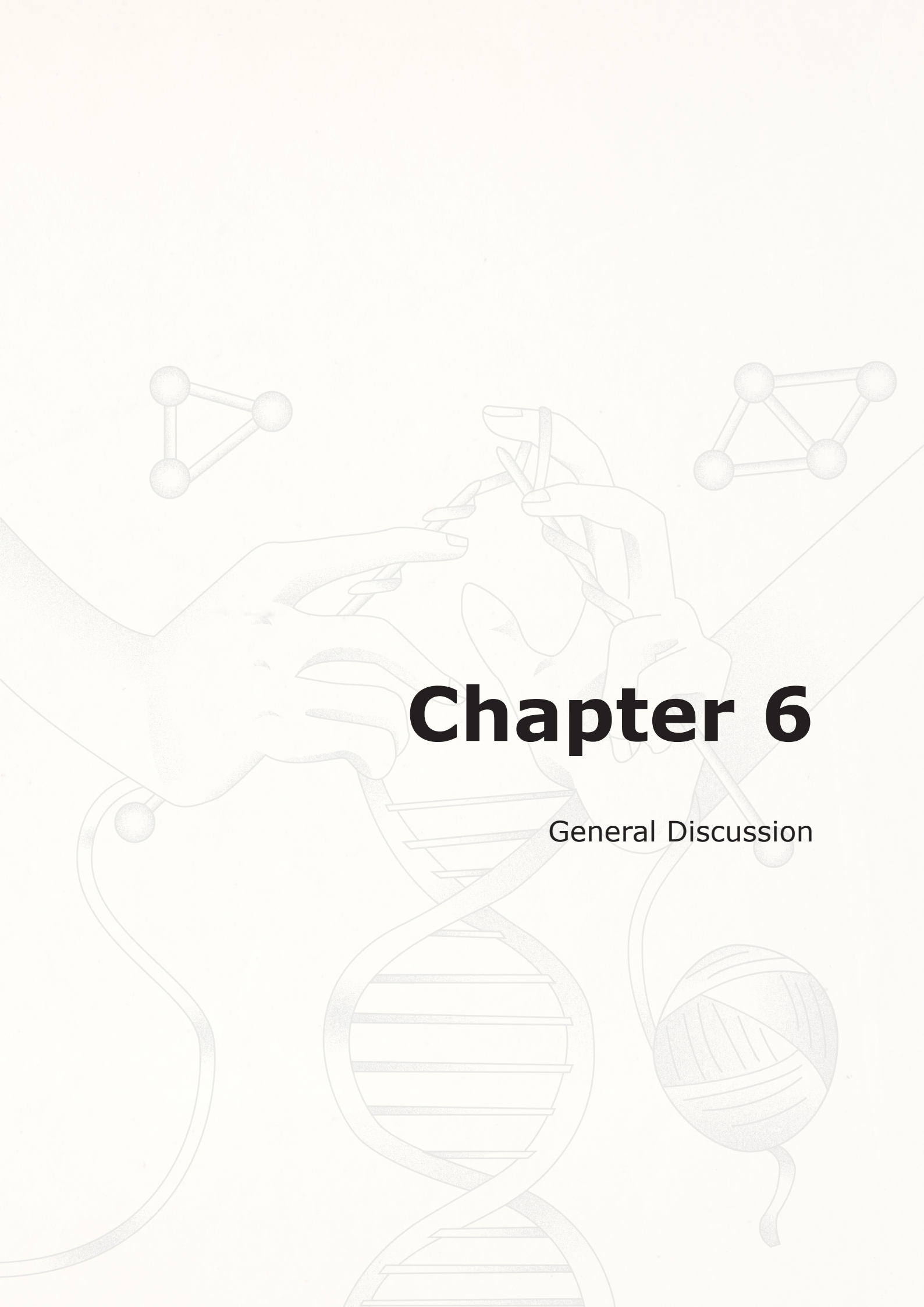

Chapter 6

General Discussion

Discussion

DNA damage can be deleterious to a cell if not properly repaired. Therefore an intricate network of DNA repair mechanisms and signalling pathways are present, which are called the DNA damage response (DDR). The DDR regulates different outcomes after DNA damage such as cell cycle arrest, apoptosis or senescence. When not properly repaired, DNA damage on its own can contribute to ageing or cancer development (1, 2).

Recently, the perspective on cancer changed from a one-dimensional disease to a disease that has a complex nature with a dynamic range of subtypes. However, all cancer types have common characteristics (3, 4) Chapter 1), which are currently exploited as treatment targets for cancer therapy. One characteristic most cancers have in common is genome instability caused by dysfunctional DNA repair machinery. Conventional cancer treatments, such as radiotherapy and chemotherapy, primarily target the DNA directly or the DNA repair machinery thereby killing the cancer cells. Although these types of treatments can be very effective, therapy resistance often occurs. Two types of resistance can be distinguished, intrinsic and acquired resistance. Intrinsic resistance is already present prior to treatment, whereas acquired resistance develops during the course of treatment (5). Since radiotherapy (RT) is a widely used treatment option, it is essential to understand the underlying mechanism of therapy resistance in order to overcome it. Several papers have already addressed the issue of acquired resistance (**Chapter 1**), however in each paper a different radiation protocol was used to generate RT resistant cell lines and are therefore difficult to compare with clinical cases. Therefore, this thesis describes the role of the DDR in acquired radiotherapy resistance induced by a clinically relevant treatment protocol using ionizing radiation (IR) (6) and the differential regulation of double strand break (DSB) repair induced by IR.

The main conclusions from this thesis can be summarized as follows: **Chapter 2** shows that long term DNA damage leads to adaptation of the DDR and subsequent RT resistance. Acquired resistance cannot solely be attributed to one component only; often multiple processes are involved. That is why in **Chapter 3** we used next generation sequencing to identify novel processes involved in acquired RT resistance. Indeed, we identified DDR pathways to be regulated in RT resistance. Interestingly, alterations in energy metabolism also contributed to RT resistance in our model. IR causes a spectrum of DNA damage of which DSBs are the most lethal to the cell (7). **Chapter 4** describes differences in transcriptional responses after different genotoxic treatments in embryonic stem cells. Based on these results we were able to identify citrullination as a post-translational modification important for proper DSB repair by homologous recombination (HR) in cancer cells. Interestingly, in **Chapter 5** we implicate the RNA binding protein (RBP) KHSRP in HR after IR.

DSB repair and post-transcriptional regulation

DSB repair is a tightly regulated process, which requires the involvement of numerous proteins and post-translational modifications (PTM). In **Chapter 5** we have identified a novel regulator in DSB repair and specifically in HR. Alternatively, DNA repair is not only regulated at the post-translational level, but also at the post-transcriptional level. Several mechanisms regulate RNA expression after DNA damage, of which microRNAs are well known. Another type of RNA regulation after DNA damage is by RNA binding proteins (RPBs) (reviewed in (8)). RBPs can, independently from their RNA-binding properties, regulate DSB repair by directly binding to core DSB recognition proteins (9), suggesting additional regulatory functions of these proteins in the DDR. Therefore in **Chapter 5**, we selected KHSRP, a RBP implicated in the DDR, to investigate its role in DSB repair after IR and found that KHSRP regulates HR. It was already shown that DDR proteins could also act as RBPs themselves and thereby regulate the DNA damage response (8, 10, 11); prominent examples are Ku70/80, BRCA1 and 53BP1 (12-15).

The DDR proteins that were identified as RBPs often bind long non-coding RNAs (lncRNA), which are also known to regulate genome organization by chromatin organization, modification and remodelling (16). Modifications of chromatin are important for DNA damage recognition and subsequent repair (17). Interestingly, histone modifiers important for DDR function, such as PRC2, Tip60 and KDM4D were also identified as RNA binding proteins (18, 19). The exact mechanism by which the interaction of chromatin modifiers and lncRNAs can regulate the DDR remains speculative, but one could argue that they are probably involved in chromatin remodelling; transcription silencing and DNA repair upon DNA damage (20). How KHSRP regulates HR is still unclear, but based on the above discussed roles of RBPs in DSB repair we can hypothesize that KHSRP may regulate HR by direct binding of HR proteins, however this hypothesis is unlikely since KHSRP is not recruited into DNA damage foci. A more feasible hypothesis is interaction of KHSRP with HR-related proteins or binding of KHSRP to RNAs involved in HR, thereby regulating chromatin condensation or transcription.

DSB repair and post-translational modifications

As mentioned previously, histone modifiers with important functions in the DDR were also identified as RBPs. Still their main function is to modify histones in response to DNA damage and thereby regulate DNA repair (17, 21, 22). The most well known PTMs upon DNA damage are phosphorylation, ubiquitylation, methylation and acetylation (23). A prominent example of a histone modification is the ATM-dependent phosphorylation of H2AX (γH2AX) upon DNA damage (24), which leads to recruitment of MDC1 to the DSB site (25). Subsequently, γH2AX spreads hundreds of kilo bases away from the break in an ATM-dependent manner (26). Furthermore, MDC1 recruits ubiquitin ligases RNF8 and RNF168, which ubiquity-

late H2A and γH2AX and as a result 53BP1 and BRCA1 are recruited (27). Dependent on cell cycle stage at which the DSB occurred and other chromatin modifications, either non-homologous end joining (NHEJ) or HR takes place to repair the break. The major determinant is the recruitment of 53BP1 and the BRCA1-CtIP complex (28). Recently, it was shown that specific (chromatin) modifications are important in determining which type of DSB repair takes place (29-31). ASF1a, which is known as a histone chaperone of the H3-H4 heterodimers to promote nucleosome assembly after DNA repair (32), was shown to have a direct role in NHEJ (29). It was shown that ASF1a interacts with MDC1 and promotes its phosphorylation by ATM. Then MDC1 is able to recruit RNF8-RNF168, which ubiquitylates H2A and H2AX and facilitates recruitment of 53BP1 and BRCA1-RAP80 (instead of BRCA1-CtIP) favouring NHEJ at the expense of HR. The data presented in this paper shows that, like RBPs, proteins with designated functions related to the DDR can also have direct, additional novel functions in DNA repair. Therefore we analysed the RNA response after DNA damage, but also to identify novel functions of proteins involved in the DDR.

In **Chapter 4** we show that citrullination is an important PTM in the regulation of HR and inhibition leads to defective HR in cancer cells. Interestingly, autoantibodies against citrullinated proteins (ACPAs) have been implicated in the pathogenesis of rheumatoid arthritis (33). Furthermore, increased or decreased citrullination of proteins were shown to enhance or inhibit cancer development or progression via various mechanisms (34-37), indicating an important role for citrullination in different disease pathologies. However, the role of citrullination in the DDR remains elusive. So far a few reports have been published linking one of the citrullination enzymes, PADI4, to p53 and HDAC2 in response to doxorubicin treatment (38-40). Whether these effects are due to the histone modifying enzyme activity of PADI4 or because of citrullination of non-histone targets is not known. However, we could speculate, based on published results by others, that citrullination of non-histone targets can lead to the observed effects. For instance it was shown that the DNA methyltransferase DNMT3a is a target of PADI4 and citrullination of DNMT3a is important for maintenance of p21 promoter methylation (41). Previously we mentioned that increased citrullination is often found in cancer as well as hypermethylation of specific promoters (42). In part, the hypermethylation patterns observed in cancer cells could be explained by overexpression of PADI4 and thereby increased expression and stabilization of DNMT3a leading to hypermethylation of specific promoters (41). In concert with the observed interaction of PADI4 with DNMT3a, PADI4 was also found to interact with histone deacetylase 2 (HDAC2) (39). Histone citrullination depended on the interaction of HDAC2 with PADI4; conversely acetylation of HDAC2 target protein p21 did not depend on PADI4. How HDAC2 influences PADI4 functioning is not known, but we could hypothesize that HDAC2 deacetylates PADI4, which is then not able to citrullinate its target histones or proteins and thereby reduces repair via HR. In line with this hypothesis are our findings in **Chapter 4** that citrullination inhibi-

tion does not affect NHEJ and it was shown that HDAC2 promotes NHEJ by deacetylating histone 3 lysine 56 and histone 4 lysine 16 specifically (43).

Regulation of DSB repair and mitochondrial metabolism upon DNA damage

A central finding in this thesis is the involvement of mitochondrial energy metabolism in response to DNA damage and acquired RT resistance (**Chapter 3; Chapter 4**). In **Chapter 2** we show that alterations in the DDR also contributed to acquired RT resistance, one of the effects we observed was stalling of RT resistant cells (RR cells) in G2- and M-phase of the cell cycle. Transition from G2-phase to M-phase is promoted by the cyclin B1/CDK1 complex, which was also found to relocate to the mitochondria during G2/M transition and thereby to increase oxygen consumption rates (OCR) and ATP production to provide sufficient energy for G2/M transition (44, 45). Interestingly, upon DNA damage by IR CDK1 also re-localized to the mitochondria and increased OCR and ATP production to favour DNA repair by HR and cell survival (46). A possible mechanism by which the cyclin B1/CDK1 complex regulates mitochondrial energy production is via SIRT3 (47). Upon exposure to IR, SIRT3 is up regulated and re-localizes together with cyclin B1/CDK1 to the mitochondria, where it is phosphorylated by cyclin B1/CDK1. Subsequently, SIRT3 phosphorylation increased and deactetylation of mitochondrial proteins; leading to lower ROS levels and increased ATP production, promoting cell survival instead of apoptosis after IR (47). Results presented in **Chapter 2** and **Chapter 3** provide a basis for this phenomenon in RR cells, as they have increased OCR and seem to require increased amounts of ATP to recover from the DNA damage.

PTMs often require intermediates from metabolic pathways, such as acetyl-CoA for acetylation, as discussed later on (see DSB repair and post-translational modifications). Under normal conditions the metabolic intermediates remain constant, however after DNA damage the demand for intermediates is increased and as a consequence these intermediates need to be replenished to maintain homeostasis of mitochondrial metabolism, which is called anaplerosis (48). Although we did not observe increased acetyl-CoA or citrate concentrations in RR cells in **Chapter 3**, it does not rule out the possibility that other metabolic intermediates are involved.

Mitochondrial regulation of post-translational modifications

As mentioned earlier Tip60 is an important chromatin modifier in the DDR. Tip60 is an acetyltransferase and upon a DSB it is recruited to the site of damage where it acetylates histones H2A, H4 and DDR proteins such as ATM and p53 (49). As a consequence of H4 acetylation, the chromatin decondensates and is more accessible for DNA repair factors (50). Acetyl-CoA is the main donor for lysine-acetyl transferases, such as Tip60, and is present in both the cytosol and nucleus. In the nucleus

acetyl-CoA is produced by ATP-citrate lyase (ACLY) from citrate, which is produced in the tri-carboxylic acid cycle (TCA cycle) in the mitochondria. A recent study shows that ACLY-dependent histone acetylation by Tip60 is an important determinant for HR in the S- and G2-phase of the cell cycle and prevention of acetylation leads to DSB repair via NHEJ (30).

Another example of how local metabolite production can contribute to DSB repair is shown by the TCA cycle enzyme fumarase (FH) (31). Upon exposure to IR FH is phosphorylated by DNA-pK and as a consequence FH binds H2A.Z and increases local production of fumarate from maltate. Subsequently, fumarate inhibited the de-methylation of H3 lysine 36 by KDM2, which is an important histone modification in NHEJ. This promotes DSB repair by NHEJ without affecting HR, indicating that this specific histone methylation mark is essential for NHEJ primarily in the G1-phase of the cell cycle.

All together these aforementioned examples show a complex wiring of DSB repair upon DNA damage. It also shows the importance of local metabolite production, which are normally produced in the mitochondria, to ensure substrate availability for histone modification enzymes. Interestingly, the results presented in **Chapter 2** and **Chapter 3** show both involvement of the DDR and mitochondrial respiration in the development of IR resistance, which leaves room for speculation about how these two pathways interact and how they together regulate modifications of histones and DDR proteins in IR resistance. Furthermore, it would be of interest to identify other non-histone targets of citrullination and to determine if the effect seen on HR is mainly due to histone citrullination or due to citrullination of for instance DDR proteins and how citrullination can contribute to acquired RT resistance. For RBPs it was already shown that they associate with cancer development and resistance to chemotherapy and radiotherapy (51-54).

Future perspective

Our findings, together with findings from others (55-62), have established a role for the DDR and energy metabolism in RT resistance (**Chapter 2 and 3**). However, the outcome of these studies is different, which suggest that characterization of individual tumours before and during treatment can help predict whether or not a tumour will respond to RT and if the regimen should be adjusted. This highlights the importance of personalized medicine, which was also emphasized by studies on the effectiveness of treatment on ex vivo breast cancer tumour slices (63, 64). A better understanding of the DDR can contribute to gaining greater insight on the role of the DDR in acquired resistance. In **Chapter 4** we used a NGS to identify novel players in the DDR and in **Chapter 5** we show that KHSRP is also involved in HR. The major advantage of our genomic approach is the identification of many different RNA species in one run without prior selection (65). This allowed us to follow, unbiased, the total change in the RNA landscape over time after DNA damage and identify novel genes in the DDR (**Chapter 4**). This approach is also interesting to use when it comes to identifying factors

involved in acquired resistance. Using biopsies taken prior to and during RT treatment the RNA response can be monitored, and based on the results, RT treatment can be adjusted when necessary. Since RBP regulation directly affects RNA biogenesis in general and has a profound effect on DSB repair either via HR (**Chapter 5**) or NHEJ (51) in different tumour types, it is not only interesting to monitor the RNA response itself during RT treatment, but also the activity of related RBPs in the tumour that could be of interest. Overall, the regulation of DSB repair at different levels and by different PTMs as discussed above, show which different pathways that are considered to function as separate entities are actually tightly intertwined. Therefore, it is important for different fields of research to work together instead of focussing solely on their specific topic. In this way it might be possible in the future to find a cure for all cancer patients.

References

1. Hoeijmakers JH. DNA damage, aging, and cancer. The New England journal of medicine. 2009;361(15):1475-85.
2. Hoeijmakers JH. Genome maintenance mechanisms for preventing cancer. Nature. 2001;411(6835):366-74.
3. Hanahan D, Weinberg RA. Hallmarks of cancer: the next generation. Cell. 2011;144(5):646-74.
4. Hanahan D, Weinberg RA. The hallmarks of cancer. Cell. 2000;100(1):57-70.
5. Holohan C, Van Schaeybroeck S, Longley DB, Johnston PG. Cancer drug resistance: an evolving paradigm. Nature reviews Cancer. 2013;13(10):714-26.
6. Incrocci L, Wortel RC, Alemayehu WG, Aluwini S, Schimmel E, Krol S, et al. Hypofractionated versus conventionally fractionated radiotherapy for patients with localised prostate cancer (HYPRO): final efficacy results from a randomised, multicentre, open-label, phase 3 trial. The Lancet Oncology. 2016;17(8):1061-9.
7. Ward JF. DNA damage produced by ionizing radiation in mammalian cells: identities, mechanisms of formation, and reparability. Progress in nucleic acid research and molecular biology. 1988;35:95-125.
8. Dutertre M, Lambert S, Carreira A, Amor-Gueret M, Vagner S. DNA damage: RNA-binding proteins protect from near and far. Trends in biochemical sciences. 2014;39(3):141-9.
9. Polo SE, Blackford AN, Chapman JR, Baskcomb L, Gravel S, Rusch A, et al. Regulation of DNA-end resection by hnRNPU-like proteins promotes DNA double-strand break signaling and repair. Molecular cell. 2012;45(4):505-16.
10. Giono LE, Nieto Moreno N, Cambindo Botto AE, Dujardin G, Munoz MJ, Kornblihtt AR. The RNA Response to DNA Damage. Journal of molecular biology. 2016;428(12):2636-51.
11. Wickramasinghe VO, Venkitaraman AR. RNA Processing and Genome Stability: Cause and Consequence. Molecular cell. 2016;61(4):496-505.
12. Lamaa A, Le Bras M, Skuli N, Britton S, Frit P, Calsou P, et al. A novel cytoprotective function for the DNA repair protein Ku in regulating p53 mRNA translation and function. EMBO reports. 2016;17(4):508-18.
13. Sharma V, Khurana S, Kubben N, Abdelmohsen K, Oberdoerffer P, Gorospe M, et al. A BRCA1-interacting lncRNA regulates homologous recombination. EMBO reports. 2015;16(11):1520-34.
14. Dalby AB, Goodrich KJ, Pfingsten JS, Cech TR. RNA recognition by the DNA end-binding Ku heterodimer. Rna. 2013;19(6):841-51.
15. Pryde F, Khalili S, Robertson K, Selfridge J, Ritchie AM, Melton DW, et al. 53BP1 exchanges slowly at the sites of DNA damage and appears to require RNA for its association with chromatin. Journal of cell science. 2005;118(Pt 9):2043-55.
16. Rinn JL, Chang HY. Genome regulation by long noncoding RNAs. Annual review of biochemistry. 2012;81:145-66.
17. Adam S, Polo SE. Blurring the line between the DNA damage response and transcription: the importance of chromatin dynamics. Expe-

rimental cell research. 2014;329(1):148-53.
18. Chen PB, Chen HV, Acharya D, Rando OJ, Fazzio TG. R loops regulate promoter-proximal chromatin architecture and cellular differentiation. Nature structural & molecular biology. 2015;22(12):999-1007.
19. Khoury-Haddad H, Nadar-Ponniah PT, Awwad S, Ayoub N. The emerging role of lysine demethylases in DNA damage response: dissecting the recruitment mode of KDM4D/JMJD2D to DNA damage sites. Cell cycle. 2015;14(7):950-8.
20. Dutertre M, Vagner S. DNA-Damage Response RNA-Binding Proteins (DDRBPs): Perspectives from a New Class of Proteins and Their RNA Targets. Journal of molecular biology. 2017;429(21):3139-45.
21. rice BD, D'Andrea AD. Chromatin remodeling at DNA double-strand breaks. Cell. 2013;152(6):1344-54.
22. Sulli G, Di Micco R, d'Adda di Fagagna F. Crosstalk between chromatin state and DNA damage response in cellular senescence and cancer. Nature reviews Cancer. 2012;12(10):709-20.
23. Lukas J, Lukas C, Bartek J. More than just a focus: The chromatin response to DNA damage and its role in genome integrity maintenance. Nature cell biology. 2011;13(10):1161-9.
24. Rogakou EP, Pilch DR, Orr AH, Ivanova VS, Bonner WM. DNA double-stranded breaks induce histone H2AX phosphorylation on serine 139. The Journal of biological chemistry. 1998;273(10):5858-68.
25. Stucki M, Jackson SP. gammaH2AX and MDC1: anchoring the DNA-damage-response machinery to broken chromosomes. DNA repair. 2006;5(5):534-43.
26. Rogakou EP, Boon C, Redon C, Bonner WM. Megabase chromatin domains involved in DNA double-strand breaks in vivo. The Journal of cell biology. 1999;146(5):905-16.
27. Doil C, Mailand N, Bekker-Jensen S, Menard P, Larsen DH, Pepperkok R, et al. RNF168 binds and amplifies ubiquitin conjugates on damaged chromosomes to allow accumulation of repair proteins. Cell. 2009;136(3):435-46.
28. Bunting SF, Callen E, Wong N, Chen HT, Polato F, Gunn A, et al. 53BP1 inhibits homologous recombination in Brca1-deficient cells by blocking resection of DNA breaks. Cell. 2010;141(2):243-54.
29. Lee KY, Im JS, Shibata E, Dutta A. ASF1a Promotes Non-homologous End Joining Repair by Facilitating Phosphorylation of MDC1 by ATM at Double-Strand Breaks. Molecular cell. 2017;68(1):61-75 e5.
30. Sivanand S, Rhoades S, Jiang Q, Lee JV, Benci J, Zhang J, et al. Nuclear Acetyl-CoA Production by ACLY Promotes Homologous Recombination. Molecular cell. 2017;67(2):252-65 e6.
31. Jiang Y, Qian X, Shen J, Wang Y, Li X, Liu R, et al. Local generation of fumarate promotes DNA repair through inhibition of histone H3 demethylation. Nature cell biology. 2015;17(9):1158-68.
32. Mello JA, Sillje HH, Roche DM, Kirschner DB, Nigg EA, Almouzni G. Human Asf1 and CAF-1 interact and synergize in a repair-coupled nucleosome assembly pathway. EMBO reports. 2002;3(4):329-34.
33. Sakkas LI, Daoussis D, Liossis SN, Bogdanos DP. The Infectious Basis of ACPA-Positive Rheumatoid Arthritis. Frontiers in microbiology. 2017;8:1853.
34. Qu Y, Olsen JR, Yuan X, Cheng PF, Levesque MP, Brokstad KA, et al. Small molecule promotes beta-catenin citrullination and inhibits Wnt signaling in cancer. Nature chemical biology. 2017.
35. Qin H, Liu X, Li F, Miao L, Li T, Xu B, et al. PAD1 promotes epithelial-mesenchymal transition and metastasis in triple-negative breast cancer cells by regulating MEK1-ERK1/2-MMP2 signaling. Cancer letters. 2017;409:30-41.
36. Wang L, Song G, Zhang X, Feng T, Pan J, Chen W, et al. PADI2-Mediated Citrullination Promotes Prostate Cancer Progression. Cancer research. 2017;77(21):5755-68.
37. Funayama R, Taniguchi H, Mizuma M, Fujishima F, Kobayashi M, Ohnuma S, et al. Protein-arginine deiminase 2 suppresses proliferation of colon cancer cells through protein citrullination. Cancer science. 2017;108(4):713-8.
38. Tanikawa C, Espinosa M, Suzuki A, Masuda K, Yamamoto K, Tsuchiya E, et al. Regulation of histone modification and chromatin structure by the p53-PADI4 pathway. Nature communications. 2012;3:676.
39. Li P, Wang D, Yao H, Doret P, Hao G, Shen Q, et al. Coordination of PAD4 and HDAC2 in the regulation of p53-target gene expression. Oncogene. 2010;29(21):3153-62.
40. Tanikawa C, Ueda K, Nakagawa H, Yoshida N, Nakamura Y, Matsuda K. Regulation of protein Citrullination through p53/PADI4 network in DNA damage response. Cancer research. 2009;69(22):8761-9.
41. Deplus R, Denis H, Putmans P, Calonne E, Fourrez M,

Yamamoto K, et al. Citrullination of DNMT3A by PADI4 regulates its stability and controls DNA methylation. Nucleic acids research. 2014;42(13):8285-96.
42. Jones PA, Baylin SB. The epigenomics of cancer. Cell. 2007;128(4):683-92.
43. Miller KM, Tjeertes JV, Coates J, Legube G, Polo SE, Britton S, et al. Human HDAC1 and HDAC2 function in the DNA-damage response to promote DNA nonhomologous end-joining. Nature structural & molecular biology. 2010;17(9):1144-51.
44. Wang Z, Fan M, Candas D, Zhang TQ, Qin L, Eldridge A, et al. Cyclin B1/Cdk1 coordinates mitochondrial respiration for cell-cycle G2/M progression. Developmental cell. 2014;29(2):217-32.
45. Lim S, Kaldis P. Cdks, cyclins and CKIs: roles beyond cell cycle regulation. Development. 2013;140(15):3079-93.
46. Qin L, Fan M, Candas D, Jiang G, Papadopoulos S, Tian L, et al. CDK1 Enhances Mitochondrial Bioenergetics for Radiation-Induced DNA Repair. Cell reports. 2015;13(10):2056-63.
47. Liu R, Fan M, Candas D, Qin L, Zhang X, Eldridge A, et al. CDK1-Mediated SIRT3 Activation Enhances Mitochondrial Function and Tumor Radioresistance. Molecular cancer therapeutics. 2015;14(9):2090-102.
48. Owen OE, Kalhan SC, Hanson RW. The key role of anaplerosis and cataplerosis for citric acid cycle function. The Journal of biological chemistry. 2002;277(34):30409-12.
49. Sun Y, Jiang X, Price BD. Tip60: connecting chromatin to DNA damage signaling. Cell cycle. 2010;9(5):930-6.
50. Kruhlak MJ, Celeste A, Dellaire G, Fernandez-Capetillo O, Muller WG, McNally JG, et al. Changes in chromatin structure and mobility in living cells at sites of DNA double-strand breaks. The Journal of cell biology. 2006;172(6):823-34.
51. Yuan M, Eberhart CG, Kai M. RNA binding protein RBM14 promotes radio-resistance in glioblastoma by regulating DNA repair and cell differentiation. Oncotarget. 2014;5(9):2820-6.
52. Kechavarzi B, Janga SC. Dissecting the expression landscape of RNA-binding proteins in human cancers. Genome biology. 2014;15(1):R14.
53. Cohen AA, Geva-Zatorsky N, Eden E, Frenkel-Morgenstern M, Issaeva I, Sigal A, et al. Dynamic proteomics of individual cancer cells in response to a drug. Science. 2008;322(5907):1511-6.
54. Ohga T, Koike K, Ono M, Makino Y, Itagaki Y, Tanimoto M, et al. Role of the human Y box-binding protein YB-1 in cellular sensitivity to the DNA-damaging agents cisplatin, mitomycin C, and ultraviolet light. Cancer research. 1996;56(18):4224-8.
55. Zhang Y, Lai J, Du Z, Gao J, Yang S, Gorityala S, et al. Targeting radioresistant breast cancer cells by single agent CHK1 inhibitor via enhancing replication stress. Oncotarget. 2016;7(23):34688-702.
56. Li Y, Li H, Peng W, He XY, Huang M, Qiu D, et al. DNA-dependent protein kinase catalytic subunit inhibitor reverses acquired radioresistance in lung adenocarcinoma by suppressing DNA repair. Molecular medicine reports. 2015;12(1):1328-34.
57. Guo L, Xiao Y, Fan M, Li JJ, Wang Y. Profiling global kinome signatures of the radioresistant MCF-7/C6 breast cancer cells using MRM-based targeted proteomics. Journal of proteome research. 2015;14(1):193-201.
58. Chang L, Graham PH, Hao J, Ni J, Bucci J, Cozzi PJ, et al. PI3K/Akt/mTOR pathway inhibitors enhance radiosensitivity in radioresistant prostate cancer cells through inducing apoptosis, reducing autophagy, suppressing NHEJ and HR repair pathways. Cell death & disease. 2014;5:e1437.
59. Peng G, Cao RB, Li YH, Zou ZW, Huang J, Ding Q. Alterations of cell cycle control proteins SHP1/2, p16, CDK4 and cyclin D1 in radioresistant nasopharyngeal carcinoma cells. Molecular medicine reports. 2014;10(4):1709-16.
60. Zhang P, Wei Y, Wang L, Debeb BG, Yuan Y, Zhang J, et al. ATM-mediated stabilization of ZEB1 promotes DNA damage response and radioresistance through CHK1. Nature cell biology. 2014;16(9):864-75.
61. Cao R, Ding Q, Li P, Xue J, Zou Z, Huang J, et al. SHP1-mediated cell cycle redistribution inhibits radiosensitivity of non-small cell lung cancer. Radiation oncology. 2013;8:178.
62. Ghosh S, Krishna M. Role of Rad52 in fractionated irradiation induced signaling in A549 lung adenocarcinoma cells. Mutation research. 2012;729(1-2):61-72.
63. Naipal KA, Verkaik NS, Sanchez H, van Deurzen CH, den Bakker MA, Hoeijmakers JH, et al. Tumor slice culture system to assess drug response of

primary breast cancer. BMC cancer. 2016;16:78.
64. Naipal KA, Verkaik NS, Ameziane N, van Deurzen CH, Ter Brugge P, Meijers M, et al. Functional ex vivo assay to select homologous recombination-deficient breast tumors for PARP inhibitor treatment. Clinical cancer research : an official journal of the American Association for Cancer Research. 2014;20(18):4816-26.
65. Derks KW, Misovic B, van den Hout MC, Kockx CE, Gomez CP, Brouwer RW, et al. Deciphering the RNA landscape by RNAome sequencing. RNA biology. 2015;12(1):30-42.

Appendix

Summary

It is estimated that the incidence of cancer will increase from 13 million to 22 million new cases each year worldwide. Cancer development is driven by changes in the DNA sequence such as mutations and chromosomal rearrangements, which occur as a consequence of DNA damage. To prevent cancer development it is important for the cell to counteract DNA damage. Thus, upon DNA damage the cell activates an adequate cellular response, which is called the DNA damage response (DDR). This response prevents cells from passing on faults in the DNA code, which, if kept, may turn into cancer cells. The DDR repairs the DNA using different repair mechanisms and DNA damage checkpoint activation, which result in different cellular outcomes such as cell death, temporary or permanent cell cycle arrest. As most, if not all cancer cells have one or more defects in the DDR, the higher sensitivity of cancer cells to DNA damage may be used to treat the cancer. Cancer therapy, such as chemotherapy or radiotherapy (RT), induces additional DNA damage that is very effective in cancer treatment. Although radiotherapy is a frequently used and effective treatment option, development of radiotherapy resistance occurs regularly.

Two types of therapy resistance can be distinguished I) intrinsic resistance, in which the resistance is already present before treatment and II) acquired resistance whereby the resistance is acquired in the course of treatment. Acquired resistance leads to recurrent and/or metastasized tumours (tumours that have spread into other places in the body), which reduce the life expectancy of the patient. Currently, limited data is available on the role of the DDR in acquired RT resistance. Therefore, we explored the role of the DDR in acquired RT resistance and the regulation of downstream processes in normal and cancer cells.

In **Chapter 2 and 3** we analysed the role of the DDR in acquired RT resistance in cancer cells and identified novel processes associated with acquired resistance. We generated radio-resistant cancer cells (RR cells) using a clinically relevant treatment protocol. RR cells were sensitised to RT after a 'RT holiday', at which RR cells were cultured for a period of time after finalizing the RT treatment (time re-sensitized RR cells). In **Chapter 2**, the DDR in RR cells was altered due to increased checkpoint activation and slower DNA repair. Interestingly, inhibition of checkpoint activation concomitantly with DNA repair sensitised RR cells to additional RT. Overall we show that the DDR in RR cells is altered and possibly contributes to the resistant phenotype.

To identify novel processes that are associated with acquired RT resistance we determined overall mRNA expression levels in RR cells and time re-sensitised RR cells in **Chapter 3**. As expected, we confirmed that the DDR is altered during RT resistance. Interestingly, energy metabolism was regulated during RT resistance in all populations tested. Verification of the mRNA data in RR cells indeed showed increased energy production by the mitochondria. Furthermore, forcing RT sensitive cancer cells to produce energy by the mitochondria induced resistance to RT. In conclusion,

using mRNA sequencing and verification with experiments we showed that energy metabolism is increased and contributes to acquired RT resistance.

To clarify the role of the DDR in acquired RT resistance, it is important to understand the factors in the DDR in healthy cells. In **Chapter 4** we studied the DDR at different time points after introduction of DNA damage with different types of DNA damaging agents. DNA damage was induced by either ionizing radiation (IR), ultraviolet light (UV) or the chemotherapeutic drug cisplatin. After treatment with these agents we analysed the overall RNA expression levels after 4, 8 and 12 hours of treatment. We observed a clear difference in mRNA and microRNA expression. MicroRNAs are small (± 22 nucleotides) non-coding RNAs that regulate gene expression by binding the target mRNA, thereby inducing mRNA degradation or translation inhibition. The mRNA response to DNA damage showed a clear DNA damage-dependent response, whereas the microRNAs showed a clear time-based distribution. The data indicate that mRNA and microRNA expression is tightly regulated upon DNA damage. Furthermore, we identified a novel modification, citrullination, in the DDR, especially in DNA repair. In summary, we made a transcriptional database with mRNA and microRNAs, which are regulated after different types of DNA damages. Additionally, citrullination was identified as a novel modification involved in the DDR.

As was shown in **Chapter 3 and 4**, the RNA response is pivotal to DDR functioning. Not only gene regulation by RNAs, but also RNA regulation itself is important. RNA binding proteins (RBPs) regulate RNA biogenesis and these proteins were also found to be involved in the DDR. Therefore, in **Chapter 5** we focussed on the role of a specific RBP, KH-Type Splicing Regulatory Protein (KHSRP), in the DDR after IR. We found that KHSRP is an important protein involved in DNA damage repair after IR as without KHSRP DNA repair after IR is less functional. These observed effects were independent from KHSRPs function in microRNA biogenesis. In conclusion, we show a novel function of KHSRP in the DDR independent from its function in microRNA biogenesis. In general, an elaborate knowledge of the DDR after IR is essential to understand the complicated nature of acquired RT resistance and the involvement of the DDR in cancer. This knowledge can then be used to develop novel targeted therapies to overcome acquired RT resistance in cancer.

Samenvatting

In de toekomst zal het aantal nieuwe gevallen van kanker wereldwijd per jaar toenemen tot 22 miljoen. Veranderingen in de nucleotidevolgorde van het DNA door bijvoorbeeld mutaties of veranderingen in het gehele chromosoom kunnen lijden tot kankerontwikkeling. Deze veranderingen treden op als gevolg van DNA-schade. Om kankerontwikkeling te voorkomen moet de cel DNA-schade tegengaan. Daarom activeert de cel in geval van DNA-schade de DNA-schaderesponse (DSR). Deze response voorkomt dat cellen fouten in de DNA-volgorde doorgeven aan de volgende generatie, welke, als ze niet gerepareerd worden, kunnen leiden tot de ontwikkeling van kankercellen. Door het gebruik van verschillende reparatiemechanismen en activatie van het DNA-schade checkpoint, wordt het DNA gerepareerd via de DSR. Dit heeft verschillende gevolgen voor de cel, zoals celdood of een tijdelijke of permanente stop van de celcyclus. De meeste, zo niet alle kankercellen hebben één of meerdere defecten in de DSR. Hierdoor hebben deze cellen een hogere gevoeligheid voor DNA-schade en kan deze hogere gevoeligheid worden gebruikt om kanker te behandelen. Kankertherapie, zoals chemotherapie of bestraling, is zeer effectief omdat ze extra DNA-schade veroorzaken. Hoewel bestraling zeer effectief is en vaak als behandelmethode wordt gebruikt, komt resistentie tegen bestraling vaak voor.

Twee typen therapieresistentie kunnen worden onderscheiden: I) intrinsieke resistentie, waarbij de resistentie voor de behandeling op voorhand al aanwezig is en II) verkregen resistentie, waarbij de resistentie tijdens de behandeling optreedt. Verkregen resistentie leidt vaak tot terugkeer of uitzaaiingen van de tumor, waardoor de levensverwachting van de patiënt daalt. Op dit moment is er beperkt data beschikbaar over de rol van de DSR in verkregen resistentie. Daarom onderzoeken wij in dit proefschrift wat de rol van de DSR in verkregen resistentie is en hoe de regulatie van de processen in de DSR verloopt in normale en kankercellen.

In **Hoofdstuk 2 en 3** hebben we de rol van de DSR in verkregen resistentie in kankercellen onderzocht. Hierbij hebben we nieuwe processen ontdekt die betrokken zijn bij de ontwikkeling van verkregen resistentie. Door het gebruik van een klinisch relevant bestralingsprotocol hebben we bestralingsresistente cellen (BR-cellen) gegenereerd. Door BR-cellen een 'bestralingsvakantie' te geven waarbij BR-cellen voor een bepaalde periode niet bestraald werden na de laatste bestralingsdosis, werden deze cellen weer gevoelig voor bestraling. In **Hoofdstuk 2** hebben we ontdekt dat de DSR veranderd is als gevolg van toegenomen checkpointactivatie en langzamer DNA-herstel. Interessant genoeg leidde remming van zowel checkpointactivatie als DNA-herstel tot gevoeligheid van BR-cellen voor extra bestraling. Alles bij elkaar genomen laten we zien dat de DSR in BR-cellen veranderd is en mogelijk bijdraagt aan de ontwikkeling van verkregen resistentie.

Om nieuwe processen te identificeren die mogelijk bijdragen aan de ontwikkeling van bestralingsresistentie, hebben we in **Hoofdstuk 3** totale mRNA-expressieniveaus bepaald in BR-cellen en BR-cel-

len die een 'bestralingsvakantie' gehad hebben. Zoals verwacht laten de data zien dat de DSR veranderd tijdens bestralingsresistentie. Een interessante bevinding is de betrokkenheid van het energiemetabolisme bij bestralingsresistentie in alle geteste samples. Verificatie van de data laat inderdaad zien dat de energieproductie door de mitochondriën verhoogd is. Daarnaast, door bestralingsgevoelige kankercellen te dwingen energie te produceren door de mitochondriën, werden ze resistent voor bestraling. Alles samenvattend laten we zien dat het gebruik van mRNA sequencing en de daarop volgende verificatie van de data met experimenten het energiemetabolisme associëren met verkregen resistentie.

Om de rol van de DSR in verkregen resistentie te verduidelijken, is het belangrijk om te begrijpen hoe de DSR werkt in gezonde cellen. Daarom hebben we in **Hoofdstuk 4** de DSR bestudeerd op verschillende tijdspunten na de introductie van DNA-schade door verschillende DNA beschadigende middelen. DNA-schade werd geïnduceerd door ioniserende straling, ultraviolet licht of het chemotherapeuticum cisplatine. Na behandeling met deze middelen hebben we de totale RNA-expressie niveaus vier, acht, en twaalf uur na behandeling geanalyseerd. We hebben een duidelijk verschil geobserveerd tussen mRNA- en microRNA-expressie. MicroRNAs zijn kleine (± 22 nucleotides groot) niet-coderende RNAs die genexpressie reguleren door het binden van specifieke mRNAs. Als gevolg hiervan wordt het mRNA afgebroken of wordt de translatie geremd. De reactie van mRNA op DNA-schade laat een duidelijk DNA-schadeafhankelijk patroon zien, terwijl de microRNAs een duidelijk tijdsgebonden patroon laten zien. De data duiden op een strikte regulatie van zowel mRNA als microRNA na DNA schade in het algemeen. Daarnaast hebben we een nieuwe modificatie in de DSR, citrullinatie genaamd, geïdentificeerd. In totaal hebben we een transcriptionele database met mRNAs en microRNAs gegenereerd, die beide worden gereguleerd na DNA-schade. Ook hebben we citrullinatie geïdentificeerd als een nieuwe modificatie die betrokken is bij de DSR.

Zoals we al laten zien in **Hoofdstuk 3 en 4** is de RNA-response essentieel voor de DSR. Niet alleen worden genen gereguleerd door RNAs, ook de regulatie van RNAs zelf is belangrijk. RNA-bindende eiwitten (RBPs) reguleren RNA-biogenese en deze eiwitten zijn ook belangrijk in de DSR. Daarom hebben we in **Hoofdstuk 5** gefocust op de rol van een specifiek RBP in de DSR na bestraling, KH-Type Splicing Regulatory Protein (KHSRP) genaamd. Wij hebben gevonden dat KHSRP een belangrijk eiwit is, dat betrokken is bij de DNA-reparatie na bestraling, sinds DNA-reparatie na bestraling zonder KHSRP minder goed functioneert. Dit geobserveerde effect was onafhankelijk van de functie van KHSRP in microRNA biogenese. Gebaseerd op de data kunnen we concluderen dat KHSRP een nieuwe functie heeft in de DSR onafhankelijk van zijn functie in de microRNA biogenese.

Om de gecompliceerde aard van verkregen resistentie en de betrokkenheid van de DSR daarbij te begrijpen, is uitgebreide kennis van de DSR onmisbaar. Deze kennis kan worden gebruikt bij de ontwikkeling van nieuwe specifieke therapieën om verkregen therapieresistentie in kanker te omzeilen.

PhD Portfolio

Name Serena Tamara Bruens
PhD period 2012 – 2017
Promotor Jan Hoeijmakers
Co-promotor Joris Pothof

Courses	Year	Workload (ECTS)
Biophysics and Biochemistry	2012	3
In vivo cellular imaging	2012	1,8
Veilig werken in het lab	2012	
Cell and Developmental Biology	2013	3
Bio-statistical methods I: Basic principles Part A	2013	2
Genetics	2014	3
Biomedical English writing	2015	3

Workshops and Conferences	Year	Workload (ECTS)
MGC PhD Workshop - Abstract (Luxemburg, Luxemburg)	2013	30 hours
NVvO Basiscursus oncologie (Ellecom, the Netherlands)	2013	40 hours
MGC PhD Workshop - Poster presentation (Münster, Germany)	2014	30 hours
PMTs in Cell signalling - Poster presentation (Copenhagen, Denmark)	2014	32 hours
MGC PhD Workshop - Oral presentation (Maastricht, the Netherlands)	2015	30 hours
Radiotherapy Research day - Oral presentation (Rotterdam, the Netherlands)	2015	8 hours

AACR Annual meeting - Poster presentation (New Orleans, USA)	2016	40 hours
Radiotherapy Research day – Oral presentation (Rotterdam, the Netherlands)	2016	8 hours

Teaching	**Year**	**Workload (ECTS)**
Werkcollege Bachelor Nanobiology	2012 - 2017	15 hours
HLO student	2013 - 2014	10 months
Master student	2015	6 months

Curriculum Vitae

Personal details

Full name: Serena Tamara Bruens
Date of birth: 15 February 1989
Place of Birth: Dordrecht, the Netherlands
Nationality: Dutch

Education

April 2017 – Present
Postdoctoral researcher on 'The influence of exogenous chemical compounds on the risk for cancer in human beings. Replacement of the chronic animal exposure test for in vitro methods using novel human tissue tests.' Department of Molecular Genetics, Erasmus Medical Centre Rotterdam, the Netherlands.

October 2012 – March 2017
PhD project 'Ionizing Radiation, DNA Damage Response and Cancer Therapy Resistance' as part of the KWO fellowship. Under supervision of Joris Pothof and Jan Hoeijmakers at the Department of Molecular Genetics, Erasmus Medical Centre Rotterdam, the Netherlands.

August 2010 – August 2012
Master of Science (MSc): Research master Infection and Immunity at Erasmus University Rotterdam (EUR), the Netherlands.

September 2007 – August 2010 ('fast track' program)
Bachelor of Applied Science (BASc): Biologie en Medisch Laboratoriumonderzoek, Hogeschool Rotterdam (HR), the Netherlands.

September 2001 – June 2007
VWO at Mgr. Frencken College, Profiel: Natuur & Gezondheid met Scheikunde 2, Oosterhout (NB), the Netherlands.

List of Publications

Serena Bruens, Marjolein Baar, Aranka Ambags, Marjolijn Ladan, Nicole Verkaik, Dik van Gent, Roland Kanaar, Wytkse van Weerden, Guido Jenster, Jan Hoeijmakers, Joris Pothof, *Persistent DNA double strand breaks and transient rewiring of the DNA damage response induce acquired radio-resistance* – Submitted

Serena Bruens, Jiang Chang, Chiara Milanese, Akos Gyenis, Kasper Derks, Marjolijn Ladan, Pier Mastroberardino, Wytkse van Weerden, Guido Jenster, Jan Hoeijmakers, Joris Pothof, *Increased metabolic activity contributes to acquired radio-resistance in cancer* – To be submitted

Serena Bruens, Jiang Chang, Kasper Derks, Akos Gyenis, Nicole Verkaik, Jan Hoeijmakers, Joris Pothof, *A time-resolved transcriptional map induced by DNA damage reveales citrullination as a novel process in the DNA damage response* – Submitted

Serena Bruens, Nicole Verkaik, Dik van Gent, Roland Kanaar, Jan Hoeijmakers, Joris Pothof, *KHSRP is involved in homologues recombination after DNA damage* – In preparation

Serena T Bruens, Benoit Stijlemans, Wouter Beumer, Maria Ochoa Gonzalez, Patrick De Baetselier, Pieter J M Leenen, *CD11b+ c-kit+ mouse bone marrow cells constitute a myeloid precursor population with distinct features* – To be submitted

Kishan A. T. Naipal, Anja Raams, **Serena T. Bruens**, Inger Brandsma, Nicole S. Verkaik, Nicolaas G. J. Jaspers, Jan H. J. Hoeijmakers, Geert J. L. H. van Leenders, Joris Pothof, Roland Kanaar, Joost Boormans, Dik C. van Gent, *Attenuated XPC Expression Is Not Associated with Impaired DNA Repair in Bladder Cancer*, PLoSOne April 30, 2015

Chinmoy Saha, Andrew Stubbs, Gaurav Dugar, Youri Hoogstrate, Gert-Jan Kremers, Gert van Cappellen, Chui-Yoke Chin, Deborah Horst-Kreft, Inez Kross, **Serena Bruens**, Duncan Gaskin, David S. Weiss, Dior Beerens, Dik van Gent, Cynthia Sharma, Johan W. Mouton, Peter J. van der Spek, Peter van Baarlen, John van der Oost, Rogier Louwen, *Saturation guide RNA loading overcomes Cas9-induced human cell death* – Submitted

Imke K. Mandermaker, **Serena T. Bruens**, Dick H. Dekkers, Pernette J. Verschure, Raghu R. Edupuganti, Eran Meshorer, Jeroen A. Demmers, Jurgen A. Marteijn, *Enhanced Histone H1 Chromatin Retention After SET Depletion Causes DNA Damage Resistance* - In preparation

Dankwoord

Nou dat was het dan… Ein-de-lijk klaar! Na bloed, zweet en een heleboel tranen ligt er dan een boekje. Deze periode heeft mij ontzettend veel geleerd. Er waren diepe dalen, maar ook hoge pieken. Uiteraard heb ik dit niet alleen voor elkaar gekregen, daarom wil ik via deze weg een aantal mensen bedanken.

Beste Jan, ik heb ontzettend veel bewondering voor je niet aflatende enthousiasme over ongeveer alles. Je bent altijd kritisch, maar met een positieve draai. Na besprekingen met jou en Joris had ik toch altijd weer het gevoel dat het allemaal goed zou komen. Ook in je drukke schema had je toch een gaatje om even bij te praten over de stand van zaken. Ik wil je bedanken dat je mij de kans hebt gegeven om mij te laten promoveren en ook dat je het vertrouwen in mij hebt om verder te gaan in en Postdoc.

Joris, hoe zal ik het zeggen… Ik ben inmiddels heel goed (maar misschien ook niet) in het managen van jou. Meer dan dat wil ik je bedanken voor het vertrouwen wat je in mij had en hebt om dit allemaal tot een goed einde te brengen. Ik waardeer onze gesprekken die altijd iets langer duurde dan de bedoeling was en ook altijd afweken van het eigenlijke onderwerp. Als ik het even niet meer zag zitten, iets met een kapotte gamma bron of zo, dan was je altijd in staat om het te relativeren en mij weer uit de put te krijgen.

Beste Roland, ontzettend bedankt voor je hulp tijdens de laatste periode van mijn promotie. Ik waardeer je Rotterdamse directheid, ook al was het af en toe even slikken. Dat je toch altijd even tijd vrijmaakte om iedereen in de goede richting te sturen (inclusief ondergetekende) heeft enorm geholpen.

Mijn paranimfen Sander en Renata, allereerst vind ik het een eer dat jullie mijn paranimf willen zijn. Lief en leed heb ik met jullie kunnen delen en het was en is nog steeds heel erg prettig dat, dat nog steeds kan. Met alle verandering is het fijn om een goede basis te hebben en die kunnen jullie ook bieden. Ik hoop dat we met z'n drieën nog lang samen kunnen lachen en het over onze kinderen/katten kunnen hebben bij de koffie. O ja, en samen kunnen werken natuurlijk ;).

Het Vermeulen lab, waar ik de eerste 2 jaar van mijn promotie door heb mogen brengen. Wim, Jurgen en Hannes, bedankt jullie bijdrage tijdens de eerste (en ook de laatste) 2 jaar van mijn promotie. Arjan, bedankt voor al je hulp met de celkweek en je slechte grappen kan ik wel waarderen ;). Franzi, Yasemin, Christina, Barbara thanks for the nice time in the lab and during conferences. I wish you all the best in your future careers.

Karen, jij verdient een eigen alineaatje. Ik wil je bedanken voor onze gesprekken in de vroege ochtend als er (bijna) niemand aanwezig was. Het heeft mij geholpen om het allemaal in perspectief te plaatsen en

toch echt voor mijzelf te kiezen en niet iedereen tevreden te willen houden. Als je kunt, sta je altijd klaar om te helpen en dat waardeer ik zeer.

Imke en Mariangela! Onze uitstapjes en etentjes waren een leuke onderbreking van het OIO bestaan. Mariangela, ik vind het zo knap dat je Nederlands geleerd hebt. Blijven oefenen en dan schrijf je, je Nederlandse samenvatting straks zelf ;). Imke, ik vind het jammer dat je naar München verhuist bent, maar dat geeft wel een goede reden om je op te komen zoeken. Na 4 jaar kan ik oprecht zeggen dat ik er 2 vriendinnen bij heb.

De laaste 2-3 jaar van mijn promotie heb ik door mogen brengen in de ageing en clock groep, ook wel bekend als 'de andere kant'. Bert, Wilbert, Peter, Ines, Maayke en Akos thank you for your input and conversations during those years and I hope we will have many more in the future. OIO-hok office mates Rana, Diana, Aida, Hester, Jiang, Astrid and Maria thank you for the great time and funny moments. I wish you all the best in obtaining your degree. Nicole, Sylvia, Yvette en Yvonne bedankt voor de gezellige tijd in het lab en aan de lunchtafel tijdens onze pauzes.

Pier, Chiara and Maria, thank you for all your help during my PhD. It was nice to work with you and I hope we can do that more often in the future. All the regular chats we had when I came for Joris and he wasn't there are highly appreciated.

Ik mag uiteraard Buurman (a.k.a. Marjolein ;)) niet vergeten. Onze gezamenlijke pogingen om experimenten te doen was niet altijd even succesvol, maar we konden er wel altijd om lachen. Het was fijn om iemand te hebben die in dezelfde situatie zit/zat als ik. Altijd kon ik bij jou terecht om even te klagen of om gewoon even gezellig te praten.

Een promotie doe je nooit alleen, zoals inmiddels wel duidelijk is en via deze weg wil ook graag de mensen van de "6e" bedanken. Nicole, Anja, Hanny, Nathalie, Dik, Kishan, Inger, Paula en Yanto. Bedankt voor alle gezellige praatjes en hulp als ik die nodig had (wat nog best vaak was eigenlijk ;)).

Jasperina en Sonja, wat is de afdeling zonder jullie? Altijd heerst er toch wel een lichte paniek als jullie er niet zijn. Bedankt voor jullie ondersteuning en hulp als ik het nodig had.

Dan de IT mensen Nils, Ton en Sjozef, bedankt voor de ondersteuning die ik regelmatig nodig had omdat er 'iets' met mijn computer was. En nee Nils, er is nu niets mis met de microscoop en m'n computer doet het gewoon nog ;).

De afdeling Moleculaire Genetica is groot en via deze weg wil ik alle andere mensen die ik niet bij naam genoemd heb, bedanken voor hun hulp en bijdrage aan de gezellige sfeer op de afdeling.

Een deel van mijn onderzoek vond ook plaats in samenwerking met de afdeling Urologie. Guido, Wytske en Hanneke ik vond het heel prettig om met jullie samen te werken. De besprekingen waren altijd open en jullie stonden altijd klaar met advies en goede ideeën om aan te werken. Ook als er geen besprekingen waren kon ik altijd even binnen lopen met nieuwe data of als ik vastgelopen was en advies nodig had, bedankt daarvoor. Ook Wilma, Sigrun, Diana, Mirella en alle anderen die ik nu vergeet, jullie stonden en staan nog steeds altijd klaar voor hulp. Dat was erg prettig en maakte het ook fijn om met jullie samen te werken.

Belangrijk zijn de mensen geweest die mij hebben geïntroduceerd in de wetenschap tijdens mijn HBO stages. Maikel, jij hebt mij enthousiast gemaakt voor het werken in het lab. Als begeleider was je prettig in omgang en je hebt mij veel geleerd. Joey! Ik heb zo ontzettend veel van jou geleerd. Maar het belangrijkste was, geef nooit op. Het was een eer om met jou te werken en om je paranimf te zijn. Helaas zit er nu een zee tussen ons, maar ik hoop nog veel te kunnen samenwerken in de toekomst.

Ondanks dat je zelf in opleiding bent, leid je zelf ook mensen op. Tijdens deze periode heb ik twee studenten gehad Aranka en Marjolijn. Ik heb ontzettend veel geluk met jullie beide gehad. Jullie waren snel zelfstandig en hebben daardoor een hoop werk kunnen verzetten. Ik heb ook veel van jullie geleerd en ik hoop jullie ook van mij. Het is ook goed om te weten dat jullie beiden goed terecht gekomen zijn en ik wens jullie veel succes.

Ontspanning is eigenlijk iets wat niet in het woordenboek van een OIO voorkomt, maar wat je toch wel nodig hebt. Ruby, Cynthia, Jantine, Chantal, Wenda, Tessa, Remco, Jacco, Jeffrey, Floris, Martijn, Freek, Doren, Ferdi, Anouk, Sander, Marit, Remco, Sjors, Dennie en Yin bedankt dat jullie hebben gezorgd voor de af en toe broodnodige afleiding en ontspanning. Ik hoop dat we nog lang samen mogen korfballen, weekendjes weg gaan, naar de film gaan, uiteten gaan of gewoon op stap gaan. Ferdi, heel erg bedankt dat je mij geholpen hebt met het ontwerpen van de kaft van mijn boekje.

Dan de familie: ooms, tantes, neven en nichten. Wat wij hebben is heel uniek en ik hoop ook zo te houden voor zo ver het gaat. Bedankt voor jullie interesse de afgelopen jaren. Ondanks het wegvallen van opa en oma, zijn we bij elkaar gebleven en hebben we het met z’n allen gezellig gemaakt. Dat er nog vele uitjes, al dan niet met (klein)kinderen mogen volgen.

Ook de schoonfamilie verdient een eervolle vermelding. Lizette, Dick, Ruby en Michiel en de rest van de familie. Het is een ontzettend warm bad waar je bij jullie in terecht komt en je graag even in blijft zitten. Als nieuweling (na bijna 10 jaar is dat natuurlijk niet echt het geval meer) wordt je met open armen ontvangen en is niets te gek. Er is een hoop

gebeurd in 10 jaar en het is heel fijn om te weten dat jullie er altijd zijn.

Het andere deel van de schoonfamilie Peter, Vera, Nikki, Nick, Jasper en Tim. Ook bij jullie werd ik gelijk in de familie opgenomen en dat was erg fijn. Jullie staan ook altijd klaar in goede en slechte tijden. We hebben tranen gehuild van verdriet, maar nog meer van het lachen en ik hoop dat, dat nog lang zo mag zijn.

Ik had dit niet kunnen doen zonder de onvoorwaardelijke steun van mijn ouders. Pap, mam bedankt dat jullie er voor gezorgd hebben dat er altijd een stabiele thuisbasis was en dat wij (ook Naomi en Dennis) ons nooit druk hebben hoeven maken of het überhaupt wel mogelijk was om te studeren. Ook al was het voor jullie onmogelijk om de naam van mijn opleiding te onthouden (iets met biologie toch?). Het ging al snel tot een onbegrijpelijk niveau en toch probeerde jullie altijd te helpen waar mogelijk. Ik kan nog steeds niet verklaren hoe het mogelijk is dat ik dit wel begrijp, maar niet weet hoe je krootjes moet koken.

Lieve Ori, je weet dat ik niet goed ben met het in woorden uitdrukken hoe blij ik met je ben. Gelukkig weet je dat ik dat absoluut wel ben. Zonder jou had ik dit niet gered, je bent er altijd voor mij en je zorgt voor de stabiele basis die ik nodig heb. Voor zover je kon heb je mij geholpen en je nuchtere kijk op dingen maakte het voor mij makkelijker om te relativeren. Nu snap je inmiddels hoe deze wereld in elkaar zit en dat je dus nooit huisvader kunt worden ;). Ik hoop echt dat we samen oud mogen worden en nog veel mooie momenten mee mogen maken.

Serena